2017

Quadrature-based models for multiphase and turbulent reacting flows

Ehsan Madadi Kandjani
Iowa State University

Quadrature-based models for multiphase and turbulent reacting flows

by

Ehsan Madadi-Kandjani

A dissertation submitted to the graduate faculty

in partial fulfillment of the requirements for the degree of

DOCTOR OF PHILOSOPHY

Major: Mechanical Engineering

Program of Study Committee:
Alberto Passalacqua, Major Professor
Rodney O. Fox
Baskar Ganapathysubramanian
Ming-Chen Hsu
Shankar Subramaniam

Iowa State University

Ames, Iowa

2017

Two heroes of my life, Hossein and Mehri

The best sister and brother-in-law, Elham and Kersten

TABLE OF CONTENTS

LIST OF TABLES

LIST OF FIGURES

ACKNOWLEDGEMENTS

This thesis represents not only my work, it is a milestone in more than a decade of work at Iowa State University specifically within the groups advised by Professor Rodney O. Fox and Professor Alberto Passalacqua. First and foremost I want to thank my advisor Professor Alberto Passalacqua. It has been an honor to be his student. I am very grateful for his patience, motivation, enthusiasm, and immense knowledge that, taken together, make him a great mentor. Since my first day at ISU, he supported me with his invaluable advice and enormous helps. I appreciate all his contributions of time, ideas, and funding to make my Ph.D. experience productive and stimulating. His advice on both research as well as on my career have been invaluable. I specially want to express my deepest gratitudes to Professor Rodney O. Fox, whose support and guidance made my thesis work possible. I have been fortunate to have him patiently guiding and helping me through difficult periods of work. Without his helps and advice, I would not be able to complete my Ph.D. studies. I would like to express my thanks to my committee members Prof. Baskar Ganapathysubramanian, Prof. Ming-Chen Hsu and Prof. Shankar Subramaniam for their support, time and advice on various aspects of conducting research and the writing of this thesis. I am grateful of having wonderful and fun group members and colleagues who helped me through useful discussions. I would like to acknowledge the financial support of the National Science Foundation. This work has been partially supported by the Division Of Advanced Cyberinfrastructure (ACI) of National Science Foundation under the award number SI2-SSE ACI-1440443 and department of mechanical engineering at ISU. Finally, I want to express my deepest love to my family and friends. In particular to my parents for devoting themselves to my life and career, and for their interminable and unconditional love and support, and to my sister and brother-in-law for being with me in frustrating times and sharing their love.

ABSTRACT

The simulation of physical systems requires accurate and robust methods with relatively low cost and it is still the challenge in many applications of engineering processes, specifically in multiphase flow systems. Soot formation, distribution of the aerosols in the atmosphere, reactive precipitation, and combustion modeling are some examples of these processes. Computer simulations of theses systems require a model that can be adapted to that reality. In this study, a quadrature based method of moments (QBMM) is used to address the problems related to the reactive multiphase flow systems. First, the log-normal kernel density function is implemented into the extended quadrature method of moments (Ln-EQMOM). Ln-EQMOM is verified reconstructing the NDF and calculating the moments of a distribution obtained by the linear combination of two log-normal distributions. Later, this numerical procedure is used for problems of aggregation and breakup of fine particles to solve the population balance equation (PBE). The results are compared to the rigorous solutions reported for the cases under consideration (Vanni, 2000). Finally, the method is verified using two analytically known problems (*e.g.* coalescence and condensation). In comparison to EQMOM with Γ kernel density function (Yuan et al., 2012), Ln-EQMOM is faster in terms of computations and it preserves the moments more accurately. Then EQMOM with β kernel density function is implemented to approximate the solution of the transport equation for the composition probability density function (PDF) of a passive scalar using the Fokker-Planck model to treat the molecular mixing term. The results then compared in a similar condition to those obtained with direct numerical simulation (DNS). The L_2 norm of the PDF is reported for two test cases that have been considered. Later the new approach is introduced to address the problems includes the mixing and reaction. Conditional quadrature method of moments (CQMOM) and using the joint composition PDF for the mixture fraction and progress variables, it is possible to address the problems with two consecutive competitive reactions, one reaction and fast reaction, all includ-

ing the mixing of reactants. direct quadrature method of moments (DQMOM) also expressed for the joint composition PDF. Results obtained with CQMOM and DQMOM are compared with each other. Finally, the CQMOM approach for mixing problems was tested considering two consecutive competitive reactions to verify the implementation and validate the proposed approach. Coupled mixing-PBE approach was then used to investigate polymer aggregation in a multi-inlet vortex reactor (MIVR), typically used to perform flash nanoprecipitation for the production of nanoparticles used in pharmaceutical applications.

CHAPTER 1. INTRODUCTION

1.1 Background

Multiphase flows are characterized by the simultaneous presence and interaction of two or more phases (*e.g.* gas, liquid and solid) in a system. These flows are encountered a multitude of applications and in nature. Examples are sediment transport in rivers, dispersion of aerosol in air, soot formation, and volcanic eruptions. Numerous industrial processes also involve multiphase mixtures. Gas bubble reactors in the chemical industry, transport of oil-water mixtures in pipes, fluidized bed combustors, and injection of fuel into the chamber of internal combustion engines are some examples.

In fluidized bed combustors, to have an optimized reaction of particles, an air jet is injected into the particle bed to make them suspended. In internal combustion engines, the fuel is injected into the chamber and fuel break into small droplets, which then evaporate and mixed with air. In soot formation process, soot begins with some precursors. Later, particles form due to the nucleation of heavy molecules. Particles then experience surface growth. Soot increases the risk of obstructive pulmonary disease and thus understanding the size and behavior of particles helps us to prevent such diseases. These examples show some general multiphase systems with different regimes and characteristics. In most of these applications, to control the final particle size distribution (PSD), it is necessary to predict the PSD evolution precisely with a reasonable computational cost.

Another essential aspect of multiphase flows is mixing, which is particularly important in turbulent flows. Turbulence enhances mixing in many geological and environmental systems. Turbulent mixing occurs in volcanic eruption columns, magma chambers and hot springs. In flash nanoprecipitation, as a particular example, the mixing affects the final size and quality

of particles. Therefore, accurate prediction of mixing is of great importance when simulating these systems. The spatial and temporal evolution of a passive scalar in a turbulent mixing process can be described using an evolution equation for the probability distribution function (PDF) of the system composition (Pope, 2000; Fox, 2003). Solutions of the composition PDF equation provide a one-point statistical description of the behavior of the scalar composition field, during its evolution from the unmixed to the mixed state (Broadwell and Breidenthal, 1982; Koochesfahani and Dimotakis, 1986; Mungal and Dimotakis, 1984; Girimaji, 1991; Cremer et al., 1994; McMurtry and Givi, 1989; Eswaran and Pope, 1988).

The common and most realistic case that happens in chemical industry applications is when mixing and reaction happens simultaneously. For some reactions, the way in which species are mixed can affect the final product (Danckwerts, 1958). In general, if chemical reactions are slow, mixing has no influence on the mean rate. In this case, the reactants will be well mixed on the smallest scales before the reactions occurs. When the time required for mixing is of the same order as, or longer than the typical time required for reactions, mixing models must be included.

In the problems mentioned before, the evolution of the system can be described using an evolution equation for the number density function (NDF) or the composition probability density function (PDF). These evolution equations, while describing different physical phenomena, have a similar mathematical structure, which allows general methods to be developed for their solution. Several methods have been developed to this purpose, which are discussed later in this chapter. We use quadrature-based moment methods (QBMM) to find approximate solutions of these equations for engineering applications. In QBMM, statistical momentsof the NDF or PDF are transported, rather than aiming at the exact reconstruction of the distribution. One of the earliest forms of QBMM is the quadrature method of moments (QMOM), in which the distribution is approximated by a weighted sum of few Dirac delta functions. Recently an extended quadrature method of moment (Yuan et al., 2012; Madadi-Kandjani and Passalacqua, 2015) was developed, which uses non-negative kernel density functions (KDF) as a base to approximate the PDF with a continuous function.

In the present work, we apply the log-normal kernel density function into an extended quadrature method of moments. Later, in this work, this method is used to address problems related to the aggregation and breakage of particles. An extended quadrature method of moments using β kernel density functions (β-EQMOM) is then adopted to approximate solutions of the evolution equation for univariate and bivariate composition probability distribution functions (PDF) of a passive scalar for binary and ternary mixing. The Fokker-Planck model is used to close the micromixing term. In this approach, the conditional scalar dissipation rate (CSDR) should be provided by the user as an input to the model. Two CSDR based on the β distribution (Fox, 2003) and the CSDR obtained using amplitude mapping closure (Pope, 1991) are used to approximate the micromixing term. These models will be described in detail later in this report. These approaches are then applied to multi-inlet vortex reactor (MIVR) to study mixing and reaction.

1.2 Existing works

In this section, we review previous studies related to the particle size distribution in polydisperse multiphase systems, turbulent mixing and turbulent reacting flows. Also, we address different approaches used in these studies.

1.2.1 Solution of PBE

Population balance equations (PBE) are used in several scientific and engineering disciplines to model complex processes, where the accurate description of the dispersed phase plays an important role in the prediction of the behavior of the system. The PBE describes the evolution of the density function associated to a particle population, and considers the various ways in which particles can either form or disappear from the system. Some examples of this type of processes are precipitation, crystallization, aerosols, bubbly flows and droplet flows (Randolph and Larson, 1988; Williams and Loyalka, 1991; Vanni, 2000; Marchisio et al., 2003b,a).

A population balance equation for chemical processes was originally derived in 1964, when two groups of researchers who studied crystal nucleation and growth, recognized that many problems involving the change in particulate systems could not be handled within the framework of

the conventional conservation equations (Randolph and Larson, 1988; Hulburt and Katz, 1964). Rather than adopting the standard continuum mechanical framework, the model derivation was based on the alternative Boltzmann-type equation familiar from classical statistical mechanics (Reyes, 1989; Lasheras et al., 2002; Carrica et al., 1999). Randolph (1964) and Randolph and Larson (1988), on the other hand, formulated a generic population balance model based on the generalized continuum mechanical framework. Different methods are proposed in the literature to solve the PBE. Some of these methods are described in upcoming sections.

1.2.2 Overview on the methods

The main methods for the solution of evolution equations of distribution functions are briefly summerized in this section. Here we discuss the existing methods and their advantage and disadvantages.

1.2.2.1 Monte-Carlo Method

The idea behind the Monte-Carlo method (Rosner and Yu, 2001; Lin et al., 2002; Smith and Matsoukas, 1998; Meimaroglou and Kiparissides, 2007; Zhao et al., 2007; Zhao and Zheng, 2013) is based on random sampling of statistical theory. It generates inputs randomly from a probability distribution over the domain of possible inputs, and aggregate the results after preforming computation over the domain. The advantage of this method is that it can deal with the high dimensional problem in a simple and straightforward manner. However, there are two drawbacks associated with the Monte-Carlo method. The Monte-Carlo method is most of the time too expensive in computational cost especially in problems related to aggregation of particles(Efendiev and Zachariah, 2002; Garcia et al., 1987; Gillespie, 1976; Goodson and Kraft, 2002; Kruis et al., 2000; Lee and Matsoukas, 2000; Liffman, 1992). Also, it is affected by statistical noise (Zhao et al., 2009), and the convergence rate of the method is slow ($1/\sqrt{N}$, e.g. quadrupling the number of sampled points halves the error, regardless of the number of dimensions).

1.2.2.2 Class and sectional methods

Another approach for problems with one internal variable is to discretize the internal coordinate in bias, called the method of classes. Equations are written for the NDF of the particles inside each interval of the size discretization (Hounslow et al., 1988; Hounslow, 1990; Kumar and Ramkrishna, 1996a,b; Puel et al., 2003; Bannari et al., 2008; Becker et al., 2011; Balakin et al., 2014). At each interval, the NDF is approximated by a polynomial. Zero order polynomials are used most commonly (Greenberg et al., 1986, 1993). However, there are methods based on higher order reconstructions in each interval (Alopaeus et al., 2006). The main advantage of these methods is that they provide the NDF distribution directly while the main disadvantages are the high computational resources required and the fact that classes must be defined a priori (Marchisio and Fox, 2005).

1.2.2.3 Method of moments

The method of moments was first developed by Hulburt and Katz (1964); Randolph and Larson (1988) for the particulate systems. In this approach, transport equations for a finite set of moments of the NDF are written, leading to a significant reduction of the computational cost compared to the methods previously mentioned. However, in general, the moment equations are not closed due to the presence of terms describing phenomena such as growth, aggregation or nucleation which are function of the NDF or of the particle size. Several approaches are possible to close the moment equations. The most common are (Falola et al., 2013):

- Assuming the functional form of the particle size distribution is known a priori (Lee, 1983; Pratsinis, 1988). However, for many particulate processes, the functional forms of the size distributions are not known a priori (Diemer and Olson, 2002; Falola et al., 2013).
- Moment inversion (Diemer and Olson, 2002; McGraw, 1997).

Of all these approaches, the second approach is the most versatile and includes the quadrature-based moment method (QBMM). In the next section, we will discuss the different types of this method.

1.2.2.4 Quadrature method of moments (QMOM)

In the context of moment methods, the closure model proposed by McGraw (1997) and then it was extensively applied to the chemical engineering applications (Marchisio et al., 2003b; Wang et al., 2005a,b; Marchisio and Fox, 2013), generates an entirely new class of methods. This method based on the idea of approximating the integrals that define the monets of the NDF with Gaussian quadrature formula, and it is called quadrature method of moments (QMOM). In this approach, the NDF can be reconstructed as a summation of weighted Dirac delta functions (or in recently developed branches of this method, the weighted summation of base functions). In QMOM, by considering the relationship between the QMOM moment closure and point distribution function (Dette, 1997) a univariate NDF can be approximated with N nodes to be an N-point distribution function as:

$$n\left(\xi;x,t\right)\approx\sum_{i=1}^{\mathrm{N}}w_i\delta\left(\xi-\xi_i\right), \tag{1.1}$$

where w_i is the i-th quadrature weight, and $\delta\left(\xi-\xi_i\right)$ represents the delta function centered at location ξ_i (abscissae), uniquely determined by means of a moment inversion algorithm. The k-th order of moment of a distribution can be expressed as:

$$M_k=\int_{\Omega_\xi}\xi^k n\left(\xi;x,t\right)\mathrm{d}\xi. \tag{1.2}$$

Applying Eq. 1.1 to the definition of the moment equation, Eq. 1.2, the moment equation can be expressed as:

$$M_k=\int_{\Omega_\xi}\sum_{i=1}^{\mathrm{N}}w_i\delta\left(\xi-\xi_i\right)\xi^k\mathrm{d}\xi. \tag{1.3}$$

Since

$$\int_{\Omega_\xi}\delta\left(\xi-\xi_i\right)\xi^k\mathrm{d}\xi=\xi_i^k, \tag{1.4}$$

the final form of Eq. 1.3 is:

$$M_k = \sum_{i=1}^{\mathrm{N}} w_i \xi_i^k. \tag{1.5}$$

Depending on the accuracy, we may need to employ the different number of weights and abscissae for calculating moments. It is worth to notice that a N-node quadrature approximation of the NDF exactly preserves the 2N moments used to determine the quadrature weights and abscissae.

1.2.2.5 The extended quadrature method of moments (EQMOM)

The Gaussian quadrature algorithm introduced in Sec. 1.2.2.4 is equivalent to approximating the univariate NDF by a sum of Dirac delta functions:

$$n\left(\xi; x, t\right) \approx \sum_{i=1}^{\mathrm{N}} w_i \delta\left(\xi - \xi_i\right). \tag{1.6}$$

The discrete representation of the NDF limits the applicability of the method to cases where a smooth representation of the NDF is needed. For example, in evaporation problems (Massot et al., 2010), the value of the NDF for the null internal coordinate is required, which is not available if the QMOM is used to approximate the NDF. Even with partial solutions in which N increases dramatically, QMOM is not accurate for N larger than 10 (Gautschi, 2004; McGraw, 1997; Wheeler, 1974). In order to overcome this limitation, Eq. 1.6 can be generalized by introducing smooth non-negative KDF with a finite (or infinite) support determined by a parameter σ shared by all the terms and of the basis:

$$n\left(\xi; x, t\right) \approx \sum_{i=1}^{\mathrm{N}} w_i \delta_\sigma\left(\xi, \xi_i\right). \tag{1.7}$$

The value of σ is determined by enforcing the preservation of one additional moment compared to QMOM. It is necessary to choose different KDF based on the case under consideration. Three kernel density functions are considered in Yuan et al. (2012), based on the support of the NDF to be reconstructed as:

- Gaussian ($\xi \in]-\infty, +\infty[$)

$$\delta_\sigma(\xi, \xi_i) \equiv \frac{1}{\sqrt{2\pi\sigma^2}} \exp\left[-\frac{(\xi - \xi_i)^2}{2\sigma^2}\right]; \tag{1.8}$$

- Gamma ($\xi \in [0, +\infty[$)

$$\delta_\sigma(\xi, \xi_i) \equiv \frac{\xi^{\lambda_i - 1} e^{\xi/\sigma}}{\Gamma(\lambda_i)\, \sigma^{\lambda_i}}, \quad \text{with} \quad \lambda_i = \xi_i/\sigma; \tag{1.9}$$

- Beta ($\xi \in [0, 1]$)

$$\delta_\sigma(\xi, \xi_i) \equiv \frac{\xi^{\lambda_i - 1}(1 - \xi)^{\mu_i - 1}}{\mathbf{B}(\lambda_i, \mu_i)}, \quad \text{with } \lambda_i = \xi_i/\sigma \text{ and } \mu_i = (1 - \xi_i)/\sigma. \tag{1.10}$$

An optional approach to formulate EQMOM is to choose the KDFs so that orthogonal polynomials are known. This choice allows the reconstructed NDF to be integrated efficiently, since the recurrence relationship for the orthogonal polynomials is known. Thus a Gaussian quadrature can be defined for each of the KDFs. These secondary weights and abscissae found in this way are then used to calculate source terms for the moment equations. Substituting Eq. 1.7 into the integral of an arbitrary function, the EQMOM closure for the integrals can be represented as (Yuan et al., 2012):

$$\int_0^\infty g(\xi)\, n(\xi)\, \mathrm{d}\xi = \int_0^\infty g(\xi) \sum_{\alpha=1}^{\mathrm{N}} w_\alpha \delta_\sigma(\xi, \xi_\alpha)\, d\xi = \sum_{\alpha=1}^{\mathrm{N}} \sum_{\beta=1}^{\mathrm{N}_\alpha} w_\alpha w_{\alpha\beta} g(\xi_{\alpha\beta}). \tag{1.11}$$

1.2.3 Solution of Fokker-Planck model using Beta-EQMOM

Mixing is an important operation in many engineering applications. Consider a scalar of a composition initially at two distinct states. These scalars constituent may be differentiated by different chemical composition, temperature, etc. The ideas of mixing to be discussed in this section, are related to the processes by which these constituents mixed at the molecular level to produce a homogeneous state. Molecular mixing models play an especially important role in describing the evolution of the probability density function of the corresponding scalars. Thus it is essential for these models to be accurate. As an example, in combustion applications, chemical

reactions can only take place when the mixing happens at the molecular level. The term related to transport in composition space due to molecular mixing (micromixing) in evolution equation, appears in unclosed form due to the appearance of the conditional expectation at PDF equation. Evolution equations for such PDFs contain further unknown terms. The micromixing term involves diffusion coefficients and composition gradients, which stem directly from the molecular diffusion term in the instantaneous species conservation equations (Meyer and Jenny, 2013). Since diffusion is important at the small scales of turbulent motion, an accurate representation of these scales is essential to the determination of the evolution of the PDF. Closure approximations constructed to represent the micromixing term must satisfy a number of properties. The most basic requirements are that the approximation leaves the means of the scalars unchanged, i.e. (Launder and Sandham, 2002):

$$\Delta \langle \phi \rangle = \langle \boldsymbol{\phi}(\mathbf{x}, t+\delta t) - \boldsymbol{\phi}(\mathbf{x}, t) \rangle = 0. \tag{1.12}$$

In addition to the general realizability condition for the PDF, $f_\phi(\boldsymbol{\psi}; \mathbf{x}, t) \geq 0$, there are additional conditions to be imposed depending on the properties of the actual scalars being considered. For example, mixing should be local in composition space, and mixing rate should depend on scalar length scales (Fox, 2003; Pope, 2000). a large number of mixing models have been proposed in literature (Curl, 1963; Villermaux and Devillon, 1972; Villermaux and Falk, 1994; Dopazo, 1994; Pope, 2000; Tsai and Fox, 1994, 1995; Fox, 1992b, 1994, 1992a). Tab. 1.1 compares the properties of six mixing models, the modified Curls (MCD) model (Curl, 1963), the interaction by exchange with the mean (IEM) model (Villermaux and Devillon, 1972; Villermaux and Falk, 1994; Dopazo, 1994), the interaction by exchange with the conditional mean (IECM) model (Fox, 2003), the Euclidean minimum spanning tree (EMST) model (Subramaniam and Pope, 1998), and the Fokker-Planck model (FP) model (Fox, 2003). The properties of these models will be briefly summarized in the following sections.

1.2.3.1 Modified Curl model

This method is based on the Curl method (Curl, 1963) which is proposed for coalescence and breakup in a dispersed two-fluid system. In the basic version of the method due to Curl (1963),

Table 1.1: Desirable properties of molecular mixing models, and characteristics of five mixing models with respect to these criteria.

No	Mixing models	MCD	IEM	IECM	EMST	FP
1	Conservation of means	✓	✓	✓	✓	✓
2	Correct decay of variances	✓	✓	✓	✓	✓
3	Localness in composition space	–	–	–	✓	✓
4	Bounded in allowable composition space	✓	✓	✓	✓	✓
5	Turbulent dispersion consistency	–	–	✓	–	✓
6	Relaxation to Gaussian	–	–	–	–	✓
7	Linearity and independence from other scalars	✓	✓	✓	–	✓
8	Differential diffusion	–	–	–	–	✓
9	Dependence on length scales of scalar field	–	–	–	–	–
10	Dependence on Re, Sc, and Da	–	–	–	–	–

the new scalar values of the particles are equal to the mean of the two values before mixing. For the modified Curl model, a few particle pairs are randomly selected from all the particles in a cell, and their individual compositions are moved toward their mean composition. For pair of particles denoted by p and q, compositions are changed as

$$\begin{aligned} \phi^{p,new} &= \phi^p + \frac{1}{2} a \left(\phi^q - \phi^p\right) \\ \phi^{q,new} &= \phi^q + \frac{1}{2} a \left(\phi^p - \phi^q\right), \end{aligned} \tag{1.13}$$

where a is a random number uniformly distributed in $]0,1[$. For the case of decaying scalar in homogeneous turbulence, the PDF relaxes to a bell-shaped distribution. Nooren et al. (1997) developed a version of the model suitable for use in Monte Carlo algorithms employing particles with unequal weights. However, the effect on the PDF introduces a dependency on the distribution of particle weights.

1.2.3.2 IEM model

The IEM model is widely employed in chemical-reaction engineering and computational combustion due to its simple form. It assumes linear relaxation of the scalar towards its mean value (Villermaux and Devillon, 1972; Pope, 2000; Fox, 2003; Choi et al., 2008):

$$\left\langle \Gamma \nabla^2 \phi' | \psi \right\rangle = \frac{1}{2} \frac{\epsilon_\phi}{\langle \phi'^2 \rangle} \left(\langle \phi \rangle - \psi \right). \tag{1.14}$$

In this model all the scalars mix at the same rate because the differential diffusion is not accounted. The most evident consequence of this is that the shape of the PDF remains unchanged in absence of mean gradients, such as in case of homogeneous turbulence. Thus the IEM model cannot represent relaxation of the scalar to a Gaussian form in homogeneous turbulence for an arbitrary initial condition.

1.2.3.3 IECM model

The IECM model differently from the IEM, allows only to the fluid particles with similar position and similar velocity to interact, while IEM model makes an unjustifiable assumption regarding the independence of the scalar mixing term with the velocity field and is inconsistent with local isotropy. On the other hand, conditioning the scalar mean on velocity is consistent with local isotropy and hence corrects the deficiency of the IEM model by performing mixing locally in velocity-physical space.

$$\left\langle \Gamma \nabla^2 \phi' | \mathbf{V}, \psi \right\rangle = \frac{\epsilon_\phi}{2 \left\langle \phi'^2 \right\rangle} \left(\langle \phi | \mathbf{V} \rangle - \psi \right). \tag{1.15}$$

The analysis show that IEM and IECM models yield the same behavior for the mean, and the conditional mean but a different behavior for the variance(Sawford, 2004, 2006; Luhar and Sawford, 2005; Cassiani et al., 2005).

1.2.3.4 EMST model

The Euclidean Minimum Spanning Tree (EMST) mixing model (Subramaniam and Pope, 1998) is a complicated particle interaction model, designed to overcome shortcomings of simpler models such as IEM. EMST is a minimum spanning tree of a set of n points in the plane, where the weight of the edge between each pair of points is the Euclidean distance between those two points. In simpler terms, an EMST connects a set of dots using lines such that the total length of all the lines is minimized and any dot can be reached from any other by following the lines. EMST model possesses the important property that it is local in composition space. It also satisfies the mean conservation and variance decay properties. Boundedness of compositions is preserved by the EMST model. However, this model does not satisfy the independence (the

evolution of the particle property of one scalar should not depend on the properties or statistics of any of the other scalars) and linearity (the set of governing equations for the evolution of scalar fields in turbulence is linear with respect to the scalar fields) properties (Subramaniam and Pope, 1998; Pope, 2013; Zhao et al., 2016; Cao et al., 2007).

1.2.3.5 Fokker-Planck model

The Fokker-Planck (FP) model is an extension of the IEM model (Fox, 1992b, 1999) to include the effect of differential diffusion, which occurs when the molecular diffusivity of the scalar fields are not the same. The idea behind this model is to find the relation between the conditional scalar Laplacian and the conditional scalar dissipation (Pope, 2000):

$$\left\langle \Gamma \nabla^2 \phi' | \psi \right\rangle = \frac{1}{2 f_\phi} \frac{\partial}{\partial \psi} \left(\left\langle \epsilon_\phi | \psi \right\rangle f_\phi \right). \tag{1.16}$$

Unlike the IEM model, implementing the FP model for the micromixing term for the transport equation, the PDF of the inert scalar relaxes to Gaussian form in homogeneous turbulence for an arbitrary initial condition (Fox, 2003). Using this method, all scalars remain in the allowable region as determined by the mixing and chemistry (Fox, 2003).

1.3 Research objectives and approaches

The principal goal of this study is to use quadrature-based moment methods to investigate problems in polydisperse multiphase systems and turbulent reacting flows. The specific research objectives that have been addressed in this study are as follows:

- Formulating an extended quadrature method of moments with log-normal kernel density functions.
- Implementing an extended quadrature method of moments to turbulent mixing problems using the Fokker-Planck model as a closure for micromixing term.
- Implementing the conditional quadrature method of moments to the turbulent reacting problems with different mixing models and reaction types.

- Address the problems with reaction and particle size change.

These specific objects are expressed below in detail.

1.3.1 Implementing the log-normal kernel density function into EQMOM

The evolution of the particle size distribution in polydisperse systems is regulated by the population balance equation (Ramkrishna, 2000). However, the particle size distribution in many systems and multiphase flows can be represented by a log-normal distribution function. Based on this consideration, we propose a variant of the extended quadrature method of moments (Yuan et al., 2012) based on log-normal kernel density functions (Madadi-Kandjani and Passalacqua, 2015). We investigate the property of the method when one or two kernel density functions are used since in these cases an analytical solution can be found to the reconstruction problem. We then validate the method against the rigorous solution of a PBE for aggregation and breakage problems obtained in Vanni (2000), the solution for coalescence and breakup problems presented in Lage (2011), and for the condensation problem examined in Yuan et al. (2012). Results for aggregation and breakage problems are compared also to the QMOM results reported in Marchisio et al. (2003b). The topic is discussed in detail in Chap. 2 of this report.

1.3.2 Solution of Fokker-Planck equation with EQMOM for turbulent mixing flows

An extended quadrature-based moment method (EQMOM) (Yuan et al., 2012; Chalons et al., 2010) is used to close the transport equation for the composition PDF. The β kernel density function is used for EQMOM since the scalar composition is represented by a scalar bounded between -1 and 1. The direct numerical simulations (DNS) of Eswaran and Pope (1988), and the amplitude mapping closure (AMC) of Pope (1991) are taken as reference solutions to establish the accuracy of the FP model in the case of binary mixing. The DNS of Juneja and Pope (1996) is used to validate the results obtained for ternary mixing. Simulations are performed with both the conditional scalar dissipation rate (CSDR) proposed by Fox (2003) and the CSDR from AMC. The shape of the PDF, important in turbulent mixing problems, is later demonstrated. The topic is discussed in detail in Chap. 3 of this report.

1.3.3 A quadrature-based CFD model for turbulent reacting flows

In previous studies (Marchisio and Fox, 2005), direct quadrature method of moments (DQMOM) is used to find the solution of the evolution equation of the composition PDF for reactive mixing flows. In this method the discrete representation of the PDF was used to derive the transport equation for the quadrature weights and weighted abscissae. However, this method is affected by shortcomings related to the conservation of moments due to the fact that weights and abscissae are not conserved quantities to transport (Yuan et al., 2012). To overcome this limitation, we use the conditional quadrature method of moments introduce by Yuan and Fox (2011) to find the solution of the evolution composition PDF. In this method, a moment-inversion algorithm based on the adaptive quadrature of conditional composition moments is used to approximate the continuous distributions. In this study, IEM and FP models are used to close the micromixing term in the joint composition PDF transport equation.
One of the shortcoming of DQMOM approach is that it introduces correction terms to the transport equations. CQMOM does not introduce these correction terms, and the optimal moments (Fox, 2009) are transported directly rather than as weights and weighted abscissas. Here, different reaction systems are considered and modeled using DQMOM and CQMOM to compare the statistical errors and computational costs of each method. The CQMOM formulation results in a robust solution algorithm for the PDF transport equation with a similar computational cost by avoiding the potentially singular correction terms arising in DQMOM (Akroyd et al., 2010). The topic is discussed in detail in Chap. 4 of this report.

1.3.4 CQMOM for turbulent mixing coupled to a population balance equation

A conditional quadrature method of moments (CQMOM) was developed in this work to solve turbulent mixing problems associated with population balance equations (PBE) by approximating the evolution equation of the composition probability density function (PDF) for the moments of the PBE. The Interaction-by-Exchange-with-the-Mean (IEM) model was used to close the PDF evolution equation. The new CQMOM methodology was coupled to a quadrature-based PBE solver. The two procedures were implemented into the OpenQBMM® framework,

which leverages the OpenFOAM® CFD toolbox. The CQMOM approach for mixing problems was first tested considering two consecutive competitive reactions to verify the implementation and validate the proposed approach. The coupled turbulent mixing-PBE approach was then used to investigate polymer aggregation in a multi-inlet vortex reactor (MIVR). Results showing the predicted mixture fraction, reactant and product concentration fields are shown. The topic is described in detail in Chap. 5.

1.4 Accomplishment and future works

Tab. 1.2 presents the completed tasks with objectives.

1.5 Outline

The outline of this report is as follows. In Chap. 2 the formulation and the implementation of log-normal kernel density function into an extended quadrature method of moments is described. In Chap. 3, an extended quadrature method of moments with β kernel density function is applied to solve the joint composition PDF for a mixing of a univariate passive scalar. The Fokker-Planck model is used to close the micromixing term for the composition PDF transport equation. In Chap. 4, the new model based on the conditional quadrature method of moments(CQMOM) and direct quadrature method of moments (DQMOM) for single phase reacting flows is presented. In Chap. 5, result for coupled mixing-PBE approach to investigate polymer aggregation in a multi-inlet vortex reactor (MIVR) is presented. Finally in Chap. 6 the summary of the performed work is presented.

Table 1.2: Accomplishments corresponding to research objectives

Objectives	**Results**	**Conclusions**
LnEQMOM	i) Implementing the log-normal kernel density function into EQMOM. ii) Introducing the adopted Hermite quadrature to calculate secondary quadrature. iii) Introducing Stieltjes-Wigert quadrature to calculate secondary quadrature. iv) Compare results obtained with LnEQMOM with analytical solution for combination of two log-normal distribution. v) Implement the LnEQMOM to the problems with aggregation and breakup for particles. vi) Compare the solution of LnEQMOM with two analytically known problems (*e.g.* coalescence and condensation).	i) LnEQMOM predicts the zero order moment and mean particle size accurately for aggregation and breakup of particles, using low number of primary quadrature nodes. ii) LnEQMOM provides more accurate results than QMOM. iii) Due to the functional form of the log-normal kernel density function, it shows some difficulties on reconstructing the distribution when the distribution is non-zero at $\xi \to 0$. iv) LnEQMOM is more robust compare to the Γ EQMOM due to the structure of the system of equations it uses during the numerical procedure.
EQMOM-FP	i) Implementing the β-EQMOM into joint composition PDF with Fokker-Planck closure for micromixing term. ii) Validate the algorithm for univariate passive scalar case in a similar condition to those obtained by direct numerical simulations.	i) There is a satisfactory agreement between the results obtained by EQMOM-FP with those obtained by DNS. ii) In all the cases under consideration the PDF evolves with time and finally it relaxes ro the gaussian distribution at the mean value.

Table 1.2: (continued)

Objectives	**Results**	**Conclusions**
EQMOM-FP	iii) Validate the algorithm for cases with initial three delta functions and compare the results to those obtained by DNS for ternary mixing. iv) Calculate the steady state solution for joint composition PDF.	iii) Conditional scalar dissipation rate has significant effect on predicting the shape of the PDF and simple CSDR provides comparable results than complicated models. iv) The steady state solution results in a β distribution for the PDF.
DQMOM-IEM	i) Obtain the closure quantities of DQMOM for mixing with two competitive consecutive reactions.	i) In all the cases under consideration DQMOM for joint composition PDF predicts the physics of problem in a fare manner. ii) DQMOM has some instabilities during the solution. iii) In DQMOM, transport equations for weights and abscissae are calculated while they are not a conservative quantities.
CQMOM modeling approach for mixing and reaction problem	i) Implementation of CQMOM for mixing and reacting problem.	i) CQMOM transports conserved quantities (moments). ii) It is faster compare to DQMOM running the same cases in the same machine.

Table 1.2: (continued)

Objectives	**Results**	**Conclusions**
EQMOM-FP	i) Couple the mixing and conditional-based PBE for flash nanoprecepitation ii) Investigate polymer aggregation in a multi-inlet vortex reactor. iii) In solving the PBE, challenging part is the computational expenses (As an example considering 50 polymers and 300 organic particles, one should solve 15000 equations.)	i) Conditional quadrature-based population balance equation is chosen since using only 8 equations, one can find the solution of the PBE for the polymers and organics. ii) The mixing weights and abscissae which represent the environments are as first solved. These quantities are then used to find the source terms for the transported PBE equations. iii) This approach doesn't provide a correct answer when the mixture fraction is 0.5 and difference between two mixture abscissae becomes zero.

CHAPTER 2. EXTENDED QUADRATURE-BASED MOMENT METHOD WITH LOG-NORMAL KERNEL DENSITY FUNCTIONS

This chapter was published as a journal article titled "An extended quadrature-based moment method with log-normal kernel density functions" in *Chemical Engineering Science* with authors E. Madadi-Kandjani and A. Passalacqua (2015).

Abstract

An extended quadrature method of moments (EQMOM) with log-normal kernel density functions is developed in this work, and applied to the solution of a population balance equation (PBE) for aggregation and breakup, coalescence, and condensation problems. The cases with one and two kernel density functions are studied analytically, and the existence of an analytical solution is shown. A numerical procedure based on the work of Yuan et al. (2012) is adopted to address cases with a larger number of kernel density functions. Results for the reconstructed number density function (NDF), the time evolution of the zero-order moment and of the mean particle size are compared with those obtained from the rigorous solution of the PBE reported by Vanni (2000) for the cases of aggregation and breakup. A problem concerning coalescence and one regarding condensation, both with analytical solution, are also examined. The results obtained with the proposed approach are compared to those provided by EQMOM with gamma kernel densities. Satisfactory results were obtained for the reconstructed distribution. Excellent agreement was observed between the rigorous solution and the approximated one for the time evolution of the total number density and the mean particle size.

2.1 Introduction

Numerous environmental, biological, medical, and technological systems involve discrete populations of particles, whose properties evolve in space and time due to continuous phenomena, such as convection and diffusion, and discontinuous phenomena, such as aggregation, breakup, nucleation, evaporation, coalescence. Notable examples are polymerization processes, dispersion of aerosols in the atmosphere, chemical reactions involving precipitation of particles, bubble column reactors, processes for the production of pharmaceuticals. The evolution of the particle population in these systems is modeled by means of a population balance equation (PBE) (Ramkrishna, 2000), which is an integro-differential equation, whose unknown is the number density function (NDF) associated to the particle population. This NDF depends, in general, on time, on a set of external coordinates, representing the spatial location, and on a set of internal coordinates, which characterize the particle properties.

In this work we concentrate on the case of a NDF with only one internal coordinate, representing the particle size. Numerous methods were developed to solve this type of equation. Hounslow et al. (1988); Hounslow (1990); Kumar and Ramkrishna (1996a,b); Puel et al. (2003); Bannari et al. (2008); Becker et al. (2011); Balakin et al. (2014) used the method of classes, which consists in discretizing the NDF with respect to the internal coordinate using a discrete number of bins (classes). Zero-order class methods assume a uniform distribution for each bin (Vanni, 2000), while high-order class methods adopt a pre-defined functional form of the distribution for each class (Muhr et al., 1996). Bove et al. (2005) developed the parallel parent and daughter class (PPDC) approach for aggregation and breakup problems. Alopaeus et al. (2006) developed a high-order moment-conserving class method to overcome the limitations of traditional class methods (Hounslow et al., 1988; Hounslow, 1990; Kumar and Ramkrishna, 1996a,b), which conserve only two moments in the discrete solution for the PBE for agglomeration and breakup. This approach was combined with a reconstruction procedure of the NDF by Alopaeus et al. (2008).

The method of classes, while intuitive and accurate, is computationally intensive due to the large number of classes required to properly discretize the NDF (Marchisio et al., 2003b). Rosner

and Yu (2001); Lin et al. (2002); Smith and Matsoukas (1998); Meimaroglou and Kiparissides (2007); Zhao et al. (2007); Zhao and Zheng (2013) used Monte Carlo methods to tackle the PBE. Hulburt and Katz (1964) solved the PBE with the standard method of moments (SMM), accurately predicting the evolution of the NDF with size-independent growth rate, aggregation and breakup terms.

A successful approach to find an approximate solution to population balance equations is the quadrature method of moments (QMOM) proposed by McGraw (1997) for aerosol applications, and extensively used in typical applications of chemical engineering (Marchisio and Fox, 2013). In this approach the NDF is represented by a weighted summation of Dirac delta functions, which is uniquely defined by the set of moments (Gordon, 1968; Wheeler, 1974).

The discrete representation of the NDF was used in the direct quadrature method of moments (DQMOM) (Marchisio and Fox, 2005) to derive transport equations for the quadrature weights and abscissae. However, shortcomings related to the conservation of moments affect the DQMOM approach, due to the fact that weights and abscissae are not conserved quantities, as mentioned in Yuan et al. (2012).

The accuracy of QMOM, DQMOM and PPDC were compared by Silva et al. (2010), who concluded that QMOM and DQMOM show similar accuracy in the aggregation and breakup problems considered in their work, while the PPDC approach showed convegence difficulties and its accuracy was not adequate.

In general, a method relying on a discrete representation of the NDF is also affected by limitations that become particularly relevant in some classes of problems. For example, some evaporation problems (Fox et al., 2008; Yuan et al., 2012) require the value of the NDF for null internal coordinate to be known, which is not the case if the QMOM discretization of the NDF is used. This challenge can only be effectively overcome with methods that rely on a continuous representation of the distribution function. One of these methods is the entropy maximization approach (Mead and Papanicolaou, 1984; Tagliani, 1999), which however is ill-posed for certain classes of problems (Massot et al., 2010; Yuan et al., 2012), and difficult to extend to cases involving a multivariate NDF (Yuan et al., 2012).

An alternative method was proposed by Athanassoulis and Gavriliadis (2002), who introduced the idea of reconstructing the NDF as a finite superposition of kernel density functions. Important advantages of this approach are that it ensures positivity of the reconstructed NDF, and it converges to the exact NDF when the number of kernel density functions used in the reconstruction is increased (Athanassoulis and Gavriliadis, 2002). The approach of Athanassoulis and Gavriliadis (2002), however, relies on the solution of a minimization problem, which only guarantees that some of the low-order moments are exactly preserved (Yuan et al., 2012). In order to overcome this limitation, Chalons et al. (2010); Yuan et al. (2012) introduced an extended quadrature method of moments (EQMOM), where continuous non-negative kernel density functions are used in place of Dirac delta functions, when approximating the NDF. This allows an approximate continuous distribution function to be determined from the transported moments. Additionally, the EQMOM procedure ensures that the reconstructed NDF preserves all the moments used for its reconstruction. The approximated NDF obtained with EQMOM can then be used to integrate the source terms in the population balance equation in a more accurate manner (Marchisio and Fox, 2013). Chalons et al. (2010) formulated the method using Gaussian kernel density functions, while Yuan et al. (2012) used beta and gamma density functions.

The present work proposes an extended quadrature method of moments using log-normal kernel density functions. Log-normal distribution functions are frequently encountered in many geological, medical, environmental (Limpert et al., 2001) and industrial (Randolph and Larson, 1988; Petitti et al., 2010; Capecelatro et al., 2014) applications involving particles, bubbles and droplets. As a consequence, being able to use log-normal kernel density functions may improve the efficiency of the EQMOM procedure in cases where distributions are nearly log-normal, reducing the number of kernel density functions required to achieve a satisfactory reconstruction. Additionally, it will be illustrated that the structure of the system of equations to be solved in the EQMOM procedure is particularly simple when log-normal kernel density functions are chosen. The cases with one and two kernel density functions are studied analytically. The existence of a solution to the moment inversion and reconstruction problem is shown for these cases. The problem of moment realizability is studied for the case with two kernel density

functions. The proposed procedure is then tested considering cases involving aggregation and breakup (Vanni, 2000), coalescence and breakup, and condensation (Lage, 2011; Yuan et al., 2012). The effect of time integration on the accuracy of the steady-state reconstructed distribution was investigated for the cases where the rigorous solution of the PBE was available in the literature (Vanni, 2000). This was achieved by numerically integrating the NDF obtained from the rigorous solution of the PBE to compute its moments, and using these moments to perform the EQMOM reconstruction.

The remainder of the article is structured as follows: Sec. 2.2 briefly summarizes the theory of population balance equations, while Sec. 2.3 introduces the details of EQMOM and focuses on formulating the extended quadrature method of moments with log-normal kernel density functions (LnEQMOM). In particular, analytical solutions for the case with one and two quadrature nodes are discussed, and a numerical solution procedure (Yuan et al., 2012) is illustrated for the general case with N kernel density functions. Finally, Sec. 2.4 illustrates a verification study performed on the proposed procedure, presents the results concerning the solution of the PBE, and discusses the problem of moment realizability for the EQMOM procedure with two log-normal kernel density functions.

2.2 PBE for aggregation and breakup problem

The population balance equation (Ramkrishna, 2000; Vanni, 2000) accounting for the evolution of the number density function only due to birth and death of particles can be written as

$$\frac{\partial n\left(\xi,\mathbf{x},t\right)}{\partial t}=\bar{B}\left(\xi,\mathbf{x},t\right)-\bar{D}\left(\xi,\mathbf{x},t\right), \tag{2.1}$$

where $n(\xi,\mathbf{x},t)$ is the number density function, depending on the single internal coordinate ξ, while $\bar{B}\left(\xi,\mathbf{x},t\right)$ and $\bar{D}\left(\xi,\mathbf{x},t\right)$ are, respectively, the rate of change of n due to birth and death. The internal coordinate ξ represents a characteristic dimension of the particle (diameter, volume, ...). The specific meaning will be clarified for each case. Both these terms are usually decomposed in the algebraic sum of the contributions due to aggregation and breakup to birth and death of particles of a given size, leading to

$$\frac{\partial n\left(\xi,\mathbf{x},t\right)}{\partial t}=\bar{B}^{a}\left(\xi,\mathbf{x},t\right)-\bar{D}^{a}\left(\xi,\mathbf{x},t\right)+\bar{B}^{b}\left(\xi,\mathbf{x},t\right)-\bar{D}^{b}\left(\xi,\mathbf{x},t\right). \tag{2.2}$$

It is worth noting that the internal coordinate ξ represents a characteristic property of the particle related to its size, such as the particle diameter or its mass. We will consider ξ as the particle size in the aggregation and breakup problems, while ξ will represent the particle mass in the two problems concerning coalescence and condensation considered in this work. According to previous studies (Randolph and Larson, 1988; Marchisio et al., 2003b; Marchisio and Fox, 2013), these terms can be written in a continuous form for a homogeneous system as:

$$\bar{B}^a\left(\xi,\mathbf{x},t\right)=\frac{\xi^2}{2}\int_0^{\xi}\frac{\beta\left(\left(\xi^3-\xi'^3\right)^{1/3},\xi'\right)}{\left(\xi^3-\xi'^3\right)^{2/3}}n\left(\left(\xi^3-\xi'^3\right)^{1/3},\mathbf{x},t\right)n\left(\xi',\mathbf{x},t\right)\mathrm{d}\xi', \tag{2.3}$$

$$\bar{D}^a\left(\xi,x,t\right)=n\left(\xi,\mathbf{x},t\right)\int_0^{\infty}\beta\left(\xi,\xi'\right)n\left(\xi',\mathbf{x},t\right)d\xi', \tag{2.4}$$

$$\bar{B}^b\left(\xi,\mathbf{x},t\right)=\int_{\xi}^{\infty}a\left(\xi'\right)b\left(\xi|\xi'\right)n\left(\xi',\mathbf{x},t\right)\mathrm{d}\xi', \tag{2.5}$$

$$\bar{D}^b\left(\xi,\mathbf{x},t\right)=a\left(\xi\right)n\left(\xi,\mathbf{x},t\right). \tag{2.6}$$

The aggregation kernel β describes the probability of particles to aggregate, and can be expressed as a product of the collision frequency and the aggregation efficiency, $a\left(\xi\right)$ is the breakup kernel and $b\left(\xi|\xi'\right)$ is the fragmentation distribution function that contains information on the fragments produced by a breakup event (Marchisio et al., 2003b). The reader interested in how to derive Eqs. 2.3 – 2.6 can refer to Marchisio et al. (2003b) for further details.

2.3 The extended quadrature method of moments

The solution of the PBE with the extended quadrature method of moments requires moment transport equations to be obtained from Eq. 2.2. This is achieved by applying of the definition of the moment of order k of the NDF

$$M_k(t)=\int_0^{\infty}n\left(\xi,\mathbf{x},t\right)\xi^k\mathrm{d}\xi \tag{2.7}$$

to each side of the PBE (Eq. 2.2), leading to

$$\frac{\partial M_k\left(\mathbf{x},t\right)}{\partial t}=\bar{B}_k^a\left(\mathbf{x},t\right)-\bar{D}_k^a\left(\mathbf{x},t\right)+\bar{B}_k^b\left(\mathbf{x},t\right)-\bar{D}_k^b\left(\mathbf{x},t\right). \tag{2.8}$$

The source terms due to birth and death as a consequence of aggregation and breakup phenomena are defined as the moments of the source terms in the original PBE, as follows:

$$\begin{aligned}
\bar{B}_k^a(\mathbf{x},t) &= \frac{1}{2}\int_0^\infty n(\xi',\mathbf{x},t)\int_0^\infty \beta(\xi,\xi')\left(\xi^3+\xi'^3\right)^{k/3} n(\xi,\mathbf{x},t)\,\mathrm{d}\xi\mathrm{d}\xi', \\
\bar{D}_k^a(\mathbf{x},t) &= \int_0^\infty \xi^k n(\xi,\mathbf{x},t)\int_0^\infty \beta(\xi,\xi')\, n(\xi',\mathbf{x},t)\,\mathrm{d}\xi'\mathrm{d}\xi, \\
\bar{B}_k^b(\mathbf{x},t) &= \int_0^\infty \xi^k \int_0^\infty a(\xi')\, b(\xi|\xi')\, n(\xi',\mathbf{x},t)\,\mathrm{d}\xi'\mathrm{d}\xi, \\
\bar{D}_k^b(\mathbf{x},t) &= \int_0^\infty \xi^k a(\xi)\, n(\xi,\mathbf{x},t)\,\mathrm{d}\xi.
\end{aligned} \tag{2.9}$$

The evaluation of the integrals in Eq. 2.9 requires the knowledge of the NDF, in addition to the kernel functions a and β. However, the NDF is not known a priori, and has to be approximated from the transported moments.

Following the procedure described in Yuan et al. (2012), we choose to approximate the NDF with a weighted sum of non-negative kernel density functions $\delta_\sigma(\xi,\xi_\alpha)$

$$n(\xi) \approx p_{\mathrm{N}}(\xi) = \sum_{\alpha=1}^{\mathrm{N}} w_\alpha \delta_\sigma(\xi,\xi_\alpha), \tag{2.10}$$

where w_α are the non-negative weights of each kernel density function, ξ_α are the corresponding quadrature abscissae, and N is the number of kernel density functions used to approximate the NDF. Since the particle size is a positive, real number, the support of the kernel density function δ_σ is chosen to be the whole real positive axis $\mathbb{R}^+$.

The approximation introduced with Eq. 2.10 allows the calculation of the integrals that appear in the source terms of Eq. 2.9 to be carried out. After substituting the equation for $p_{\mathrm{N}}(\xi)$, and approximating the integrals with quadrature formulae, the following expression is obtained (Yuan et al., 2012):

$$\int_0^\infty g(\xi)\, p_{\mathrm{N}}(\xi)\,\mathrm{d}\xi = \int_0^\infty g(\xi)\sum_{\alpha=1}^{\mathrm{N}} w_\alpha \delta_\sigma(\xi,\xi_\alpha)\,d\xi = \sum_{\alpha=1}^{\mathrm{N}}\sum_{\beta=1}^{\mathrm{N}_\alpha} w_\alpha w_{\alpha\beta} g(\xi_{\alpha\beta}). \tag{2.11}$$

The N *primary* weights w_α, the corresponding primary abscissae ξ_α, together with the parameter σ are determined from the first $2\mathrm{N}+1$ integer moments of the NDF, as illustrated in Sec. 2.3.1. The N_α quantities $w_{\alpha\beta}$ and $\xi_{\alpha\beta}$, called *secondary* weights and abscissae, are computed using the standard Gaussian quadrature formulae for known orthogonal polynomials

to the kernel NDF. This allows each kernel density function to be evaluated at an arbitrary number of points, depending on the desired level of accuracy.

Introducing the approximated integrals of the source terms into Eq. 2.9 leads to the following semi-discrete form of the moment transport equations:

$$\frac{\partial M_k}{\partial t} = \frac{1}{2}\sum_{\alpha_1=1}^{\mathrm{N}}\sum_{\beta_1=1}^{\mathrm{N}_\alpha} w_{\alpha_1} w_{\alpha_1\beta_1} \sum_{\alpha_2=1}^{\mathrm{N}}\sum_{\beta_2=1}^{\mathrm{N}_\alpha} w_{\alpha_2} w_{\alpha_2\beta_2} \left(\xi^3_{\alpha_1\beta_1} + \xi^3_{\alpha_2\beta_2}\right)^{k/3} \beta_{\alpha_1\beta_1\alpha_2\beta_2} - \sum_{\alpha_1=1}^{\mathrm{N}}\sum_{\beta_1=1}^{\mathrm{N}_\alpha} \xi^k_{\alpha_1\beta_1} w_{\alpha_1} w_{\alpha_1\beta_1} \sum_{\alpha_2=1}^{\mathrm{N}}\sum_{\beta_2=1}^{\mathrm{N}_\alpha} w_{\alpha_2} w_{\alpha_2\beta_2} \beta_{\alpha_1\beta_1\alpha_2\beta_2} + \sum_{\alpha=1}^{\mathrm{N}}\sum_{\beta=1}^{\mathrm{N}_\alpha} a_{\alpha\beta}\bar{b}^k_{\alpha\beta} w_{\alpha\beta} - \sum_{\alpha=1}^{\mathrm{N}}\sum_{\beta=1}^{\mathrm{N}_\alpha} \xi^k_{\alpha\beta} a_{\alpha\beta} w_{\alpha\beta}. \quad (2.12)$$

2.3.1 The EQMOM numerical procedure

The numerical procedure to solve Eq. 2.12 is illustrated in this section. The starting point to define the EQMOM numerical solution procedure is to choose the functional form of the kernel density function. The choice is made based on the support of the NDF that has to be reconstructed. In other words, if the reconstructed NDF has support $\mathbb{R}$, Gaussian kernel functions may be used, while if the support is $\mathbb{R}_0^+$, gamma or log-normal kernel functions can be chosen. Beta kernel functions are suitable to reconstruct an NDF with bounded support (Yuan et al., 2012). As we mentioned in the introduction, we deal with the log-normal kernel density function in this work, which we write as

$$\delta_\sigma(\xi,\mu) = \frac{1}{\xi\sigma\sqrt{2\pi}}\, \mathrm{e}^{-\frac{(\ln\xi-\mu)^2}{2\sigma^2}}, \quad \xi,\sigma\in\mathbb{R}^+, \mu\in\mathbb{R}. \quad (2.13)$$

The integer moment of order k of the log-normal distribution can be found analytically using the Mellin transform, leading to (Magnus et al., 1966):

$$M_k(\mu,\sigma) = \mathrm{e}^{k\mu+\frac{k^2\sigma^2}{2}}. \quad (2.14)$$

2.3.2 The one-node case

The case when only one kernel density function is used is trivial, and an analytical solution can be found for σ. To this purpose, it suffices to consider the first three moments of the NDF

$\{M_0, M_1, M_2\}$, and impose that the moments of the approximated NDF

$$p_1(\xi) = w_1 \delta_\sigma(\xi, \xi_1) = \frac{w_1}{\xi\sigma\sqrt{2\pi}} \, \mathrm{e}^{-\frac{(\ln\xi - \xi_1)^2}{2\sigma^2}} \tag{2.15}$$

are equal. This leads to the following non-linear system of equations:

$$\begin{cases} M_0 = w_1 \\ M_1 = w_1 \, \mathrm{e}^{\xi_1 + \sigma^2/2} \\ M_2 = w_1 \, \mathrm{e}^{2\xi_1 + 2\sigma^2} \end{cases}, \tag{2.16}$$

which can be solved analytically by setting $z = \mathrm{e}^{\sigma^2/2}$, and $\chi_1 = \mathrm{e}^{\xi_1}$. Eliminating w_1 and ξ_1, and taking the only positive z root leads to:

$$z = \frac{1}{M_1}\sqrt{M_0 M_2} \Rightarrow \sigma^2 = 2\ln\left(\frac{1}{M_1}\sqrt{M_0 M_2}\right), \tag{2.17}$$

which is always defined because the moments of the NDF are strictly positive. The complete solution for the one-node case is then:

$$\begin{cases} w_1 = M_0 \\ \xi_1 = \ln \dfrac{M_1^2}{M_0\sqrt{M_0 M_1}} \\ \sigma = \sqrt{2\ln\left(\dfrac{1}{M_1}\sqrt{M_0 M_2}\right)} \end{cases}. \tag{2.18}$$

2.3.3 The two-node case

The two-node case is obtained when two kernel density functions are used to approximate the NDF. Following Chalons et al. (2010), the approximated NDF is written as:

$$p_2(\xi) = w_1 \delta_\sigma(\xi, \xi_1) + w_2 \delta_\sigma(\xi, \xi_2) = \frac{w_1}{\xi\sigma\sqrt{2\pi}} \, \mathrm{e}^{-\frac{(\ln\xi - \xi_1)^2}{2\sigma^2}} + \frac{w_2}{\xi\sigma\sqrt{2\pi}} \, \mathrm{e}^{-\frac{(\ln\xi - \xi_2)^2}{2\sigma^2}}. \tag{2.19}$$

It is worth reminding at this time that the parameter σ is assumed to be the same for both the kernel density functions, in order to obtain a single non-linear equation for σ, rather than a system of non-linear equations, which would significantly increase the complexity of the problem (Chalons et al., 2010; Yuan et al., 2012). The effect of this assumption on the accuracy of the reconstructed NDF is shown in Sec. 2.4.1.

The following non-linear system of equations is found imposing that the first five transported moments are exactly represented by the approximated NDF (Chalons et al., 2010):

$$\begin{cases} M_0 = w_1 + w_2 \\ M_1 = w_1\, \mathrm{e}^{\xi_1+\sigma^2/2} + w_2\, \mathrm{e}^{\xi_2+\sigma^2/2} \\ M_2 = w_1\, \mathrm{e}^{2(\xi_1+\sigma^2)} + w_2\, \mathrm{e}^{2(\xi_2+\sigma^2)} \\ M_3 = w_1\, \mathrm{e}^{3\xi_1+9/2\sigma^2} + w_2\, \mathrm{e}^{3\xi_2+9/2\sigma^2} \\ M_4 = w_1\, \mathrm{e}^{4\xi_1+8\sigma^2} + w_2\, \mathrm{e}^{4\xi_2+8\sigma^2}\,. \end{cases} \tag{2.20}$$

Setting

$$z = \mathrm{e}^{\sigma^2/2}, \chi_1 = \mathrm{e}^{\xi_1}, \chi_2 = \mathrm{e}^{\xi_2} \tag{2.21}$$

leads to

$$\begin{cases} M_0 = w_1 + w_2 = M_0^* \\ M_1 = z\,(w_1\chi_1 + w_2\chi_2) = zM_1^* \\ M_2 = z^4\left(w_1\chi_1^2 + w_2\chi_2^2\right) = z^4 M_2^* \\ M_3 = z^9\left(w_1\chi_1^3 + w_2\chi_2^3\right) = z^9 M_3^* \\ M_4 = z^{16}\left(w_1\chi_1^4 + w_2\chi_2^4\right) = z^{16} M_4^*. \end{cases} \tag{2.22}$$

It is immediately apparent that Eq. 2.22, which relates the transported moments M_k to the moments of the approximated NDF M_k^*, shows a simpler structure than the corresponding system for EQMOM based on gamma kernel densities (Yuan et al., 2012). In particular, the system of equations in Eq. 2.22 is diagonal, while the one for gamma EQMOM is lower-triangular, as described in Yuan et al. (2012). This property is also maintained for the cases with N > 2.

Eliminating w_1, ξ_1, w_2, ξ_2 from Eq. 2.22, the following polynomial equation is found:

$$f(z) = M_2^3 z^8 - 2M_1M_2M_3z^6 + \left(M_0M_3^2 + M_1^2M_4\right)z^2 - M_0M_2M_4 = 0. \tag{2.23}$$

Recalling that all the moments of our NDF are positive quantities, the application of Descartes rule of signs shows that this polynomial equation has a maximum of three positive real roots and of three negative roots.

We now show that at least a positive real root σ exists for Eq. 2.23, if the moments are positive. To this purpose, we observe that the coefficient of the leading power of the polynomial in Eq. 2.23 is positive because $M_2 > 0$. This implies that $\lim_{z\to+\infty} f(z) = +\infty$. We also note that $f(z=0) = -M_0 M_2 M_4 < 0$. As a consequence, because $f \in C^0(\mathbb{R})$, we conclude that at least one value of $z \in \mathbb{R}^+$ so that $f(z) = 0$.

We also observe that, in general, it is not possible to show that such a root is unique, as discussed before. Only additional constraints on the moment realizability may further limit the number of real roots. Analytical expressions for the real roots of Eq. 2.23 can be found by solving Eq. 2.23, and obtaining the corresponding square roots of the result. However, the complexity of the expressions obtained with this procedure makes them unpractical, and a numerical solution is favored in this work, as illustrated for the general case in Sec. 2.3.4.

2.3.4 The general case

The general case with N kernel density functions is treated in the same way illustrated for the two-node case. An equation for z is found imposing that the first $2\mathrm{N}+1$ moments are exactly represented by the approximated NDF, leading to the polynomial expression

$$J_{2\mathrm{N}}(z) = M_{2\mathrm{N}} - z^{(2\mathrm{N})^2} M^*_{2\mathrm{N}}, \tag{2.24}$$

where

$$M^*_{2\mathrm{N}} = \sum_{\alpha=1}^{\mathrm{N}} w_\alpha \chi_\alpha^{2\mathrm{N}}. \tag{2.25}$$

It is worth noting that the $2\mathrm{N}+1$ equations are coupled, since the values of both w_α and χ_α depend on z. Such system can be solved iteratively as illustrated in Yuan et al. (2012), and briefly summarized below:

i) Guess σ, and compute the corresponding value of $z = \mathrm{e}^{\sigma^2/2}$.

ii) Compute $M^*_k = M_k z^{-(2k)^2}, k = 0, \ldots, 2\mathrm{N}-1$ moments, using the guessed value for z.

iii) Apply the Wheeler algorithm (Wheeler, 1974) to the first 2N M^* moments to obtain the weights w_α and the abscissae χ_α.

iv) Compute M^*_{2N} with the new values of weights and abscissae.

v) Construct the $J(z)$ function, and determine z with a bounded numerical root finding procedure.

vi) Repeat from ii) until $|J(z)| < \varepsilon$, with ε a small value close to machine precision.

Gaussian quadrature formulae with log-normal weight function can be computed with two approaches, which we briefly summarize in A, referring the interested reader to Weisstein (1998); Wilck (2001); Gautschi (2004) for further details. We compared the numerical results obtained with both Hermite and Stieltjes-Wigert quadrature formulae (comparison not reported here), and we did not find significant differences for the cases discussed in this work. As a consequence, we used Hermite quadrature to approximate the integrals in the source terms of the PBE. This choice also makes the numerical procedure more efficient, because the algorithm to compute Hermite quadrature weights and nodes does not involve the parameter σ, as opposed to the one for the Stieltjes-Wigert quadrature.

2.4 Results and discussion

2.4.1 Verification of the Ln-EQMOM implementation

We verify the numerical procedure to reconstruct the NDF with LnEQMOM by considering a distribution obtained as a linear combination of two log-normal distributions with different parameters μ and σ. The functional form of this distribution is shown in Eq. 2.26

$$f(x) = \frac{1}{2}\left[\frac{1}{x\sigma_1\sqrt{2\pi}}\,\mathrm{e}^{-\frac{(\ln x-\mu_1)^2}{2\sigma_1^2}} + \frac{1}{x\sigma_2\sqrt{2\pi}}\,\mathrm{e}^{-\frac{(\ln x-\mu_2)^2}{2\sigma_2^2}}\right], \tag{2.26}$$

while the values of the parameters used in each case are summarized in Tab. 2.1. The reconstructed distributions obtained with four-node LnEQMOM are reported in Fig. 2.1. As expected, the reconstruction obtained in case 1 exactly matches the analytical solution, because the exact distribution is log-normal. We observe that, in general, the reconstructed distribution agrees well with the analytical function. However, as it is clear from Fig. 2.1(d), the agreement deteriorates for increasingly different values of the parameter σ. This is a consequence of

Table 2.1: Parameters used in the cases concerning the linear combination of two log-normal distributions.

Case	μ_1	σ_1	μ_2	σ_2
1	3	0.6	3	0.6
2	1.2	0.6	3	0.6
3	3	0.6	5	0.5
4	3	0.6	1	0.8

the assumption that the kernel density functions used to define the approximated distribution (Eq. 2.10) share the same value of σ.

We first verify that the moments of the reconstructed distributions match the moments of the analytical one. To this purpose, we consider the relative error affecting the moments, defined as

$$E_i = \left| \frac{M_{i,\text{analytical}} - M_{i,\text{reconstruction}}}{M_{i,\text{analytical}}} \right|. \tag{2.27}$$

As shown in Tab. 2.2, the first $2\text{N} + 1$ moments are preserved by EQMOM with errors of the order of $1.0 \cdot 10^{-16}$ for cases 1 – 3, and with errors of the order of $1.0 \cdot 10^{-12}$ for case 4. We then consider the L^2 norm of the difference between the analytical distribution function and the approximated one, normalized with respect to M_0:

$$d = \frac{||f(\xi) - p(\xi)||_2}{M_0}. \tag{2.28}$$

As shown in Tab. 2.3, d is between $6.04 \cdot 10^{-16}(\text{N} = 4)$ and $1.90 \cdot 10^{-13}(\text{N} = 2)$ for case 1, when the analytical distribution is itself log-normal. The error is between $3.90 \cdot 10^{-14}(\text{N} = 4)$ and $2.88 \cdot 10^{-12}(\text{N} = 2)$ in case 2, when $\sigma_1 = \sigma_2$, with different values of μ_1 and μ_2. However, a significantly larger error (order between 10^{-3} and 10^{-1}) is observed when different values of σ_1 and σ_2 are chosen. We can also observe that the error increases when the difference between σ_1 and σ_2 increases, as expected as a consequence of the assumption that kernel densities share the same value of σ. Finally, we notice that increasing the number of primary quadrature nodes from two to four reduces the relative error of one order of magnitude in cases 1 – 3, but only marginally affects the error in case 4.

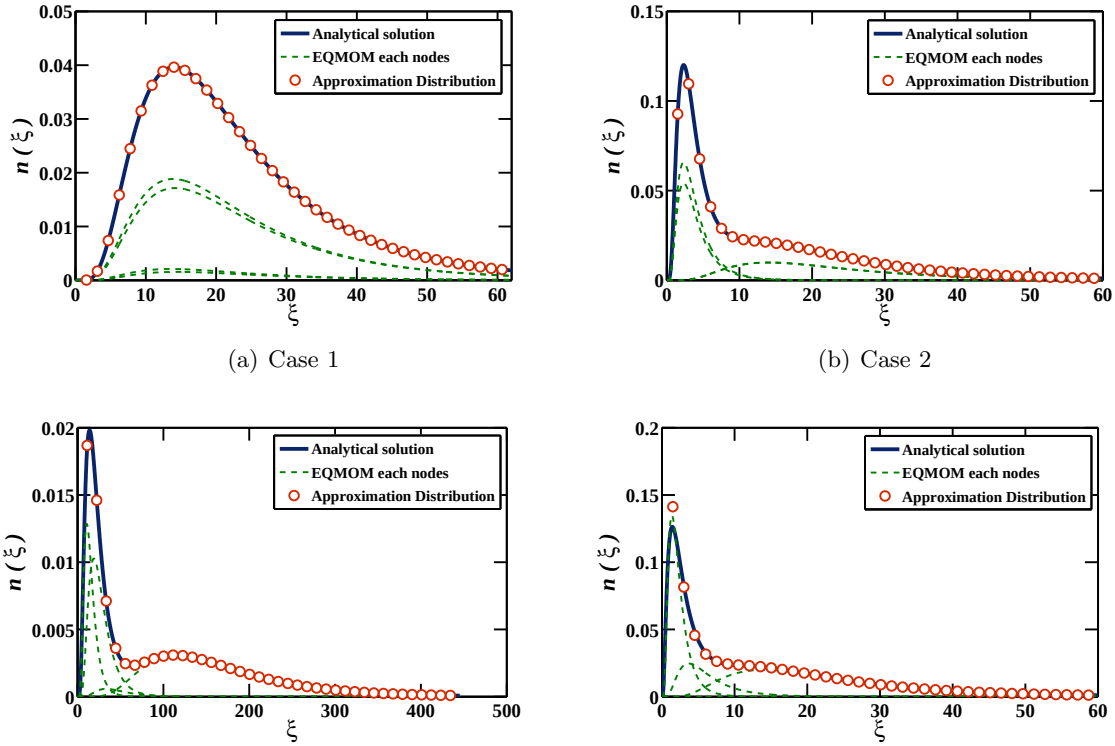

(a) Case 1

(b) Case 2

(c) Case 3

(d) Case 4

Figure 2.1: Comparison between the analytical and the approximated distribution obtained with LnEQMOM using four primary quadrature nodes (N = 4) for cases 1-4.

Table 2.2: Relative error affecting the moments of the reconstructed distribution as a function of the number of primary nodes N.

Case	N = 2		N = 3		N = 4	
1	E_0	1.34×10^{-16}	E_0	1.41×10^{-16}	E_0	4.36×10^{-16}
	E_1	1.48×10^{-16}	E_1	1.48×10^{-16}	E_1	1.47×10^{-16}
	E_2	2.74×10^{-16}	E_2	2.74×10^{-16}	E_2	2.74×10^{-16}
	E_3	8.88×10^{-16}	E_3	8.88×10^{-16}	E_3	8.88×10^{-16}
	E_4	9.64×10^{-16}	E_4	9.64×10^{-16}	E_4	9.64×10^{-16}
			E_5	2.03×10^{-16}	E_5	2.03×10^{-16}
			E_6	3.56×10^{-16}	E_6	3.56×10^{-16}
					E_7	2.18×10^{-16}
					E_8	4.12×10^{-16}
2	E_0	1.35×10^{-16}	E_0	1.37×10^{-16}	E_0	4.35×10^{-16}
	E_1	1.27×10^{-16}	E_1	1.27×10^{-16}	E_1	1.27×10^{-16}
	E_2	2.67×10^{-16}	E_2	2.67×10^{-16}	E_2	2.67×10^{-16}
	E_3	8.84×10^{-16}	E_3	8.84×10^{-16}	E_3	8.84×10^{-16}
	E_4	9.63×10^{-16}	E_4	9.63×10^{-16}	E_4	9.63×10^{-16}
			E_5	2.03×10^{-16}	E_5	2.03×10^{-16}
			E_6	1.78×10^{-16}	E_6	1.78×10^{-16}
					E_7	2.19×10^{-16}
					E_8	4.12×10^{-15}
3	E_0	1.48×10^{-16}	E_0	1.97×10^{-16}	E_0	2.71×10^{-16}
	E_1	1.47×10^{-16}	E_1	1.48×10^{-16}	E_1	1.48×10^{-16}
	E_2	2.22×10^{-16}	E_2	2.22×10^{-16}	E_2	2.22×10^{-16}
	E_3	4.36×10^{-16}	E_3	4.36×10^{-16}	E_3	4.36×10^{-16}
	E_4	6.08×10^{-16}	E_4	6.08×10^{-16}	E_4	6.08×10^{-16}
			E_5	7.81×10^{-16}	E_5	7.81×10^{-16}
			E_6	8.21×10^{-16}	E_6	8.21×10^{-16}
					E_7	1.30×10^{-16}
					E_8	1.87×10^{-16}
4	E_0	1.34×10^{-15}	E_0	1.40×10^{-15}	E_0	4.36×10^{-15}
	E_1	1.28×10^{-14}	E_1	1.28×10^{-14}	E_1	1.27×10^{-12}
	E_2	2.66×10^{-14}	E_2	2.66×10^{-14}	E_2	2.66×10^{-12}
	E_3	8.81×10^{-14}	E_3	8.81×10^{-14}	E_3	8.81×10^{-12}
	E_4	9.61×10^{-14}	E_4	9.61×10^{-14}	E_4	9.61×10^{-12}
			E_5	2.02×10^{-14}	E_5	2.02×10^{-12}
			E_6	3.56×10^{-14}	E_6	3.56×10^{-12}
					E_7	2.19×10^{-12}
					E_8	4.12×10^{-12}

Table 2.3: Normalized L^2 norm of the difference d between the analytical and the approximated distribution.

Case	N = 2	N = 3	N = 4
1	1.90×10^{-13}	2.21×10^{-14}	6.04×10^{-16}
2	2.88×10^{-12}	3.93×10^{-14}	3.90×10^{-14}
3	2.68×10^{-2}	6.68×10^{-3}	2.04×10^{-3}
4	2.76×10^{-1}	1.10×10^{-1}	1.07×10^{-1}

Table 2.4: Cases examined for the aggregation and breakup process.

Case	$\beta(\xi, \xi')$	$a(\xi)$	$b(\xi\|\xi')$	$M_k(t=0)$
5	1	$\begin{cases} 0 & \xi = 1 \\ 0.02 & \xi > 1 \end{cases}$	1, Tab. 2.7	$M_k = 1, k = 0, \ldots, 6$
6	$\xi^3 + \xi'^3$	$\begin{cases} 0 & \xi = 1 \\ 0.02\xi^3 & \xi > 1 \end{cases}$	1, Tab. 2.7	$M_k = 1, k = 0, \ldots, 6$
7	$(\xi + \xi')^3$	$\begin{cases} 0 & \xi = 1 \\ 0.1\, e^{0.01\xi^3} & \xi > 1 \end{cases}$	1, Tab. 2.7	$M_k = 1, k = 0, \ldots, 6$
8	$(\xi + \xi')^2 \lvert\xi^2 - \xi'^2\rvert$	$\begin{cases} 0 & \xi = 1 \\ 0.01\xi^6 & \xi > 1 \end{cases}$	2, Tab. 2.7	$\begin{cases} M_0 = 1 \\ M_1 = 1.13 \\ M_2 = 1.294 \\ M_3 = 1.5 \\ M_4 = 1.760 \\ M_5 = 2.087 \\ M_6 = 2.087 \end{cases}$
9	$(\xi + \xi')^3$	$\begin{cases} 0 & \xi < \sqrt[3]{5} \\ 0.1\, e^{0.01\xi^3} & \xi \geq \sqrt[3]{5} \end{cases}$	3, Tab. 2.7	$M_k = 1, k = 0, \ldots, 6$

2.4.2 PBE for aggregation and breakup problems

We discuss in this section the solution of the PBE for aggregation and breakup problems. We refer to the work of Vanni (2000), who reported the rigorous solution for the aggregation and breakup problems considered here. In particular, we study the five cases summarized in Tab. 2.4, where the kernels for aggregation and breakup reported in Tabs. 2.5 and 2.6 were used, together with the daughter distribution functions listed in Tab. 2.7.

Two types of calculation were performed to investigate the predictive capabilities of LnEQ-MOM:

Table 2.5: Aggregation kernels.

Kernel	$\beta(\xi, \xi')$
Constant	1
Sum	$\xi^3 + \xi'^3$
Hydrodynamic	$(\xi + \xi')^3$
Differential force	$(\xi + \xi')^2 \lvert\xi^2 - \xi'^2\rvert$

Table 2.6: Breakup kernels.

Kernel	$a(\xi)$
Constant	1
Power law	ξ^α
Exponential	$\mathrm{e}^{\delta\xi^3}$

Table 2.7: Daughter distribution functions and their moment transforms.

No.	Mechanism	$b(\xi\lvert\xi')$	$\bar{b}^k$
1	Symmetric fragmentation	$\begin{cases} 2 & \xi = \xi'/2^{1/3} \\ 0 & \text{otherwise} \end{cases}$	$2^{(3-k)/3}\xi^k$
2	Uniform	$\begin{cases} 6\xi^2/\xi'^3 & \xi \in]0, \xi'[\\ 0 & \text{otherwise} \end{cases}$	$6\xi^k/(k+3)$
3	Mass ratio 1 to 4	$\begin{cases} 1 & \xi = \xi' \left(\frac{1}{5}\right)^{1/3} \\ 1 & \xi = \xi' \left(\frac{4}{5}\right)^{1/3} \\ 0 & \text{otherwise} \end{cases}$	$\xi^k \frac{4^{k/3}+1}{5^{k/3}}$

i) The moments of the rigorous NDF reported by Vanni (2000) were computed for each of the cases considered in this section. Numerical integration of the data extracted from the figures reported in Vanni (2000) was performed with the trapezoidal rule, in order to calculate these moments. The computed moments were then used as input to LnEQMOM to obtain the reconstructed NDF. Results were compared to the rigorous NDF and to the reconstruction obtained with Gamma EQMOM (Yuan et al., 2012).

ii) The moment transport equations with LnEQMOM closures with the appropriate source terms, were integrated to obtain the approximate distribution for each of the cases under consideration, starting from the initial conditions reported in the last column of Tab. 2.4.

This procedure was designed to isolate the error in the NDF reconstruction from the error due to the approximation in the time integration of the source terms that appear in the PBE. This is particularly relevant in some of the cases under examination, where the initial condition is characterized by a uniform NDF, which causes LnEQMOM to degenerate into QMOM, affecting the accuracy of the integration of the kernels.

Results obtained by integrating the moment equations with LnEQMOM were also compared to those previously obtained by Marchisio et al. (2003b) using a three-node standard QMOM procedure. Time integration was performed with a two-stage Runge-Kutta method (RK-2), until a steady-state solution was achieved. For each case, the particle number density M_0, the mean particle size $d_{43} = M_4/M_3$, and the particle size distribution are reported.

Fig. 2.2 shows the results obtained for case 5 using LnEQMOM to reconstruct the NDF from the moments of the exact distribution reported in Vanni (2000), as a function of the number of nodes. LnEQMOM satisfactorily approximates the distribution function for large values of ξ when N = 1 and N = 2, however when a larger number of primary quadrature nodes is used, the reconstructed distribution shows oscillations that are not present in the rigorous NDF. It is worth noting that the cases with N $>$ 2 were obtained forcing the number of primary quadrature nodes to be constant. However, the adoption of the adaptive Wheeler algorithm (Yuan and Fox, 2011; Marchisio and Fox, 2013), with realistic adaption criteria, the number of nodes would likely be automatically reduced, limiting the oscillatory behavior.

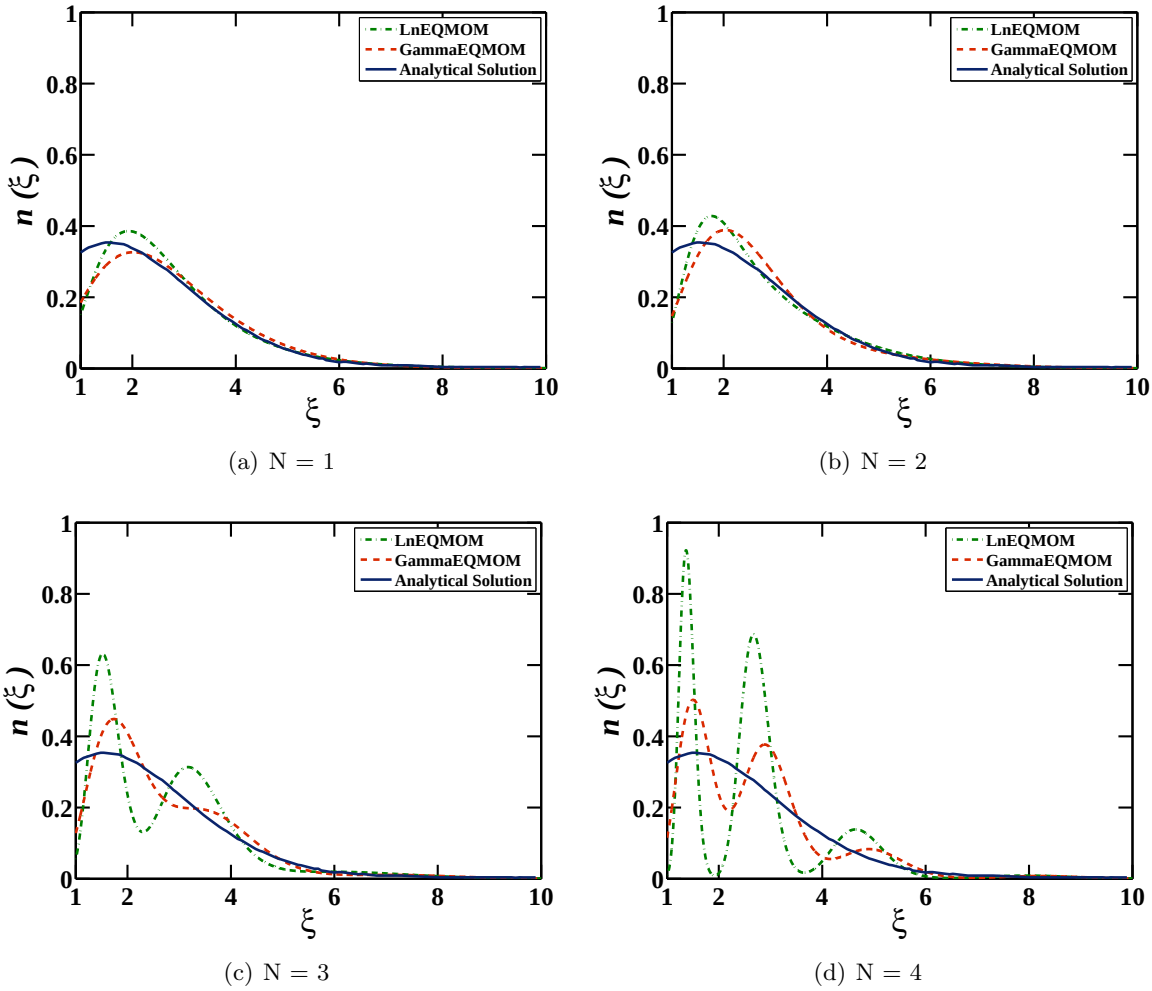

(a) N = 1 (b) N = 2

(c) N = 3 (d) N = 4

Figure 2.2: Case 5 – Comparison of the reconstructed NDF from the exact moments of the rigorous solution of the PBE with LnEQMOM and Gamma EQMOM, as a function of the number of primary quadrature nodes N.

As expected, due to the functional form of the kernel function used in LnEQMOM, the reconstructed NDF does not tend to the correct limit for $\xi \to 0^+$. However, by definition, the reconstructed NDF has the same moments of the rigorous solution up to order $2N+1$. Finally, we observe that similar predictions were obtained with Gamma kernel density functions.

Results obtained from the solution of the PBE with LnEQMOM for case 5 are reported in Fig. 2.3, for $t = 200$ s. As observed above, the right tail of the distribution is well captured by the approximate solution. However, important differences are observed for smaller values of ξ. Both QMOM and LnEQMOM (Fig. 2.3(c) and 2.3(d)) predict the time evolution of the

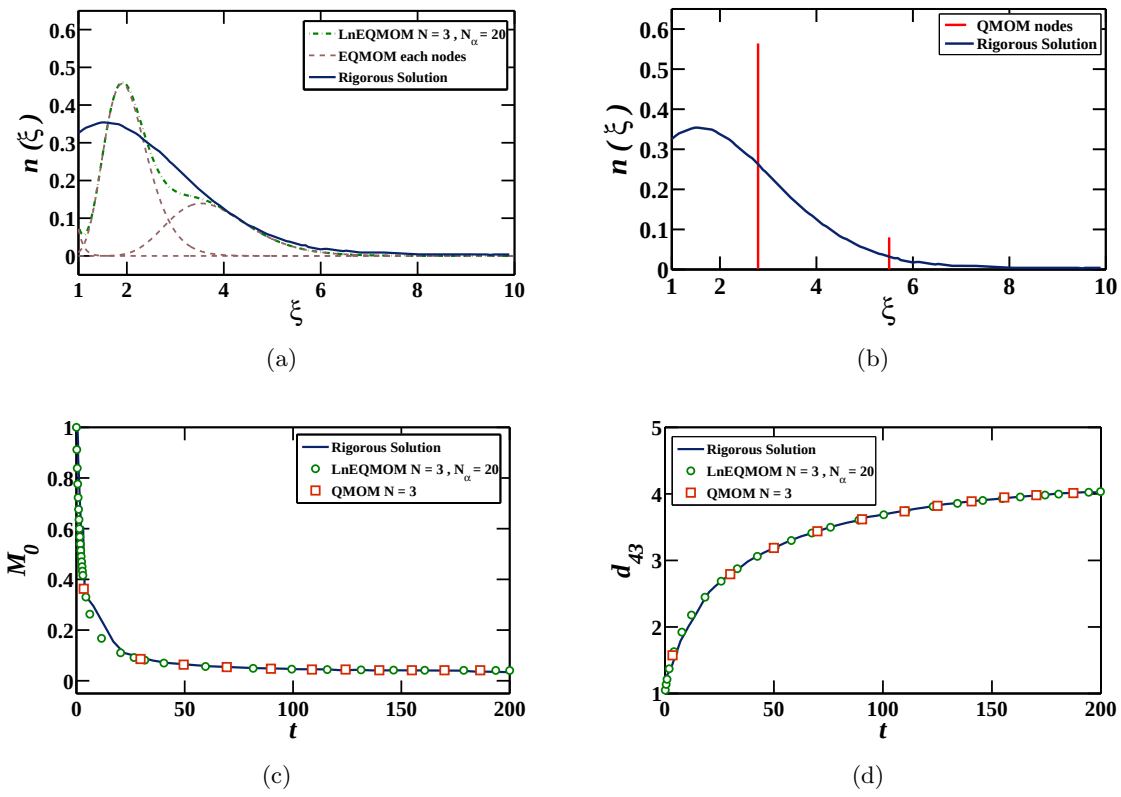

Figure 2.3: Case 5 – (a) NDF from the rigorous solution and LnEQMOM, (b) NDF from the rigorous solution and QMOM, (c) zero-order moment of the NDF, (d) mean particle size d_{43}.

particle number density M_0 and of the mean particle size d_{43} with comparable accuracy. Results obtained with LnEQMOM and Gamma EQMOM applied to the moments of the rigorous solution for case 6 are reported in Fig. 2.4. In this case, two primary quadrature nodes are sufficient to obtain an excellent match of the reconstruction with the exact distribution, with the LnEQMOM results exactly overlapping the curve of the rigorous NDF. The reconstructed NDF provided by EQMOM with gamma kernel densities for this case is also in good agreement with the rigorous solution, but it shows larger differences compared to the result obtained with LnEQMOM. Fig. 2.5 shows the results obtained integrating the moment equations for case 6 in Tab. 2.4, where the sum aggregation kernel was used. The daughter distribution for symmetric fragmentation was adopted. The reconstructed distribution agrees well with the rigorous solution, however, the height of its peak is slightly overestimated. The time evolution of the total number density M_0 (Fig. 2.5(c)) is in excellent agreement with the rigorous solution, and

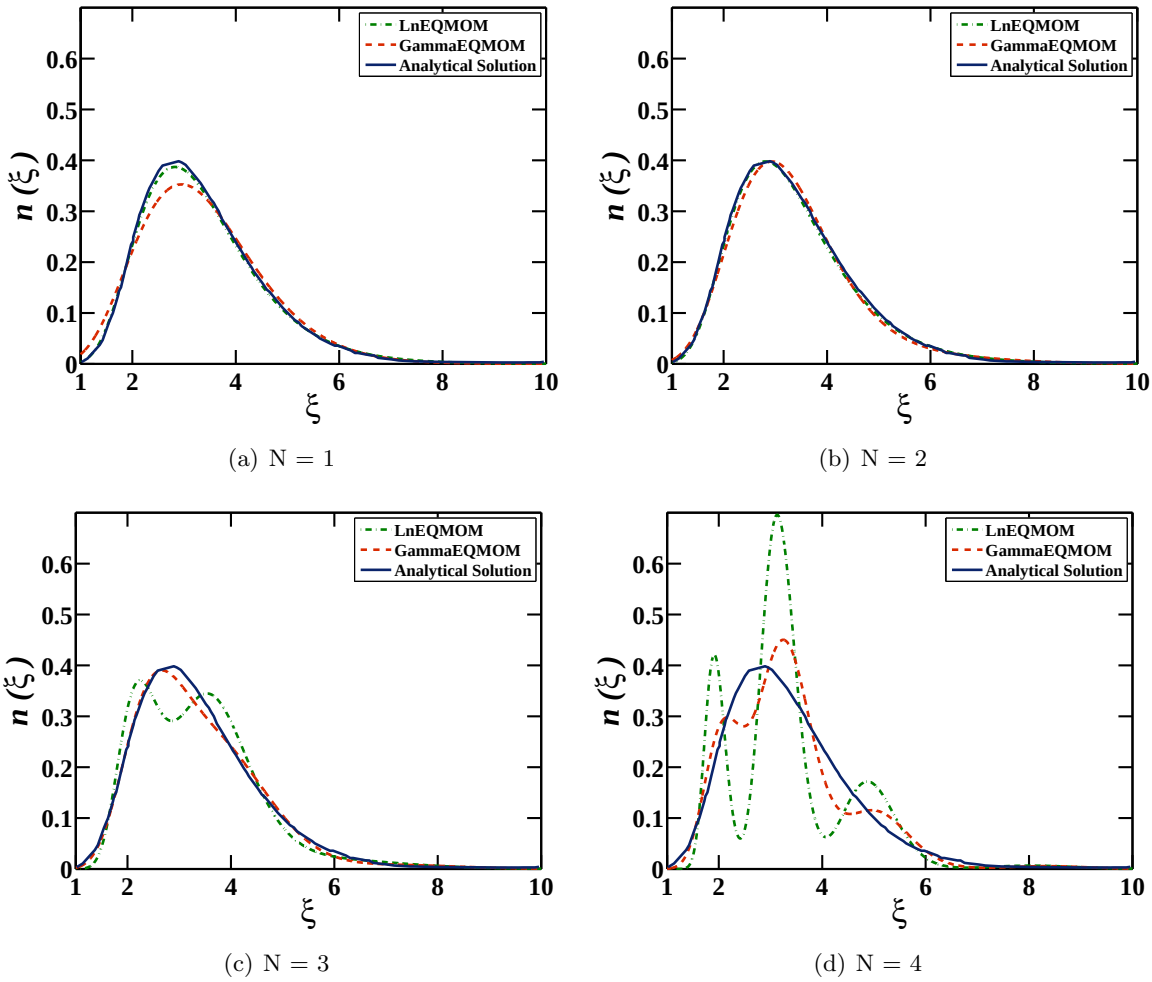

(a) N = 1

(b) N = 2

(c) N = 3

(d) N = 4

Figure 2.4: Case 6 – Comparison of the reconstructed NDF from the exact moments of the rigorous solution of the PBE with LnEQMOM and Gamma EQMOM, as a function of the number of primary quadrature nodes N.

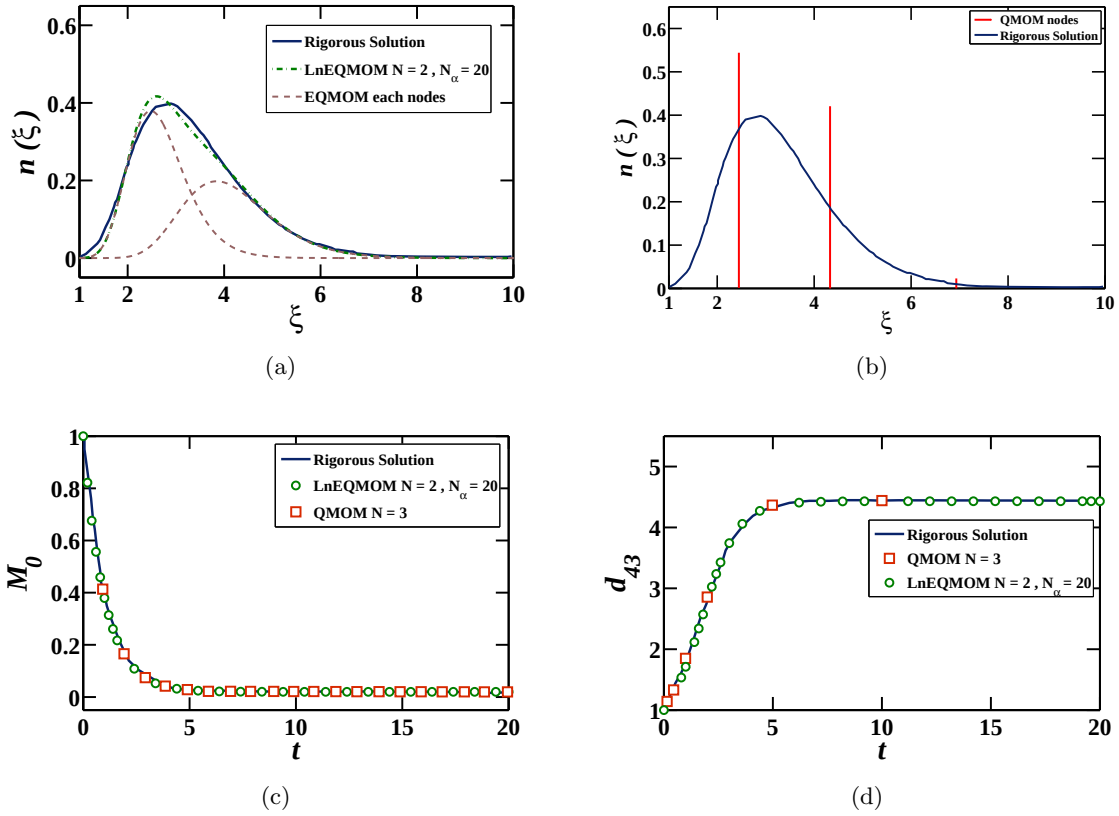

Figure 2.5: Case 6 – (a) NDF from the rigorous solution and LnEQMOM, (b) NDF from the rigorous solution and QMOM, (c) zero-order moment of the NDF, (d) mean particle size d_{43}.

with the QMOM prediction. Similar conclusions can be drawn for the time evolution of the particle mean diameter d_{43}, reported in Fig. 2.5(d).

Results concerning case 7 are reported in Figs. 2.6 and 2.7. The agreement between the reconstructed distribution obtained from the moments of the rigorous solution of the PBE and the rigorous solution itself is satisfactory. The tails of the distribution are well reproduced, however the shape of the central part of the distribution, and the maximum value of the NDF are not properly captured by the EQMOM procedure. The reconstructed NDF obtained integrating the moment transport equations (Fig. 2.7(a)) shows poorer agreement with the rigorous solution, if compared to the NDF reconstructed directly from the moments of the exact NDF. This may be caused by the accumulation of error during the integration process, in particular at the initial stages of the simulation, when the uniform initial condition forces the procedure to

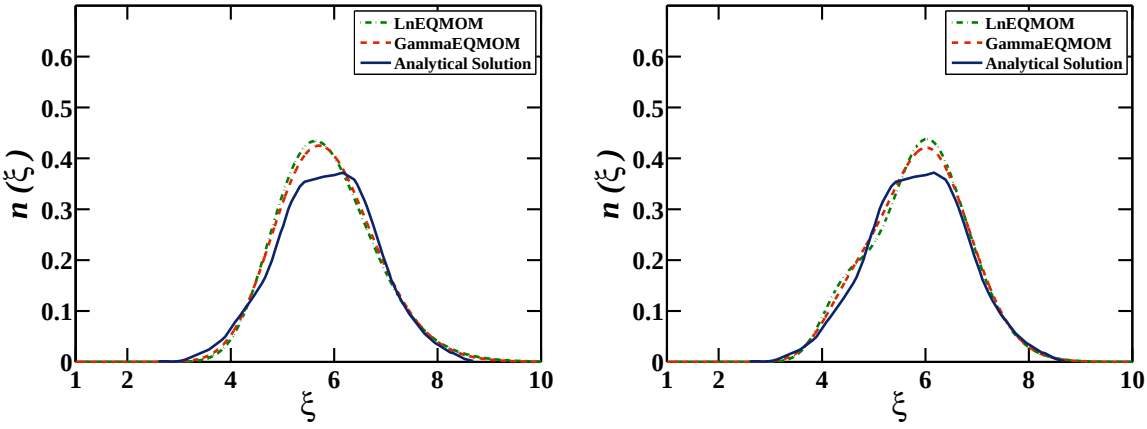

(a) N = 1 (b) N = 2

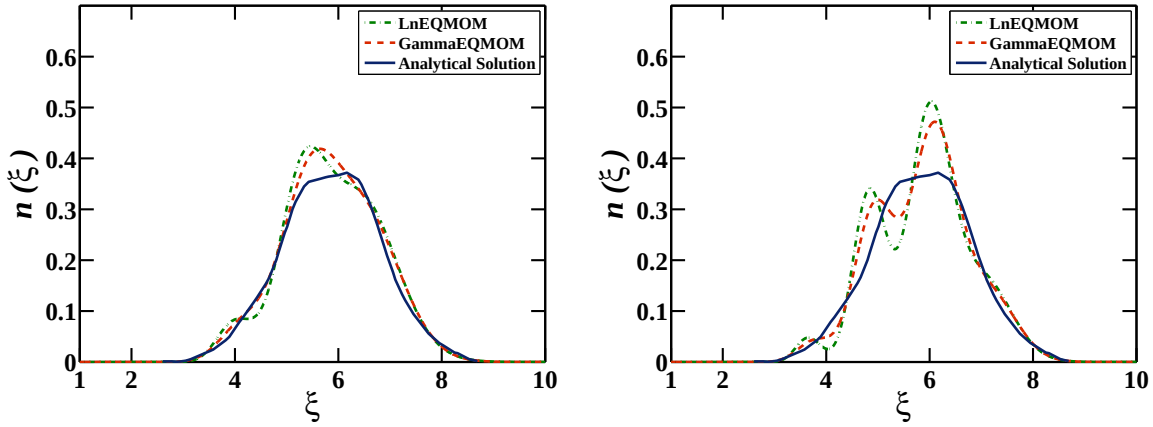

(c) N = 3 (d) N = 4

Figure 2.6: Case 7 – Comparison of the reconstructed NDF from the exact moments of the rigorous solution of the PBE with LnEQMOM and Gamma EQMOM, as a function of the number of primary quadrature nodes N.

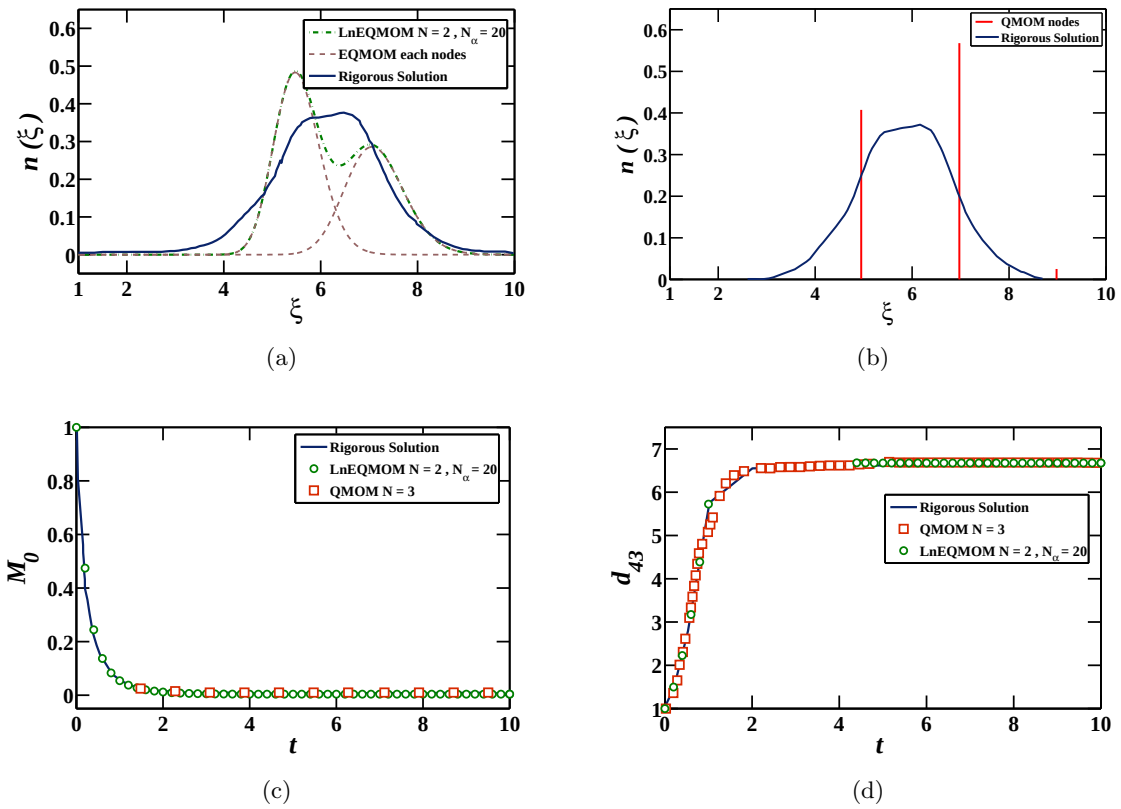

Figure 2.7: Case 7 – (a) NDF from the rigorous solution and LnEQMOM, (b) NDF from the rigorous solution and QMOM, (c) zero-order moment of the NDF, (d) mean particle size d_{43}.

rely on the delta function representation of the NDF to integrate the source terms of the PBE. It is worth reminding that the EQMOM procedure smoothly and automatically degenerates into QMOM when a continuous reconstruction cannot be determined (Chalons et al., 2010; Yuan et al., 2012), allowing the calculation to proceed. The time evolution of the zero-order moment of the NDF (Fig. 2.7(c)), and of the mean diameter d_{43} (Fig. 2.7(d)) are in excellent agreement with those reported for the rigorous solution by Marchisio et al. (2003b). Similar observations to those made for the reconstructed NDF of case 7 apply to case 8, as illustrated in Figs. 2.8 and 2.9. It is worth to highlight, however, that in this case the time evolution of the zero-order moment of the NDF (Fig. 2.9(c)) and of d_{43} (Fig. 2.9(d)) obtained with LnEQMOM show a significant improvement in comparison to the same quantities predicted by the standard QMOM procedure. In particular, the results provided by LnEQMOM for these two averaged quantities are in excellent agreement with those obtained with the rigorous solution of the PBE

(Vanni, 2000), while those provided by QMOM (Marchisio et al., 2003b) show a slight under-estimation of the zero-order moment and an important over-estimation of d_{43} for $t \in [0, 4]$. The reader should also notice that the predictions reported for cases 6 – 8 were obtained using two quadrature nodes for the EQMOM procedure, as opposed to the three quadrature nodes used in QMOM. As a consequence, EQMOM not only provides a satisfactory reconstruction of the continuous NDF, and a significant improvement in the prediction of the time evolution of M_0 and d_{43} for cases 7 and 8, but it also allows a reduction of the number of quadrature nodes to be achieved. This positively impacts the computational cost of the procedure, because the eigenproblem solved to perform the moment inversion involves a smaller matrix, and can be treated analytically.

LnEQMOM with N = 3 and N = 4 provides a satisfactory reconstruction of the NDF of case 9 (Fig. 2.10), when the moments of the rigorous NDF are used to perform the reconstruction. The cases with N = 1 and N = 2 are unable to reproduce the complex shape of the distribution, which presents three local maxima. As shown in Fig. 2.11, the NDF obtained integrating the moment equations presents significant differences with respect to the rigorous solution. However, the time evolution of the zero-order moment (Fig. 2.11(c)) and of the mean particle size d_{43} (Fig. 2.11(d)) are in excellent agreement with those obtained by Marchisio et al. (2003b) for the rigorous solution.

2.4.3 Coalescence problem

We now consider a problem concerning coalescence, for which an analytical solution can be found. In this case $a(t, \xi, \xi') = \xi + \xi'$ (sum kernel) is used, where ξ, the size variable, is volume. Since only coalescence is considered, no other kernel needs to be defined. The initial condition for this problem has been reported (Lage, 2011; Yuan et al., 2012) as:

$$n(0, \xi) = \mathrm{e}^{-\xi}. \tag{2.29}$$

The exact NDF for this problem is known (Gelbard and Seinfeld, 1978) and can be written as:

$$n(t, \xi) = \frac{\mathrm{e}^{-t-2\xi+\xi\,\mathrm{e}^{-t}}}{\xi\sqrt{1-\mathrm{e}^{-t}}}\,\mathrm{I}_1\left(2\xi\sqrt{1-\mathrm{e}^{-t}}\right), \tag{2.30}$$

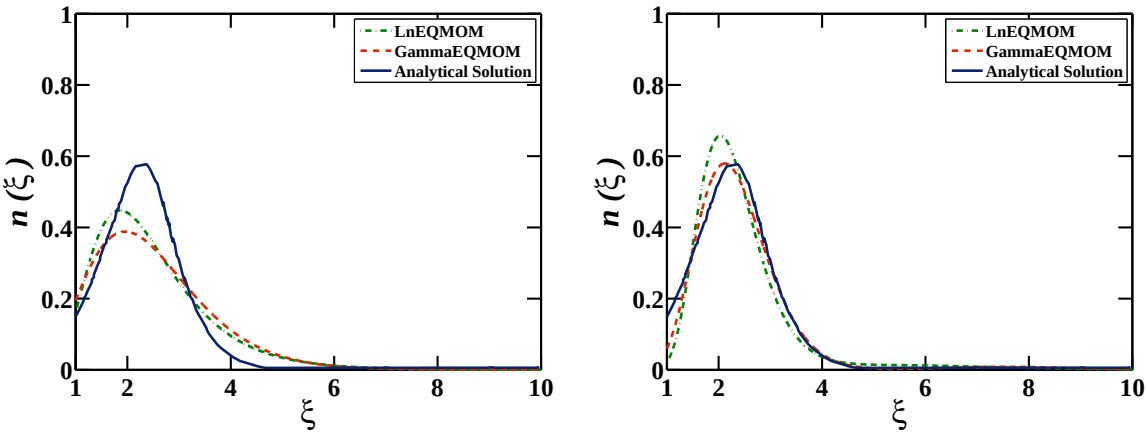

(a) N = 1

(b) N = 2

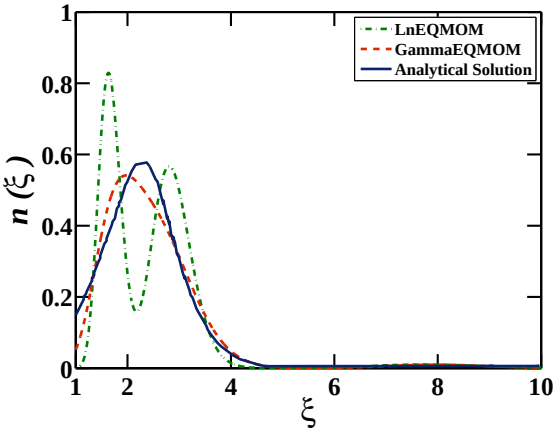

(c) N = 3

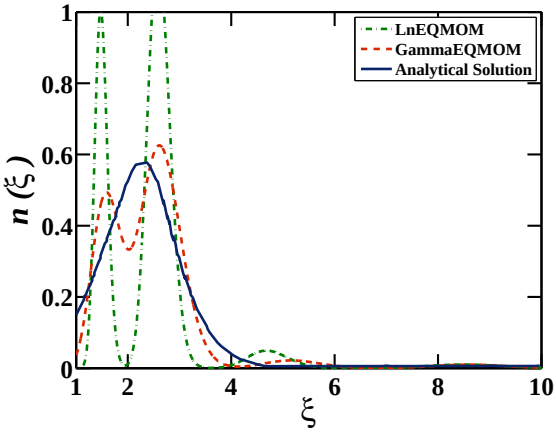

(d) N = 4

Figure 2.8: Case 8 – Comparison of the reconstructed NDF from the exact moments of the rigorous solution of the PBE with LnEQMOM and Gamma EQMOM, as a function of the number of primary quadrature nodes N.

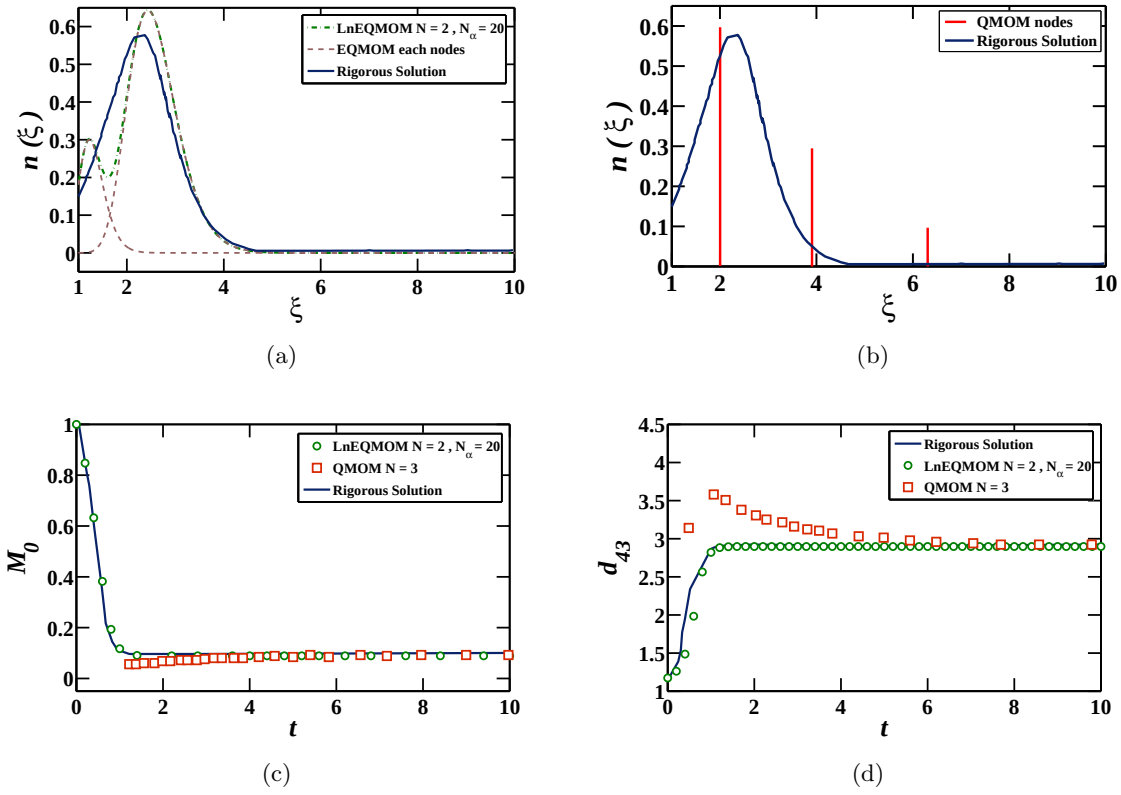

Figure 2.9: Case 8 – (a) NDF from the rigorous solution and LnEQMOM, (b) NDF from the rigorous solution and QMOM, (c) zero-order moment of the NDF, (d) mean particle size d_{43}.

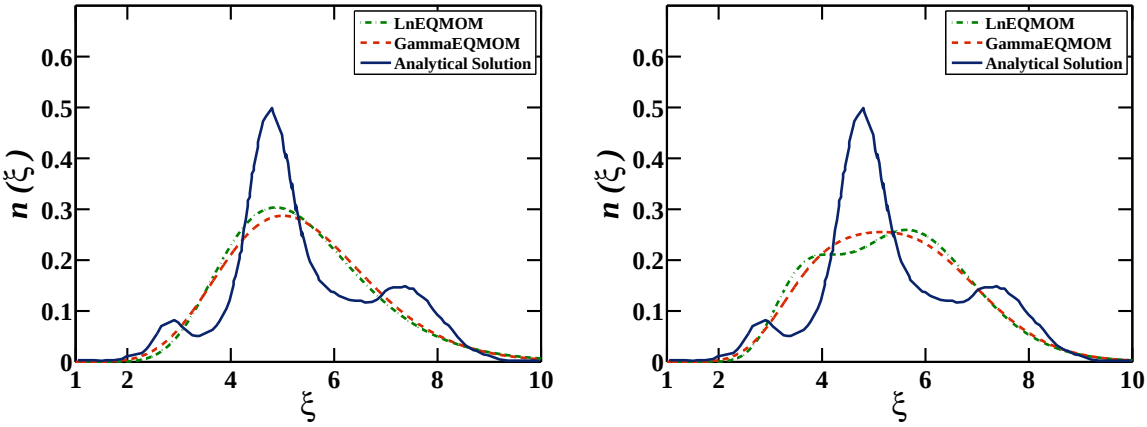

(a) N = 1 (b) N = 2

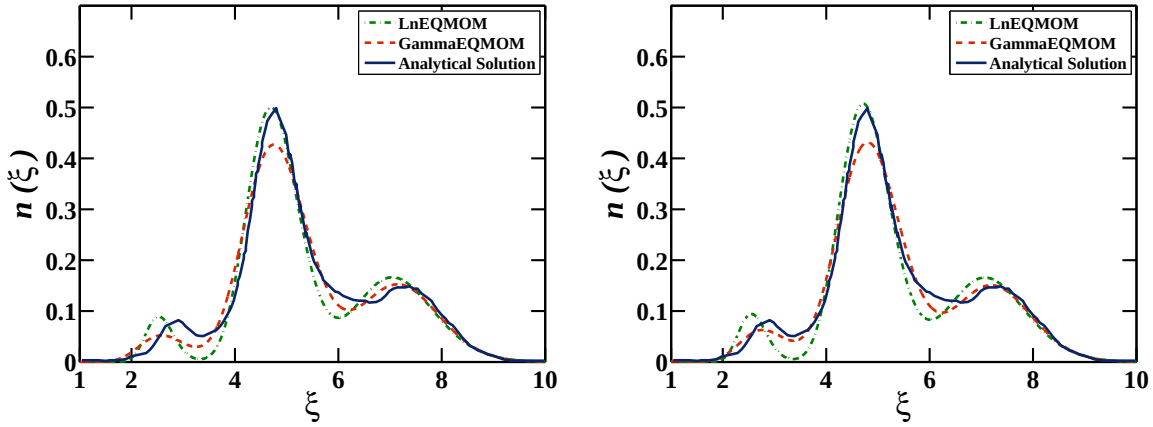

(c) N = 3 (d) N = 4

Figure 2.10: Case 9 – Comparison of the reconstructed NDF from the exact moments of the rigorous solution of the PBE with LnEQMOM and Gamma EQMOM, as a function of the number of primary quadrature nodes N.

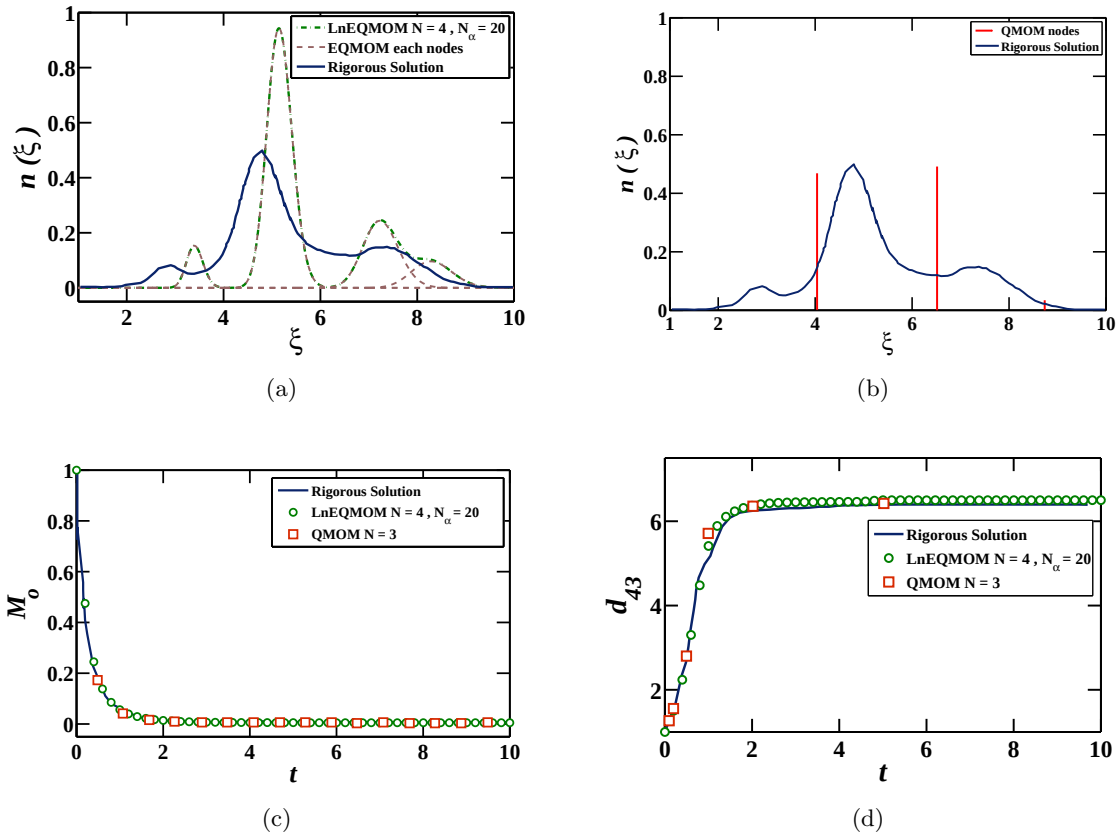

Figure 2.11: Case 9 – (a) NDF from the rigorous solution and LnEQMOM, (b) NDF from the rigorous solution and QMOM, (c) zero-order moment of the NDF, (d) mean particle size d_{43}.

where I_1 is the modified Bessel function. Results were obtained as a function of the number of primary quadrature nodes. The reconstructed NDF was obtained from the moments of the exact NDF, without integrating the moment transport equations. Increasing the number of primary quadrature nodes improves the accuracy of the reconstructed distribution, as illustrated in Fig. 2.12. The numerical approximation matches the analytical solution, properly predicting the slope of the tail of the distribution, and its behavior for large values of ξ.

2.4.4 Condensation problem

We consider here the reconstruction of the NDF in a condensation problem, where ξ is chosen to be particle volume. In this case, the PBE is (Yuan et al., 2012)

$$\frac{\partial n\left(\xi,\mathbf{x},t\right)}{\partial t}+\frac{\partial}{\partial\xi}\left[g\left(\xi,\mathbf{x},t\right)n\left(\xi,\mathbf{x},t\right)\right]=0, \tag{2.31}$$

and the corresponding moment transport equations are

$$\frac{\partial M_k\left(\mathbf{x},t\right)}{\partial t}=-\left.g\left(\xi,\mathbf{x},t\right)n\left(\xi,\mathbf{x},t\right)\right)\xi^k\right|_0^{+\infty}+\int_0^{+\infty}k\xi^{k-1}g\left(\xi,\mathbf{x},t\right)n\left(\xi,\mathbf{x},t\right)\mathrm{d}\xi. \tag{2.32}$$

We consider the case in which $g\left(t,\xi\right)=\xi/2$, and with initial condition expressed as (Lage, 2011):

$$n\left(0,\xi\right)=6\xi^3\,\mathrm{e}^{-\xi}. \tag{2.33}$$

The exact NDF for this problem can be written as (Lage, 2011):

$$n\left(t,\xi\right)=\frac{\left(\xi\,\mathrm{e}^{-t/2}\right)^3\mathrm{e}^{-\xi\,\mathrm{e}^{-t/2}}}{6\,\mathrm{e}^{t/2}}. \tag{2.34}$$

The LnEQMOM reconstruction is only tested considering the exact moments of the analytical solution for brevity. Fig. 2.13 shows the LnEQMOM reconstruction obtained with an increased number of primary quadrature nodes. It is clear that increasing the number of the nodes will lead to more precise results for large values of ξ. However, oscillations appear when a large number of nodes is used. The reconstructed distribution agrees satisfactorily with the analytical solution, and the slope of its tail is properly captured by the reconstructed NDF.

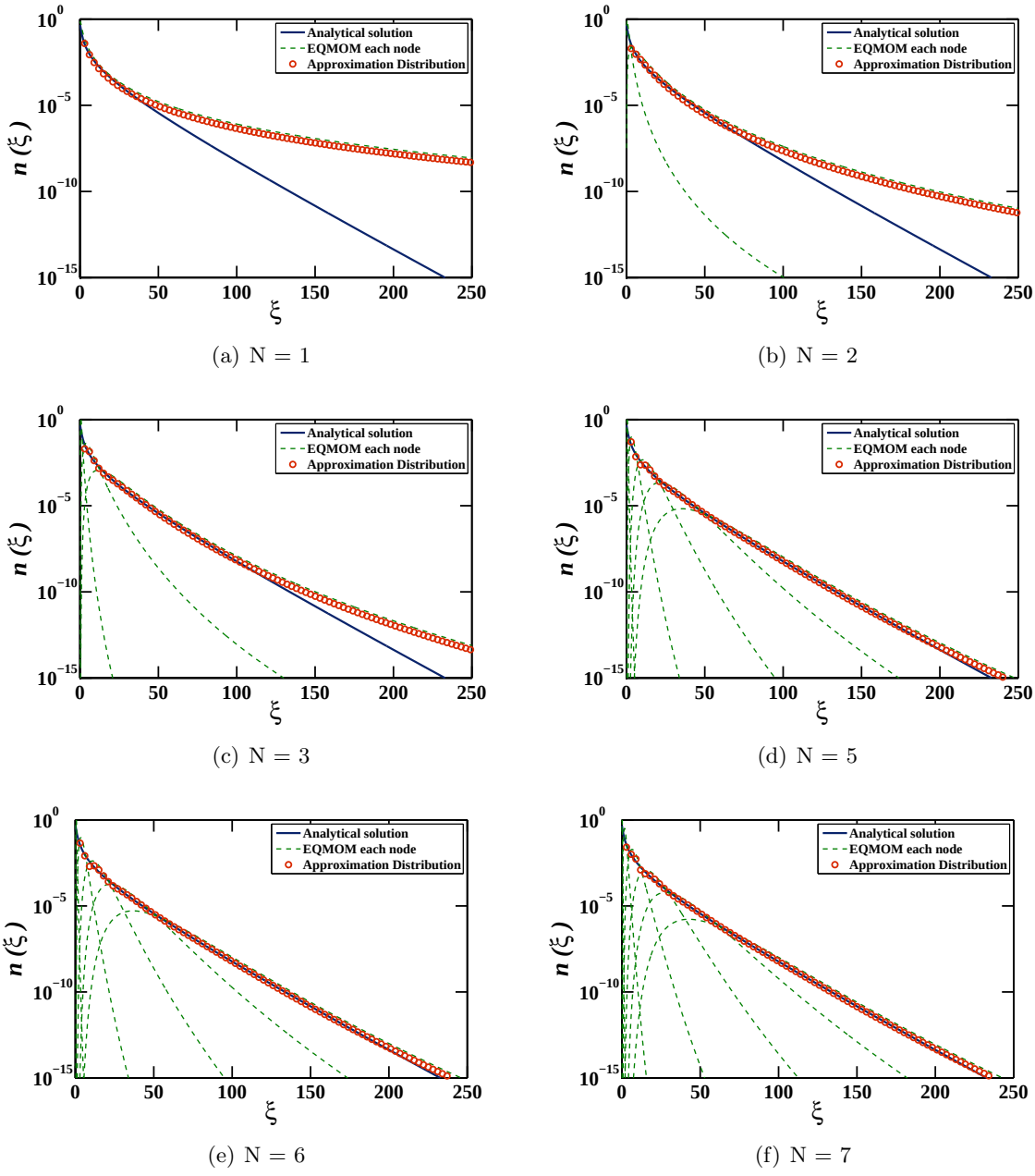

(a) N = 1

(b) N = 2

(c) N = 3

(d) N = 5

(e) N = 6

(f) N = 7

Figure 2.12: Case 10 – Reconstructed distribution as a function of the number of nodes used in the primary quadrature obtained from the exact moments of the analytical solution.

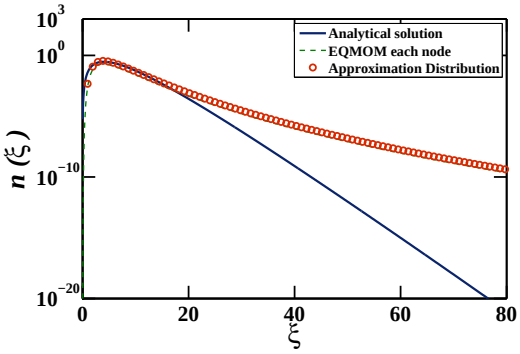

(a) N = 1

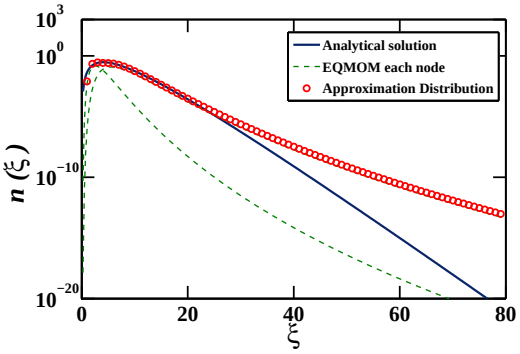

(b) N = 2

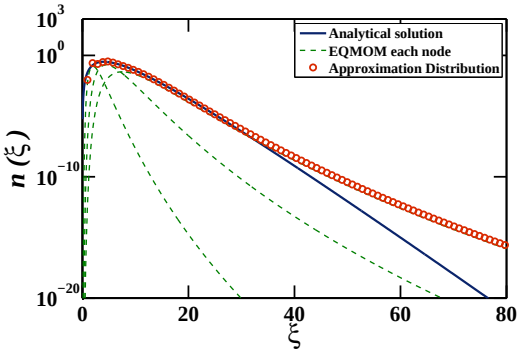

(c) N = 3

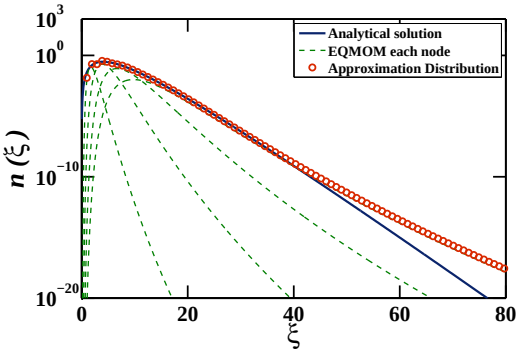

(d) N = 5

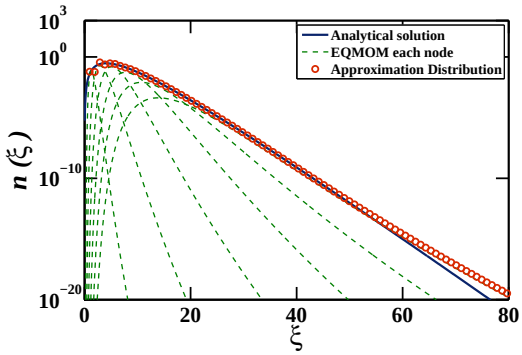

(e) N = 6

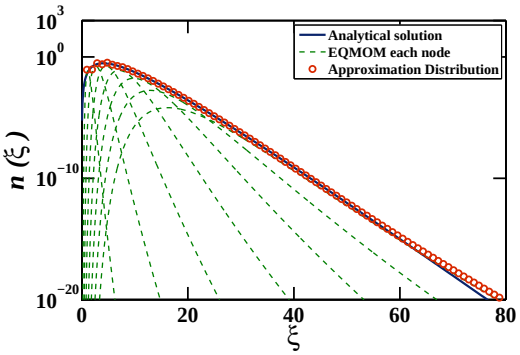

(f) N = 7

Figure 2.13: Case 11 – Reconstructed distribution as a function of the number of nodes used in the primary quadrature obtained from the exact moments of the analytical solution.

Table 2.8: Values of σ, σ_{H_0}, and σ_{H_1} for cases 5 – 9.

Case	σ	σ_{H_0}	σ_{H_1}
5	0.580	0.624	0.612
6	0.600	0.881	0.682
7	0.502	0.836	0.586
8	0.604	0.893	0.672
9	0.355	0.450	0.381

2.4.5 Realizability of transformed moments

The LnEQMOM algorithm will succeed if the transformed moments are realizable. To this purpose, it is necessary to have an algorithm to check the moment realizability (Shohat and Tamarkin, 1943; Dette, 1997; Yuan et al., 2012; Vikas et al., 2013a). A set of real values is a set of moments of a distribution function if the Hankel determinants are non-negative. The Hankel determinants for our case can be written as (Dette, 1997; Wright, 2007):

$$\Delta_{i,j} = \begin{vmatrix} M^*_i & M^*_{i+1} & \cdots & M^*_{i+j} \\ M^*_{i+1} & M^*_{i+2} & \cdots & M^*_{i+j+1} \\ \vdots & \vdots & \ddots & \vdots \\ M^*_{i+j} & M^*_{i+j+1} & \cdots & M^*_{i+2j} \end{vmatrix}, \tag{2.35}$$

where $i = 0, 1$, $j = 0, \ldots, \mathrm{N}-1$. Fig. 2.14 shows the graphs for the target function $J(\sigma)$ and the graphs of the Hankel determinants as a function of σ for the case with $\mathrm{N} = 2$ primary quadrature nodes. The values of the parameter σ which set the target function J to zero are reported in the first column of Tab. 2.8. We indicate with σ_{H_0} and σ_{H_1} the values of σ which set the Hankel determinants H_0 and H_1 to zero. It is clear from the values reported in Tab. 2.8 that, for cases 5 to 9,

$$\sigma < \sigma_{H_0} \wedge \sigma < \sigma_{H_1}.$$

Examining Fig. 2.14, it is evident that both Hankel determinants H_0 and H_1 are positive for the value of σ at which $J = 0$, indicated by the red vertical lines. As a consequence, the set of moments considered in the reconstruction is realizable for such a value of the parameter σ. Whether these determinants become negative, the moments will be non-realizable and the moment inversion procedure will fail. We generally choose the smallest positive value of σ

which sets our target function to zero, as described in (Yuan et al., 2012), however when such value leads to non-realizable moments, we search larger values of σ and choose one that ensures the realizability of the moment set.

2.5 Conclusion

An extended quadrature method of moments with log-normal kernel density function (LnEQMOM) was presented in this study. The analytical solution to the cases with one and two primary nodes was studied, and a numerical procedure was described for cases involving larger number of quadrature nodes. The existence of at least one positive real value of the parameter σ was proven for the case with two primary quadrature nodes.

The proposed numerical approach was tested against cases concerning aggregation and breakup, coalescence, and condensation problems, demonstrating that LnEQMOM is capable of accurately predicting the time evolution of the zero-order moment and of the mean particle size in all the cases considered in this work, with results in excellent agreement with those obtained with the rigorous solution of the PBE, using a relatively low number of primary quadrature nodes (N = 2 or 3 depending on the case). In particular, LnEQMOM provides more accurate results for the time evolution of the zero-order moment and of the mean particle size than QMOM for aggregation and breakup problems with symmetric and uniform daughter distributions (cases 7 and 8). This improvement is achieved using a lower number of primary quadrature nodes than the standard QMOM procedure.

Overall, satisfactory accuracy was achieved for what concerns the reconstructed number density function. In particular, LnEQMOM correctly predicts the tails of the NDF in the cases we considered. However, due to the functional form of the log-normal kernel, the method shows some difficulties in reconstructing distributions whose value for $\xi \to 0$ is not zero. LnEQMOM also appeared to be numerically more robust when compared to Gamma EQMOM, due to the structure of the system of equations used in the numerical procedure.

Some discrepancy was observed between the reconstructed NDF from the moments of the rigorous solution of the PBE, and the NDF obtained integrating in time the moment transport equations with LnEQMOM. This discrepancy may be attributed to the propagation of errors

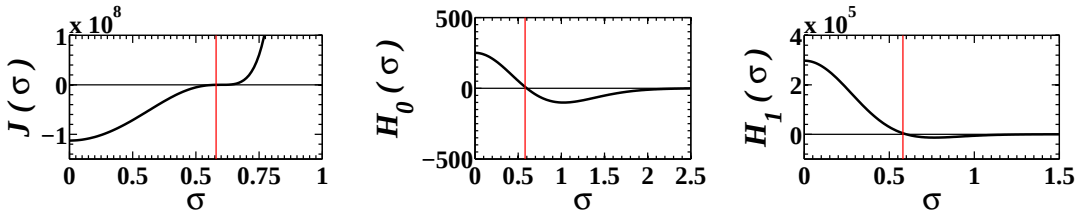

(a) Case 5

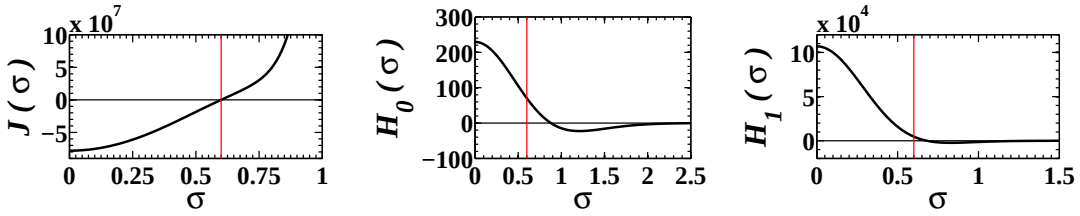

(b) Case 6

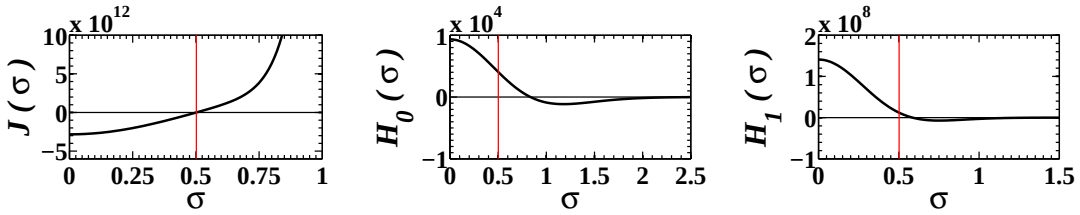

(c) Case 7

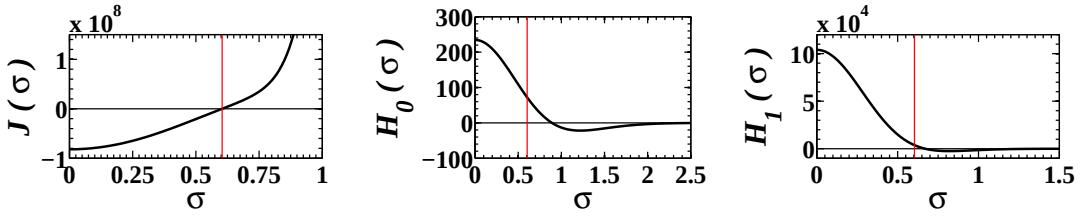

(d) Case 8

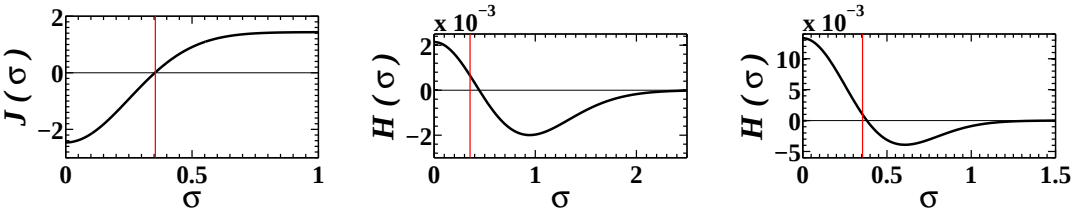

(e) Case 9

Figure 2.14: Target function and Hankel determinants for cases 5 – 9 with N = 2.

in the time-integration procedure, and to the fact that the uniform initial condition required delta functions to be used in the evaluation of the integrals involved in the source terms of the PBE. This aspect of the numerical procedure deserves a more in-depth study, in order to improve its accuracy, and it will be object of future work.

2.6 Acknowledgments

The authors would like to thank Prof. Rodney O. Fox and Dr. Xiaofei Hu for the precious feedback they provided about this manuscript.

2.7 Bibliography

Akroyd, J., Smith, A. J., McGlashan, L. R., and Kraft, M. (2010). Numerical investigation of DQMOM-IEM as a turbulent reaction closure. *Chemical Engineering Science*, 65(6):1915–1924.

Alopaeus, V., Laakkonen, M., and Aittamaa, J. (2006). Solution of population balances with breakage and agglomeration by high-order moment-conserving method of classes. *Chemical Engineering Science*, 61(20):6732–6752.

Alopaeus, V., Laakkonen, M., and Aittamaa, J. (2008). Solution of population balances by high order moment-conserving method of classes: reconstruction of a non-negative density distribution. *Chemical Engineering Science*, 63(10):2741–2751.

Athanassoulis, G. A. and Gavriliadis, P. N. (2002). The truncated Hausdorff moment problem solved by using kernel density functions. *Probabilistic Engineering Mechanics*, 17(3):273–291.

Balakin, B. V., Hoffmann, A. C., and Kosinski, P. (2014). Coupling STAR-CD with a population-balance technique based on the classes method. *Powder Technology*, 257:47–54.

Bannari, R., Kerdouss, F., Selma, B., Bannari, A., and Proulx, P. (2008). Three-dimensional mathematical modeling of dispersed two-phase flow using class method of population balance in bubble columns. *Computers & Chemical Engineering*, 32(12):3224–3237.

Becker, P. J., Puel, F., Henry, R., and Sheibat-Othman, N. (2011). Investigation of discrete population balance models and breakage kernels for dilute emulsification systems. *Industrial & Engineering Chemistry Research*, 50(19):11358–11374.

Bove, S., Solberg, T., and Hjertager, B. H. (2005). A novel algorithm for solving population balance equations: the parallel parent and daughter classes. Derivation, analysis and testing. *Chemical Engineering Science*, 60(5):1449–1464.

Broadwell, J. E. and Breidenthal, R. E. (1982). A simple model of mixing and chemical reaction in a turbulent shear layer. *Journal of Fluid Mechanics*, 125:397–410.

Cao, R. R., Wang, H., and Pope, S. B. (2007). The effect of mixing models in PDF calculations of piloted jet flames. *Proceedings of the Combustion Institute*, 31(1):1543–1550.

Capecelatro, J., Desjardins, O., and Fox, R. (2014). Numerical study of collisional particle dynamics in cluster-induced turbulence. *Journal of Fluid Mechanics*, 747:R2–1–R2–13.

Carrica, P. M., Drew, D., Bonetto, F., and Lahey Jr, R. T. (1999). A polydisperse model for bubbly two-phase flow around a surface ship. *International Journal of Multiphase Flow*, 25(2):257–305.

Cassiani, M., Franzese, P., and Giostra, U. (2005). A PDF micromixing model of dispersion for atmospheric flow. Part I: development of the model, application to homogeneous turbulence and to neutral boundary layer. *Atmospheric Environment*, 39(8):1457–1469.

Chalons, C., Fox, R., and Massot, M. (2010). A multi-Gaussian quadrature method of moments for gas-particle flows in a LES framework. *Studying Turbulence Using Numerical Simulation Databases, Center for Turbulence Research, Summer Program 2010, Stanford University*, pages 347–358.

Chen, H., Chen, S., and Kraichnan, R. H. (1989). Probability distribution of a stochastically advected scalar field. *Physical Review Letters*, 63(24):2657–2660.

Cheng, J. C. (2010). A comrehensive model study for Flash Nanoprecipitation: computational fluid dynamics, micro- particle image velocimetry, and population balance modeling. *Iowa State University, Ames, Iowa, USA*.

Cheng, J. C. and Fox, R. O. (2010). Kinetic Modeling of Nanoprecipitation using CFD Coupled with a Population Balance. *Industrial & Engineering Chemistry Research*, 49(21):10651–10662.

Cheng, J. C., Vigil, R., and Fox, R. (2010). A competitive aggregation model for Flash Nano-Precipitation. *Journal of Colloid and Interface Science*, 351(2):330–342.

Choi, H. S., Park, T. S., and Suzuki, K. (2008). Turbulent mixing of a passive scalar in confined multiple jet flows of a micro combustor. *International Journal of Heat and Mass Transfer*, 51(17–18):4276–4286.

Cremer, M. A., McMurtry, P. A., and Kerstein, A. R. (1994). Effects of turbulence length scale distribution on scalar mixing in homogeneous turbulent flow. *Physics of Fluids*, 6(6):2143–2153.

Curl, R. L. (1963). Dispersed phase mixing: I. Theory and effects in simple reactors. *AIChE Journal*, 9(2):175–181.

Danckwerts, P. V. (1958). The effect of incomplete mixing on homogeneous reactions. *Chemical Engineering Science*, 8(12):93–102.

Desjardins, O., Fox, R., and Villedieu, P. (2008). A quadrature-based moment method for dilute fluid-particle flows. *Journal of Computational Physics*, 227(4):2514–2539.

Dette, H. (1997). *The Theory of Canonical Moments with Applications in Statistics, Probability and Analysis*. John Wiley & Sons, New York.

Diemer, R. B. and Olson, J. H. (2002). A moment methodology for coagulation and breakage problems: Part 2moment models and distribution reconstruction. *Chemical Engineering Science*, 57(12):2211–2228.

Dopazo, C. (1994). Recent development in pdf methods. In Libby, P. A. and Williams, F. A., editors, *Turbulent Reacting Flows*, pages 357–474. New York: Academic Press.

Dopazo, C. and O'Brien, E. E. (1973). Isochoric turbulent mixing of two rapidly reacting chemical species with chemical heat release. *Physics of Fluids*, 16(12):2075–2081.

Efendiev, Y. and Zachariah, M. R. (2002). Hybrid Monte Carlo Method for Simulation of Two-Component Aerosol Coagulation and Phase Segregation. *Journal of Colloid and Interface Science*, 249(1):30–43.

Eswaran, V. and Pope, S. B. (1988). Direct numerical simulations of the turbulent mixing of a passive scalar. *Physics of Fluids*, 31:506–520.

Falola, A., Borissova, A., and Wang, X. Z. (2013). Extended method of moment for general population balance models including size dependent growth rate, aggregation and breakage kernels. *Computers & Chemical Engineering*, 56:1–11.

Fokker, A. D. (1914). Die mittlere Energie rotierender elektrischer Dipole im Strahlungsfeld. *Annalen der Physik*, 348(5):810–820.

Fox, R., Laurent, F., and Massot, M. (2008). Numerical simulation of spray coalescence in an Eulerian framework: Direct quadrature method of moments and multi-fluid method. *Journal of Computational Physics*, 227(6):3058–3088.

Fox, R. O. (1992a). Computation of turbulent reactive flows: first- principles macro/micromixing models using probability density function methods. *Chemical Engineering Science*, 47(9–11):2853–2858.

Fox, R. O. (1992b). The Fokker–Planck closure for turbulent molecular mixing: Passive scalars. *Physics of Fluids*, 4(6):1230–1244.

Fox, R. O. (1994). Improved Fokker–Planck model for the joint scalar, scalar gradient PDF. *Physics of Fluids*, 6(1):334–348.

Fox, R. O. (1998). On the relationship between Lagrangian micromixing models and computational fluid dynamics. *Chemical Engineering and Processing: Process Intensification*, 37(6):521–535.

Fox, R. O. (1999). The Lagrangian spectral relaxation model for differential diffusion in homogeneous turbulence. *Physics of Fluids*, 11(6):1550–1571.

Fox, R. O. (2003). Computational models for turbulent reacting flows. Cambridge University Press.

Fox, R. O. (2009). Optimal Moment Sets for Multivariate Direct Quadrature Method of Moments. *Industrial & Engineering Chemistry Research*, 48(21):9686–9696.

Frankel, S. H., Madnia, C. K., and Givi, P. (1992). Modeling of the reactant conversion rate in a turbulent shear flow. *Chemical Engineering Communications*, 113(1):197–209.

Garcia, A. L., van den Broeck, C., Aertsens, M., and Serneels, R. (1987). A Monte Carlo simulation of coagulation. *Physica A: Statistical Mechanics and its Applications*, 143(3):535–546.

Garmory, A., Kim, I. S., Britter, R. E., and Mastorakos, E. (2009). Simulations of the dispersion of reactive pollutants in a street canyon, considering different chemical mechanisms and micromixing. *Atmospheric Environment*, 43(31):4670–4680.

Garmory, A. and Mastorakos, E. (2008). Aerosol nucleation and growth in a turbulent jet using the Stochastic Fields method. *Chemical Engineering Science*, 63(16):4078–4089.

Garmory, A., Richardson, E. S., and Mastorakos, E. (2006). Micromixing effects in a reacting plume by the Stochastic Fields method. *Atmospheric Environment*, 40(6):1078–1091.

Gautschi, W. (2004). *Orthogonal Polynomials: Computation and Approximation*. Oxford University Press.

Gavi, E., Rivautella, L., Marchisio, D. L., Vanni, M., Barresi, A. A., and Baldi, G. (2007). CFD modelling of nano-particle precipitation in confined impinging jet reactors. *Chemical Engineering Research and Design*, 85(5):735–744.

Gelbard, F. and Seinfeld, J. H. (1978). Numerical solution of the dynamic equation for particulate systems. *Journal of Computational Physics*, 28(3):357–375.

Gillespie, D. T. (1976). A general method for numerically simulating the stochastic time evolution of coupled chemical reactions. *Journal of Computational Physics*, 22(4):403–434.

Girimaji, S. S. (1991). Assumed β-pdf model for turbulent mixing: validation and extension to multiple scalar mixing. *Combustion Science and Technology*, 78:177.

Golub, G. H. and Welsch, J. H. (1969). Calculation of gauss quadrature rules. *Mathematics of Computation*, 23(106):221–230.

Goodson, M. and Kraft, M. (2002). An efficient stochastic algorithm for simulating nanoparticle dynamics. *Journal of Computational Physics*, 183(1):210–232.

Gordon, R. G. (1968). Error bounds in equilibrium statistical mechanics. *Journal of Mathematical Physics*, 9:655–662.

Greenberg, J. B., Alibagli, D., and Tambour, Y. (1986). An opposed jet quasi-monodisperse spray diffusion flame. *Combustion Science and Technology*, 50(4-6):255–270.

Greenberg, J. B., Silverman, I., and Tambour, Y. (1993). On the origins of spray sectional conservation equations. *Combustion and Flame*, 93(12):90–96.

Hounslow, M., Ryall, R., and Marshall, V. (1988). Discretized population balance for nucleation, growth, and aggregation. *AIChE Journal*, 34(11):1821–1832.

Hounslow, M. J. (1990). A discretized population balance for continuous systems at steady state. *AIChE Journal*, 36(1):106–116.

Hu, X., Passalacqua, A., and Fox, R. O. (2015). Application of quadrature-based uncertainty quantification to the NETL small-scale challenge problem SSCP-I. *Powder Technology*, 272:100–112.

Hulburt, H. M. and Katz, S. (1964). Some problems in particle technology: A statistical mechanical formulation. *Chemical Engineering Science*, 19(8):555–574.

Johnson, B. K. and Prud'homme, R. K. (2003). Chemical processing and micromixing in confined impinging jets. *AIChE Journal*, 49(9):2264–2282.

Jones, W. P. and Navarro-Martinez, S. (2007). Large eddy simulation of autoignition with a subgrid probability density function method. *Combustion and Flame*, 150(3):170–187.

Jones, W. P. and Navarro-Martinez, S. (2009). Numerical Study of n-Heptane Auto-ignition Using LES-PDF Methods. *Flow, Turbulence and Combustion*, 83(3):407–423.

Jones, W. P., Navarro-Martinez, S., and Rhl, O. (2007). Large eddy simulation of hydrogen auto-ignition with a probability density function method. *Proceedings of the Combustion Institute*, 31(2):1765–1771.

Juneja, A. and Pope, S. B. (1996). A DNS study of turbulent mixing of two passive scalars. *Physics of Fluids*, 8(8):2161–2184.

Kolmogoroff, A. (1931). ber die analytischen Methoden in der Wahrscheinlichkeitsrechnung. *Mathematische Annalen*, 104(1):415–458.

Koochesfahani, M. M. and Dimotakis, P. E. (1986). Mixing and chemical reactions in a turbulent liquid mixing layer. *Journal of Fluid Mechanics*, 170:83–112.

Kraichnan, R. H. (1989). Closures for probability distributions. *Bulletin of the American Physical Society*, 34:2298.

Kraichnan, R. H. (1990). Models of intermittency in hydrodynamic turbulence. *Physical Review Letters*, 65(5):575–578.

Kruis, F. E., Maisels, A., and Fissan, H. (2000). Direct simulation Monte Carlo method for particle coagulation and aggregation. *AIChE Journal*, 46(9):1735–1742.

Kumar, P. and Narayanan, S. (2006). Solution of Fokker-Planck equation by finite element and finite difference methods for nonlinear systems. *Sadhana - Academy Proceedings in Engineering Sciences*, 31:445–461.

Kumar, S. and Ramkrishna, D. (1996a). On the solution of population balance equations by discretization – I. A fixed pivot technique. *Chemical Engineering Science*, 51(8):1311–1332.

Kumar, S. and Ramkrishna, D. (1996b). On the solution of population balance equations by discretization – II. A moving pivot technique. *Chemical Engineering Science*, 51(8):1333–1342.

Lage, P. L. C. (2011). On the representation of QMOM as a weighted-residual method – The dual-quadrature method of generalized moments. *Computers & Chemical Engineering*, 35(11):2186–2203.

Lasheras, J. C., Eastwood, C., Martinez-Bazan, C., and Montanes, J. L. (2002). A review of statistical models for the break-up of an immiscible fluid immersed into a fully developed turbulent flow. *International Journal of Multiphase Flow*, 28(2):247–278.

Launder, B. E. and Sandham, N. D. (2002). *Closure Strategies for Turbulent and Transitional Flows*. Cambridge University Press, Cambridge.

Laurent, F. and Nguyen, T. T. (2017). Realizable second-order finite-volume schemes for the advection of moment sets of the particle size distribution. *Journal of Computational Physics*, 337:309–338.

Lee, K. and Matsoukas, T. (2000). Simultaneous coagulation and break-up using constant-n monte carlo. *Powder Technology*, 110(12):82–89.

Lee, K. W. (1983). Change of particle size distribution during Brownian coagulation. *Journal of Colloid and Interface Science*, 92(2):315–325.

Liffman, K. (1992). A direct simulation Monte-Carlo method for cluster coagulation. *Journal of Computational Physics*, 100(1):116–127.

Limpert, E., Stahel, W. A., and Abbt, M. (2001). Log-normal distribution across the sciences: keys and clues. *BioScience*, 51(5):341–352.

Lin, Y., Lee, K., and Matsoukas, T. (2002). Solution of the population balance equation using constant-number Monte Carlo. *Chemical Engineering Science*, 57(12):2241–2252.

Liu, Y., Cheng, C., Liu, Y., Prudhomme, R. K., and Fox, R. O. (2008). Mixing in a multi-inlet vortex mixer (MIVM) for flash nano-precipitation. *Chemical Engineering Science*, 63(11):2829–2842.

Liu, Z., Fox, R. O., Hill, J. C., and Olsen, M. G. (2015). A Batchelor Vortex Model for Mean Velocity of Turbulent Swirling Flow in a Macroscale Multi-Inlet Vortex Reactor. *Journal of Fluids Engineering*, 137(4):041204–041204.

Liu, Z., Passalacqua, A., Olsen, M. G., Fox, R. O., and Hill, J. C. (2016). Dynamic delayed detached eddy simulation of a multi-inlet vortex reactor. *AIChE Journal*, 62(7):2570–2578.

Luhar, A. K. and Sawford, B. L. (2005). Micromixing modelling of mean and fluctuating scalar fields in the convective boundary layer. *Atmospheric Environment*, 39(35):6673–6685.

Madadi-Kandjani, E. and Passalacqua, A. (2015). An extended quadrature-based moment method with log-normal kernel density functions. *Chemical Engineering Science*, 131:323–339.

Madnia, C. K., Frankel, S. H., and Givi, P. (1991). Direct numerical simulations of the unmixedness in a homogeneous reacting turbulent flow. *Chemical Engineering Communications*, 109(1):19–29.

Magnus, W., Oberhettinger, F., and Soni, R. P. (1966). *Formulas and theorems for the special functions of mathematical physics*. Springer–Verlag, Berlin.

Marchisio, D. L. and Fox, R. O. (2005). Solution of population balance equations using the direct quadrature method of moments. *Journal of Aerosol Science*, 36(1):43–73.

Marchisio, D. L. and Fox, R. O. (2013). *Computational Models for Polydisperse Particulate and Multiphase Systems*. Cambridge University Press, Cambridge.

Marchisio, D. L., Pikturna, J. T., Fox, R. O., Vigil, R. D., and Barresi, A. A. (2003a). Quadrature method of moments for population-balance equations. *AIChE Journal*, 49(5):1266–1276.

Marchisio, D. L., Vigil, R., and Fox, R. O. (2003b). Quadrature method of moments for aggregation-breakage processes. *Journal of Colloid and Interface Science*, 258(2):322–334.

Massot, M., Laurent, F., Kah, D., and de Chaisemartin, S. (2010). A robust moment method for evaluation of the disappearance rate of evaporating sprays. *SIAM Journal on Applied Mathematics*, 70(8):3203–3234.

McGraw, R. (1997). Description of aerosol dynamics by the quadrature method of moments. *Aerosol Science and Technology*, 27(2):255–265.

McMurtry, P. A. and Givi, P. (1989). Direct numerical simulations of mixing and reaction in a nonpremixed homogeneous turbulent flow. *Combustion and Flame*, 77(2):171–185.

Mead, L. R. and Papanicolaou, N. (1984). Maximum entropy in the problem of moments. *Journal of Mathematical Physics*, 25(8):2404–2417.

Meimaroglou, D. and Kiparissides, C. (2007). Monte Carlo simulation for the solution of the bi-variate dynamic population balance equation in batch particulate systems. *Chemical Engineering Science*, 62(1820):5295–5299.

Meyer, D. W. (2010). A new particle interaction mixing model for turbulent dispersion and turbulent reactive flows. *Physics of Fluids*, 22(3):035103.

Meyer, D. W. and Jenny, P. (2006). A mixing model for turbulent flows based on parameterized scalar profiles. *Physics of Fluids*, 18(3):035105.

Meyer, D. W. and Jenny, P. (2009). Micromixing models for turbulent flows. *Journal of Computational Physics*, 228(4):1275–1293.

Meyer, D. W. and Jenny, P. (2013). Accurate and computationally efficient mixing models for the simulation of turbulent mixing with PDF methods. *Journal of Computational Physics*, 247:192–207.

Muhr, H., David, R., Villermaux, J., and Jezequel, P. H. (1996). Crystallization and precipitation engineering-VI. Solving population balance in the case of the precipitation of silver bromide crystals with high primary nucleation rates by using the first order upwind differentiation. *Chemical Engineering Science*, 51(2):309–319.

Mungal, M. G. and Dimotakis, P. E. (1984). Mixing and combustion with low heat release in a turbulent shear layer. *Journal of Fluid Mechanics*, 148:349–382.

Nguyen, T. T., Laurent, F., Fox, R. O., and Massot, M. (2016). Solution of population balance equations in applications with fine particles: Mathematical modeling and numerical schemes. *Journal of Computational Physics*, 325:129–156.

Nooren, P. A., Wouters, H. A., Peeters, T. W. J., Roekaerts, D., Maas, U., and Schmidt, D. (1997). Monte Carlo PDF modelling of a turbulent natural-gas diffusion flame. *Combustion Theory and Modelling*, 1(1):79–96.

O'Brien, E. E. (1980). The probability density function (pdf) approach to reacting turbulent flows. In Libby, P. A. and Williams, F. A., editors, *Turbulent Reacting Flows*, number 44 in Topics in Applied Physics, pages 185–218. Springer Berlin Heidelberg.

O'Brien, E. E. and Jiang, T.-L. (1991). The conditional dissipation rate of an initially binary scalar in homogeneous turbulence. *Physics of Fluids A: Fluid Dynamics*, 3(12):3121–3123.

Overholt, M. R. and Pope, S. B. (1996). Direct numerical simulation of a passive scalar with imposed mean gradient in isotropic turbulence. *Physics of Fluids*, 8(11):3128–3148.

Perthame, B. (1992). Second-Order Boltzmann Schemes for Compressible Euler Equations in One and Two Space Dimensions. *SIAM Journal on Numerical Analysis*, 29(1):1–19.

Peters, N. (2000). *Turbulent Combustion*. Cambridge University Press, Cambridge, 1 edition.

Petitti, M., Nasuti, A., Marchisio, D. L., Vanni, M., Baldi, G., Mancini, N., and Podenzani, F. (2010). Bubble size distribution modeling in stirred gas-liquid reactors with QMOM augmented by a new correction algorithm. *AIChE Journal*, 56(1):36–53.

Pitsch, H. (2006). Large-Eddy Simulation of Turbulent Combustion. *Annual Review of Fluid Mechanics*, 38(1):453–482.

Poinsot, T. and Veynante, D. (2005). *Theoretical and Numerical Combustion, Second Edition*. R.T. Edwards, Inc., Philadelphia, 2 edition.

Pope, S. B. (1991). Mapping closures for turbulent mixing and reaction. *Theoretical and Computational Fluid Dynamics*, 2(5-6):255–270.

Pope, S. B. (2000). *Turbulent Flows*. Cambridge University Press, Cambridge.

Pope, S. B. (2013). A model for turbulent mixing based on shadow-position conditioning. *Physics of Fluids*, 25(11):110803.

Popov, P. P. and Pope, S. B. (2014). Large eddy simulation/probability density function simulations of bluff body stabilized flames. *Combustion and Flame*, 161(12):3100–3133.

Popov, P. P., Wang, H., and Pope, S. B. (2015). Specific volume coupling and convergence properties in hybrid particle/finite volume algorithms for turbulent reactive flows. *Journal of Computational Physics*, 294:110–126.

Pratsinis, S. E. (1988). Simultaneous nucleation, condensation, and coagulation in aerosol reactors. *Journal of Colloid and Interface Science*, 124(2):416–427.

Puel, F., Fevotte, G., and Klein, J. P. (2003). Simulation and analysis of industrial crystallization processes through multidimensional population balance equations. part 1: a resolution algorithm based on the method of classes. *Chemical Engineering Science*, 58(16):3715–3727.

Raman, V. and Pitsch, H. (2007). A consistent LES/filtered-density function formulation for the simulation of turbulent flames with detailed chemistry. *Proceedings of the Combustion Institute*, 31(2):1711–1719.

Ramkrishna, D. (2000). *Population balances: theory and applications to particulate systems in engineering*. Academic Press.

Randolph, A. (1964). A population balance for countable entities. *The Canadian Journal of Chemical Engineering*, 42(6):280–281.

Randolph, A. D. and Larson, M. A. (1988). *Theory of particulate processes: analysis and techniques of continuous crystallization*. Academic Press.

Reyes, J. N. J. (1989). Statistically derived conservation equations for fluid particle flows.

Richardson, E. S. and Chen, J. H. (2012). Application of PDF mixing models to premixed flames with differential diffusion. *Combustion and Flame*, 159(7):2398–2414.

Risken, H. (1989). *The Fokker-Planck Equation*, volume 18 of *Springer Series in Synergetics*. Springer Berlin Heidelberg, Berlin, Heidelberg.

Rosner, D. E. and Yu, S. (2001). MC simulation of aerosol aggregation and simultaneous spheroidization. *AIChE Journal*, 47(3):545–561.

Sabelnikov, V. and Soulard, O. (2005). Rapidly decorrelating velocity-field model as a tool for solving one-point Fokker-Planck equations for probability density functions of turbulent reactive scalars. *Physical Review E*, 72(1):016301.

Sabelnikov, V. and Soulard, O. (2006). White in Time Scalar Advection Model as a Tool for Solving Joint Composition PDF Equations. *Flow, Turbulence and Combustion*, 77(1-4):333–357.

Sawford, B. L. (2004). Micro-mixing modelling of scalar fluctuations for plumes in homogeneous turbulence. *Flow, Turbulence and Combustion*, 72(2-4):133–160.

Sawford, B. L. (2006). Lagrangian modeling of scalar statistics in a double scalar mixing layer. *Physics of Fluids*, 18(8):085108.

Shohat, J. A. and Tamarkin, J. D. (1943). *The Problem of Moments*. American Mathematical Soc.

Silva, L. F. L. R., Rodrigues, R. C., Mitre, J. F., and Lage, P. L. C. (2010). Comparison of the accuracy and performance of quadrature-based methods for population balance problems with simultaneous breakage and aggregation. *Computers & Chemical Engineering*, 34(3):286–297.

Smith, M. and Matsoukas, T. (1998). Constant-number Monte Carlo simulation of population balances. *Chemical Engineering Science*, 53(9):1777–1786.

Smoluchowski, M. v. (1916). Drei vortrge ber diffusion, brownsche bewegung und koagulation von kolloidteilchen. In Simon, H. T. and Debye, P., editors, *Physikalische Zeitschrift*, number 17, pages 557–585. S. Hirzel, Leipzig.

Spencer, B. F. and Bergman, L. A. (1993). On the numerical solution of the Fokker-Planck equation for nonlinear stochastic systems. *Nonlinear Dynamics*, 4(4):357–372.

Stollinger, M. and Heinz, S. (2010). Evaluation of scalar mixing and time scale models in PDF simulations of a turbulent premixed flame. *Combustion and Flame*, 157(9):1671–1685.

Subramaniam, S. and Pope, S. B. (1998). A mixing model for turbulent reactive flows based on Euclidean minimum spanning trees. *Combustion and Flame*, 115(4):487–514.

Sundaram, B., Klimenko, A. Y., Cleary, M. J., and Ge, Y. (2016). A direct approach to generalized multiple mapping conditioning for selected turbulent diffusion flame cases. *Combustion Theory and Modelling*, 20(4):735–764.

Tagliani, A. (1999). Hausdorff moment problem and maximum entropy: A unified approach. *Applied Mathematics and Computation*, 105(23):291–305.

Tsai, K. and Fox, R. O. (1994). PDF simulation of a turbulent seriesparallel reaction in an axisymmetric reactor. *Chemical Engineering Science*, 49(24):5141–5158.

Tsai, K. and Fox, R. O. (1995). Modeling multiple reactive scalar mixing with the generalized IEM model. *Physics of Fluids*, 7(11):2820–2830.

Valino, L. (1998). A Field Monte Carlo Formulation for Calculating the Probability Density Function of a Single Scalar in a Turbulent Flow. *Flow, Turbulence and Combustion*, 60(2):157–172.

Vanni, M. (2000). Approximate population balance equations for aggregation-breakage processes. *Journal of Colloid and Interface Science*, 221(2):143–160.

Vikas, V., Hauck, C., Wang, Z., and Fox, R. (2013a). Radiation transport modeling using extended quadrature method of moments. *Journal of Computational Physics*, 246:221–241.

Vikas, V., Wang, Z. J., and Fox, R. O. (2013b). Realizable high-order finite-volume schemes for quadrature-based moment methods applied to diffusion population balance equations. *Journal of Computational Physics*, 249:162–179.

Vikas, V., Wang, Z. J., Passalacqua, A., and Fox, R. O. (2011). Realizable high-order finite-volume schemes for quadrature-based moment methods. *Journal of Computational Physics*, 230(13):5328–5352.

Villermaux, J. and Devillon (1972). Represntation de la coalescence et de la redispersion des domaines de sgrgation dans un fluide par un modle d'interaction phnomnologique. In *In Proceedings of the 2nd International Symposium on Chemical Reaction Engineering*, pages 1–13. New York: Elsevier.

Villermaux, J. and Falk, L. (1994). A generalized mixing model for initial contacting of reactive fluids. *Chemical Engineering Science*, 49(24, Part 2):5127–5140.

Wang, H. and Kim, K. (2015). Effect of molecular transport on PDF modeling of turbulent non-premixed flames. *Proceedings of the Combustion Institute*, 35(2):1137–1145.

Wang, L. and Fox, R. O. (2004). Comparison of micromixing models for CFD simulation of nanoparticle formation. *AIChE Journal*, 50(9):2217–2232.

Wang, L., Marchisio, D., Vigil, R., and Fox, R. (2005a). CFD simulation of aggregation and breakage processes in laminar Taylor–Couette flow. *Journal of Colloid and Interface Science*, 282(2):380–396.

Wang, L., Vigil, R. D., and Fox, R. O. (2005b). CFD simulation of shear-induced aggregation and breakage in turbulent Taylor–Couette flow. *Journal of Colloid and Interface Science*, 285(1):167–178.

Weisstein, E. W. (1998). *CRC Concise Encyclopedia of Mathematics*. CRC Press.

Wheeler, J. C. (1974). Modified moments and Gaussian quadratures. *Rocky Mountain Journal of Mathematics*, 4:287–296.

Wilck, M. (2001). A general approximation method for solving integrals containing a lognormal weighting function. *Journal of Aerosol Science*, 32(9):1111–1116.

Wilf, H. S. (1962). *Mathematics for the Physical Sciences*. Dover Publications, New York.

Williams, M. M. R. and Loyalka, S. K. (1991). *Aerosol Science: Theory and Practice*. Pergamon, Oxford ; New York, 1^{st} edition.

Wright, D. L. (2007). Numerical advection of moments of the particle size distribution in eulerian models. *Journal of Aerosol Science*, 38(3):352–369.

Yeung, P. K., Donzis, D. A., and Sreenivasan, K. R. (2005). High-Reynolds-number simulation of turbulent mixing. *Physics of Fluids*, 17(8):081703.

Yeung, P. K., Xu, S., and Sreenivasan, K. R. (2002). Schmidt number effects on turbulent transport with uniform mean scalar gradient. *Physics of Fluids*, 14(12):4178–4191.

Yuan, C. and Fox, R. (2011). Conditional quadrature method of moments for kinetic equations. *Journal of Computational Physics*, 230(22):8216–8246.

Yuan, C., Laurent, F., and Fox, R. (2012). An extended quadrature method of moments for population balance equations. *Journal of Aerosol Science*, 51:1–23.

Zhao, H., Kruis, F. E., and Zheng, C. (2009). Reducing statistical noise and extending the size spectrum by applying weighted simulation particles in Monte Carlo simulation of coagulation. *Aerosol Science and Technology*, 43(8):781–793.

Zhao, H., Maisels, A., Matsoukas, T., and Zheng, C. (2007). Analysis of four Monte Carlo methods for the solution of population balances in dispersed systems. *Powder Technology*, 173(1):38–50.

Zhao, H. and Zheng, C. (2013). A population balance-Monte Carlo method for particle coagulation in spatially inhomogeneous systems. *Computers & Fluids*, 71:196–207.

Zhao, X.-Y., Bhagatwala, A., Chen, J. H., Haworth, D. C., and Pope, S. B. (2016). An a priori DNS study of the shadow-position mixing model. *Combustion and Flame*, 165:223–245.

CHAPTER 3. APPLICATION OF THE FOKKER-PLANCK MOLECULAR MIXING MODEL TO TURBULENT SCALAR MIXING USING MOMENT METHODS

This chapter was published as a journal article titled "Application of the Fokker-Planck molecular mixing model to turbulent scalar mixing using moment methods" in *Physics of Fluids* with authors E. Madadi-Kandjani R. O. Fox and A. Passalacqua (2017).

Abstract

An extended quadrature method of moments using the β kernel density function (β-EQMOM) is used to approximate solutions to the evolution equation for univariate and bivariate composition probability distribution functions (PDF) of a passive scalar for binary and ternary mixing. The key element of interest is the molecular mixing term, which is described using the Fokker–Planck (FP) molecular mixing model. The direct numerical simulations (DNS) of Eswaran & Pope (Physics of Fluids 31, 506, 1988), and the amplitude mapping closure (AMC) of Pope (Theoretical and Computational Fluid Dynamics 2, 255, 1991) are taken as reference solutions to establish the accuracy of the FP model in the case of binary mixing. The DNS of Juneja & Pope (Physics of Fluids 8, 2161, 1996) are used to validate the results obtained for ternary mixing. Simulations are performed with both the conditional scalar dissipation rate (CSDR) proposed by Fox (*Computational Methods for Turbulent Reacting Flows*, Cambridge University Press, 2003) and the CSDR from AMC. Using scalar moments up to fourth order, the ability of the FP model to capture the evolution of the shape of the PDF, important in turbulent mixing problems, is demonstrated. Compared to the widely used assumed β-PDF model (Girimaji,

Combustion Science & Technology 78, 177 1991), the β-EQMOM solution to the FP model more accurately describes the initial mixing process with a relatively small increase in computational cost.

3.1 Introduction

The spatial and temporal evolution of a passive scalar in a turbulent mixing process can be described using an evolution equation for the probability density function (PDF) of the system composition (Pope, 2000; Fox, 2003). Solutions of the equation for the composition PDF provide a one-point statistical description of the behavior of the scalar composition field, during its evolution from the unmixed to the mixed state (Broadwell and Breidenthal, 1982; Kooches-fahani and Dimotakis, 1986; Mungal and Dimotakis, 1984; Girimaji, 1991; Cremer et al., 1994; McMurtry and Givi, 1989; Eswaran and Pope, 1988). Due to the importance of turbulent mixing in industrial and environmental applications, several methods have been developed to obtain such solutions.

Before summarizing the most common approaches used to obtain the composition PDF from its evolution equation, it is worth reminding that the most accurate approach for modeling turbulent mixing is direct numerical simulation (DNS) (Eswaran and Pope, 1988; O'Brien and Jiang, 1991; Overholt and Pope, 1996; Yeung et al., 2005, 2002), which consists in directly discretizing the physical space, and solving the transport equation for the passive scalar along with the Navier-Stokes equation (Pope, 2000). However, this method is computationally prohibitive when applied to practical problems, due to the requirements in terms of spatial resolution, which needs to explicitly resolve the smallest of the Kolmogorov and Batchelor scales. Other strategies include large-eddy simulation, such as those discussed in (Pitsch, 2006; Popov and Pope, 2014; Popov et al., 2015). In the context of PDF methods, which aim at finding approximate solutions for the evolution equation of the composition PDF, Lagrangian PDF methods Pope (2000); Fox (2003); Meyer and Jenny (2006); Meyer (2010) are computationally more affordable than DNS, but still computationally intensive for many practical applications at the industrial and environmental scales. Stochastic field methods were proposed Valino (1998); Sabelnikov and Soulard (2005); Jones et al. (2007); Jones and Navarro-Martinez (2007, 2009); Garmory

et al. (2006); Garmory and Mastorakos (2008); Garmory et al. (2009); Sabelnikov and Soulard (2006), in which the evolution of the composition PDF is approximated using a set of Eulerian stochastic fields, defined over the entire computational domain. The spatio-temporal evolution of these fields is regulated by stochastic partial differential equations (PDEs). A number of PDEs equal to the product between the number of composition variables, and the number of stochastic fields need to be solved. For practical applications, Reynolds-averaged Navier-Stokes (RANS) simulations are particularly attractive to describe turbulent mixing processes due to their low computational cost. In RANS methods, the evolution equation of the composition PDF is closed by introducing molecular mixing models, which are defined in terms of one-point turbulence statistics. As it will be illustrated later, these models typically require the scalar dissipation rate to be modeled, which may not be a trivial task in general non-homogeneous problems.

In many applications, a presumed β-PDF model is employed to describe the mixture fraction (Girimaji, 1991), which requires the solution of two RANS equations: one for the mixture-fraction mean, and one for its variance. To go beyond the β-PDF model, the Fokker–Planck (FP) model (Fox, 1992b, 1994, 2003) can be used to close the molecular mixing term in the composition PDF transport equation. The resulting nonlinear FP equation must then be solved, which is a nontrivial task.

The Fokker-Planck equation was developed by Fokker (1914) and Planck (Risken, 1989), to describe the time evolution of the velocity PDF of a particle under the effect of random motions and drag forces. Kolmogoroff (1931) also obtained the equation independently, while Smoluchowski (1916) obtained the equivalent of the Fokker-Planck equation for the particle position in Brownian motion.

Analytical solutions for FP equations are possible only in a limited set of cases (Risken, 1989). As a consequence, numerical methods have been developed to find approximate solutions in cases of general interest. Spencer and Bergman (1993) and Kumar and Narayanan (2006) used the finite-difference method to directly discretize the spatial and composition spaces. As with Lagrangian PDF methods, due to the transient nature of mixing problems and to the dimensionality of the composition PDF, this approach still carries a significant computational cost,

which makes it unattractive for many applications. As a consequence, alternative approaches have been developed to compute moments of the composition PDF, rather than to capture its entire evolution. These methods are based on the idea that the quantities of interest in most applications can be related to the calculated moments. However, when applied to reactive scalars with nonlinear chemical source terms, integrals with respect to the unknown composition PDF must be evaluated Fox (2003); Pitsch (2006). For this purpose, an efficient and accurate method for reconstructing the composition PDF from its moments is required (Marchisio and Fox, 2013).

In this work, the extended quadrature method of moments (EQMOM) with β kernel density functions (Yuan et al., 2012) is adopted to approximate solutions to the statistically homogeneous composition PDF equation, which is closed using the FP model for molecular mixing. EQMOM is an extension of the quadrature method of moments (QMOM), initially proposed by McGraw (1997) for problems involving aerosols, and later applied to chemical engineering problems by Marchisio et al. (2003b). In the EQMOM approach (Yuan et al., 2012), the composition PDF is approximated by a discrete sum of positive kernel density functions (KDF), instead of the Dirac delta functions used in QMOM. This allows a continuous reconstruction of the PDF to be obtained from a finite set of integer moments. The choice of the functional form of the kernel density function is based on the support of the PDF whose moments are to be reconstructed, and on the explicit knowledge of the recurrence relation of the polynomials orthogonal to such kernel density function. In particular, if the PDF is defined on the compact support $[0, 1]$, the β density function is an appropriate choice, while for a PDF defined on the positive real like, the gamma or log-normal density functions would be adequate.

It is worth noting that, differently from the direct QMOM (Marchisio and Fox, 2005) used in multi-environment PDF models (Fox, 1998, 2003; Wang and Fox, 2004), which directly computes the quadrature weights and abscissae associated to the moments of the composition PDF, EQMOM solves for the moments of the PDF, which are conserved quantities in the calculation. For spatially inhomogeneous cases, this feature allows a realizable finite-volume scheme to be formulated, as illustrated in Vikas et al. (2011, 2013b). While we consider homogeneous problems in this case, a brief discussion of the extension to non-homogeneous

problems is provided in the conclusions. Hereinafter, the turbulent mixing model resulting from the application of β-EQMOM to the composition PDF equation, closed with the FP model, will be referred to as the β-EQMOM-FP model.

The primary objectives of the work are two fold. First, the version of the FP molecular mixing model proposed by Fox (2003) is validated against DNS for binary (Eswaran and Pope, 1988) and ternary (Juneja and Pope, 1996) mixing. To the best of our knowledge, this step has not been previously reported for the FP model. In doing so, we demonstrate that the FP model for binary mixing is essentially identical to the amplitude mapping closure (AMC) (Pope, 1991), including at very short times, where the β-PDF model yields poor predictions. Second, the β-EQMOM approach is shown to yield accurate approximations for the composition PDF equation using as few as four moments (i.e. $\langle\phi\rangle$, $\langle\phi^2\rangle$, $\langle\phi^3\rangle$, $\langle\phi^4\rangle$) for binary mixing. This result opens the possibility of applying the β-EQMOM-FP model in practical computational fluid dynamic (CFD) simulations of complex flows as an alternative to the widely used assumed β-PDF model. In addition, we demonstrate that the β-EQMOM-FP model can be used for ternary mixing problems for which assumed PDF models are not available (Fox, 2003).

The remainder of the paper is structured as follows. In Sec. 3.2 the evolution equation for the composition PDF is reported, and the FP molecular mixing model is summarized. The β-EQMOM approach is introduced in Sec. 3.4, while the moment transport equations and the corresponding source terms originating from the equation forthe composition PDF are presented in Sec. 3.3. The AMC, used as a reference to validate the FP model, is summarized in Sec. 3.5. Next, the β-EQMOM-FP approach is validated in Sec. 3.6. In particular, Sec. 3.6.3 shows the validation results for the binary mixing cases of Eswaran and Pope (1988) using the conditional scalar dissipation rate (CSDR) proposed by Fox (2003), and Sec. 3.6.4 presents the corresponding results obtained using the CSDR from AMC. Section 3.6.5 concludes with the application of the β-EQMOM-FP approach to the ternary mixing case of Juneja and Pope (1996).

3.2 Evolution equation for the composition PDF

The evolution equation of the composition PDF $f_{\boldsymbol{\phi}}(\boldsymbol{\psi}; \mathbf{x}, t)$ for nonreacting, passive scalars, assuming constant density, reads (Pope, 2000; Fox, 2003)

$$\underbrace{\frac{\partial f_{\boldsymbol{\phi}}}{\partial t}}_{\substack{\text{rate of change}}} + \underbrace{\langle U_i \rangle \frac{\partial f_{\boldsymbol{\phi}}}{\partial x_i}}_{\substack{\text{convection in physical space} \\ \text{due to the mean velocity} \\ \text{(macromixing)}}} + \underbrace{\frac{\partial}{\partial x_i}\left(\langle u_i | \boldsymbol{\psi} \rangle f_{\boldsymbol{\phi}}\right)}_{\substack{\text{convection in physical space due to} \\ \text{the scalar conditioned velocity fluctuations} \\ \text{(mesomixing)}}} =$$

$$\underbrace{-\frac{\partial}{\partial \psi_i}\left(\left\langle \Gamma_i \nabla^2 \phi_i' | \boldsymbol{\psi} \right\rangle f_{\boldsymbol{\phi}}\right) - \frac{\partial}{\partial \psi_i}\left[\left(\Gamma_i \nabla^2 \langle \phi_i \rangle\right) f_{\boldsymbol{\phi}}\right]}_{\substack{\text{transport in composition space} \\ \text{due to the molecular mixing} \\ \text{(micromixing)}}}, \quad (3.1)$$

where repeated indices imply summation. The i-th composition variable is denoted by ϕ_i, and its phase-space component by ψ_i. Fluctuations about the mean are denoted with a prime: ϕ_i'. In this work, we consider only statistically homogeneous cases for which the convection in physical space is null. The molecular diffusivity of species i is denoted by Γ_i. For statistically homogeneous systems, $\nabla^2 \langle \phi_i \rangle$ is null, leaving only the first term on the right-hand side of (5.1). In order to close this term, a molecular mixing model is needed. Two models will be considered in this work: the interaction-by-exchange-with-the-mean (IEM) model (Villermaux and Falk, 1994; Dopazo and O'Brien, 1973) and the FP model (Fox, 1992b, 1994, 1999, 2003).

The IEM model is the simplest mixing model as it assumes a linear relaxation of the concentration towards its mean (Fox, 2003; Pope, 2000). The generalized IEM expression for the conditional diffusion is

$$\left\langle \Gamma_i \nabla^2 \phi_i' | \boldsymbol{\psi} \right\rangle = \sum_{j,k} \frac{1}{2} \varepsilon_{ij} \left\langle \phi_j' \phi_k' \right\rangle^{-1} \left(\langle \phi_k \rangle - \psi_k\right) \quad (3.2)$$

where $\varepsilon_{ij} = \left\langle (\Gamma_i \Gamma_j)^{1/2} \nabla \phi_i' \cdot \nabla \phi_j' \right\rangle$ is the scalar covariance dissipation rate (SDR) for component i, j, $\langle \phi_i \rangle$ is the scalar mean for component i, and $\left\langle \phi_j' \phi_k' \right\rangle^{-1}$ is the i, j component of the inverse covariance matrix of the scalars (Fox, 2003). In applications, it is almost always assumed the timescales $1/\tau_{ii} = \sum_j \varepsilon_{ij} \left\langle \phi_j' \phi_i' \right\rangle^{-1}$ are the same for all components i. Moreover, it is also assumed that the scalars are independent so that $\sum_j \varepsilon_{ij} \left\langle \phi_j' \phi_k' \right\rangle^{-1} = 0$ when $i \neq k$ (Fox, 2003; Pope, 2000). While the IEM model has been widely used, in its original formulation Dopazo

and O'Brien (1973), it does not account for differential diffusion (see Richardson and Chen (2012) for an extension including this effect), and it assumes that all the scalars mix with a single timescale. As a consequence, in the absence of gradients in the scalar mean, the shape of the scalar PDF does not evolve with time.

In order to capture the change in shape, Fox (1992b, 1994) introduced the FP molecular mixing model, as possible solution to the limitations of the IEM model. By observing that when the Γ_i are equal, the conditional diffusion can be related to the joint CSDR $\langle \epsilon_{ij} | \boldsymbol{\psi} \rangle = \left\langle (\Gamma_i \Gamma_j)^{1/2} \nabla \phi_i' \cdot \nabla \phi_j' | \boldsymbol{\psi} \right\rangle$ by (Fox, 2003)

$$\left\langle \Gamma_i \nabla^2 \phi_i' | \boldsymbol{\psi} \right\rangle = \frac{1}{2 f_{\boldsymbol{\phi}}} \sum_j \frac{\partial}{\partial \psi_j} \left(\langle \epsilon_{ij} | \boldsymbol{\psi} \rangle \, f_{\boldsymbol{\phi}} \right). \tag{3.3}$$

However, Eq. (3.3) leads to negative diffusion in phase space, as discussed by Pope (2000). To avoid this problem, in the FP model the conditional diffusion is modeled as (Fox, 2003)

$$\left\langle \Gamma_i \nabla^2 \phi_i' | \boldsymbol{\psi} \right\rangle = (c_{\mathrm{FP}} + 1) \left\langle \Gamma_i \nabla^2 \phi_i' | \boldsymbol{\psi} \right\rangle - \frac{c_{\mathrm{FP}}}{2 f_{\boldsymbol{\phi}}} \sum_j \frac{\partial}{\partial \psi_j} \left(\langle \epsilon_{ij} | \boldsymbol{\psi} \rangle \, f_{\boldsymbol{\phi}} \right) \tag{3.4}$$

where c_{FP} is a positive constant that controls the diffusive relaxation rate for the shape of the PDF. The generalized IEM model in (5.3) is then used to close the first term on the right-hand side of Eq. (3.4) (Fox, 2003):

$$\left\langle \Gamma_i \nabla^2 \phi_i' | \boldsymbol{\psi} \right\rangle = \left(\frac{c_{\mathrm{FP}} + 1}{2} \right) \sum_{j,k} \varepsilon_{ij} \left\langle \phi_j' \phi_k' \right\rangle^{-1} \left(\langle \phi_k \rangle - \psi_k \right) - \frac{c_{\mathrm{FP}}}{2 f_{\boldsymbol{\phi}}} \sum_j \frac{\partial}{\partial \psi_j} \left(\langle \epsilon_{ij} | \boldsymbol{\psi} \rangle \, f_{\boldsymbol{\phi}} \right). \tag{3.5}$$

This formulation yields the generalized IEM model in the case of $c_{\mathrm{FP}} = 0$. Here, $c_{\mathrm{FP}} = 10$ is chosen to ensure an accurate reproduction of the results obtained in comparison with AMC (see Section 3.6.2 for details).

Eliminating the terms representing transport in physical space, the evolution equation for a univariate composition PDF can be written as

$$\frac{\partial f_\phi}{\partial t} = R\left(\psi; t\right) \tag{3.6}$$

where $f_\phi = f_\phi\left(\psi; t\right)$, and $R\left(\psi; t\right)$ is the source term due to micromixing. The models for $R\left(\psi; t\right)$ using the IEM and FP models are, respectively,

$$R_{\mathrm{IEM}}\left(\psi; t\right) = -\frac{\partial}{\partial \psi} \left[\frac{\varepsilon_\phi}{2 \left\langle \phi'^2 \right\rangle} \left(\langle \phi \rangle - \psi \right) f_\phi \right], \tag{3.7}$$

$$R_{\mathrm{FP}}\left(\psi;t\right)=-\frac{c_{\mathrm{FP}}+1}{2}\frac{\partial}{\partial\psi}\left[\frac{\varepsilon_{\phi}}{\langle\phi'^{2}\rangle}\left(\langle\phi\rangle-\psi\right)f_{\phi}\right]+\frac{c_{\mathrm{FP}}}{2}\frac{\partial^{2}}{\partial\psi^{2}}\left(\langle\epsilon_{\phi}|\psi\rangle\,f_{\phi}\right) \tag{3.8}$$

where the SDR ε_{ϕ} is the expected value of the CSDR, which we indicate with $\langle\epsilon_{\phi}|\psi\rangle$. The form of the CSDR must be provided by the user to close the FP model (Fox, 2003). In Sec. 3.3.1, we consider two possible closures based on the β PDF (Fox, 2003) and AMC (Pope, 1991).

In the case of a bivariate composition PDF for the mixture-fraction vector $\boldsymbol{\xi}$ with phase-space vector $\boldsymbol{\zeta}$ (Fox, 2003), the statistically homogeneous version of Eq. (5.1) with the mixing term closed using the FP model yields

$$\frac{\partial f_{\boldsymbol{\xi}}}{\partial t}=-\frac{c_{\mathrm{FP}}+1}{2}\sum_{i,j,k=1}^{2}\frac{\partial}{\partial\zeta_{i}}\left[\varepsilon_{ij}\left\langle\xi_{j}'\xi_{k}'\right\rangle^{-1}\left(\langle\xi_{k}\rangle-\zeta_{k}\right)f_{\boldsymbol{\xi}}\right]+\frac{c_{\mathrm{FP}}}{2}\sum_{i,j=1}^{2}\frac{\partial^{2}}{\partial\zeta_{i}\partial\zeta_{j}}\left(\langle\epsilon_{ij}|\zeta_{1},\zeta_{2}\rangle\,f_{\boldsymbol{\xi}}\right) \tag{3.9}$$

where ε_{ij} is the expected value of the joint CSDR $\langle\epsilon_{ij}|\zeta_{1},\zeta_{2}\rangle$. The components of the inverse covariance matrix are defined by

$$\begin{aligned}
\left\langle\xi_{1}'\xi_{1}'\right\rangle^{-1}&=\frac{\left\langle\xi_{2}'^{2}\right\rangle}{\left\langle\xi_{1}'^{2}\right\rangle\left\langle\xi_{2}'^{2}\right\rangle-\left\langle\xi_{1}'\xi_{2}'\right\rangle^{2}},\\
\left\langle\xi_{1}'\xi_{2}'\right\rangle^{-1}&=-\frac{\left\langle\xi_{1}'\xi_{2}'\right\rangle}{\left\langle\xi_{1}'^{2}\right\rangle\left\langle\xi_{2}'^{2}\right\rangle-\left\langle\xi_{1}'\xi_{2}'\right\rangle^{2}},\\
\left\langle\xi_{2}'\xi_{2}'\right\rangle^{-1}&=\frac{\left\langle\xi_{1}'^{2}\right\rangle}{\left\langle\xi_{1}'^{2}\right\rangle\left\langle\xi_{2}'^{2}\right\rangle-\left\langle\xi_{1}'\xi_{2}'\right\rangle^{2}}.
\end{aligned} \tag{3.10}$$

As in the univariate case, a closure is required for the joint CSDR. Fox (2003) proposed the following closure:

$$\begin{aligned}
\langle\epsilon_{11}|\zeta_{1},\zeta_{2}\rangle&=\alpha\zeta_{1}\left(1-\zeta_{1}-\zeta_{2}\right)-\beta\zeta_{1}\zeta_{2},\\
\langle\epsilon_{12}|\zeta_{1},\zeta_{2}\rangle&=\beta\zeta_{1}\zeta_{2},\\
\langle\epsilon_{22}|\zeta_{1},\zeta_{2}\rangle&=\gamma\zeta_{2}\left(1-\zeta_{1}-\zeta_{2}\right)-\beta\zeta_{1}\zeta_{2}
\end{aligned} \tag{3.11}$$

where

$$\alpha=\frac{\varepsilon_{11}+\varepsilon_{12}}{\langle\xi_{1}\left(1-\xi_{1}-\xi_{2}\right)\rangle},\ \beta=\frac{\varepsilon_{12}}{\langle\xi_{1}\xi_{2}\rangle},\ \gamma=\frac{\varepsilon_{22}+\varepsilon_{12}}{\langle\xi_{2}\left(1-\xi_{1}-\xi_{2}\right)\rangle}. \tag{3.12}$$

As described in Fox (2003), this closure ensures that the joint PDF found by solving (3.9) is nonzero only inside the phase-space triangle defined by $0\leq\zeta_{i}$ and $0\leq\zeta_{1}+\zeta_{2}\leq1$ (i.e., the phase-space diffusive flux is null in the direction normal to the boundary). The three SDR components in (3.12) must be supplied by a separate model for the scalar covariance dissipation rate. By definition the 2×2 matrix with components ε_{ij} has to be symmetric and non-negative.

In Sec. 3.6.5 we relate $\boldsymbol{\xi}$ to the two scalars (ϕ_1, ϕ_2) used in the ternary mixing case of Juneja and Pope (1996), for which the covariance and the cross SDR (i.e. ε_{12}) are null.

3.3 Transport equations for the moments of the composition PDF

Transport equations for the moments are now obtained for the univariate and bivariate cases considered in the present work.

3.3.1 Univariate case

The moment of order m of the univariate PDF $f_\phi(\psi;t)$ is defined as

$$\langle \phi^m \rangle (t) = \int f_\phi(\psi;t)\, \psi^m \mathrm{d}\psi. \tag{3.13}$$

Multiplying both sides of Eq. (3.6) by ψ^m and integrating with respect to ψ, we obtain

$$\int \psi^m \frac{\partial f_\phi}{\partial t} \mathrm{d}\psi = \int \psi^m R(\psi;t)\, \mathrm{d}\psi. \tag{3.14}$$

Observing that differentiation and integration commute on the left-hand side of Eq. (3.14), and indicating with $R_m(t)$ the moment of order m of $R(\psi,t)$

$$R_m(t) = \int \psi^m R(\psi;t)\, \mathrm{d}\psi, \tag{3.15}$$

the transport equations for the moments of $f_\phi(\psi;t)$ are obtained:

$$\frac{\partial \langle \phi^m \rangle}{\partial t} = R_m(t). \tag{3.16}$$

The expression for the source term obtained from the IEM model is

$$R_{m,\mathrm{IEM}}(t) = \frac{m\varepsilon_\phi}{2\langle \phi'^2 \rangle} \left(\langle \phi^{m-1} \rangle \langle \phi \rangle - \langle \phi^m \rangle \right) \tag{3.17}$$

where $\langle \phi'^2 \rangle = \langle \phi^2 \rangle - \langle \phi \rangle^2$. Note that this expression is closed for the integer moments up to order $m \geq 0$.

The form of the source term $R_{m,\mathrm{FP}}$ for the FP model depends on the choice for the functional form of the CSDR. As this choice essentially determines the predicted shape of the scalar PDF,

it is the most important part of the FP model. Based on the β PDF with support $[0,1]$, Fox (2003) proposed

$$\langle \epsilon_\phi | \psi \rangle = \varepsilon_\phi \frac{\psi\left(1-\psi\right)}{\langle \phi \rangle - \langle \phi^2 \rangle}, \tag{3.18}$$

which leads to a source term for the moment transport equations given by

$$R_{m,\mathrm{FP}}\left(t\right) = \frac{c_{\mathrm{FP}}+1}{2}\frac{m\varepsilon_\phi}{\langle \phi'^2 \rangle}\left(\left\langle \phi^{m-1}\right\rangle \langle \phi \rangle - \langle \phi^m \rangle\right) + \frac{m\left(m-1\right)c_{\mathrm{FP}}\varepsilon_\phi\left(\left\langle \phi^{m-1}\right\rangle - \langle \phi^m \rangle\right)}{2\left(\langle \phi \rangle - \langle \phi^2 \rangle\right)}. \tag{3.19}$$

It is important to note that (3.19) is closed for the moments up to order $m \geq 0$. (The cases $m = 0, 1$ are trivial.) In other words, the predicted values of the moments will not depend on how the scalar PDF is reconstructed from the moments (e.g. using β-EQMOM). The case of a scalar PDF with support $[-1,1]$ is treated by applying a linear transformation to map the support to $[0,1]$, in which case the numerator of (3.18) is $1-\psi^2$ (Fox, 2003). In Sec. 3.5 we introduce an alternative choice to (3.18) based on the AMC (Pope, 1991).

3.3.2 Bivariate case

The moments of the joint mixture-fraction PDF $f_{\boldsymbol{\xi}}\left(\boldsymbol{\zeta};t\right)$, in which $\boldsymbol{\zeta} = \left(\zeta_1,\zeta_2\right) \in \Omega = \{0 \leq \zeta_i,\ 0 \leq \zeta_1+\zeta_2 \leq 1\}$, are defined as

$$\langle \xi_1^m \xi_2^n \rangle\left(t\right) = \int_\Omega f_{\boldsymbol{\xi}}\left(\zeta_1,\zeta_2;t\right)\zeta_1^m\zeta_2^n \mathrm{d}\zeta_1\mathrm{d}\zeta_2. \tag{3.20}$$

Multiplying both sides of Eq. (3.9) by $\zeta_1^m\zeta_2^n$, and integrating with respect to ζ_1 and ζ_2, yields the transport equations for the moments of $f_{\boldsymbol{\xi}}\left(\zeta_1,\zeta_2;t\right)$:

$$\frac{\partial \langle \xi_1^m \xi_2^n \rangle}{\partial t} = R_{mn}\left(t\right) \tag{3.21}$$

where $R_{mn}\left(t\right)$ is the moment of the source term

$$R_{mn}\left(t\right) = \int_\Omega R\left(\zeta_1,\zeta_2;t\right)\zeta_1^m\zeta_2^n \mathrm{d}\zeta_1\mathrm{d}\zeta_2 \tag{3.22}$$

For the FP model with the joint CSDR closure in (3.11), this yields

$$
\begin{aligned}
R_{mn,\mathrm{FP}}(t) = {} & \frac{c_{\mathrm{FP}}+1}{2} m \left(\varepsilon_{11}\left\langle \xi_1'\xi_1' \right\rangle^{-1} + \varepsilon_{12}\left\langle \xi_1'\xi_2' \right\rangle^{-1}\right)\left(\left\langle \xi_1^{m-1}\xi_2^{n}\right\rangle \left\langle \xi_1\right\rangle - \left\langle \xi_1^{m}\xi_2^{n}\right\rangle\right) \\
& + \frac{c_{\mathrm{FP}}+1}{2} m \left(\varepsilon_{11}\left\langle \xi_1'\xi_2' \right\rangle^{-1} + \varepsilon_{12}\left\langle \xi_2'\xi_2' \right\rangle^{-1}\right)\left(\left\langle \xi_1^{m-1}\xi_2^{n}\right\rangle \left\langle \xi_2\right\rangle - \left\langle \xi_1^{m-1}\xi_2^{n+1}\right\rangle\right) \\
& + \frac{c_{\mathrm{FP}}+1}{2} n \left(\varepsilon_{12}\left\langle \xi_1'\xi_1' \right\rangle^{-1} + \varepsilon_{22}\left\langle \xi_1'\xi_2' \right\rangle^{-1}\right)\left(\left\langle \xi_1^{m}\xi_2^{n-1}\right\rangle \left\langle \xi_1\right\rangle - \left\langle \xi_1^{m+1}\xi_2^{n-1}\right\rangle\right) \\
& + \frac{c_{\mathrm{FP}}+1}{2} n \left(\varepsilon_{12}\left\langle \xi_1'\xi_2' \right\rangle^{-1} + \varepsilon_{22}\left\langle \xi_2'\xi_2' \right\rangle^{-1}\right)\left(\left\langle \xi_1^{m}\xi_2^{n-1}\right\rangle \left\langle \xi_2\right\rangle - \left\langle \xi_1^{m}\xi_2^{n}\right\rangle\right) \\
& + \frac{c_{\mathrm{FP}}}{2} m(m-1)\left[\alpha\left(\left\langle \xi_1^{m-1}\xi_2^{n}\right\rangle - \left\langle \xi_1^{m}\xi_2^{n}\right\rangle - \left\langle \xi_1^{m-1}\xi_2^{n+1}\right\rangle\right) - \beta\left\langle \xi_1^{m-1}\xi_2^{n+1}\right\rangle\right] \\
& + \frac{c_{\mathrm{FP}}}{2} n(n-1)\left[\gamma\left(\left\langle \xi_1^{m}\xi_2^{n-1}\right\rangle - \left\langle \xi_1^{m+1}\xi_2^{n-1}\right\rangle - \left\langle \xi_1^{m}\xi_2^{n}\right\rangle\right) - \beta\left\langle \xi_1^{m+1}\xi_2^{n-1}\right\rangle\right] \\
& + c_{\mathrm{FP}} mn\beta \left\langle \xi_1^{m}\xi_2^{n}\right\rangle
\end{aligned}
\tag{3.23}
$$

where $\left\langle \xi_i'\xi_j' \right\rangle^{-1}$ are the inverse components defined in (3.10). If we denote the maximum moment order by K (i.e., $0 \leq n+m \leq K$), it can be observed that (3.23) is closed for the set of bivariate moments up to order K. Thus, as in the univariate case in (3.19), the FP model solution for the bivariate moments does not depend on how the joint mixture-fraction PDF is reconstructed.

If the time scales $1/\tau_i = \sum_j \varepsilon_{ij}\left\langle \xi_j'\xi_i' \right\rangle^{-1}$ are assumed to be equal to τ_ϕ, then $\varepsilon_{12} = \left\langle \xi_1'\xi_2' \right\rangle/\tau_\phi$ in the standard model. The time scale τ_ϕ must then be related to the turbulence time scales to close the FP model. In this work, we either take τ_ϕ directly from the DNS data, or simply use it as a fixed parameter to rescale the time t in the moment evolution equations.

3.4 Extended quadrature method of moments

The β-EQMOM (Madadi-Kandjani and Passalacqua, 2015; Marchisio and Fox, 2013; Yuan et al., 2012; Chalons et al., 2010; Nguyen et al., 2016) is used in this study to compute an approximate solution to the univariate PDF transport equation. In this method, a univariate PDF is approximated by a weighted sum of non-negative KDFs $\delta_\sigma(\psi, \psi_i)$:

$$
f(\psi;t) \approx \sum_{\alpha=1}^{\mathrm{N}} w_\alpha \delta_\sigma\left(\psi, \left\langle \phi \right\rangle_\alpha\right) \tag{3.24}
$$

where w_α and $\left\langle \phi \right\rangle_\alpha$ are, respectively, the weights and abscissae associated with the Gaussian quadrature computed from the first 2N transported moments. The right-hand side of Eq. (3.24)

contains $2\mathrm{N}+1$ unknowns: N weights $(w_1, w_2, \cdots, w_\mathrm{N})$, N abscissae $(\langle\phi\rangle_1, \langle\phi\rangle_2, \cdots, \langle\phi\rangle_\mathrm{N})$ and the parameter σ, assumed to be common for all KDFs (Yuan et al., 2012). The value of σ is determined by enforcing that the last moment of a set with an odd number of moments (a total of $2\mathrm{N}+1$ moments) is preserved by the approximated PDF (Nguyen et al., 2016).

The choice of the KDF depends on the support of the PDF to be reconstructed and on the ease of computation of the orthogonal polynomials associated with the KDF. Previous works on the validation of the assumed PDF approach in turbulent mixing (Madnia et al., 1991; Frankel et al., 1992) compared the β-PDF with the mixture-fraction PDF reconstructed from DNS in both homogeneous flow and turbulent shear flow. In general, it was found that the assumed β-PDF gives a reasonable approximation of the mixture-fraction PDF, especially when the mixture-fraction variance is much less than one. We will then use the β KDF (Yuan et al., 2012) to formulate the β-EQMOM closures used in this work. In theory, any other KDF with support $[0, 1]$ could be used for this purpose (Yuan et al., 2012).

The β KDF is defined as

$$\delta_\sigma\left(\psi, \langle\phi\rangle_\alpha\right) = \frac{\psi^{\lambda_\alpha - 1}\left(1-\psi\right)^{\mu_\alpha - 1}}{\mathrm{B}\left(\lambda_\alpha, \mu_\alpha\right)}, \ \psi \in [0,1] \tag{3.25}$$

where $\lambda_\alpha = \langle\phi\rangle_\alpha/\sigma$, $\mu_\alpha = \left(1-\langle\phi\rangle_\alpha\right)/\sigma$, and

$$\mathrm{B}\left(\lambda_\alpha, \mu_\alpha\right) = \int_0^1 \theta^{\lambda_\alpha - 1}(1-\theta)^{\mu_\alpha - 1}\mathrm{d}\theta \tag{3.26}$$

represents the beta function.

A linear transformation allows this distribution to be defined on the arbitrary compact support $[a, b]$ (Hu et al., 2015). The integer moment of order k of the β KDF is

$$M_k\left(\psi, \sigma\right) = \frac{\psi + \left(k-1\right)\sigma}{1 + \left(k-1\right)\sigma} M_{k-1} \quad \text{for} \quad k > 0, \tag{3.27}$$

with $M_0 = 1$. Thus, the integer moments of the scalar PDF to be approximated as in (3.24) can be written as

$$\left\langle \phi^k \right\rangle = \sum_{\alpha=1}^{\mathrm{N}} w_\alpha G_k\left(\langle\phi\rangle_\alpha, \sigma\right) \tag{3.28}$$

where

$$G_k\left(\langle\phi\rangle_\alpha, \sigma\right) = \begin{cases} 1 & \text{if} \quad k = 0, \\ \prod_{i=0}^{k-1}\left(\frac{\langle\phi\rangle_i + i\sigma}{1+i\sigma}\right) & \text{if} \quad k \geq 1. \end{cases} \tag{3.29}$$

Eq. (3.28) defines a lower triangular system of equations to find the $2\mathrm{N}+1$ unknowns, i.e. N weights, N abscissae and σ:

$$\left\langle \phi^k \right\rangle = \chi_k M_k^* + \chi_{k-1} M_{k-1}^* + \cdots + \chi_1 M_1^* \tag{3.30}$$

where the non-negative coefficients χ_k depend only on σ, and $M_k^* = \sum_{\alpha=1}^{\mathrm{N}} w_\alpha \langle\phi\rangle_\alpha^k$. The improved version (Nguyen et al., 2016) of the iterative procedure of Yuan et al. (2012) is used to compute the values of the quadrature weights, abscissae and of the parameter σ from the $2\mathrm{N}+1$ transported scalar moments $(1, \langle\phi\rangle, \langle\phi^2\rangle, \ldots, \langle\phi^{2\mathrm{N}}\rangle)$. Note that fixing $\mathrm{N}=1$ reduces β-EQMOM to the assumed β-PDF approximation Girimaji (1991).

As illustrated in Section 3.6.5, the bivariate cases considered in this work are reduced to the application of the univariate β-EQMOM procedure for each of the scalars, argument of the joint composition PDF, by means of a linear mapping. This is possible because only the marginal composition PDFs, and not the joint composition PDF, are reconstructed in the bivariate case concerning ternary mixing.

3.5 Mapping closure

Mapping closures were initially developed by Kraichnan (1989, 1990) and Chen et al. (1989) and were applied to model tubulent scalar mixing. Pope (1991) used the same approach to study the evolution of an inert scalar in isotropic turbulence decaying from a PDF initially set to be constituted by a double delta function. He compared the results obtained from the solution of the mapping closure with those obtained from the DNS of Eswaran and Pope (1988), and demonstrated the agreement between the two models. An analytical expression for the PDF is (Pope, 1991)

$$f_\phi(\psi, t) = \frac{1}{2}\Sigma(t) \exp\left(-\frac{1}{2}\eta^2\left[1-\Sigma(t)^{-2}\right]\right) \tag{3.31}$$

where

$$\Sigma(t)^2 = \mathrm{e}^{2t} - 1, \eta = \sqrt{2}\Sigma(t)\,\mathrm{erf}^{-1}(\psi)\,. \tag{3.32}$$

As pointed out by Pope (1991), the time t enters into (3.31) only through the scalar variance. In other words, for a fixed scalar variance the shape of the PDF does not depend on t. Similar

behavior was observed by Eswaran and Pope (1988). In the literature, the AMC in (3.31) is considered to be the best model for binary mixing in the case of homogeneous turbulence, and hence it has often been used for validating other molecular mixing models Meyer and Jenny (2006); Meyer (2010).

Using the AMC, the CSDR can be expressed as (Fox, 2003)

$$\langle \epsilon_\phi | \psi \rangle_{\mathrm{AMC}} = \mathcal{N}(t) \varepsilon_\phi \exp\left[-2 \left(\mathrm{erf}^{-1}\left(2\psi - 1\right) \right)^2 \right] \tag{3.33}$$

where

$$\mathcal{N}(t) = \left\{ \int_0^1 \exp\left[-2 \left(\mathrm{erf}^{-1}\left(2\psi - 1\right) \right)^2 \right] f_\phi\left(\psi; t\right) \mathrm{d}\psi \right\}^{-1}. \tag{3.34}$$

The expression for R_m in Eq. (3.16) obtained from the AMC model is

$$\begin{aligned} R_{m,\mathrm{AMC}}\left(t\right) = & \frac{c_{\mathrm{FP}} + 1}{2} \frac{m \varepsilon_\phi}{\langle \phi'^2 \rangle} \left(\left\langle \phi^{m-1} \right\rangle \langle \phi \rangle - \langle \phi^m \rangle \right) \\ & + \frac{m\left(m-1\right) c_{\mathrm{FP}} \varepsilon_\phi}{2} \mathcal{N}_{\mathrm{N}} \sum_{i=1}^{\mathrm{N}} \sum_{j=1}^{\mathrm{N}_i} w_i w_{ij} \exp\left[-2 \left(\mathrm{erf}^{-1}\left(2\psi_{ij} - 1\right) \right)^2 \right] \psi_{ij}^{m-2} \end{aligned} \tag{3.35}$$

where $N_{\mathrm{N}}(t)$ is found by substituting the quadrature representation of the PDF into Eq. (3.34) (Yuan et al., 2012):

$$\mathcal{N}_{\mathrm{N}}(t) = \left\{ \sum_{i=1}^{\mathrm{N}} \sum_{j=1}^{\mathrm{N}_i} w_i w_{ij} \exp\left[-2 \left(\mathrm{erf}^{-1}\left(2\psi_{ij} - 1\right) \right)^2 \right] \right\}^{-1} \tag{3.36}$$

with $\mathrm{N}_i \geq \mathrm{N}+1$. The secondary weights w_{ij} and abscissae ψ_{ij} are the Gauss-Jacobi quadrature corresponding to the β KDF, which can be computed using the methodology described in Yuan et al. (2012). The value of N_i is chosen large enough that the numerical value of $\mathcal{N}_{\mathrm{N}}$ is insensitive to N_i. Compared to (3.19), the choice of the AMC CSDR leads to an unclosed moment system due to (3.34). We are thus interested to know which choice (3.18) or (3.33) performs best in the FP model.

3.6 Results and discussion

In order to investigate its capability to capture the known shape of the PDF, and to determine the required number of KDFs, β-EQMOM is applied first to reconstruct the composition PDF using the moments from AMC. After establishing this capability, a set of simulations is then

performed using β-EQMOM-FP to determine the effect of the model constant c_{FP}, in order to match the AMC PDF. Finally, the β-EQMOM-FP model is validated against the results of the DNS of binary mixing reported in Eswaran and Pope (1988), and of ternary mixing reported in Juneja and Pope (1996).

3.6.1 Verification of β-EQMOM

The first step to verify that the β-EQMOM is able to accurately reconstruct the PDF obtained with AMC in Sec. 3.5, and to determine the number of KDFs required to achieve this result. The reader should note that this step is of pure numerical interest, and does not involve the FP closure model, but simply the β-EQMOM procedure. Moments of the AMC PDF are computed and provided as input to β-EQMOM, and the number N of KDFs is varied to determine its effect on the shape of the reconstructed PDF. Figure 3.1 shows the results obtained using from one to four KDFs. It is possible to observe that with $\mathrm{N} = 1$, the agreement at the initial time is poor, but β-EQMOM closely matches the AMC PDF at later times. As noted earlier, the latter is expected because both the AMC and the β PDF approach a Gaussian PDF for large times. Results with $\mathrm{N} \geq 2$ show that the reconstructed PDFs agree closely with the AMC PDFs at all times. These results demonstrate that β-EQMOM is capable of reconstructing the shape of the PDFs of interest in the binary mixing problems given a known set of moments as input. Moreover, as the difference between $\mathrm{N} = 2$ and 3 is negligible, it is possible to conclude that for binary mixing only two KDFs are required to accurately reproduce the AMC PDF. Thus, CFD models for turbulent mixing can make use of the FP model by solving for as few as four mixture-fraction moments: $\langle\xi\rangle$, $\langle\xi^2\rangle$, $\langle\xi^3\rangle$, $\langle\xi^4\rangle$. Compared to the assumed β-PDF model, the two additional moments are needed to capture the shape of the PDF when the variance is near its maximum value (i.e., the PDF is close to two Dirac delta functions) as seen in Fig. 3.1.

3.6.2 Choice of the value of the diffusive relaxation rate constant

The constant c_{FP}, which appears in the FP model, controls the diffusive relaxation rate of the PDF. In this section, we obtain solutions with different values of c_{FP}, and compare the results with those obtained with the AMC. Figure 3.2 shows that as c_{FP} increases, the distributions

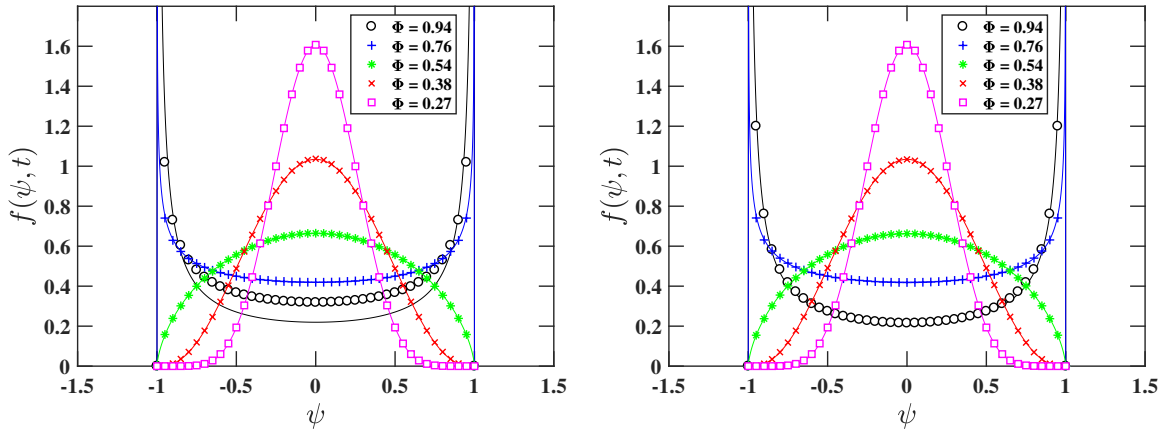

(a) N = 1

(b) N = 2

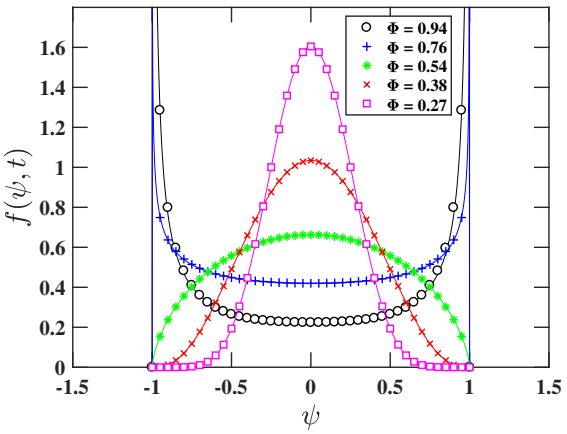

(c) N = 3

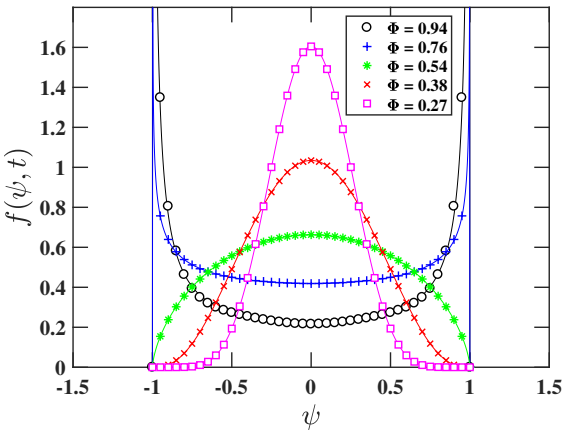

(d) N = 4

Figure 3.1: Comparison between the analytical solution obtained with the mapping closures (Pope, 1991) (solid lines) and the approximated distribution obtained with β-EQMOM (symbols) using different numbers of quadrature nodes N. Each curve represents a fixed value of scalar variance $\langle \phi'^2 \rangle (t)$.

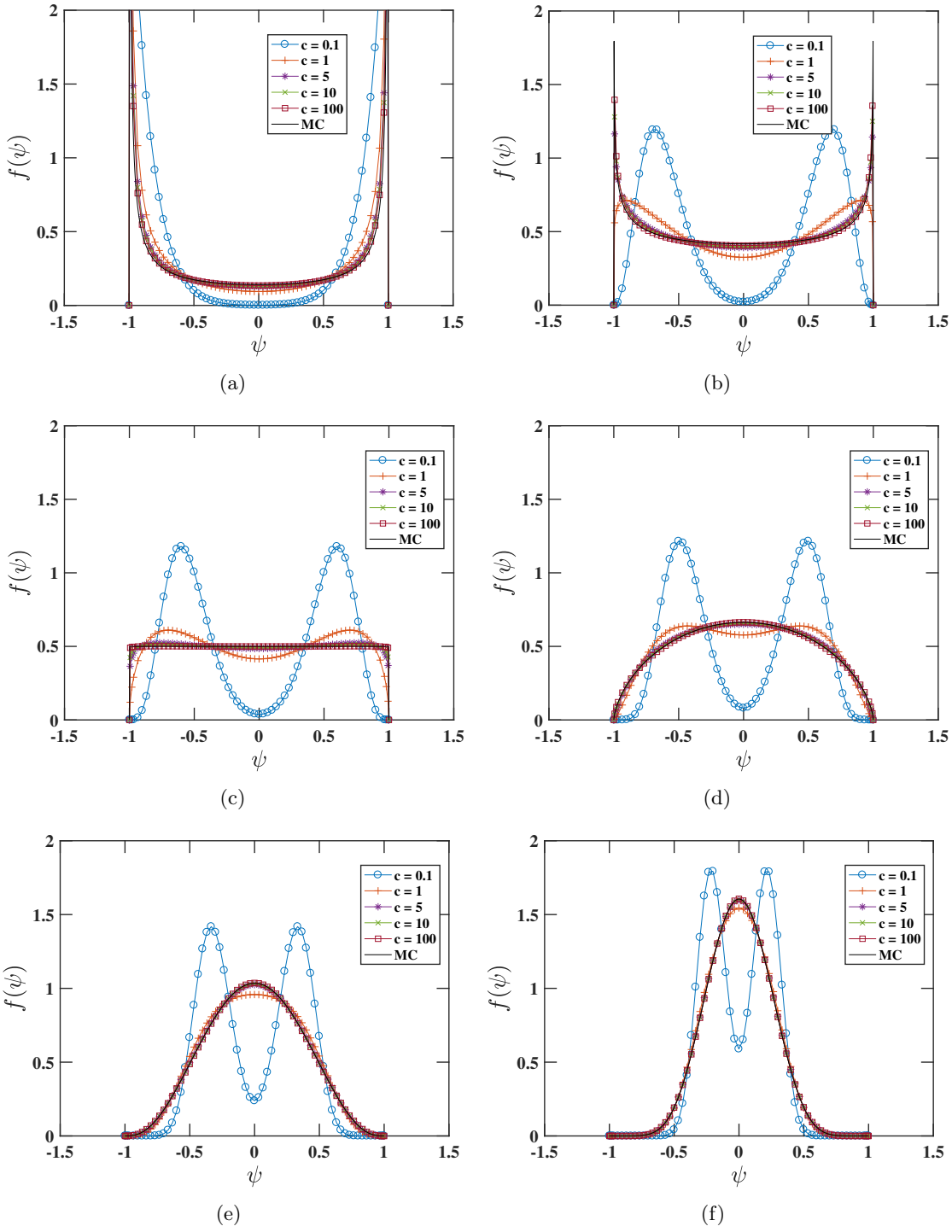

Figure 3.2: Comparison of the PDF found from the β-EQMOM-FP model with different c_{FP} and variances with the results obtained from the mapping closure model.

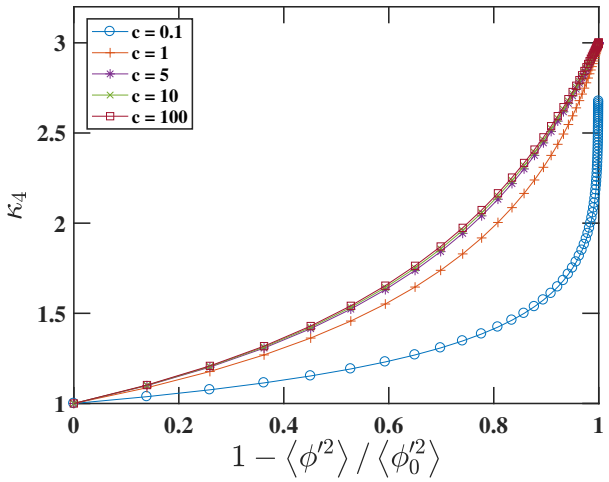

Figure 3.3: Time-evolution of scaled fourth-order central moment $\kappa_4 = \langle \phi'^4 \rangle / \langle \phi'^2 \rangle^2$ using β-EQMOM-FP with N = 2 at different values of c_{FP} for a symmetric PDF with support $[-1, 1]$.

are comparable to those obtained with AMC. In particular, a value of $c_{\mathrm{FP}} = 10$ or higher yields results in good agreement with AMC. For smaller values of c_{FP}, the PDF is closer to that predicted with the IEM model. As c_{FP} fixes the time scale for diffusive relaxation, it is reminiscent of the "generation time" used in the multiple mapping closure (MMC) as described by Sundaram et al. (2016). Here, as in MMC, it is necessary to consider two micromixing time scales: τ_ϕ and $\tau_\phi / c_{\mathrm{FP}}$. Thus, if the FP model is used for a reactive scalar, a second Damköhler number will arise to describe the timescale ratio between diffusive relaxation and chemical reactions. It can be anticipated that this new Damköhler number will better characterize ignition/extinction phenomena than the one based on integral-scale mixing τ_ϕ.

It is worth noting that the moments $\langle \phi \rangle$ and $\langle \phi^2 \rangle$ do not depend on c_{FP}. Thus, changing its value only affects moments of orders higher than two. In general, in order to recover the AMC PDF, c_{FP} must be set large enough that it no longer affects these higher-order moments. In fact, if the only requirement were to recover the AMC PDF then we can set $c_{\mathrm{FP}} = \infty$ and use algebraic expressions for the third- and fourth-order moments. These observations are confirmed in Fig. 3.3, which shows for large times the scaled fourth-order central moment relaxes to 3, which is the value for the Gaussian distribution. The curves for different c_{FP} overlap for values higher than 5. For pure mixing problems like the ones considered in this work, the value of c_{FP} can be set arbitrarily large. However, when additional physics are included in the PDF

transport equation, a more precise definition will be needed for fixing its value relative to other timescales. The theoretical estimates developed for the MMC (Sundaram et al., 2016) may be helpful in this respect. Nonetheless, as the AMC PDF holds for purely diffusive problems Fox (1992b, 1994), one cannot link *a priori* the value of c_{FP} to the turbulence time scales without considering the length scales of molecular diffusion. For fully developed turbulent flows for which $\tau_\phi \propto k/\varepsilon$ where k is the turbulent kinetic energy and ε its dissipation, if the Schmidt number is greater than one, then the diffusion time scale would yield $c_{\mathrm{FP}} \propto k/\sqrt{\varepsilon\nu}$ where ν is the kinematic viscosity of the fluid.

3.6.3 Validation of β-EQMOM-FP model against DNS of binary mixing

Three cases of mixing in homogeneous isotropic turbulence, with different time evolutions of the scalar dissipation rate (Figure 3.4), are now considered to validate the β-EQMOM-FP model against the DNS results of Eswaran and Pope (1988). In these cases, the initial scalar fields are constituted by two Dirac delta functions, located at points -1 and 1 in composition space, to represent a binary mixing problem, characterized by the presence of the scalar at two different states. The time-dependent SDR ($\varepsilon_\phi(t)$) obtained from the DNS Eswaran and Pope (1988), for the three cases, is provided as input to the β-EQMOM-FP model. The evolution of ε_ϕ as a function of the dimensionless time τ is shown in Fig. 3.4 for the three cases considered here. The SDR is combined with the moment source term in (3.19) to solve for the closed system of moments $\langle\phi^m\rangle$ for $m \in \{1, 2, 3, 4\}$. The parameter $c_{\mathrm{FP}} = 10$ was chosen to reproduce the AMC behavior as described in Section 3.6.2.

Figure 3.5 shows the scalar PDF reported by Eswaran and Pope (1988) compared to the results obtained using β-EQMOM-FP at different values of the scalar variance Φ, for case 1. Two KDFs (N = 2) were used to obtain these results. It is apparent that the results provided by β-EQMOM-FP after the first few time steps differ from those of the DNS (Eswaran and Pope, 1988). This difference, however, can be explained by noting that the initial condition defined in the DNS simulations (Eswaran and Pope, 1988) is not an exact pair of Dirac delta functions, due to the difficulties of generating this configuration in a discretized space. However, with β-EQMOM-FP, as with AMC, it is possible to have an exact initial definition of the scalar

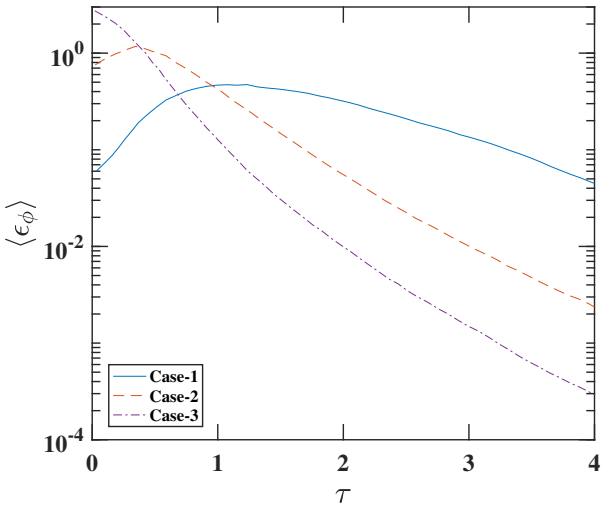

Figure 3.4: Evolution of the scalar dissipation rate for three test cases as functions of the dimensionless time from Eswaran and Pope (1988).

PDF. Further advancing the β-EQMOM-FP solution in time shows that the model predicts the evolution towards the well-mixed condition in reasonable agreement with the DNS results, and converges towards a Gaussian PDF (Fig. 3.5(e)).

Figures 3.6 and 3.7 show the results obtained for Cases 2 and 3, respectively. In both cases, the β-EQMOM-FP model satisfactorily predicts the evolution of the PDF, and its relaxation to a Gaussian distribution, as it is observed in the DNS. The satisfactory performance of the β-EQMOM-FP model for binary mixing is a direct reflection of its agreement with AMC as seen in Section 3.6.2. We show next that the quality of the predictions depends on the choice of the CSDR.

3.6.4 β-EQMOM-FP model of binary mixing with the AMC CSDR

The solution for the three cases considered in Sec. 3.6.3 using the AMC CSDR found by solving (3.35) is considered here. Two KDFs (N = 2) and eight secondary nodes ($N_i = 5$) were used to study the evolution of the PDF with the AMC CSDR. Figure 3.8 shows the results obtained using the AMC CSDR for Cases 1 and 2. Using the AMC CSDR, the PDF relaxes to a Gaussian distribution as expected. However, the agreement with the DNS and AMC is not as good as with the CSDR given in (3.18). It is worth mentioning that increasing the number of

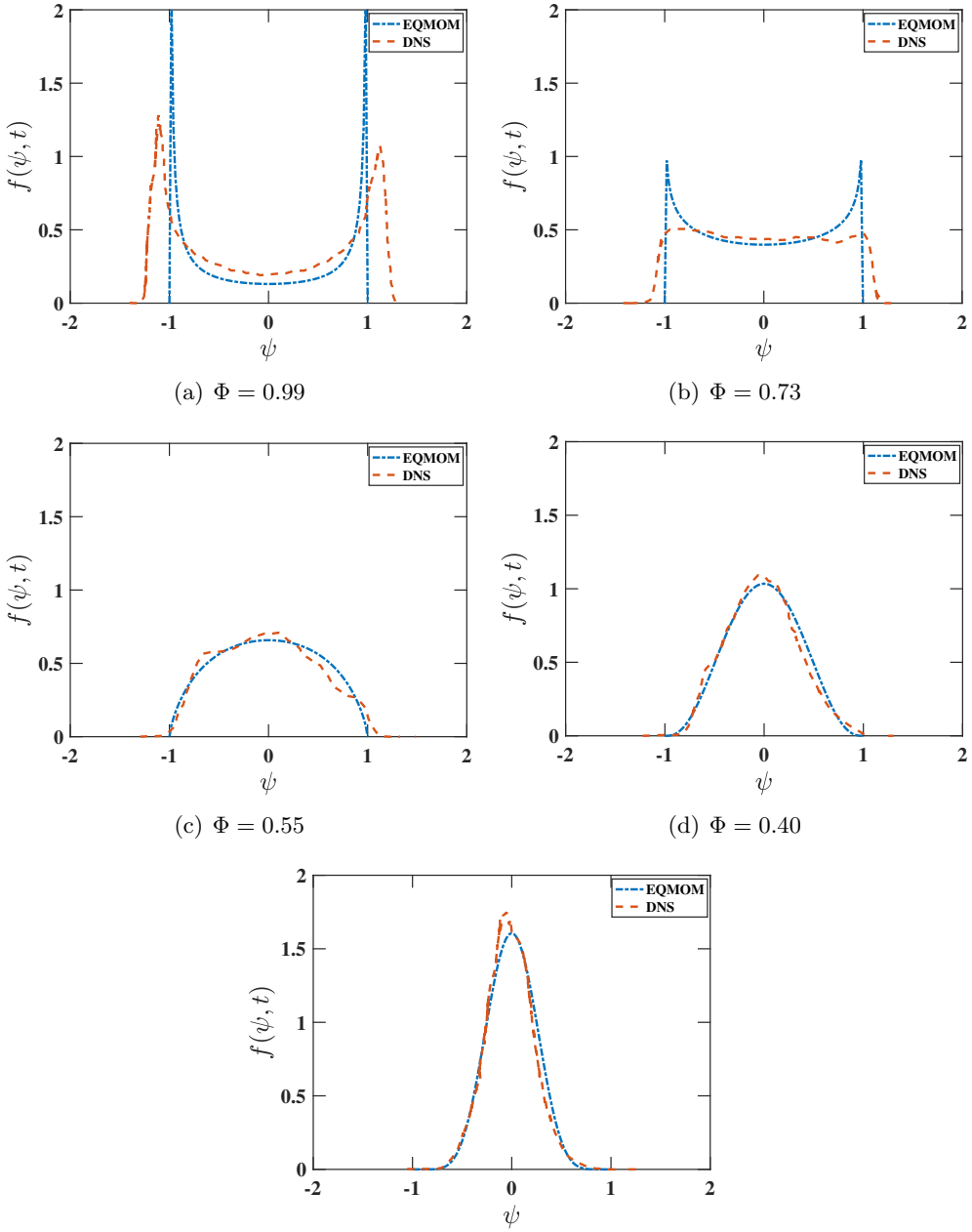

(a) $\Phi = 0.99$

(b) $\Phi = 0.73$

(c) $\Phi = 0.55$

(d) $\Phi = 0.40$

(e) $\Phi = 0.27$

Figure 3.5: Evolution of scalar PDF for Case 1 at different variances.

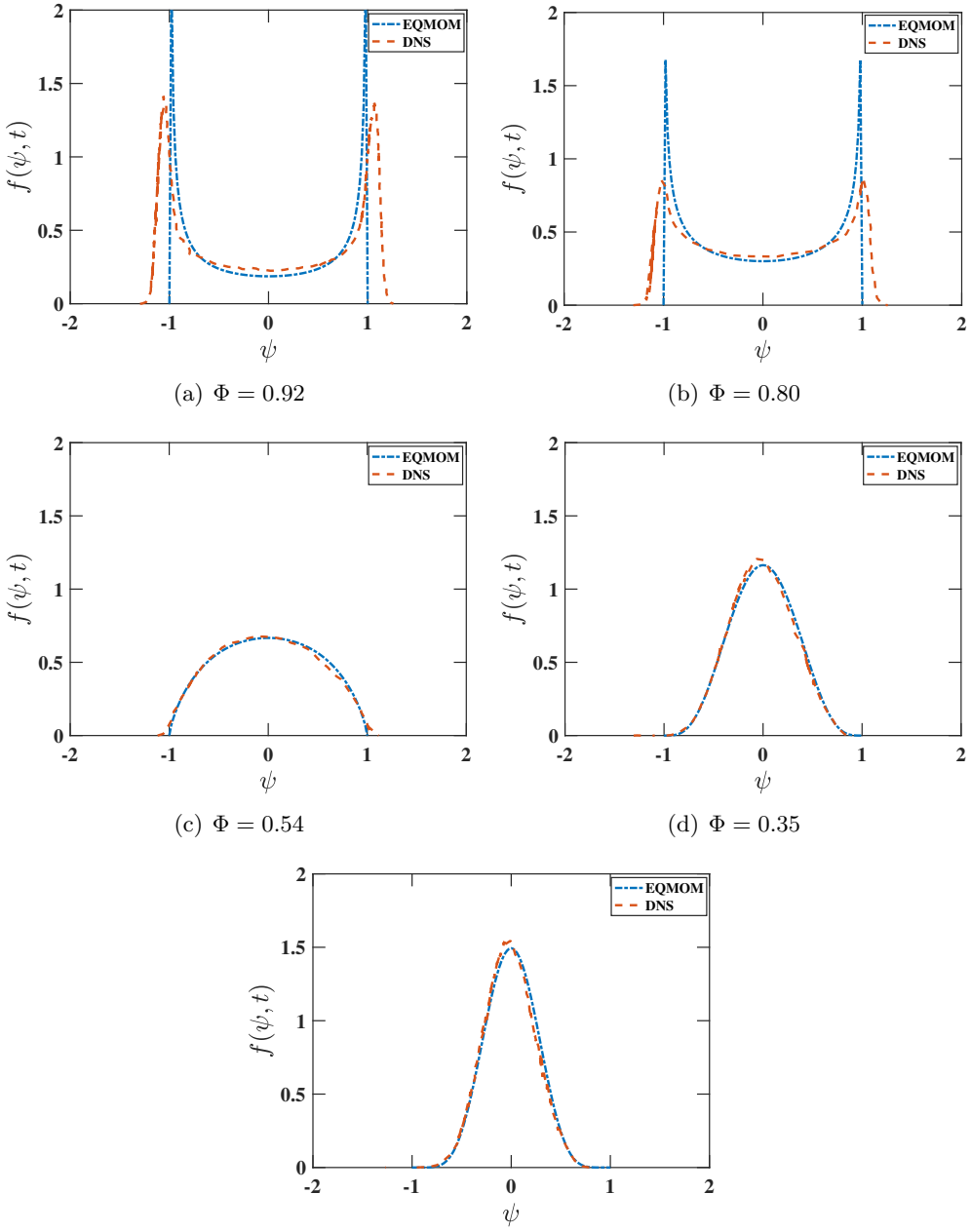

(a) $\Phi = 0.92$

(b) $\Phi = 0.80$

(c) $\Phi = 0.54$

(d) $\Phi = 0.35$

(e) $\Phi = 0.28$

Figure 3.6: Evolution of scalar PDF for Case 2 at different variances.

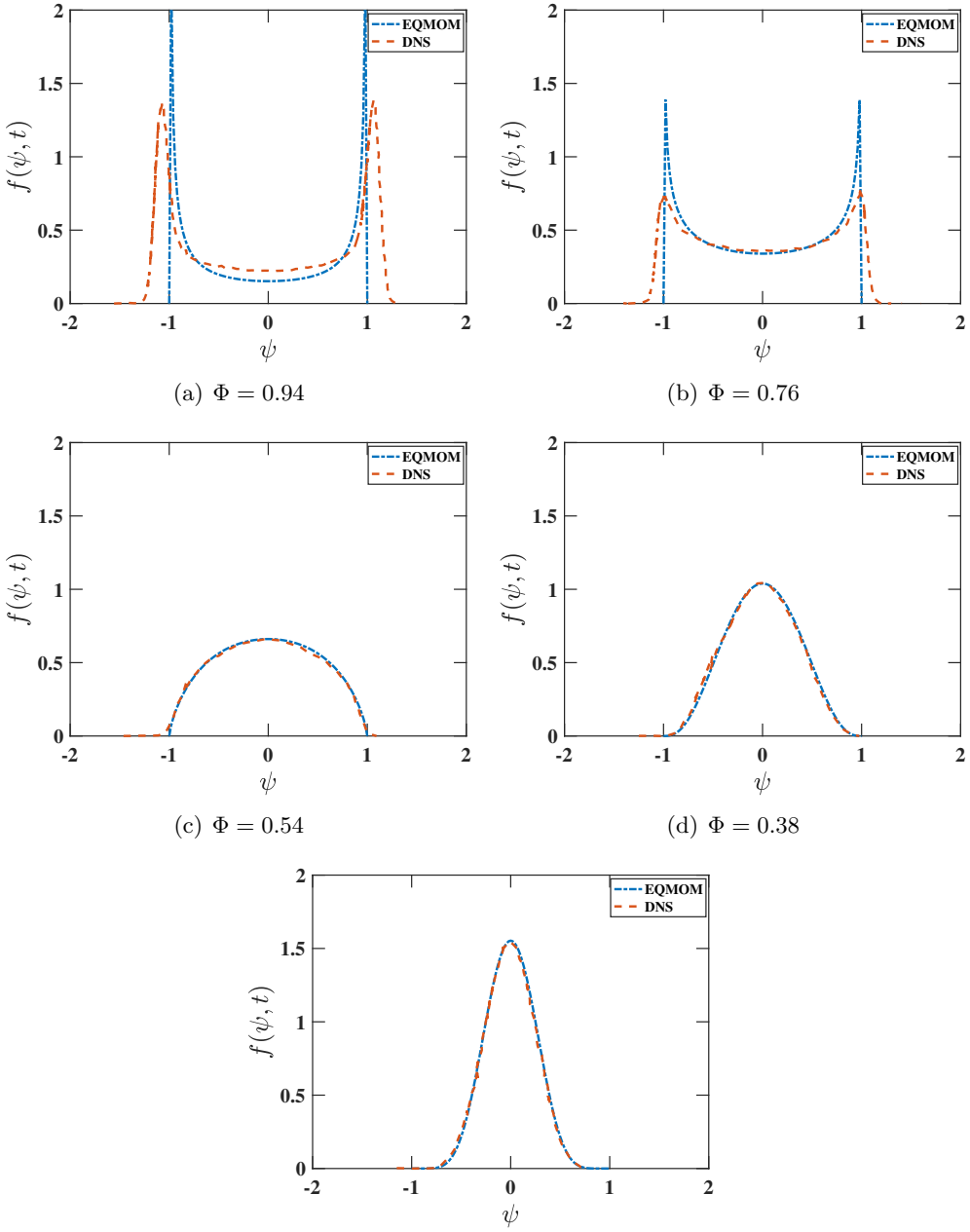

(a) $\Phi = 0.94$

(b) $\Phi = 0.76$

(c) $\Phi = 0.54$

(d) $\Phi = 0.38$

(e) $\Phi = 0.27$

Figure 3.7: Evolution of scalar PDF for Case 3 at different variances.

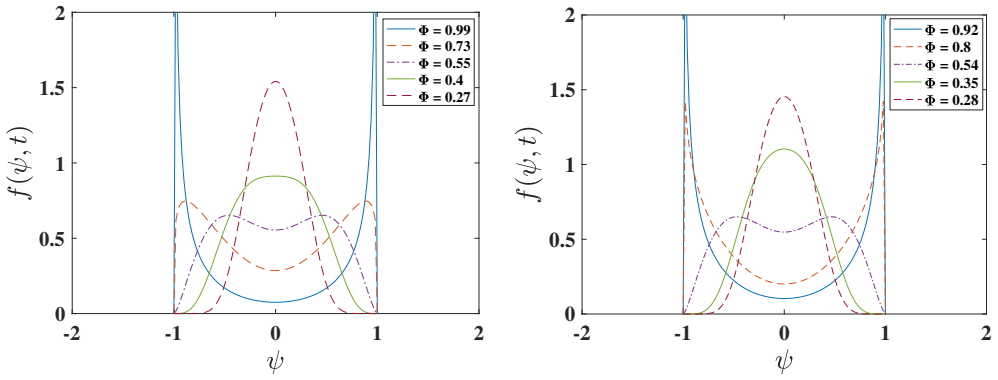

(a) Case 1 (b) Case 2

Figure 3.8: Evolution of scalar PDF using β-EQMOM-FP with AMC CSDR at different variances.

KDFs does not improve the predicted shape of the PDF. Quadrature methods are accurate for $N_i \geq 2N + 1$ secondary nodes (Yuan et al., 2012) and increasing N_i does not affect the results. Different values for c_{FP} were tested, and smaller values make the result closer to the IEM model while values of 10 or higher do not improve the prediction of the PDF. Using AMC CSDR, the moment transport equations must be closed using the quadrature representation of the PDF. This increases the cost of computation in the sense that an inversion is required at each time step to compute the source terms.

3.6.5 Validation of β-EQMOM-FP model against DNS of ternary mixing

In realistic problems, such as in chemical reacting flows, it is not infrequent to have reactants introduced in more than two inlets. In order to show that the β-EQMOM-FP model is capable of describing such cases, we consider the ternary mixing problem studied by Juneja and Pope (1996), who reported the evolution of the joint PDF $f_{\boldsymbol{\phi}}(\psi_1, \psi_2; t)$ of the two scalars. We will use their results for the marginal PDFs to validate the results obtained with β-EQMOM-FP, starting from the bivariate mixture-fraction model introduced in Sec. 3.3.2.

Juneja and Pope (1996) considered two scalars with an initial joint PDF constituted by a triple delta function, corresponding to blobs of fluids at three distinct states. Figure 3.9(b) shows the bivariate phase space. The three states corresponds to the vertices of an equilateral triangle.

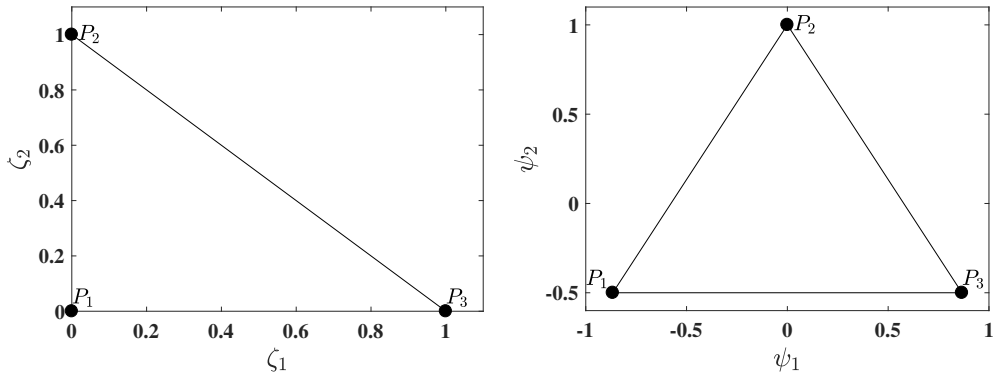

(a) Ternary mixing in $\boldsymbol{\zeta}$-phase space (b) Ternary mixing in $\boldsymbol{\psi}$-phase space

Figure 3.9: Phase-space transformation between bivariate mixture fraction and two scalars used for ternary mixing in (Juneja and Pope, 1996). The points P_1, P_2 and P_3 define the affine mapping between the two spaces.

The initial states have equal probability, and therefore the means $\langle\phi_1\rangle$ and $\langle\phi_2\rangle$ are zero, which ensures the three-way symmetry of the initial state in composition phase space. The setup is designed so that the bivariate PDF relaxes to zero for both ψ_1 and ψ_2. Additionally, the two scalars are uncorrelated so that $\langle\phi_1\phi_2\rangle = 0$ (Juneja and Pope, 1996), and hence the cross SDR is also zero when written in terms of $\boldsymbol{\phi}$.

In order to solve the problem using the mixture-fraction PDF, the composition phase space $\boldsymbol{\psi}$ is mapped linearly onto the mixture-fraction phase space $\boldsymbol{\zeta}$, so that the matrix for the joint CSDR introduced in Fox (2003), defined in terms of $\boldsymbol{\zeta}$, can be used. A graphical representation of this mapping is illustrated in Fig. 3.9. The linear mapping is defined by the following linear algebraic equation:

$$\begin{bmatrix}\psi_1\\ \psi_2\end{bmatrix} = \begin{bmatrix}\sqrt{3} & \frac{\sqrt{3}}{2}\\ 0 & \frac{3}{2}\end{bmatrix}\begin{bmatrix}\zeta_1\\ \zeta_2\end{bmatrix} - \begin{bmatrix}\frac{\sqrt{3}}{2}\\ \frac{1}{2}\end{bmatrix}. \tag{3.37}$$

After simplifying, the relationship between the components of $\boldsymbol{\zeta}$ and $\boldsymbol{\psi}$ is found:

$$\begin{aligned}\psi_1 &= \sqrt{3}\left(\zeta_1 + \frac{1}{2}\zeta_2 - \frac{1}{2}\right)\\ \psi_2 &= \frac{3}{2}\zeta_2 - \frac{1}{2}\end{aligned} \quad\Longleftrightarrow\quad \begin{aligned}\zeta_1 &= \frac{\sqrt{3}}{3}\psi_1 - \frac{1}{3}\psi_2 + \frac{1}{3}\\ \zeta_2 &= \frac{2}{3}\psi_2 + \frac{1}{3}\end{aligned}. \tag{3.38}$$

Note that using these transformation it is straightforward to write the moments $\langle\phi_1^m\phi_2^n\rangle$ in terms of the moments $\langle\xi_1^m\xi_2^n\rangle$. Also note that $\langle\xi_1\rangle = \langle\xi_2\rangle = 1/3$, and the mixture-fraction

variances are $\langle \xi_1'^2 \rangle = \frac{1}{3}\langle \phi_1^2 \rangle + \frac{1}{9}\langle \phi_2^2 \rangle$ and $\langle \xi_2'^2 \rangle = \frac{4}{9}\langle \phi_2^2 \rangle$, while the mixture-fraction covariance $\langle \xi_1' \xi_2' \rangle = -\frac{2}{9}\langle \phi_2^2 \rangle$ is negative for this example.

In order to employ the FP model for the mixture-fraction moments in (3.23), we must relate the SDR components defined in terms of $\boldsymbol{\xi}$ to those defined in terms of $\boldsymbol{\phi}$ by using the second part of (3.38). The transformed joint scalar dissipation matrix can be written as

$$\begin{bmatrix} \varepsilon_{11} & \varepsilon_{12} \\ \varepsilon_{12} & \varepsilon_{22} \end{bmatrix} = \frac{1}{9}\begin{bmatrix} 3\varepsilon_{\phi_{11}} + \varepsilon_{\phi_{22}} & -2\varepsilon_{\phi_{22}} \\ -2\varepsilon_{\phi_{22}} & 4\varepsilon_{\phi_{22}} \end{bmatrix} = \frac{1}{\tau_\phi}\begin{bmatrix} \langle \xi_1'^2 \rangle & \langle \xi_1' \xi_2' \rangle \\ \langle \xi_1' \xi_2' \rangle & \langle \xi_2'^2 \rangle \end{bmatrix} \tag{3.39}$$

where $\varepsilon_{\phi_{11}} = \langle \phi_1^2 \rangle / \tau_\phi$ and $\varepsilon_{\phi_{22}} = \langle \phi_2^2 \rangle / \tau_\phi$ are the SDR components for $\boldsymbol{\phi}$, and the scalar mixing time τ_ϕ is found from the DNS. Note that (3.39) implies that $\sum_j \varepsilon_{ij} \left\langle \xi_j' \xi_k' \right\rangle^{-1} = \frac{1}{\tau_\phi}\delta_{i,k}$ in (3.9), which is just the single scalar timescale model used in the IEM model Fox (2003).

Univariate moments defined over the space $\boldsymbol{\psi}$ are obtained from the bivariate moments over $\boldsymbol{\zeta}$ by means of Eq. (3.38), leading to

$$\langle \phi_1^m \rangle = 3^{m/2} \left\langle \left(\xi_1' + \frac{1}{2}\xi_2' \right)^m \right\rangle, \quad \langle \phi_2^n \rangle = \left(\frac{3}{2} \right)^n \langle \xi_2'^n \rangle . \tag{3.40}$$

By expanding the right-hand side of (3.40), the univariate moments needed for β-EQMOM-FP reconstruction of the two marginal PDFs for ϕ_1 and ϕ_2 can be related to the bivariate moments of mixture fraction. In this study N = 3 KDFs are used to reconstruct each of the two marginal PDFs. The number of primary quadrature nodes was chosen to be able to exactly represent the initial condition, which is constituted by three Dirac delta distributions. As a consequence of this choice of N, 27 joint mixture-fraction moments up to sixth order are computed:

$$\begin{array}{cccccccc} & \langle \xi_2 \rangle & \langle \xi_2^2 \rangle & \langle \xi_2^3 \rangle & \langle \xi_2^4 \rangle & \langle \xi_2^5 \rangle & \langle \xi_2^6 \rangle \\ \langle \xi_1 \rangle & \langle \xi_1\xi_2 \rangle & \langle \xi_1\xi_2^2 \rangle & \langle \xi_1\xi_2^3 \rangle & \langle \xi_1\xi_2^4 \rangle & \langle \xi_1\xi_2^5 \rangle & \\ \langle \xi_1^2 \rangle & \langle \xi_1^2\xi_2 \rangle & \langle \xi_1^2\xi_2^2 \rangle & \langle \xi_1^2\xi_2^3 \rangle & \langle \xi_1^2\xi_2^4 \rangle & & \\ \langle \xi_1^3 \rangle & \langle \xi_1^3\xi_2 \rangle & \langle \xi_1^3\xi_2^2 \rangle & \langle \xi_1^3\xi_2^3 \rangle & & & \\ \langle \xi_1^4 \rangle & \langle \xi_1^4\xi_2 \rangle & \langle \xi_1^4\xi_2^2 \rangle & & & & \\ \langle \xi_1^5 \rangle & \langle \xi_1^5\xi_2 \rangle & & & & & \\ \langle \xi_1^6 \rangle & & & & & & \end{array} \tag{3.41}$$

The initial conditions for this moment set are easily found from the known bivariate PDF. Recall from Sec. 3.3.2 that the 27 moment transport equations are closed. Thus, their values

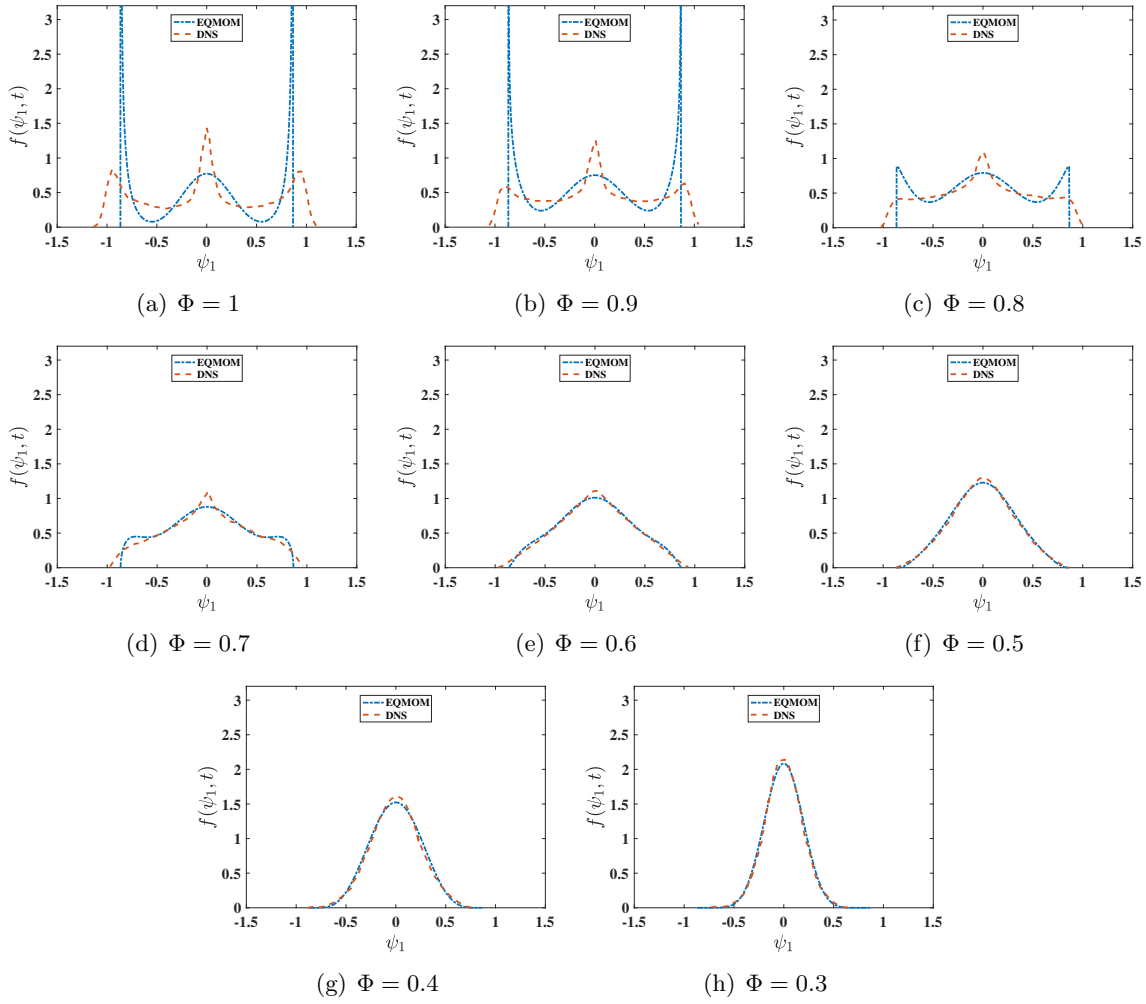

(a) $\Phi = 1$ (b) $\Phi = 0.9$ (c) $\Phi = 0.8$

(d) $\Phi = 0.7$ (e) $\Phi = 0.6$ (f) $\Phi = 0.5$

(g) $\Phi = 0.4$ (h) $\Phi = 0.3$

Figure 3.10: Evolution of marginal scalar PDFs for ϕ_1 at different variances. β-EQMOM-FP compared to the DNS of Juneja and Pope (1996).

do not depend on how the PDFs are reconstructed from the moments. For the results presented here, the diffusive relaxation parameter is again $c_{\text{FP}} = 10$.

Figure 3.10 shows the results for the marginal PDFs of ϕ_1 and Figure 3.11 for ϕ_2 obtained with β-EQMOM-FP, compared to the DNS (Juneja and Pope, 1996). The marginal PDFs are evolving and finally converge to Gaussian distributions. The marginal PDF of ϕ_2 obtained using β-EQMOM-FP with unequal initial conditions is in very good agreement with that obtained by DNS. As the scalar ϕ_2 represents binary mixing with unequal volumes, this result demonstrates the ability of the FP model to treat such cases. For ϕ_1, β-EQMOM-FP captures the peak in the middle for the marginal PDF; however, it is not as sharp as the one obtained by the DNS.

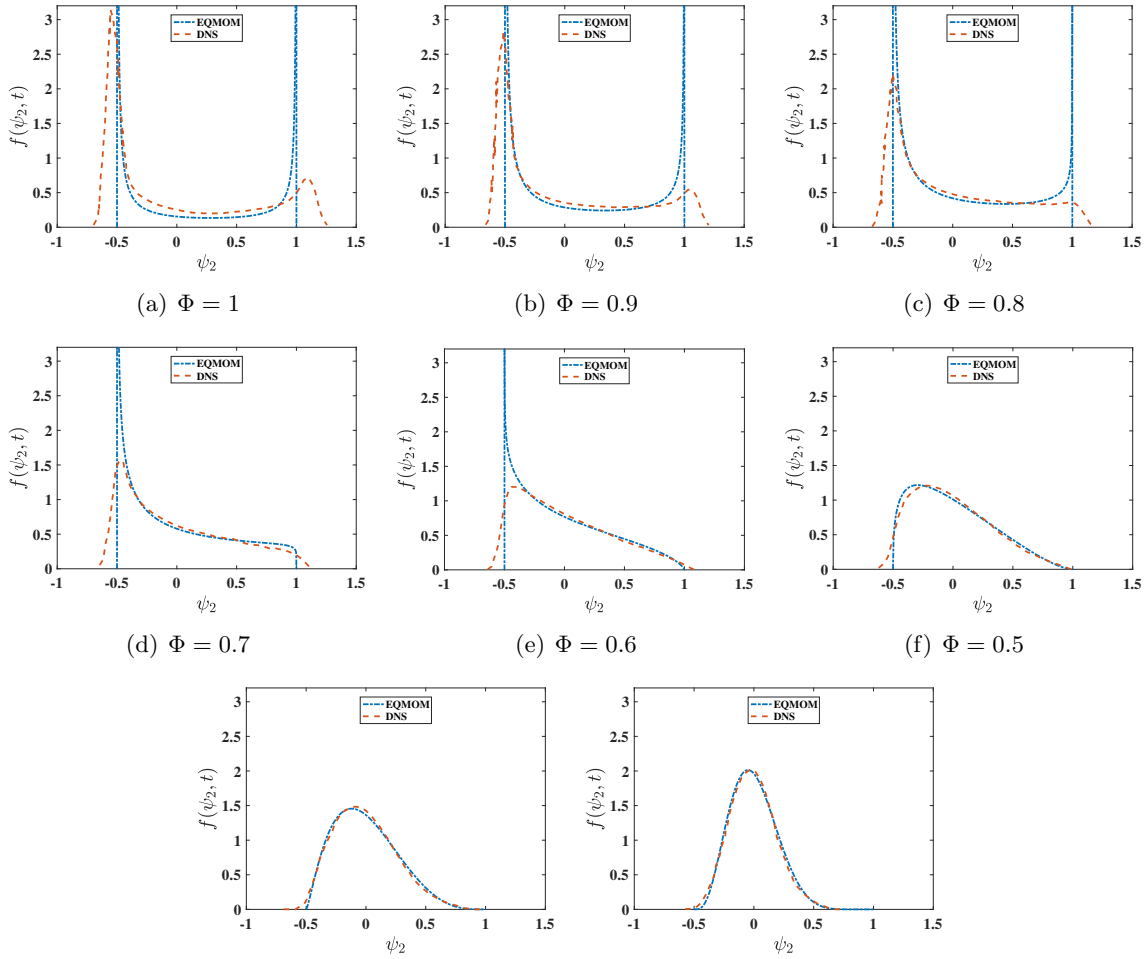

(a) $\Phi = 1$ (b) $\Phi = 0.9$ (c) $\Phi = 0.8$

(d) $\Phi = 0.7$ (e) $\Phi = 0.6$ (f) $\Phi = 0.5$

(g) $\Phi = 0.4$ (h) $\Phi = 0.3$

Figure 3.11: Evolution of marginal scalar PDFs for ϕ_2 at different variances. β-EQMOM-FP compared to the DNS of Juneja and Pope (1996).

This is a result of the β-EQMOM reconstruction methodology not accounting for the fact that the marginal PDF is a projection of the bivariate PDF for the correlated variables ξ_1 and ξ_2. Thus, in order to improve the reconstruction, it would be necessary to reconstruct the bivariate mixture-fraction PDF using a method such as CQMOM Cheng (2010); Yuan and Fox (2011). However, before this can be done in a general way, further work will be needed to extend CQMOM to bounded convex domains in phase space such as those in Fig. 3.9. Given that binary mixing required moments up to fourth order, it is likely that a bivariate CQMOM using fourth-order moments will be successful for most applications, thereby reducing the number of moments in (3.41) that would have to be computed for ternary mixing.

3.7 Conclusions

For the first time, the extended quadrature method of moments with β KDFs has been applied to find approximate solutions for the composition PDF using the FP molecular mixing model (Fox, 1992b, 2003). This approach allows any form of the conditional scalar dissipation rate $\langle \epsilon_\phi | \psi \rangle$ to be used in the calculations. Differently from models relying on a β PDF to approximate the mixture-fraction PDF, it is able to represent any form of the scalar PDF, due to its capability of reproducing the moments of arbitrary distributions. For example, here we have shown that the mixture-fraction PDF can be better captured using moments up to fourth order.

Two mixing cases were used to validate the β-EQMOM-FP against results obtained with the DNS (Eswaran and Pope, 1988; Juneja and Pope, 1996). For binary mixing, the initial scalar PDF is specified as two delta functions at different locations in composition space. Results show that the β-EQMOM-FP predicts the evolution of scalar PDF in agreement with AMC (Pope, 1991) and the DNS results in the cases examined. For ternary mixing, the capability of the β-EQMOM-FP to predict the time evolution of the moments of the bivariate scalar PDF was demonstrated considering the DNS of Juneja and Pope (1996). Here, the β-EQMOM-FP approach predicted the evolution of the marginal PDFs towards Gaussian. However, for the true ternary mixing problem with three delta functions for the univariate PDF, the middle peak was not as well captured. Nonetheless, the applicability of the β-EQMOM-FP approach

to solve turbulent mixing problems has been demonstrated for the first time.

Finally, the closure for the conditional scalar dissipation rate in the FP model was shown to have a strong effect on the predictions, and it was found that the simplest closure produces the best results. This conclusion was initially verified by reconstructing the PDF obtained with known moments from the AMC. In this manner, it was demonstrated how the diffusive relaxation time scale in the FP model affects the solution.

Future work should focus on applying quadrature-based moment methods (QBMM) with the PDF transport equation to investigate turbulent reacting scalars. In principle, once the PDF equation has been closed (e.g., using the FP molecular mixing model), its solution can be approximated using QBMM.

The extension of the proposed approach to non-homogeneous problems can be achieved by keeping the spatial transport terms in the moment transport equations obtained from (5.1). These will consist of a diffusion and an advection term, in physical space, for each moment. The solution of the moment transport equations obtained in this way has to be performed with a numerical scheme that ensures the realizability of the transported moment set. As discussed in Vikas et al. (2013b), the discretization of the moment diffusion term does not present difficulties, if a traditional second-order finite-volume scheme is used. More difficulties are faced when dealing with the discretization of the moment advection term, which is known to be problematic Wright (2007), because it may compromise the realizability of the set of transported moments, when using numerical schemes other than the first order upwind. In the framework of quadrature-based moment methods, the closure of the advection term can be achieved using a kinetic-based flux Perthame (1992); Desjardins et al. (2008); Fox et al. (2008). In these schemes, the PDF reconstructed by means of the quadrature approximation is used to close the convective term of the moment transport equations, as illustrated in Desjardins et al. (2008); Fox et al. (2008). These schemes were extended to higher order of discretization in Vikas et al. (2011); Laurent and Nguyen (2017), where the technical details of the discretization of the moment transport equations are provided.

3.8 Acknowledgments

The authors gratefully acknowledge the support of the US National Science Foundation under the SI^2–SSE award NSF–ACI 1440443.

3.9 Bibliography

Akroyd, J., Smith, A. J., McGlashan, L. R., and Kraft, M. (2010). Numerical investigation of DQMOM-IEM as a turbulent reaction closure. *Chemical Engineering Science*, 65(6):1915–1924.

Alopaeus, V., Laakkonen, M., and Aittamaa, J. (2006). Solution of population balances with breakage and agglomeration by high-order moment-conserving method of classes. *Chemical Engineering Science*, 61(20):6732–6752.

Alopaeus, V., Laakkonen, M., and Aittamaa, J. (2008). Solution of population balances by high order moment-conserving method of classes: reconstruction of a non-negative density distribution. *Chemical Engineering Science*, 63(10):2741–2751.

Athanassoulis, G. A. and Gavriliadis, P. N. (2002). The truncated Hausdorff moment problem solved by using kernel density functions. *Probabilistic Engineering Mechanics*, 17(3):273–291.

Balakin, B. V., Hoffmann, A. C., and Kosinski, P. (2014). Coupling STAR-CD with a population-balance technique based on the classes method. *Powder Technology*, 257:47–54.

Bannari, R., Kerdouss, F., Selma, B., Bannari, A., and Proulx, P. (2008). Three-dimensional mathematical modeling of dispersed two-phase flow using class method of population balance in bubble columns. *Computers & Chemical Engineering*, 32(12):3224–3237.

Becker, P. J., Puel, F., Henry, R., and Sheibat-Othman, N. (2011). Investigation of discrete population balance models and breakage kernels for dilute emulsification systems. *Industrial & Engineering Chemistry Research*, 50(19):11358–11374.

Bove, S., Solberg, T., and Hjertager, B. H. (2005). A novel algorithm for solving population balance equations: the parallel parent and daughter classes. Derivation, analysis and testing. *Chemical Engineering Science*, 60(5):1449–1464.

Broadwell, J. E. and Breidenthal, R. E. (1982). A simple model of mixing and chemical reaction in a turbulent shear layer. *Journal of Fluid Mechanics*, 125:397–410.

Cao, R. R., Wang, H., and Pope, S. B. (2007). The effect of mixing models in PDF calculations of piloted jet flames. *Proceedings of the Combustion Institute*, 31(1):1543–1550.

Capecelatro, J., Desjardins, O., and Fox, R. (2014). Numerical study of collisional particle dynamics in cluster-induced turbulence. *Journal of Fluid Mechanics*, 747:R2–1–R2–13.

Carrica, P. M., Drew, D., Bonetto, F., and Lahey Jr, R. T. (1999). A polydisperse model for bubbly two-phase flow around a surface ship. *International Journal of Multiphase Flow*, 25(2):257–305.

Cassiani, M., Franzese, P., and Giostra, U. (2005). A PDF micromixing model of dispersion for atmospheric flow. Part I: development of the model, application to homogeneous turbulence and to neutral boundary layer. *Atmospheric Environment*, 39(8):1457–1469.

Chalons, C., Fox, R., and Massot, M. (2010). A multi-Gaussian quadrature method of moments for gas-particle flows in a LES framework. *Studying Turbulence Using Numerical Simulation Databases, Center for Turbulence Research, Summer Program 2010, Stanford University*, pages 347–358.

Chen, H., Chen, S., and Kraichnan, R. H. (1989). Probability distribution of a stochastically advected scalar field. *Physical Review Letters*, 63(24):2657–2660.

Cheng, J. C. (2010). A comrehensive model study for Flash Nanoprecipitation: computational fluid dynamics, micro- particle image velocimetry, and population balance modeling. *Iowa State University, Ames, Iowa, USA*.

Cheng, J. C. and Fox, R. O. (2010). Kinetic Modeling of Nanoprecipitation using CFD Coupled with a Population Balance. *Industrial & Engineering Chemistry Research*, 49(21):10651–10662.

Cheng, J. C., Vigil, R., and Fox, R. (2010). A competitive aggregation model for Flash Nano-Precipitation. *Journal of Colloid and Interface Science*, 351(2):330–342.

Choi, H. S., Park, T. S., and Suzuki, K. (2008). Turbulent mixing of a passive scalar in confined multiple jet flows of a micro combustor. *International Journal of Heat and Mass Transfer*, 51(17–18):4276–4286.

Cremer, M. A., McMurtry, P. A., and Kerstein, A. R. (1994). Effects of turbulence length scale distribution on scalar mixing in homogeneous turbulent flow. *Physics of Fluids*, 6(6):2143–2153.

Curl, R. L. (1963). Dispersed phase mixing: I. Theory and effects in simple reactors. *AIChE Journal*, 9(2):175–181.

Danckwerts, P. V. (1958). The effect of incomplete mixing on homogeneous reactions. *Chemical Engineering Science*, 8(12):93–102.

Desjardins, O., Fox, R., and Villedieu, P. (2008). A quadrature-based moment method for dilute fluid-particle flows. *Journal of Computational Physics*, 227(4):2514–2539.

Dette, H. (1997). *The Theory of Canonical Moments with Applications in Statistics, Probability and Analysis*. John Wiley & Sons, New York.

Diemer, R. B. and Olson, J. H. (2002). A moment methodology for coagulation and breakage problems: Part 2moment models and distribution reconstruction. *Chemical Engineering Science*, 57(12):2211–2228.

Dopazo, C. (1994). Recent development in pdf methods. In Libby, P. A. and Williams, F. A., editors, *Turbulent Reacting Flows*, pages 357–474. New York: Academic Press.

Dopazo, C. and O'Brien, E. E. (1973). Isochoric turbulent mixing of two rapidly reacting chemical species with chemical heat release. *Physics of Fluids*, 16(12):2075–2081.

Efendiev, Y. and Zachariah, M. R. (2002). Hybrid Monte Carlo Method for Simulation of Two-Component Aerosol Coagulation and Phase Segregation. *Journal of Colloid and Interface Science*, 249(1):30–43.

Eswaran, V. and Pope, S. B. (1988). Direct numerical simulations of the turbulent mixing of a passive scalar. *Physics of Fluids*, 31:506–520.

Falola, A., Borissova, A., and Wang, X. Z. (2013). Extended method of moment for general population balance models including size dependent growth rate, aggregation and breakage kernels. *Computers & Chemical Engineering*, 56:1–11.

Fokker, A. D. (1914). Die mittlere Energie rotierender elektrischer Dipole im Strahlungsfeld. *Annalen der Physik*, 348(5):810–820.

Fox, R., Laurent, F., and Massot, M. (2008). Numerical simulation of spray coalescence in an Eulerian framework: Direct quadrature method of moments and multi-fluid method. *Journal of Computational Physics*, 227(6):3058–3088.

Fox, R. O. (1992a). Computation of turbulent reactive flows: first- principles macro/micromixing models using probability density function methods. *Chemical Engineering Science*, 47(9–11):2853–2858.

Fox, R. O. (1992b). The Fokker–Planck closure for turbulent molecular mixing: Passive scalars. *Physics of Fluids*, 4(6):1230–1244.

Fox, R. O. (1994). Improved Fokker–Planck model for the joint scalar, scalar gradient PDF. *Physics of Fluids*, 6(1):334–348.

Fox, R. O. (1998). On the relationship between Lagrangian micromixing models and computational fluid dynamics. *Chemical Engineering and Processing: Process Intensification*, 37(6):521–535.

Fox, R. O. (1999). The Lagrangian spectral relaxation model for differential diffusion in homogeneous turbulence. *Physics of Fluids*, 11(6):1550–1571.

Fox, R. O. (2003). Computational models for turbulent reacting flows. Cambridge University Press.

Fox, R. O. (2009). Optimal Moment Sets for Multivariate Direct Quadrature Method of Moments. *Industrial & Engineering Chemistry Research*, 48(21):9686–9696.

Frankel, S. H., Madnia, C. K., and Givi, P. (1992). Modeling of the reactant conversion rate in a turbulent shear flow. *Chemical Engineering Communications*, 113(1):197–209.

Garcia, A. L., van den Broeck, C., Aertsens, M., and Serneels, R. (1987). A Monte Carlo simulation of coagulation. *Physica A: Statistical Mechanics and its Applications*, 143(3):535–546.

Garmory, A., Kim, I. S., Britter, R. E., and Mastorakos, E. (2009). Simulations of the dispersion of reactive pollutants in a street canyon, considering different chemical mechanisms and micromixing. *Atmospheric Environment*, 43(31):4670–4680.

Garmory, A. and Mastorakos, E. (2008). Aerosol nucleation and growth in a turbulent jet using the Stochastic Fields method. *Chemical Engineering Science*, 63(16):4078–4089.

Garmory, A., Richardson, E. S., and Mastorakos, E. (2006). Micromixing effects in a reacting plume by the Stochastic Fields method. *Atmospheric Environment*, 40(6):1078–1091.

Gautschi, W. (2004). *Orthogonal Polynomials: Computation and Approximation*. Oxford University Press.

Gavi, E., Rivautella, L., Marchisio, D. L., Vanni, M., Barresi, A. A., and Baldi, G. (2007). CFD modelling of nano-particle precipitation in confined impinging jet reactors. *Chemical Engineering Research and Design*, 85(5):735–744.

Gelbard, F. and Seinfeld, J. H. (1978). Numerical solution of the dynamic equation for particulate systems. *Journal of Computational Physics*, 28(3):357–375.

Gillespie, D. T. (1976). A general method for numerically simulating the stochastic time evolution of coupled chemical reactions. *Journal of Computational Physics*, 22(4):403–434.

Girimaji, S. S. (1991). Assumed β-pdf model for turbulent mixing: validation and extension to multiple scalar mixing. *Combustion Science and Technology*, 78:177.

Golub, G. H. and Welsch, J. H. (1969). Calculation of gauss quadrature rules. *Mathematics of Computation*, 23(106):221–230.

Goodson, M. and Kraft, M. (2002). An efficient stochastic algorithm for simulating nano-particle dynamics. *Journal of Computational Physics*, 183(1):210–232.

Gordon, R. G. (1968). Error bounds in equilibrium statistical mechanics. *Journal of Mathematical Physics*, 9:655–662.

Greenberg, J. B., Alibagli, D., and Tambour, Y. (1986). An opposed jet quasi-monodisperse spray diffusion flame. *Combustion Science and Technology*, 50(4-6):255–270.

Greenberg, J. B., Silverman, I., and Tambour, Y. (1993). On the origins of spray sectional conservation equations. *Combustion and Flame*, 93(12):90–96.

Hounslow, M., Ryall, R., and Marshall, V. (1988). Discretized population balance for nucleation, growth, and aggregation. *AIChE Journal*, 34(11):1821–1832.

Hounslow, M. J. (1990). A discretized population balance for continuous systems at steady state. *AIChE Journal*, 36(1):106–116.

Hu, X., Passalacqua, A., and Fox, R. O. (2015). Application of quadrature-based uncertainty quantification to the NETL small-scale challenge problem SSCP-I. *Powder Technology*, 272:100–112.

Hulburt, H. M. and Katz, S. (1964). Some problems in particle technology: A statistical mechanical formulation. *Chemical Engineering Science*, 19(8):555–574.

Johnson, B. K. and Prud'homme, R. K. (2003). Chemical processing and micromixing in confined impinging jets. *AIChE Journal*, 49(9):2264–2282.

Jones, W. P. and Navarro-Martinez, S. (2007). Large eddy simulation of autoignition with a subgrid probability density function method. *Combustion and Flame*, 150(3):170–187.

Jones, W. P. and Navarro-Martinez, S. (2009). Numerical Study of n-Heptane Auto-ignition Using LES-PDF Methods. *Flow, Turbulence and Combustion*, 83(3):407–423.

Jones, W. P., Navarro-Martinez, S., and Rhl, O. (2007). Large eddy simulation of hydrogen auto-ignition with a probability density function method. *Proceedings of the Combustion Institute*, 31(2):1765–1771.

Juneja, A. and Pope, S. B. (1996). A DNS study of turbulent mixing of two passive scalars. *Physics of Fluids*, 8(8):2161–2184.

Kolmogoroff, A. (1931). ber die analytischen Methoden in der Wahrscheinlichkeitsrechnung. *Mathematische Annalen*, 104(1):415–458.

Koochesfahani, M. M. and Dimotakis, P. E. (1986). Mixing and chemical reactions in a turbulent liquid mixing layer. *Journal of Fluid Mechanics*, 170:83–112.

Kraichnan, R. H. (1989). Closures for probability distributions. *Bulletin of the American Physical Society*, 34:2298.

Kraichnan, R. H. (1990). Models of intermittency in hydrodynamic turbulence. *Physical Review Letters*, 65(5):575–578.

Kruis, F. E., Maisels, A., and Fissan, H. (2000). Direct simulation Monte Carlo method for particle coagulation and aggregation. *AIChE Journal*, 46(9):1735–1742.

Kumar, P. and Narayanan, S. (2006). Solution of Fokker-Planck equation by finite element and finite difference methods for nonlinear systems. *Sadhana - Academy Proceedings in Engineering Sciences*, 31:445–461.

Kumar, S. and Ramkrishna, D. (1996a). On the solution of population balance equations by discretization – I. A fixed pivot technique. *Chemical Engineering Science*, 51(8):1311–1332.

Kumar, S. and Ramkrishna, D. (1996b). On the solution of population balance equations by discretization – II. A moving pivot technique. *Chemical Engineering Science*, 51(8):1333–1342.

Lage, P. L. C. (2011). On the representation of QMOM as a weighted-residual method – The dual-quadrature method of generalized moments. *Computers & Chemical Engineering*, 35(11):2186–2203.

Lasheras, J. C., Eastwood, C., Martinez-Bazan, C., and Montanes, J. L. (2002). A review of statistical models for the break-up of an immiscible fluid immersed into a fully developed turbulent flow. *International Journal of Multiphase Flow*, 28(2):247–278.

Launder, B. E. and Sandham, N. D. (2002). *Closure Strategies for Turbulent and Transitional Flows*. Cambridge University Press, Cambridge.

Laurent, F. and Nguyen, T. T. (2017). Realizable second-order finite-volume schemes for the advection of moment sets of the particle size distribution. *Journal of Computational Physics*, 337:309–338.

Lee, K. and Matsoukas, T. (2000). Simultaneous coagulation and break-up using constant-n monte carlo. *Powder Technology*, 110(12):82–89.

Lee, K. W. (1983). Change of particle size distribution during Brownian coagulation. *Journal of Colloid and Interface Science*, 92(2):315–325.

Liffman, K. (1992). A direct simulation Monte-Carlo method for cluster coagulation. *Journal of Computational Physics*, 100(1):116–127.

Limpert, E., Stahel, W. A., and Abbt, M. (2001). Log-normal distribution across the sciences: keys and clues. *BioScience*, 51(5):341–352.

Lin, Y., Lee, K., and Matsoukas, T. (2002). Solution of the population balance equation using constant-number Monte Carlo. *Chemical Engineering Science*, 57(12):2241–2252.

Liu, Y., Cheng, C., Liu, Y., Prudhomme, R. K., and Fox, R. O. (2008). Mixing in a multi-inlet vortex mixer (MIVM) for flash nano-precipitation. *Chemical Engineering Science*, 63(11):2829–2842.

Liu, Z., Fox, R. O., Hill, J. C., and Olsen, M. G. (2015). A Batchelor Vortex Model for Mean Velocity of Turbulent Swirling Flow in a Macroscale Multi-Inlet Vortex Reactor. *Journal of Fluids Engineering*, 137(4):041204–041204.

Liu, Z., Passalacqua, A., Olsen, M. G., Fox, R. O., and Hill, J. C. (2016). Dynamic delayed detached eddy simulation of a multi-inlet vortex reactor. *AIChE Journal*, 62(7):2570–2578.

Luhar, A. K. and Sawford, B. L. (2005). Micromixing modelling of mean and fluctuating scalar fields in the convective boundary layer. *Atmospheric Environment*, 39(35):6673–6685.

Madadi-Kandjani, E. and Passalacqua, A. (2015). An extended quadrature-based moment method with log-normal kernel density functions. *Chemical Engineering Science*, 131:323–339.

Madnia, C. K., Frankel, S. H., and Givi, P. (1991). Direct numerical simulations of the unmixedness in a homogeneous reacting turbulent flow. *Chemical Engineering Communications*, 109(1):19–29.

Magnus, W., Oberhettinger, F., and Soni, R. P. (1966). *Formulas and theorems for the special functions of mathematical physics*. Springer–Verlag, Berlin.

Marchisio, D. L. and Fox, R. O. (2005). Solution of population balance equations using the direct quadrature method of moments. *Journal of Aerosol Science*, 36(1):43–73.

Marchisio, D. L. and Fox, R. O. (2013). *Computational Models for Polydisperse Particulate and Multiphase Systems*. Cambridge University Press, Cambridge.

Marchisio, D. L., Pikturna, J. T., Fox, R. O., Vigil, R. D., and Barresi, A. A. (2003a). Quadrature method of moments for population-balance equations. *AIChE Journal*, 49(5):1266–1276.

Marchisio, D. L., Vigil, R., and Fox, R. O. (2003b). Quadrature method of moments for aggregation-breakage processes. *Journal of Colloid and Interface Science*, 258(2):322–334.

Massot, M., Laurent, F., Kah, D., and de Chaisemartin, S. (2010). A robust moment method for evaluation of the disappearance rate of evaporating sprays. *SIAM Journal on Applied Mathematics*, 70(8):3203–3234.

McGraw, R. (1997). Description of aerosol dynamics by the quadrature method of moments. *Aerosol Science and Technology*, 27(2):255–265.

McMurtry, P. A. and Givi, P. (1989). Direct numerical simulations of mixing and reaction in a nonpremixed homogeneous turbulent flow. *Combustion and Flame*, 77(2):171–185.

Mead, L. R. and Papanicolaou, N. (1984). Maximum entropy in the problem of moments. *Journal of Mathematical Physics*, 25(8):2404–2417.

Meimaroglou, D. and Kiparissides, C. (2007). Monte Carlo simulation for the solution of the bi-variate dynamic population balance equation in batch particulate systems. *Chemical Engineering Science*, 62(1820):5295–5299.

Meyer, D. W. (2010). A new particle interaction mixing model for turbulent dispersion and turbulent reactive flows. *Physics of Fluids*, 22(3):035103.

Meyer, D. W. and Jenny, P. (2006). A mixing model for turbulent flows based on parameterized scalar profiles. *Physics of Fluids*, 18(3):035105.

Meyer, D. W. and Jenny, P. (2009). Micromixing models for turbulent flows. *Journal of Computational Physics*, 228(4):1275–1293.

Meyer, D. W. and Jenny, P. (2013). Accurate and computationally efficient mixing models for the simulation of turbulent mixing with PDF methods. *Journal of Computational Physics*, 247:192–207.

Muhr, H., David, R., Villermaux, J., and Jezequel, P. H. (1996). Crystallization and precipitation engineering-VI. Solving population balance in the case of the precipitation of silver bromide crystals with high primary nucleation rates by using the first order upwind differentiation. *Chemical Engineering Science*, 51(2):309–319.

Mungal, M. G. and Dimotakis, P. E. (1984). Mixing and combustion with low heat release in a turbulent shear layer. *Journal of Fluid Mechanics*, 148:349–382.

Nguyen, T. T., Laurent, F., Fox, R. O., and Massot, M. (2016). Solution of population balance equations in applications with fine particles: Mathematical modeling and numerical schemes. *Journal of Computational Physics*, 325:129–156.

Nooren, P. A., Wouters, H. A., Peeters, T. W. J., Roekaerts, D., Maas, U., and Schmidt, D. (1997). Monte Carlo PDF modelling of a turbulent natural-gas diffusion flame. *Combustion Theory and Modelling*, 1(1):79–96.

O'Brien, E. E. (1980). The probability density function (pdf) approach to reacting turbulent flows. In Libby, P. A. and Williams, F. A., editors, *Turbulent Reacting Flows*, number 44 in Topics in Applied Physics, pages 185–218. Springer Berlin Heidelberg.

O'Brien, E. E. and Jiang, T.-L. (1991). The conditional dissipation rate of an initially binary scalar in homogeneous turbulence. *Physics of Fluids A: Fluid Dynamics*, 3(12):3121–3123.

Overholt, M. R. and Pope, S. B. (1996). Direct numerical simulation of a passive scalar with imposed mean gradient in isotropic turbulence. *Physics of Fluids*, 8(11):3128–3148.

Perthame, B. (1992). Second-Order Boltzmann Schemes for Compressible Euler Equations in One and Two Space Dimensions. *SIAM Journal on Numerical Analysis*, 29(1):1–19.

Peters, N. (2000). *Turbulent Combustion*. Cambridge University Press, Cambridge, 1 edition.

Petitti, M., Nasuti, A., Marchisio, D. L., Vanni, M., Baldi, G., Mancini, N., and Podenzani, F. (2010). Bubble size distribution modeling in stirred gas-liquid reactors with QMOM augmented by a new correction algorithm. *AIChE Journal*, 56(1):36–53.

Pitsch, H. (2006). Large-Eddy Simulation of Turbulent Combustion. *Annual Review of Fluid Mechanics*, 38(1):453–482.

Poinsot, T. and Veynante, D. (2005). *Theoretical and Numerical Combustion, Second Edition*. R.T. Edwards, Inc., Philadelphia, 2 edition.

Pope, S. B. (1991). Mapping closures for turbulent mixing and reaction. *Theoretical and Computational Fluid Dynamics*, 2(5-6):255–270.

Pope, S. B. (2000). *Turbulent Flows*. Cambridge University Press, Cambridge.

Pope, S. B. (2013). A model for turbulent mixing based on shadow-position conditioning. *Physics of Fluids*, 25(11):110803.

Popov, P. P. and Pope, S. B. (2014). Large eddy simulation/probability density function simulations of bluff body stabilized flames. *Combustion and Flame*, 161(12):3100–3133.

Popov, P. P., Wang, H., and Pope, S. B. (2015). Specific volume coupling and convergence properties in hybrid particle/finite volume algorithms for turbulent reactive flows. *Journal of Computational Physics*, 294:110–126.

Pratsinis, S. E. (1988). Simultaneous nucleation, condensation, and coagulation in aerosol reactors. *Journal of Colloid and Interface Science*, 124(2):416–427.

Puel, F., Fevotte, G., and Klein, J. P. (2003). Simulation and analysis of industrial crystallization processes through multidimensional population balance equations. part 1: a resolution algorithm based on the method of classes. *Chemical Engineering Science*, 58(16):3715–3727.

Raman, V. and Pitsch, H. (2007). A consistent LES/filtered-density function formulation for the simulation of turbulent flames with detailed chemistry. *Proceedings of the Combustion Institute*, 31(2):1711–1719.

Ramkrishna, D. (2000). *Population balances: theory and applications to particulate systems in engineering*. Academic Press.

Randolph, A. (1964). A population balance for countable entities. *The Canadian Journal of Chemical Engineering*, 42(6):280–281.

Randolph, A. D. and Larson, M. A. (1988). *Theory of particulate processes: analysis and techniques of continuous crystallization*. Academic Press.

Reyes, J. N. J. (1989). Statistically derived conservation equations for fluid particle flows.

Richardson, E. S. and Chen, J. H. (2012). Application of PDF mixing models to premixed flames with differential diffusion. *Combustion and Flame*, 159(7):2398–2414.

Risken, H. (1989). *The Fokker-Planck Equation*, volume 18 of *Springer Series in Synergetics*. Springer Berlin Heidelberg, Berlin, Heidelberg.

Rosner, D. E. and Yu, S. (2001). MC simulation of aerosol aggregation and simultaneous spheroidization. *AIChE Journal*, 47(3):545–561.

Sabelnikov, V. and Soulard, O. (2005). Rapidly decorrelating velocity-field model as a tool for solving one-point Fokker-Planck equations for probability density functions of turbulent reactive scalars. *Physical Review E*, 72(1):016301.

Sabelnikov, V. and Soulard, O. (2006). White in Time Scalar Advection Model as a Tool for Solving Joint Composition PDF Equations. *Flow, Turbulence and Combustion*, 77(1-4):333–357.

Sawford, B. L. (2004). Micro-mixing modelling of scalar fluctuations for plumes in homogeneous turbulence. *Flow, Turbulence and Combustion*, 72(2-4):133–160.

Sawford, B. L. (2006). Lagrangian modeling of scalar statistics in a double scalar mixing layer. *Physics of Fluids*, 18(8):085108.

Shohat, J. A. and Tamarkin, J. D. (1943). *The Problem of Moments*. American Mathematical Soc.

Silva, L. F. L. R., Rodrigues, R. C., Mitre, J. F., and Lage, P. L. C. (2010). Comparison of the accuracy and performance of quadrature-based methods for population balance problems with simultaneous breakage and aggregation. *Computers & Chemical Engineering*, 34(3):286–297.

Smith, M. and Matsoukas, T. (1998). Constant-number Monte Carlo simulation of population balances. *Chemical Engineering Science*, 53(9):1777–1786.

Smoluchowski, M. v. (1916). Drei vortrge ber diffusion, brownsche bewegung und koagulation von kolloidteilchen. In Simon, H. T. and Debye, P., editors, *Physikalische Zeitschrift*, number 17, pages 557–585. S. Hirzel, Leipzig.

Spencer, B. F. and Bergman, L. A. (1993). On the numerical solution of the Fokker-Planck equation for nonlinear stochastic systems. *Nonlinear Dynamics*, 4(4):357–372.

Stollinger, M. and Heinz, S. (2010). Evaluation of scalar mixing and time scale models in PDF simulations of a turbulent premixed flame. *Combustion and Flame*, 157(9):1671–1685.

Subramaniam, S. and Pope, S. B. (1998). A mixing model for turbulent reactive flows based on Euclidean minimum spanning trees. *Combustion and Flame*, 115(4):487–514.

Sundaram, B., Klimenko, A. Y., Cleary, M. J., and Ge, Y. (2016). A direct approach to generalized multiple mapping conditioning for selected turbulent diffusion flame cases. *Combustion Theory and Modelling*, 20(4):735–764.

Tagliani, A. (1999). Hausdorff moment problem and maximum entropy: A unified approach. *Applied Mathematics and Computation*, 105(23):291–305.

Tsai, K. and Fox, R. O. (1994). PDF simulation of a turbulent seriesparallel reaction in an axisymmetric reactor. *Chemical Engineering Science*, 49(24):5141–5158.

Tsai, K. and Fox, R. O. (1995). Modeling multiple reactive scalar mixing with the generalized IEM model. *Physics of Fluids*, 7(11):2820–2830.

Valino, L. (1998). A Field Monte Carlo Formulation for Calculating the Probability Density Function of a Single Scalar in a Turbulent Flow. *Flow, Turbulence and Combustion*, 60(2):157–172.

Vanni, M. (2000). Approximate population balance equations for aggregation-breakage processes. *Journal of Colloid and Interface Science*, 221(2):143–160.

Vikas, V., Hauck, C., Wang, Z., and Fox, R. (2013a). Radiation transport modeling using extended quadrature method of moments. *Journal of Computational Physics*, 246:221–241.

Vikas, V., Wang, Z. J., and Fox, R. O. (2013b). Realizable high-order finite-volume schemes for quadrature-based moment methods applied to diffusion population balance equations. *Journal of Computational Physics*, 249:162–179.

Vikas, V., Wang, Z. J., Passalacqua, A., and Fox, R. O. (2011). Realizable high-order finite-volume schemes for quadrature-based moment methods. *Journal of Computational Physics*, 230(13):5328–5352.

Villermaux, J. and Devillon (1972). Represntation de la coalescence et de la redispersion des domaines de sgrgation dans un fluide par un modle d'interaction phnomnologique. In *In Proceedings of the 2nd International Symposium on Chemical Reaction Engineering*, pages 1–13. New York: Elsevier.

Villermaux, J. and Falk, L. (1994). A generalized mixing model for initial contacting of reactive fluids. *Chemical Engineering Science*, 49(24, Part 2):5127–5140.

Wang, H. and Kim, K. (2015). Effect of molecular transport on PDF modeling of turbulent non-premixed flames. *Proceedings of the Combustion Institute*, 35(2):1137–1145.

Wang, L. and Fox, R. O. (2004). Comparison of micromixing models for CFD simulation of nanoparticle formation. *AIChE Journal*, 50(9):2217–2232.

Wang, L., Marchisio, D., Vigil, R., and Fox, R. (2005a). CFD simulation of aggregation and breakage processes in laminar Taylor–Couette flow. *Journal of Colloid and Interface Science*, 282(2):380–396.

Wang, L., Vigil, R. D., and Fox, R. O. (2005b). CFD simulation of shear-induced aggregation and breakage in turbulent Taylor–Couette flow. *Journal of Colloid and Interface Science*, 285(1):167–178.

Weisstein, E. W. (1998). *CRC Concise Encyclopedia of Mathematics*. CRC Press.

Wheeler, J. C. (1974). Modified moments and Gaussian quadratures. *Rocky Mountain Journal of Mathematics*, 4:287–296.

Wilck, M. (2001). A general approximation method for solving integrals containing a lognormal weighting function. *Journal of Aerosol Science*, 32(9):1111–1116.

Wilf, H. S. (1962). *Mathematics for the Physical Sciences*. Dover Publications, New York.

Williams, M. M. R. and Loyalka, S. K. (1991). *Aerosol Science: Theory and Practice*. Pergamon, Oxford ; New York, 1^{st} edition.

Wright, D. L. (2007). Numerical advection of moments of the particle size distribution in eulerian models. *Journal of Aerosol Science*, 38(3):352–369.

Yeung, P. K., Donzis, D. A., and Sreenivasan, K. R. (2005). High-Reynolds-number simulation of turbulent mixing. *Physics of Fluids*, 17(8):081703.

Yeung, P. K., Xu, S., and Sreenivasan, K. R. (2002). Schmidt number effects on turbulent transport with uniform mean scalar gradient. *Physics of Fluids*, 14(12):4178–4191.

Yuan, C. and Fox, R. (2011). Conditional quadrature method of moments for kinetic equations. *Journal of Computational Physics*, 230(22):8216–8246.

Yuan, C., Laurent, F., and Fox, R. (2012). An extended quadrature method of moments for population balance equations. *Journal of Aerosol Science*, 51:1–23.

Zhao, H., Kruis, F. E., and Zheng, C. (2009). Reducing statistical noise and extending the size spectrum by applying weighted simulation particles in Monte Carlo simulation of coagulation. *Aerosol Science and Technology*, 43(8):781–793.

Zhao, H., Maisels, A., Matsoukas, T., and Zheng, C. (2007). Analysis of four Monte Carlo methods for the solution of population balances in dispersed systems. *Powder Technology*, 173(1):38–50.

Zhao, H. and Zheng, C. (2013). A population balance-Monte Carlo method for particle coagulation in spatially inhomogeneous systems. *Computers & Fluids*, 71:196–207.

Zhao, X.-Y., Bhagatwala, A., Chen, J. H., Haworth, D. C., and Pope, S. B. (2016). An a priori DNS study of the shadow-position mixing model. *Combustion and Flame*, 165:223–245.

CHAPTER 4. A QUADRATURE-BASED CFD MODEL FOR SINGLE-PHASE TURBULENT REACTING FLOWS

Abstract

In this study, a new model based on quadrature-based moments method is used to investigate the single-phase turbulent reacting flows. Transport equation based on the join composition probability density function is introduced for the mixture fraction and reaction progress variables as internal coordinates. Later the conditional quadrature method of moments (CQMOM) (Yuan and Fox, 2011) is used to close the transport equation. Interaction by exchange with the mean and the Fokker-Planck mixing models are used for the term related to the mixing in composition space. A numerical procedure is then adopted to address the reaction of two species in a string. The direct quadrature method of moments (DQMOM) is also employed and the correction terms related to DQMOM is derived for this problem. The results obtained by CQMOM with different mixing models and different reaction mechanisms are then compared to those obtained by DQMOM.

4.1 Introduction

Turbulent reacting flows are an important field of study. Understanding the behavior of these flows are of great importance. Computational fluid dynamics is one of the convenient tools to simulate such complex flow. It is the branch of study that expands fast by growing the power of computers. Turbulent reactive flows mostly happen in engineering applications. For example, in combustion, where different species start reacting with each other during the burning process to produce heat and work, it is being used to increase the fuel efficiency and reduce soot and NO_x. Moreover in reacting flows, chemical compositions can be determined

by turbulent mixing and chemical reactions. In current flow simulations, as an example in Reynolds-averaged Navier-Stokes (RANS) equations, transport equations are solved for averaged components (Pope, 2000; Fox, 2003). In such models, there is a need to close terms arising from the fluctuating components. In chemically reacting flows, the chemical source terms that occur in material and energy balance equations are unclosed (Meyer and Jenny, 2009; Akroyd et al., 2010) and modeling of these components are necessary.

Large number of models are introduced for chemical source terms in previous studies (Fox, 2003; O'Brien, 1980; Peters, 2000; Poinsot and Veynante, 2005). In this study, to overcome the closure problem in turbulent transport and chemical reaction, PDF methods are applied. The advantage of using PDF method is that it provides the entire information on joint composition PDF. However, there is a need of mixing models for molecular diffusion.

Large number of mixing models have been proposed in literature (Curl, 1963; Villermaux and Falk, 1994; Tsai and Fox, 1995; Fox, 1992b, 1994; Subramaniam and Pope, 1998; Meyer and Jenny, 2009). In this study Interaction by exchange with the mean and Fokker-Planck models are considered to close the molecular diffusion.

Approximation solution of PDF transport equation can be determined using several approaches. Monte Carlo solution techniques (Lin et al., 2002; Meimaroglou and Kiparissides, 2007; Rosner and Yu, 2001; Smith and Matsoukas, 1998; Zhao et al., 2007) and method of classes (Balakin et al., 2014; Bannari et al., 2008; Becker et al., 2011; Hounslow et al., 1988; Hounslow, 1990; Kumar and Ramkrishna, 1996a,b; Puel et al., 2003) are some examples of those methods. Although these methods are intuitive and accurate, they are computationally expensive to be used in large-scale CFD simulations. A sufficiently accurate approach to finding the solution of the PDF is the quadrature-based moment methods. Quadrature method of moments (QMOM) is initially proposed by McGraw (1997) for aerosols application and later used by Marchisio et al. (2003b) for chemical engineering applications. Later direct quadrature method of moments introduced by Marchisio and Fox (2005) in the context of population balance equation. The shortcoming of this method is that it uses the discrete representation of the PDF and it does not guarantee the conservation of moments as the non-conserved quantities of weights and abscissae are being transported.

In order to overcome this limitation, we use the conditional quadrature method of moments introduce by Yuan and Fox (2011). In this method, a moment-inversion algorithm based on the adaptive quadrature of conditional composition moments is used to approximate the continuous distributions. It has been shown that this method always yields realizable distribution functions Yuan and Fox (2011).

The remainder of this chapter is structured as below. In Sec. 4.2 we present the joint composition PDF transport equation for turbulent reactive flows. Different reactions such as one reaction, two competitive consecutive reaction, and fast reactions are considered in this study and the model is adopted for such reactions. Two mixing models e.g. interaction by exchange with the mean and Fokker-Planck models are used to close the molecular diffusion term. In Sec. 4.3, we introduce the new model based on conditional quadrature method of moments. This method is implemented to turbulent reactive flows to overcome the closure problem in turbulent transport and chemical reaction terms. In Sec. 4.4 we review the algorithm we use to compute the mixture fraction and progress variables depending on the reaction type. In Sec. 4.5, we provide a solution of turbulent reacting flows using the direct quadrature method of moments. Finally in Sec.4.6 we compare the results obtained by CQMOM with DQMOM with different mixing models and different reaction types.

4.2 Transported PDF method for turbulent reacting flow

The joint composition transport equation which treats both the velocity and the compositions as random variables is derived in previous studies (Fox, 2003). The composition PDF evolves by macromixing (convective transport in real space due to the mean velocity), mesomixing (convective transport in composition space due to the scalar-conditioned velocity fluctuations), micromixing (transport in composition space due to the molecular mixing) and chemical reactions. Thus, depending on the problem, we can identify the transport equation with different micromixing terms and different chemical reaction conditions.To model a problem that involves mixing, it is possible to define the source terms in two ways. These two types of source term can lead us to the two transport equations which can be defined as:

- Interaction by exchange with the mean (IEM)

$$\mathcal{L}\{f\} = -\frac{\partial}{\partial \xi}\left[\frac{\varepsilon_\xi}{\langle \xi'^2 \rangle}\left(\langle \xi \rangle - \xi\right) f\right] \tag{4.1}$$

- Fokker-Planck

$$\mathcal{L}\{f\} = -\frac{\partial}{\partial \xi}\left[\frac{\varepsilon_\xi}{\langle \xi'^2 \rangle}\left(\langle \xi \rangle - \xi\right) f\right] + \frac{1}{2}\frac{\partial^2}{\partial \xi^2}\left[\langle \varepsilon \mid \xi \rangle f\right] \tag{4.2}$$

where

$$\mathcal{L}\{\} = \frac{\partial}{\partial t} + \langle U \rangle \frac{\partial}{\partial \mathbf{x}} - \frac{\partial}{\partial \mathbf{x}}\left(\Gamma_t \frac{\partial}{\partial \mathbf{x}}\right), \tag{4.3}$$

ξ is mixture fraction, $\langle \xi \rangle$ is mean mixture fraction, f probability density function, $\langle \xi'^2 \rangle$ is variance of the mixture fraction, ε_ξ is dissipation factor, t is time, $\langle U \rangle$ is mean velocity and Γ_t denotes turbulent diffusivity. If the problem under study also involves the reaction, source terms for the reaction would be defined in three ways depend on the nature of the reaction. These three kinds of reaction can be defined as:

- Competitive consecutive reaction

$$\begin{aligned} A + B &\rightarrow R \\ B + R &\rightarrow S \end{aligned} \tag{4.4}$$

- Fast competitive consecutive reaction

$$\begin{aligned} A + B &\rightarrow R \\ B + R &\rightarrow S \end{aligned} \tag{4.5}$$

- One step reaction

$$A + B \rightarrow R \tag{4.6}$$

where the A and B are the reactants, R is the primary product and S is the bi-product. Thus chemical source terms can be defined as:

- Competitive consecutive reaction

$$\begin{aligned} \mathcal{R}_1(\xi, Y_1, Y_2) &= \xi_{st} k_1 c_{B_0}\left(\frac{1-\xi}{1-\xi_{st}} - Y_1\right)\left(\frac{\xi}{\xi_{st}} - Y_1 - Y_2\right), \\ \mathcal{R}_2(\xi, Y_1, Y_2) &= \xi_{st} k_2 c_{B_0}\left(Y_1 - Y_2\right)\left(\frac{\xi}{\xi_{st}} - Y_1 - Y_2\right). \end{aligned} \tag{4.7}$$

- Fast competitive consecutive reaction

$$\mathcal{R}\left(\xi, Y_2\right) = \xi_{st} k_2 c_{B_0} h_1\left(\xi, Y_2\right) h_2\left(\xi, Y_2\right). \tag{4.8}$$

with

$$\begin{aligned} h_1\left(\xi, Y_2\right) &= \frac{1-\xi}{1-\xi_{st}} - Y_2 \\ h_2\left(\xi, Y_2\right) &= \frac{\xi-\xi_{st}}{\xi_{st}\left(1-\xi_{st}\right)} - Y_2 \end{aligned} \tag{4.9}$$

It should be mention here that in the limit where $k_1 c_{B_0} \to \infty$, the first reaction can be written in terms of Y_2 and ξ.

$$Y_1\left(\xi, Y_2\right) = \min\left(\frac{\xi}{\xi_{st}} - Y_2, \frac{1-\xi}{1-\xi_{st}}\right) \tag{4.10}$$

- one step reaction

$$\mathcal{R}\left(\xi, Y_1\right) = \xi_{st} k_1 c_{B_0}\left(\frac{1-\xi}{1-\xi_{st}} - Y_1\right)\left(\frac{\xi}{\xi_{st}} - Y_1\right). \tag{4.11}$$

where Y_1 denotes progress variable for the first reaction, Y_2 progress variable for the second reaction, ξ mixture fraction, c_{A_0} initial concentration of a reactant A, c_{B_0} initial concentration of a reactant B, k_1 reaction rate constant for the first reaction, k_2 reaction rate constant for the second reaction and the ξ_{st} stoichiometric mixture fraction can be described as

$$\xi_{st} = \frac{c_{A_0}}{c_{A_0} + c_{B_0}}. \tag{4.12}$$

Implementing the reaction source terms, transport equation for different reaction condition with different micromixing terms can be introduced as:

- IEM mixing with competitive consecutive reaction

$$\begin{aligned} \mathcal{L}\left\{f\right\} = -\frac{\partial}{\partial \xi}\left[\frac{\varepsilon_\xi}{\langle \xi'^2 \rangle}\left(\langle \xi \rangle - \xi\right) f\right] - \frac{\partial}{\partial Y_1}\left[\mathcal{R}_1\left(\xi, Y_1, Y_2\right) f\right] \\ - \frac{\partial}{\partial Y_2}\left[\mathcal{R}_2\left(\xi, Y_1, Y_2\right) f\right] \end{aligned} \tag{4.13}$$

- IEM mixing with fast competitive consecutive reaction

$$\mathcal{L}\left\{f\right\} = -\frac{\partial}{\partial \xi}\left[\frac{\varepsilon_\xi}{\langle \xi'^2 \rangle}\left(\langle \xi \rangle - \xi\right) f\right] - \frac{\partial}{\partial Y_2}\left[\mathcal{R}_2\left(\xi, Y_2\right) f\right] \tag{4.14}$$

- IEM mixing with one step reaction

$$\mathcal{L}\{f\} = -\frac{\partial}{\partial \xi}\left[\frac{\varepsilon_\xi}{\langle \xi'^2 \rangle}\left(\langle \xi \rangle - \xi\right) f\right] - \frac{\partial}{\partial Y_1}\left[\mathcal{R}_1\left(\xi, Y_1\right) f\right] \tag{4.15}$$

- Fokker-Planck mixing with competitive consecutive reaction

$$\mathcal{L}\{f\} = -\frac{\partial}{\partial \xi}\left[\frac{\varepsilon_\xi}{\langle \xi'^2 \rangle}\left(\langle \xi \rangle - \xi\right) f\right] + \frac{1}{2}\frac{\partial^2}{\partial \xi^2}\left[\langle \varepsilon \mid \xi \rangle f\right] - \frac{\partial}{\partial Y_1}\left[\mathcal{R}_1\left(\xi, Y_1, Y_2\right) f\right] - \frac{\partial}{\partial Y_2}\left[\mathcal{R}_2\left(\xi, Y_1, Y_2\right) f\right] \tag{4.16}$$

- Fokker-Planck mixing with fast competitive consecutive reaction

$$\mathcal{L}\{f\} = -\frac{\partial}{\partial \xi}\left[\frac{\varepsilon_\xi}{\langle \xi'^2 \rangle}\left(\langle \xi \rangle - \xi\right) f\right] + \frac{1}{2}\frac{\partial^2}{\partial \xi^2}\left[\langle \varepsilon \mid \xi \rangle f\right] - \frac{\partial}{\partial Y_2}\left[\mathcal{R}_2\left(\xi, Y_2\right) f\right] \tag{4.17}$$

- Fokker-Planck mixing with one step reaction

$$\mathcal{L}\{f\} = -\frac{\partial}{\partial \xi}\left[\frac{\varepsilon_\xi}{\langle \xi'^2 \rangle}\left(\langle \xi \rangle - \xi\right) f\right] + \frac{1}{2}\frac{\partial^2}{\partial \xi^2}\left[\langle \varepsilon \mid \xi \rangle f\right] - \frac{\partial}{\partial Y_1}\left[\mathcal{R}_1\left(\xi, Y_1\right) f\right] \tag{4.18}$$

4.3 Solution of the turbulent reacting flow using the conditional quadrature method of moments (CQMOM)

It is convenient to introduce the conditional density functions $f\left(Y_2 \mid \xi, Y_1\right)$ and $f\left(Y_1 \mid \xi\right)$ which are corresponds to the conditional density function for Y_2, given fixed values for the ξ and Y_1, and the conditional density function for Y_1, given fixed values for the ξ respectively. Then the conditional density function related to the mixture fraction and the progress variables can be expressed as:

$$f = f\left(\xi, Y_1, Y_2\right) = f\left(Y_2 \mid \xi, Y_1\right) f\left(\xi, Y_1\right) = f\left(Y_2 \mid \xi, Y_1\right) f\left(Y_1 \mid \xi\right) f\left(\xi\right). \tag{4.19}$$

The conditional moments can be expressed using the conditional density functions and can be defined by

$$\left\langle Y_1^j \right\rangle \left(\xi\right) \equiv \int Y_1^j f\left(Y_1 \mid \xi\right) \mathrm{d}Y_1 \tag{4.20}$$

and

$$\left\langle Y_2^j \right\rangle (\xi, Y_1) \equiv \int Y_2^j f\left(Y_2 \mid \xi, Y_1\right) \mathrm{d}Y_2 \tag{4.21}$$

Let M_{njk} denote the moments of f, where the non-negative integers n,j and k represents the order for each scalar, e.g. mixture fraction and progress variable one and progress variable two. Thus the moments in integral form is defined as:

$$M_{njk}(\mathbf{x}, t) = \iiint \xi^n Y_1^j Y_2^k f\left(\xi, Y_1, Y_2; \mathbf{x}, t\right) \mathrm{d}\xi \mathrm{d}Y_1 \mathrm{d}Y_2. \tag{4.22}$$

Using the same definition it is possible to show that:

$$M_{nj0} = \iint \xi^n Y_1^j f\left(\xi, Y_1\right) \mathrm{d}\xi \mathrm{d}Y_1 = \int \xi^n \left\langle Y_1^j \right\rangle (\xi) f\left(\xi\right) \mathrm{d}\xi \tag{4.23}$$

and

$$M_{njk} = \iint \xi^n Y_1^j \left\langle Y_2^k \right\rangle (\xi, Y_1) f\left(\xi, Y_1\right) \mathrm{d}\xi \mathrm{d}Y_1 \tag{4.24}$$

In quadrature-based moment method (QBMM) the scalar distribution function can be represented by:

$$f(\boldsymbol{\phi}) = \sum_{\alpha=1}^{\mathrm{N}} w_\alpha \delta\left(\phi - \phi_\alpha\right), \tag{4.25}$$

where $\phi_\alpha = (\xi, Y_1, Y_2)$ represent the scalar of interest, w_α are the weights. For clarity, we will assume that only mean values for the conditional scalars are necessary, e.g. we assume that $\mathrm{N}_2 = \mathrm{N}_3 = 1$. The number of the primary nodes are $\mathrm{N}_1 = 2$. This assumption yields to the fact that the conditional weights becomes unity by definition. We also assume that the primary moments represent the mixture fraction while the conditional moments are represent the progress variables, Y_1 and Y_2. Implementing Eq. 5.15 into Eq. 5.14 can be expressed as:

$$f\left(\xi, Y_1, Y_2\right) = \sum_{\alpha=1}^{\mathrm{N}_1} w_\alpha \delta\left(\xi - \xi_\alpha\right) \delta\left(Y_1 - Y_{1;\alpha}\right) \delta\left(Y_2 - Y_{2;\alpha}\right). \tag{4.26}$$

Given the assumptions above, we reconstruct the coefficient matrices for the CQMOM:

$$\mathbf{V} = \begin{bmatrix} 1 & 1 \\ \xi_1 & \xi_2 \end{bmatrix}, \quad \text{and} \quad \mathbf{R} = \begin{bmatrix} w_1 & 0 \\ 0 & w_2 \end{bmatrix}. \tag{4.27}$$

Using the coefficient matrices, the set of the equation can be written to find the conditional moments from the original transported moments. These equations can be expressed as:

$$\mathbf{VR} \begin{bmatrix} Y_{1;1} & Y_{2;1} \\ Y_{1;2} & Y_{2;2} \end{bmatrix} = \begin{bmatrix} M_{010} & M_{001} \\ M_{110} & M_{101} \end{bmatrix}. \tag{4.28}$$

$$\begin{bmatrix} Y_{1;1} & Y_{2;1} \\ Y_{1;2} & Y_{2;2} \end{bmatrix} = \frac{1}{w_1 w_2 \xi_2 - w_1 w_2 \xi_1} \begin{bmatrix} w_2 \xi_2 & -w_2 \\ -w_1 \xi_1 & w_1 \end{bmatrix} \begin{bmatrix} M_{010} & M_{001} \\ M_{110} & M_{101} \end{bmatrix}. \tag{4.29}$$

In other words we can express the conditional moments as:

$$\begin{aligned} Y_{1;1} &= \frac{1}{w_1 (\xi_2 - \xi_1)} \left[\xi_2 M_{010} - M_{110} \right], \\ Y_{1;2} &= \frac{1}{w_2 (\xi_2 - \xi_1)} \left[-\xi_1 M_{010} + M_{110} \right], \\ Y_{2;1} &= \frac{1}{w_1 (\xi_2 - \xi_1)} \left[\xi_2 M_{001} - M_{101} \right], \\ Y_{2;2} &= \frac{1}{w_2 (\xi_2 - \xi_1)} \left[-\xi_1 M_{001} + M_{101} \right]. \end{aligned} \tag{4.30}$$

In terms of the moments, Eq. 5.16 can be expressed for the assumed case as:

$$M_{njk} = \sum_{\alpha=1}^{\mathrm{N}_1} w_\alpha \xi_\alpha^n Y_{1;\alpha}^j Y_{2;\alpha}^k. \tag{4.31}$$

Using the definition for the moments, we can rewrite the transport equations in the form of moments for each problem. Thus the moments transport equations will be defined as:

- Pure IEM mixing

$$\mathcal{L}\{M_n\} = \frac{n \varepsilon_\xi}{\langle \xi'^2 \rangle} \left(M_{n-1} M_1 - M_n \right). \tag{4.32}$$

- Pure Fokker-Planck mixing

$$\mathcal{L}\{M_n\} = \frac{n \varepsilon_\xi}{\langle \xi'^2 \rangle} \left(M_{n-1} M_1 - M_n \right) + \frac{n (n-1) \varepsilon_\xi}{2 (M_1 - M_2)} \left(M_{n-1} - M_n \right). \tag{4.33}$$

- IEM mixing with competitive consecutive reaction

$$\mathcal{L}\{M_{njk}\} = \frac{n\varepsilon_\xi}{\langle \xi'^2 \rangle}\left(M_{n-1}M_{100} - M_n\right) + \sum_{\alpha=1}^{\mathrm{N}_1} w_\alpha \mathcal{R}_1\left(\xi_\alpha, Y_{1;\alpha}, Y_{2;\alpha}\right)\left(j\xi_\alpha^n Y_{1;\alpha}^{j-1} Y_{2;\alpha}^k\right) + \sum_{\alpha=1}^{\mathrm{N}_1} w_\alpha \mathcal{R}_2\left(\xi_\alpha, Y_{1;\alpha}, Y_{2;\alpha}\right)\left(k\xi_\alpha^n Y_{1;\alpha}^j Y_{2;\alpha}^{k-1}\right). \quad (4.34)$$

- IEM mixing with fast competitive consecutive reaction

$$\mathcal{L}\{M_{nk}\} = \frac{n\varepsilon_\xi}{\langle \xi'^2 \rangle}\left(M_{n-1}M_{10} - M_n\right) + \sum_{\alpha=1}^{\mathrm{N}_1} w_\alpha \mathcal{R}\left(\xi_\alpha, Y_{2,\alpha}\right)\left(k\xi_\alpha^n Y_{2,\alpha}^{k-1}\right). \quad (4.35)$$

- IEM mixing with one step reaction

$$\mathcal{L}\{M_{nj}\} = \frac{n\varepsilon_\xi}{\langle \xi'^2 \rangle}\left(M_{n-1}M_{10} - M_n\right) + \sum_{\alpha=1}^{\mathrm{N}_1} w_\alpha \mathcal{R}_1\left(\xi_\alpha, Y_{1,\alpha}\right)\left(j\xi_\alpha^n Y_{1,\alpha}^{j-1}\right). \quad (4.36)$$

- Fokker-Planck mixing with competitive consecutive reaction

$$\mathcal{L}\{M_{njk}\} = \frac{n\varepsilon_\xi}{\langle \xi'^2 \rangle}\left(M_{n-1}M_{100} - M_n\right) + \frac{n\left(n-1\right)\varepsilon_\xi}{2\left(M_{100} - M_{200}\right)}\left(M_{n-1} - M_n\right) + \sum_{\alpha=1}^{\mathrm{N}_1} w_\alpha \mathcal{R}_1\left(\xi_\alpha, Y_{1;\alpha}, Y_{2;\alpha}\right)\left(j\xi_\alpha^n Y_{1;\alpha}^{j-1} Y_{2;\alpha}^k\right) + \sum_{\alpha=1}^{\mathrm{N}_1} w_\alpha \mathcal{R}_2\left(\xi_\alpha, Y_{1;\alpha}, Y_{2;\alpha}\right)\left(k\xi_\alpha^n Y_{1;\alpha}^j Y_{2;\alpha}^{k-1}\right). \quad (4.37)$$

- Fokker-Planck mixing with fast competitive consecutive reaction

$$\mathcal{L}\{M_{nk}\} = \frac{n\varepsilon_\xi}{\langle \xi'^2 \rangle}\left(M_{n-1}M_{10} - M_n\right) + \frac{n\left(n-1\right)\varepsilon_\xi}{2\left(M_{10} - M_{20}\right)}\left(M_{n-1} - M_n\right) + \sum_{\alpha=1}^{\mathrm{N}_1} w_\alpha \mathcal{R}\left(\xi_\alpha, Y_{2,\alpha}\right)\left(k\xi_\alpha^n Y_{2,\alpha}^{k-1}\right). \quad (4.38)$$

- Fokker-Planck mixing with one step reaction

$$\mathcal{L}\{M_{nj}\} = \frac{n\varepsilon_\xi}{\langle \xi'^2 \rangle}\left(M_{n-1}M_{10} - M_n\right) + \frac{n\left(n-1\right)\varepsilon_\xi}{2\left(M_{10} - M_{20}\right)}\left(M_{n-1} - M_n\right) + \sum_{\alpha=1}^{\mathrm{N}_1} w_\alpha \mathcal{R}_1\left(\xi_\alpha, Y_{1,\alpha}\right)\left(j\xi_\alpha^n Y_{1,\alpha}^{j-1}\right). \quad (4.39)$$

4.4 CQMOM algorithm and chemical kinetics

Here, we present the procedure we used to implement the CQMOM model. The mixture fraction is considered to be the primary direction and the progress variable one and progress variable two are considered to be the conditional directions. Below we describe the algorithm:

- Initialize the number of nodes per each direction (our problem has three dimensions, e.g. mixture fraction, progress variable one and progress variable two.
- We consider the two primary nodes and one conditional node for the second and third direction. Choosing of one node is due to the fact that there is no information and closure for the cross terms that may appear on the right-hand side of the equation between mixture fraction and chemical reactions. Also, we are only interested in the mean values of the progress variables for the first and second reaction.
- We use initial values for the concentrations to calculate the stoichiometric mixture fraction.
- We initialize moments of PDF. Depend on reaction condition, we use set of moments as it is stated below:
  - Pure mixing (one dimension)

$$M_{000} \quad M_{100} \quad M_{200} \quad M_{300} \tag{4.40}$$

  - Mixing with competitive consecutive reaction (three dimension)

$$\begin{array}{lll} M_{000} & M_{010} & M_{001} \\ M_{100} & M_{110} & M_{101} \\ M_{200} & & \\ M_{300} & & \end{array} \tag{4.41}$$

– Mixing with fast competitive consecutive reaction (two dimension)

$$\begin{matrix} M_{000} & M_{001} \\ M_{100} & M_{101} \\ M_{200} & \\ M_{300} & \end{matrix} \tag{4.42}$$

– Mixing with one step reaction (two dimension)

$$\begin{matrix} M_{000} & M_{010} \\ M_{100} & M_{110} \\ M_{200} & \\ M_{300} & \end{matrix} \tag{4.43}$$

- Invert the moments of the mixture fraction dimension e.g. M_{000}, M_{100}, M_{200} and M_{300} using the adaptive Wheeler algorithm to obtain the primary weights, w_α, and primary abscissae, ξ_α.

- Using the conditional moments of the second direction to find the abscissae of the progress variable one for the node 1 and node 2:

$$\begin{aligned} Y_{1;1} &= \frac{1}{w_1\left(\xi_2 - \xi_1\right)}\left[\xi_2 M_{010} - M_{110}\right], \\ Y_{1;2} &= \frac{1}{w_2\left(\xi_2 - \xi_1\right)}\left[-\xi_1 M_{010} + M_{110}\right]. \end{aligned} \tag{4.44}$$

- Using the conditional moments of the third direction to find the abscissae of the progress variable two for the node 1 and node 2:

$$\begin{aligned} Y_{2;1} &= \frac{1}{w_1\left(\xi_2 - \xi_1\right)}\left[\xi_2 M_{001} - M_{101}\right], \\ Y_{2;2} &= \frac{1}{w_2\left(\xi_2 - \xi_1\right)}\left[-\xi_1 M_{001} + M_{101}\right]. \end{aligned} \tag{4.45}$$

  This step depends on the problem if we have the third direction or not.

- For fast competitive consecutive reaction, the value for the abscissae of progress variable one for the node 1 and node 2 will be calculated after solving the transport equations for the moments of progress variable:

$$Y_1\left(\xi, Y_2\right) = \min\left(\frac{\xi}{\xi_{st}} - Y_2, \frac{1-\xi}{1-\xi_{st}}\right). \tag{4.46}$$

- Solve the transport equations for the moments with the source terms described before for each problem with the different model for the mixing and different type of reaction.

- Use the mean values for the mixture fraction (M_{100}), progress variable one (M_{010}) and progress variable two (M_{001}) to calculate the concentration using the equations below (for pure mixing there is no concentration included in calculations):

  – Mixing with competitive consecutive reaction

$$\begin{aligned} c_A &= c_{A_0}\left[1-\xi-\left(1-\xi_{st}\right)Y_1\right], \\ c_B &= c_{B_0}\left[\xi-\xi_{st}\left(Y_1+Y_2\right)\right], \\ c_R &= c_{B_0}\xi_{st}\left(Y_1-Y_2\right), \\ c_S &= c_{B_0}\xi_{st}Y_2. \end{aligned} \tag{4.47}$$

  – Mixing with fast competitive consecutive reaction

$$\begin{aligned} c_A &= c_{A_0}\left[1-\xi-\left(1-\xi_{st}\right)Y_1\right], \\ c_B &= c_{B_0}\left[\xi-\xi_{st}\left(Y_1+Y_2\right)\right], \\ c_R &= c_{B_0}\xi_{st}\left(Y_1-Y_2\right), \\ c_S &= c_{B_0}\xi_{st}Y_2. \end{aligned} \tag{4.48}$$

  – Mixing with one step reaction

$$\begin{aligned} c_A &= c_{A_0}\left[1-\xi-\left(1-\xi_{st}\right)Y_1\right], \\ c_B &= c_{B_0}\left[\xi-\xi_{st}\left(Y_1\right)\right], \\ c_R &= c_{B_0}\xi_{st}Y_1. \end{aligned} \tag{4.49}$$

- Use the current values of the moments for the next time step and implement the same procedure for the next step until the end of the simulation.

4.5 Solution of the turbulent reacting flow using the direct quadrature method of moments (DQMOM)

In order to compare the results obtained by CQMOM and DQMOM, we follow the path presented before in Fox (2003). Here we only consider the evolution equation for joint composition

PDF for three scalar, ξ, Y_1 and Y_2 with IEM model and two competitive consecutive reaction which is defined in Eq. 4.13. Thus the PDF can be approximated as:

$$f\left(\xi, Y_1, Y_2\right) = \sum_{\alpha=1}^{\mathrm{N}} w_\alpha \delta\left(\xi - \xi_\alpha\right) \delta\left(Y_1 - Y_{1,\alpha}\right) \delta\left(Y_2 - Y_{2,\alpha}\right), \tag{4.50}$$

We begin derivation of the DQMOM by implementing the Eq. 4.50 into the Eq. 4.13. We assume that

$$\begin{aligned}
&\frac{\partial w_\alpha}{\partial t} + \langle U \rangle \frac{\partial w_\alpha}{\partial \mathbf{x}} - \frac{\partial}{\partial \mathbf{x}}\left(\Gamma_t \frac{\partial w_\alpha}{\partial \mathbf{x}}\right) = a_\alpha \\
&\frac{\partial w_\alpha \langle \xi \rangle_\alpha}{\partial t} + \langle U \rangle \frac{\partial w_\alpha \langle \xi \rangle_\alpha}{\partial \mathbf{x}} - \frac{\partial}{\partial \mathbf{x}}\left(\Gamma_t \frac{\partial w_\alpha \langle \xi \rangle_\alpha}{\partial \mathbf{x}}\right) = b_{1\alpha} \\
&\frac{\partial w_\alpha \langle Y_1 \rangle_\alpha}{\partial t} + \langle U \rangle \frac{\partial w_\alpha \langle Y_1 \rangle_\alpha}{\partial \mathbf{x}} - \frac{\partial}{\partial \mathbf{x}}\left(\Gamma_t \frac{\partial w_\alpha \langle Y_1 \rangle_\alpha}{\partial \mathbf{x}}\right) = b_{2\alpha} \\
&\frac{\partial w_\alpha \langle Y_2 \rangle_\alpha}{\partial t} + \langle U \rangle \frac{\partial w_\alpha \langle Y_2 \rangle_\alpha}{\partial \mathbf{x}} - \frac{\partial}{\partial \mathbf{x}}\left(\Gamma_t \frac{\partial w_\alpha \langle Y_2 \rangle_\alpha}{\partial \mathbf{x}}\right) = b_{3\alpha}
\end{aligned} \tag{4.51}$$

Inserting Eq. 4.50 into 4.13 and using Eq. 4.51 and some trivial algebra we have

$$
\begin{aligned}
&\sum_{\alpha=1}^{\mathrm{N}} \delta\left(\xi-\xi_\alpha\right)\delta\left(Y_1-Y_{1,\alpha}\right)\delta\left(Y_2-Y_{2,\alpha}\right)a_\alpha \\
&\qquad -\sum_{\alpha=1}^{\mathrm{N}} \delta^{(1)}\left(\xi-\xi_\alpha\right)\delta\left(Y_1-Y_{1,\alpha}\right)\delta\left(Y_2-Y_{2,\alpha}\right)\left[b_{1\alpha}-\xi_\alpha a_\alpha\right] \\
&\qquad -\sum_{\alpha=1}^{\mathrm{N}} \delta\left(\xi-\xi_\alpha\right)\delta^{(1)}\left(Y_1-Y_{1,\alpha}\right)\delta\left(Y_2-Y_{2,\alpha}\right)\left[b_{2\alpha}-Y_{1,\alpha}a_\alpha\right] \\
&\qquad -\sum_{\alpha=1}^{\mathrm{N}} \delta\left(\xi-\xi_\alpha\right)\delta\left(Y_1-Y_{1,\alpha}\right)\delta^{(1)}\left(Y_2-Y_{2,\alpha}\right)\left[b_{3\alpha}-Y_{2,\alpha}a_\alpha\right] \\
&\quad = R_m + 2\sum_{\alpha=1}^{\mathrm{N}} \delta^{(1)}\left(\xi-\xi_\alpha\right)\delta^{(1)}\left(Y_1-Y_{1,\alpha}\right)\delta\left(Y_2-Y_{2,\alpha}\right)w_\alpha c_{12\alpha} \\
&\qquad + 2\sum_{\alpha=1}^{\mathrm{N}} \delta^{(1)}\left(\xi-\xi_\alpha\right)\delta\left(Y_1-Y_{1,\alpha}\right)\delta^{(1)}\left(Y_2-Y_{2,\alpha}\right)w_\alpha c_{13\alpha} \\
&\qquad + 2\sum_{\alpha=1}^{\mathrm{N}} \delta\left(\xi-\xi_\alpha\right)\delta^{(1)}\left(Y_1-Y_{1,\alpha}\right)\delta^{(1)}\left(Y_2-Y_{2,\alpha}\right)w_\alpha c_{23\alpha} \\
&\qquad + \sum_{\alpha=1}^{\mathrm{N}} \delta^{(2)}\left(\xi-\xi_\alpha\right)\delta\left(Y_1-Y_{1,\alpha}\right)\delta\left(Y_2-Y_{2,\alpha}\right)w_\alpha c_{11\alpha} \\
&\qquad + \sum_{\alpha=1}^{\mathrm{N}} \delta\left(\xi-\xi_\alpha\right)\delta^{(2)}\left(Y_1-Y_{1,\alpha}\right)\delta\left(Y_2-Y_{2,\alpha}\right)w_\alpha c_{22\alpha} \\
&\qquad\qquad + \sum_{\alpha=1}^{\mathrm{N}} \delta\left(\xi-\xi_\alpha\right)\delta\left(Y_1-Y_{1,\alpha}\right)\delta^{(2)}\left(Y_2-Y_{2,\alpha}\right)w_\alpha c_{33\alpha}, \quad (4.52)
\end{aligned}
$$

where

$$
\begin{aligned}
c_{11\alpha} &= \Gamma_t \frac{\partial \xi_\alpha}{\partial \mathbf{x}}\frac{\partial \xi_\alpha}{\partial \mathbf{x}}, \qquad c_{22\alpha} = \Gamma_t \frac{\partial Y_{1,\alpha}}{\partial \mathbf{x}}\frac{\partial Y_{1,\alpha}}{\partial \mathbf{x}}, \quad c_{33\alpha} = \Gamma_t \frac{\partial Y_{2,\alpha}}{\partial \mathbf{x}}\frac{\partial Y_{2,\alpha}}{\partial \mathbf{x}} \\
c_{12\alpha} &= \Gamma_t \frac{\partial \xi_\alpha}{\partial \mathbf{x}}\frac{\partial Y_{1,\alpha}}{\partial \mathbf{x}}, \qquad c_{13\alpha} = \Gamma_t \frac{\partial \xi_\alpha}{\partial \mathbf{x}}\frac{\partial Y_{2,\alpha}}{\partial \mathbf{x}}, \quad c_{23\alpha} = \Gamma_t \frac{\partial Y_{1,\alpha}}{\partial \mathbf{x}}\frac{\partial Y_{2,\alpha}}{\partial \mathbf{x}}.
\end{aligned} \quad (4.53)
$$

If we write the integer moments of the joint PDF, and considering that the derivatives of delta function is defined as (Pope, 2000)

$$
\int \delta^{(m)}\left(x-s\right)g\left(x\right)\mathrm{d}x = (-1)^m\, g^{(m)}\left(s\right) \quad (4.54)
$$

where $g^{(m)}\left(s\right)$ is the mth derivative of the $g\left(x\right)$, yields to

$$\begin{aligned}\sum_{\alpha=1}^{\mathrm{N}}\left(1-n-j-k\right)\xi_{\alpha}^{n}Y_{1,\alpha}^{j}Y_{2,\alpha}^{k}a_{\alpha}+\sum_{\alpha=1}^{\mathrm{N}}n\xi_{\alpha}^{n-1}Y_{1,\alpha}^{j}Y_{2,\alpha}^{k}b_{1\alpha}\\ +\sum_{\alpha=1}^{\mathrm{N}}j\xi_{\alpha}^{n}Y_{1,\alpha}^{j-1}Y_{2,\alpha}^{k}b_{2\alpha}+\sum_{\alpha=1}^{\mathrm{N}}k\xi_{\alpha}^{n}Y_{1,\alpha}^{j}Y_{2,\alpha}^{k-1}b_{3\alpha}\\ =R_{m}+2\sum_{\alpha=1}^{\mathrm{N}}nj\xi_{\alpha}^{n-1}Y_{1,\alpha}^{j-1}Y_{2,\alpha}^{k}w_{\alpha}c_{12\alpha}+2\sum_{\alpha=1}^{\mathrm{N}}nk\xi_{\alpha}^{n-1}Y_{1,\alpha}^{j}Y_{2,\alpha}^{k-1}w_{\alpha}c_{13\alpha}\\ +2\sum_{\alpha=1}^{\mathrm{N}}jk\xi_{\alpha}^{n}Y_{1,\alpha}^{j-1}Y_{2,\alpha}^{k-1}w_{\alpha}c_{23\alpha}+\sum_{\alpha=1}^{\mathrm{N}}n\left(n-1\right)\xi_{\alpha}^{n-2}Y_{1,\alpha}^{j}Y_{2,\alpha}^{k}w_{\alpha}c_{11\alpha}\\ +\sum_{\alpha=1}^{\mathrm{N}}j\left(j-1\right)\xi_{\alpha}^{n}Y_{1,\alpha}^{j-2}Y_{2,\alpha}^{k}w_{\alpha}c_{22\alpha}+\sum_{\alpha=1}^{\mathrm{N}}k\left(k-1\right)\xi_{\alpha}^{n}Y_{1,\alpha}^{j}Y_{2,\alpha}^{k-2}w_{\alpha}c_{33\alpha},\end{aligned}\tag{4.55}$$

where the moments of the source terms can be represented as

$$\begin{aligned}R_{m}=\sum_{\alpha=1}^{\mathrm{N}}\frac{n\varepsilon_{\xi}}{\langle\xi''^{2}\rangle}w_{\alpha}\left(\langle\xi\rangle-\xi_{\alpha}\right)\xi_{\alpha}^{n-1}Y_{1,\alpha}^{j}Y_{2,\alpha}^{k}\\ +\sum_{\alpha=1}^{\mathrm{N}}jw_{\alpha}\mathcal{R}_{1}\xi_{\alpha}^{n}Y_{1,\alpha}^{j-1}Y_{2,\alpha}^{k}+\sum_{\alpha=1}^{\mathrm{N}}kw_{\alpha}\mathcal{R}_{2}\xi_{\alpha}^{n}Y_{1,\alpha}^{j}Y_{2,\alpha}^{k-1}.\end{aligned}\tag{4.56}$$

As it is mentioned before, we consider two primary nodes in mixture fraction direction and only one node for each progress variable. Thus we need to find the solution for the moment set as below:

$$\begin{matrix}M_{000} & M_{010} & M_{001}\\ M_{100} & M_{110} & M_{101}\\ M_{200} & & \\ M_{300} & & \end{matrix}\tag{4.57}$$

In order to find the solution for unknown parameters in the above equations, we first consider the part which only contains the information related to the mixture fraction. Thus we have a linear system of the form

$$\mathbf{A_1}\boldsymbol{\alpha}_1=\boldsymbol{\beta}_1,\tag{4.58}$$

where

$$\boldsymbol{\alpha}_1^{\mathrm{T}} = \begin{bmatrix} a_1 & a_2 & b_{11} & b_{12} \end{bmatrix} = \begin{bmatrix} \mathbf{a} \\ \mathbf{b_1} \end{bmatrix}^{\mathrm{T}}, \tag{4.59}$$

and

$$\mathbf{A_1} = \left[\begin{array}{cc|cc} 1 & 1 & 0 & 0 \\ 0 & 0 & 1 & 1 \\ -\langle\xi\rangle_1^2 & -\langle\xi\rangle_2^2 & 2\langle\xi\rangle_1 & 2\langle\xi\rangle_2 \\ -2\langle\xi\rangle_1^3 & -2\langle\xi\rangle_2^3 & 3\langle\xi\rangle_1^2 & 3\langle\xi\rangle_2^2 \end{array}\right]. \tag{4.60}$$

The right hand side of Eq. 4.58 can be written as

$$\boldsymbol{\beta}_1 = \mathbf{A_2 W c_1} + \mathbf{A_3 W r}, \tag{4.61}$$

where

$$\mathbf{W} = \mathbf{diag}\left(w_1, w_2\right), \tag{4.62}$$

$$\mathbf{c_1}^{\mathrm{T}} = \begin{bmatrix} c_{111} & c_{112} \end{bmatrix}, \tag{4.63}$$

$$\mathbf{A_2} = \begin{bmatrix} 0 & 0 \\ 0 & 0 \\ 2 & 2 \\ 6\langle\xi\rangle_1 & 6\langle\xi\rangle_2 \end{bmatrix}, \tag{4.64}$$

$$\mathbf{A_3} = \begin{bmatrix} 0 & 0 \\ 1 & 1 \\ 2\langle\xi\rangle_1 & 2\langle\xi\rangle_2 \\ 3\langle\xi\rangle_1^2 & 3\langle\xi\rangle_2^2 \end{bmatrix}, \tag{4.65}$$

and

$$\mathbf{r_1} = \begin{bmatrix} \frac{\varepsilon_\xi}{\langle \xi'^2 \rangle} \left(\langle \xi \rangle - \langle \xi \rangle_1 \right) \\ \frac{\varepsilon_\xi}{\langle \xi'^2 \rangle} \left(\langle \xi \rangle - \langle \xi \rangle_2 \right) \end{bmatrix} = \begin{bmatrix} r_{11} \\ r_{12} \end{bmatrix}. \tag{4.66}$$

If we assume $\mathbf{a} = 0$, then we have

$$\begin{aligned} b_{11} &= w_1 r_{11} + \frac{w_1 c_{111} + w_2 c_{112}}{\langle \xi \rangle_1 - \langle \xi \rangle_2}, \\ b_{12} &= w_2 r_{12} + \frac{w_1 c_{111} + w_2 c_{112}}{\langle \xi \rangle_2 - \langle \xi \rangle_1}. \end{aligned} \tag{4.67}$$

With known values for the four parameters related to the mixture fraction, a_1,a_2,b_{11} and b_{12}, we use the other four linear system of equations to obtain the remaining unknown parameters, Thus we can write the system of equations as

$$\mathbf{A_4} \boldsymbol{\alpha}_2 = \boldsymbol{\beta}_2, \tag{4.68}$$

where

$$\mathbf{A_4} = \left[\begin{array}{cc|cc} 1 & 1 & 0 & 0 \\ \langle \xi \rangle_1 & \langle \xi \rangle_2 & 0 & 0 \\ 0 & 0 & 1 & 1 \\ 0 & 0 & \langle \xi \rangle_1 & \langle \xi \rangle_2 \end{array}\right], \tag{4.69}$$

$$\boldsymbol{\alpha}_2^{\mathrm{T}} = \begin{bmatrix} b_{21} & b_{22} & b_{31} & b_{32} \end{bmatrix} = \begin{bmatrix} \mathbf{b_2} \\ \mathbf{b_3} \end{bmatrix}^{\mathrm{T}}. \tag{4.70}$$

The right hand side of Eq. 4.68 can be written as

$$\boldsymbol{\beta}_2 = \mathbf{A_5 W c_2} + \mathbf{A_6 W c_3} - \mathbf{A_7 \alpha_1} + \mathbf{r}, \tag{4.71}$$

where

$$\mathbf{c_2}^{\mathrm{T}} = \begin{bmatrix} c_{121} & c_{122} \end{bmatrix}, \tag{4.72}$$

$$\mathbf{c_3}^{\mathrm{T}} = \begin{bmatrix} c_{131} & c_{132} \end{bmatrix}, \tag{4.73}$$

$$\mathbf{A_5} = \begin{bmatrix} 0 & 0 \\ 2 & 2 \\ 0 & 0 \\ 0 & 0 \end{bmatrix}, \tag{4.74}$$

$$\mathbf{A_6} = \begin{bmatrix} 0 & 0 \\ 0 & 0 \\ 0 & 0 \\ 2 & 2 \end{bmatrix}, \tag{4.75}$$

$$\mathbf{A_7} = \left[\begin{array}{cc|cc} 0 & 0 & 0 & 0 \\ -\langle\xi\rangle_1 \langle Y_1\rangle_1 & -\langle\xi\rangle_2 \langle Y_1\rangle_2 & \langle Y_1\rangle_1 & \langle Y_1\rangle_2 \\ 0 & 0 & 0 & 0 \\ -\langle\xi\rangle_1 \langle Y_2\rangle_1 & -\langle\xi\rangle_2 \langle Y_2\rangle_2 & \langle Y_2\rangle_1 & \langle Y_2\rangle_2 \end{array}\right], \tag{4.76}$$

and

$$\mathbf{r} = \begin{bmatrix} w_1\mathcal{R}_{21} + w_2\mathcal{R}_{22} \\ w_1 \langle\xi\rangle_1 \mathcal{R}_{21} + w_2 \langle\xi\rangle_2 \mathcal{R}_{22} \\ w_1\mathcal{R}_{31} + w_2\mathcal{R}_{32} \\ w_1 \langle\xi\rangle_1 \mathcal{R}_{31} + w_2 \langle\xi\rangle_2 \mathcal{R}_{32} \end{bmatrix} = \begin{bmatrix} r_{21} \\ r_{22} \\ r_{31} \\ r_{32} \end{bmatrix} = \begin{bmatrix} \mathbf{r_2} \\ \mathbf{r_3} \end{bmatrix}. \tag{4.77}$$

Finally we can obtain the terms as

$$\begin{aligned} b_{21} &= w_1 r_{21} + \frac{2w_1c_{121} + 2w_2c_{122} - \langle Y_1\rangle_1 b_{11} - \langle Y_1\rangle_2 b_{12}}{\langle\xi\rangle_1 - \langle\xi\rangle_2}, \\ b_{22} &= w_2 r_{22} + \frac{2w_1c_{121} + 2w_2c_{122} - \langle Y_1\rangle_1 b_{11} - \langle Y_1\rangle_2 b_{12}}{\langle\xi\rangle_2 - \langle\xi\rangle_1}, \\ b_{31} &= w_1 r_{31} + \frac{2w_1c_{131} + 2w_2c_{132} - \langle Y_2\rangle_1 b_{11} - \langle Y_2\rangle_2 b_{12}}{\langle\xi\rangle_1 - \langle\xi\rangle_2}, \\ b_{32} &= w_2 r_{32} + \frac{2w_1c_{131} + 2w_2c_{132} - \langle Y_2\rangle_1 b_{11} - \langle Y_2\rangle_2 b_{12}}{\langle\xi\rangle_2 - \langle\xi\rangle_1}, \end{aligned} \tag{4.78}$$

4.6 Results and discussion

In this section, we propose a test case similar to those proposed by Akroyd et al. (2010). It is a one-dimensional reactive mixing problem where two species A and B are initialized at the right and left of a string respectively. The two species start to mix and react and produce the R product and S bi-product

$$\begin{aligned} A + B &\xrightarrow{k_1} R \\ B + R &\xrightarrow{k_2} S \end{aligned} \tag{4.79}$$

Reaction system can be considered as a competitive consecutive in which the first reaction happens between A and B and produces R with reaction rate constant of k_1. Then in regions where the mixing is slow relative to the second reaction, the product R in a parallel reaction, reacts with B and produces S with reaction rate constant of k_2. In chemical engineering application usually, the first reaction is assumed to be faster than the second one. Fig. 4.1 shows the configuration of the problem under investigation.

Figure 4.1: The schematic of one dimensional reactive mixing problem

In this study we assume $k_1 = 5.0 \times 10^6$ $\mathrm{m^3/kmol\,s}$ and $k_2 = 1.8 \times 10^3$ $\mathrm{m^3/kmol\,s}$. Initial concentration of species A and B are 2.97 $\mathrm{mol/m^3}$ and 2.86 $\mathrm{mol/m^3}$ respectively. Fluxes are imposed to be zero at walls (Neumann conditions). Initial condition for two streams are presented at Tab. 4.1.

Fig. 4.2 shows the evolution of species concentration. As it is shown the almost 5 seconds B reacts with A. After the species B are reacted, the concentration of species A diffuse and become homogeneous in the system. Also, this figure shows that most production of R happens

Table 4.1: Initial condition for N = 2.

Variable	**A**	**B**	**Variable**	**A**	**B**
w_1	1	0	$Y_{1;1}$	0	0
w_2	0	1	$Y_{1;2}$	0	0
ξ_1	0	0	$Y_{2;1}$	0	0
ξ_2	1	1	$Y_{2;2}$	0	0

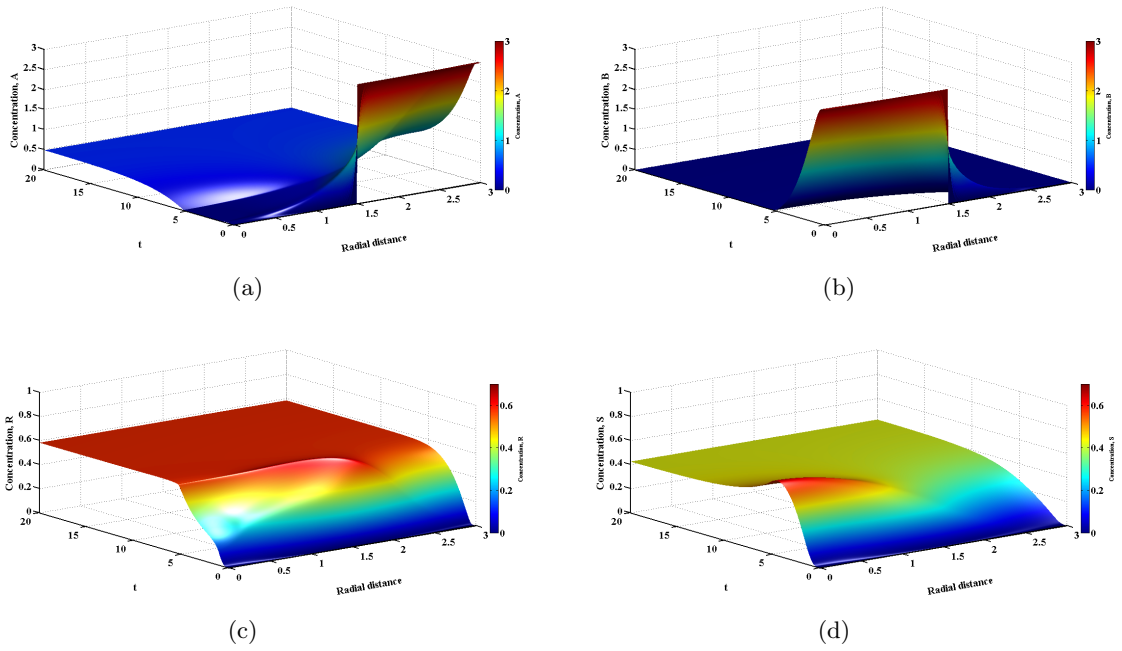

(a) (b)

(c) (d)

Figure 4.2: CQMOM-IEM – (a) concentration of species A, (b) concentration of species B, (c) concentration of species R, (d) concentration of species S.

in the middle. Maximum production of bi-product S happens near to B stream and after there is a sufficient R produced and still B is present in the system.

Fig. 4.3 shows the evolution of mixture fraction, the variance of mixture fraction and two progress variables. As it is shown in Fig. 4.3(a), two species are starting to mix and relaxes to the average mixture fraction of 0.5. The variance of the mixture fraction is high at initial time steps in the middle of the stream where two species mostly meet each other. Also since the first reaction is faster than the second one, the progress variable one relaxes to a higher value than the one for the second progress variable.

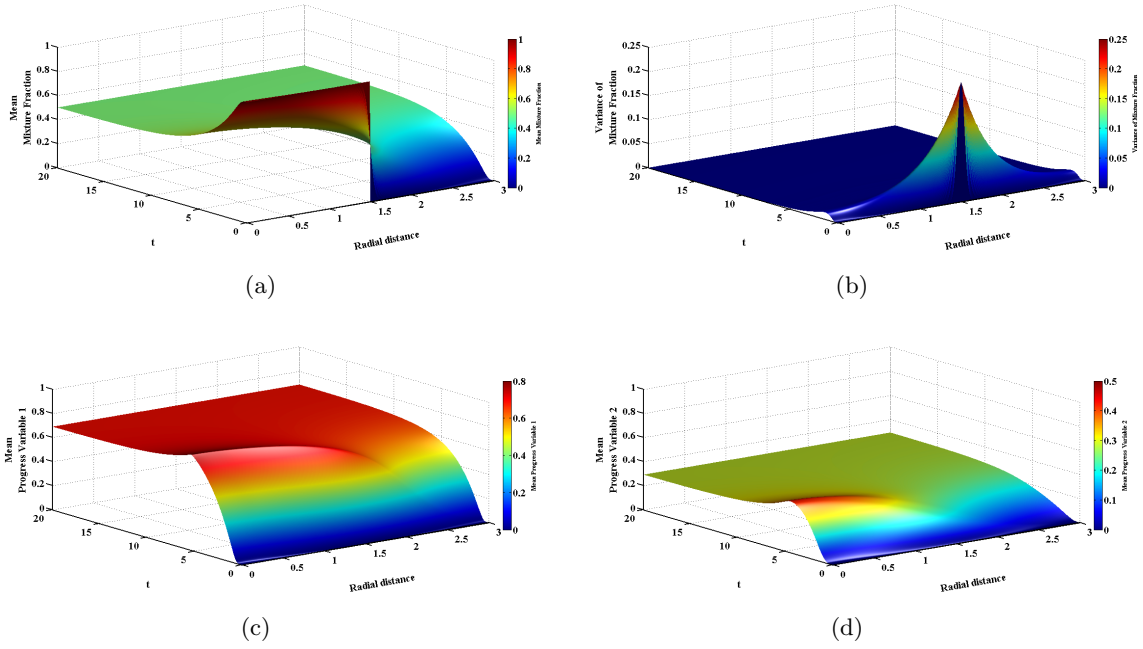

Figure 4.3: CQMOM-IEM – (a) mean mixture fraction, (b) mean mixture fraction variance, (c) progress variable one, (d) progress variable two.

Fig. 4.4 and Fig. 4.5 show similar results obtained by FP model for micromixing. However since the FP model includes the effect of differential diffusion, homogeneous results for Y_1 and Y_2 have %1.9 and %4 difference respectively.

Fig. 4.6 and Fig. 4.7 shows the results obtained using the DQMOM-IEM. The same behavior is predicted by the DQMOM-IEM in consistent to those observed by CQMOM-IEM and CQMOM-FP. However DQMOM-IEM predicts the production of R less than CQMOM those predicted by CQMOM.

In chemical engineering applications, the competitive consecutive reactions are studied in t0he limit where $k_1 c_{B_0} \rightarrow \infty$. In this limit, the first reaction progress variable can be written in terms of ξ and Y_2 which is shown at Eq. 4.10. Fig. 4.8 show the concentration of reactant and products for fast reactions using the IEM model. As it is shown in this figure, at the early time steps, high production of R happens in the middle where A and B contacts with each other. In this case, the amount of bi-product S is less and most of produced at the side near to B.

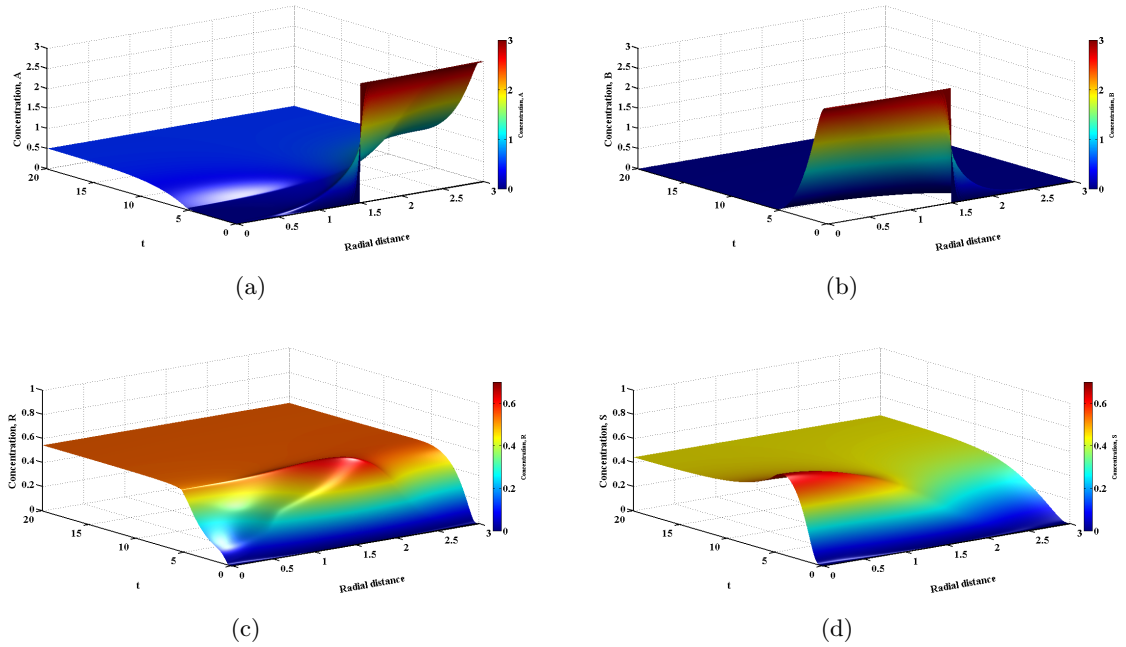

Figure 4.4: CQMOM-FP – (a) concentration of species A, (b) concentration of species B, (c) concentration of species R, (d) concentration of species S.

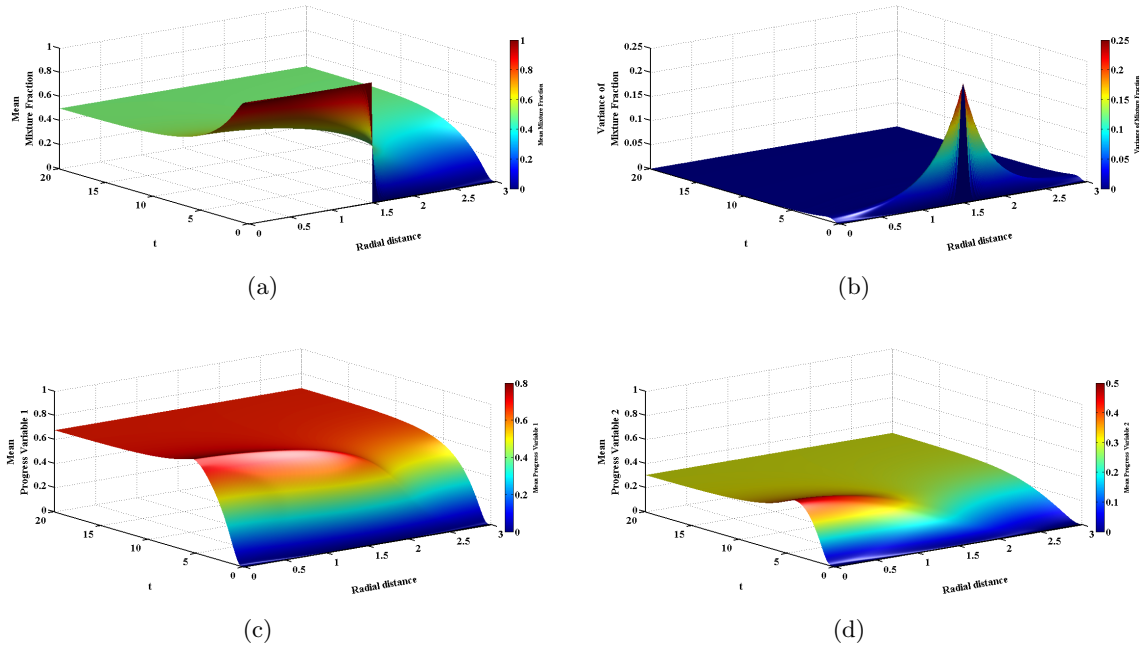

Figure 4.5: CQMOM-FP – (a) mean mixture fraction, (b) mean mixture fraction variance, (c) progress variable one, (d) progress variable two.

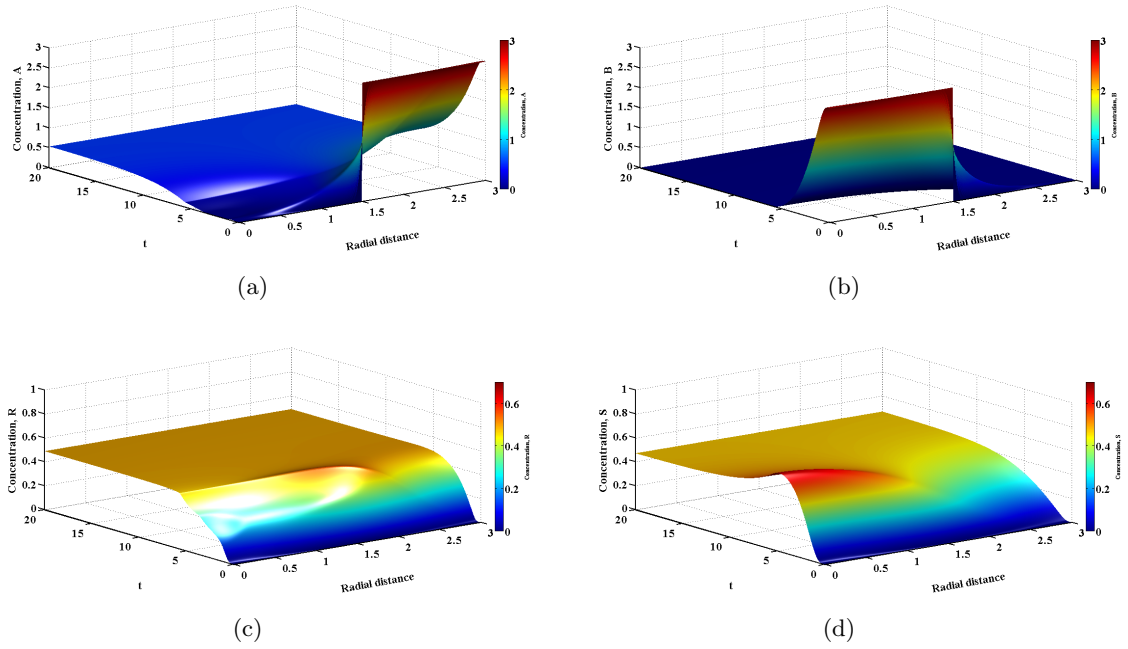

Figure 4.6: DQMOM-IEM – (a) concentration of species A, (b) concentration of species B, (c) concentration of species R, (d) concentration of species S.

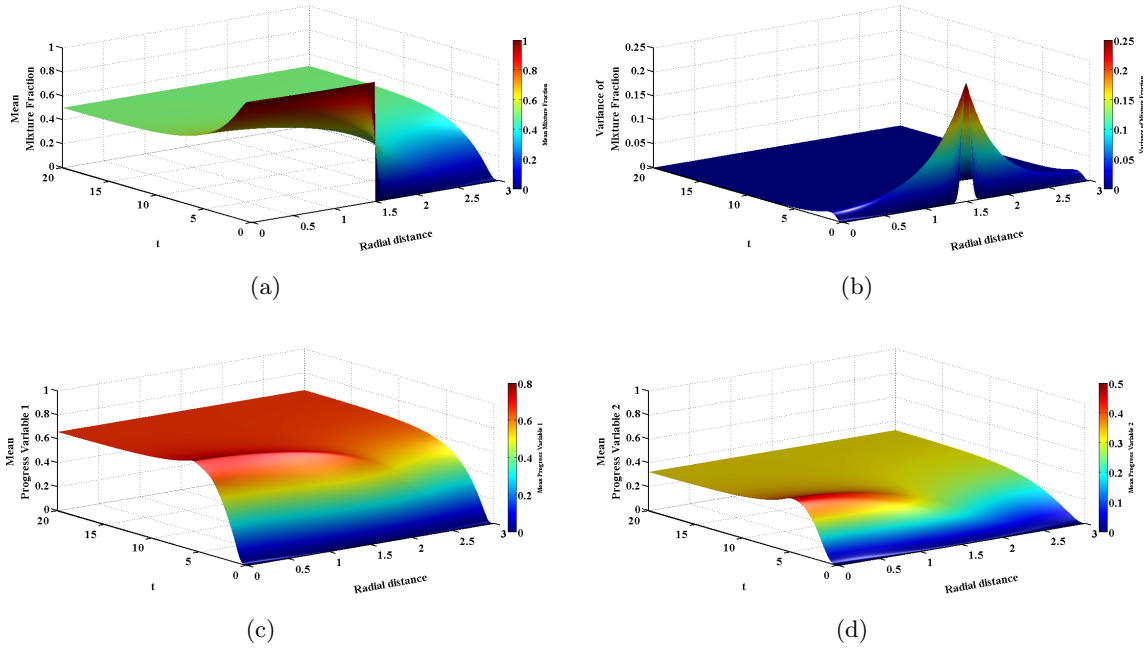

Figure 4.7: DQMOM-IEM – (a) mean mixture fraction, (b) mean mixture fraction variance, (c) progress variable one, (d) progress variable two.

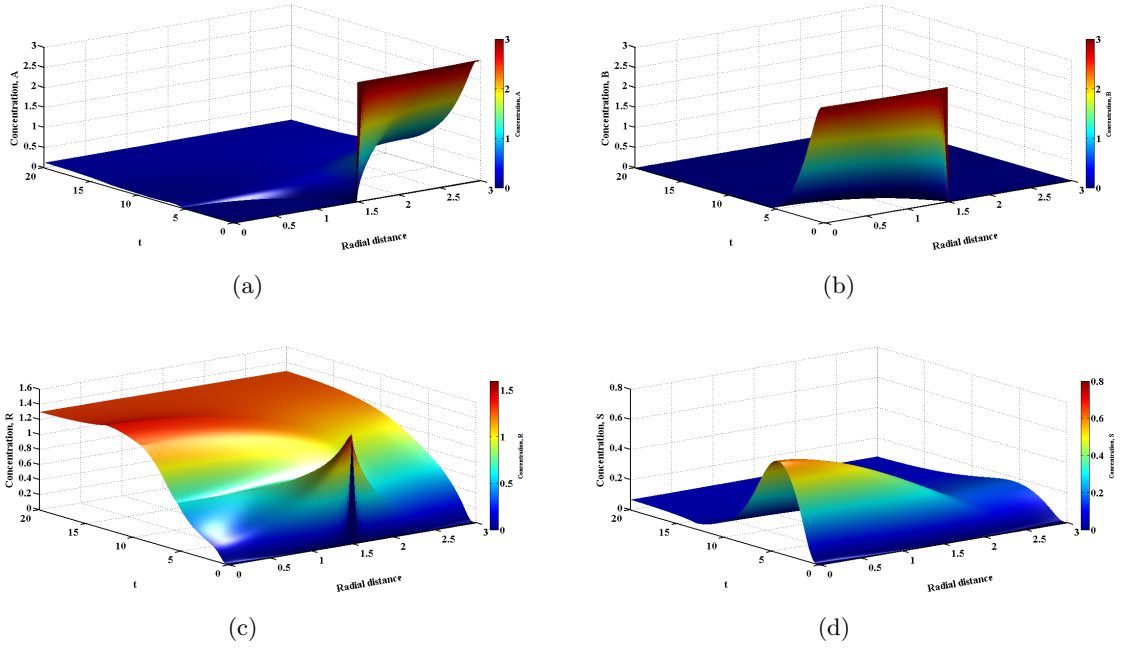

Figure 4.8: CQMOM-IEM fast reaction – (a) concentration of species A, (b) concentration of species B, (c) concentration of species R, (d) concentration of species S.

Similar behavior is obtained for the fast reaction modeled by CQMOM-FP and the results are consistent with those obtained by CQMOM-IEM model.

4.7 Conclusion

In this study, CQMOM approach is introduced for the turbulent reacting flows. The joint composition PDF for the mixture fraction and progress variables of two parallel reactions is introduced. Interaction by exchange with the mean (IEM) and Fokker-Planck (FP) with β distribution are considered for the micromixing term. The transport equation for the moments of PDF is introduced for the cases with competitive consecutive reactions and fast reactions. Analytical closure terms of DQMOM-IEM method for specified joint composition PDF is also derived and reported. As it is stated before (Akroyd et al., 2010; Tsai and Fox, 1994), in this method the diffusion term may cause a loss of boundedness.

The numerical behavior of CQMOM-IEM, CQMOM-FP and DQMOM-IEM are presented for different reaction and mixing models. The results present satisfactory agreement between the

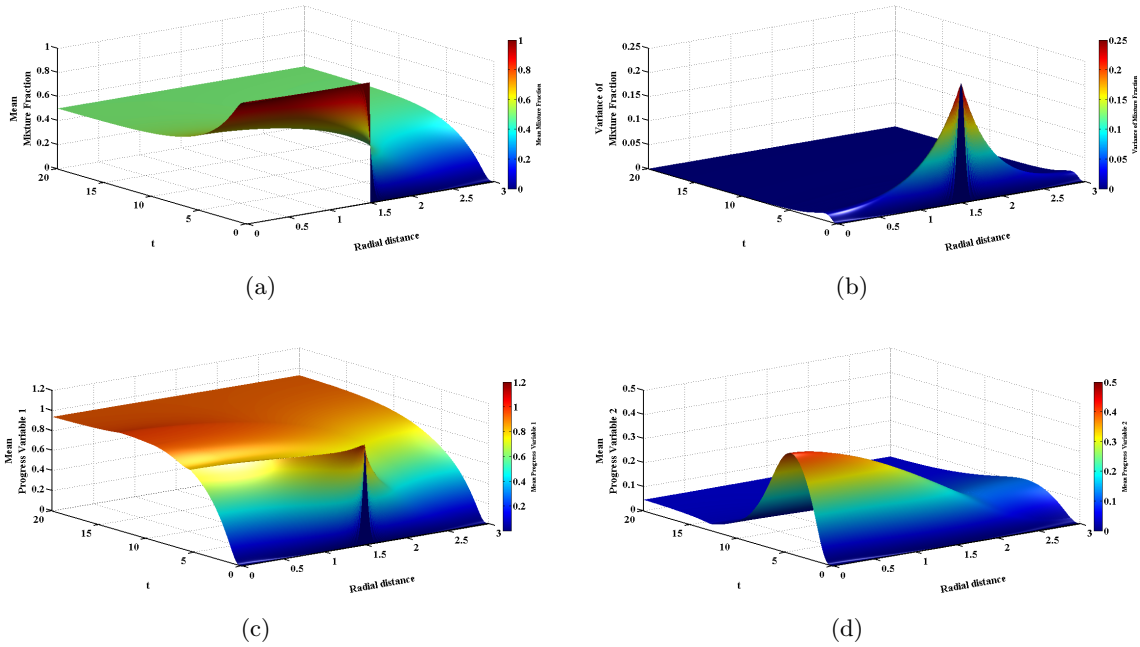

Figure 4.9: CQMOM-IEM fast reaction – (a) mean mixture fraction, (b) mean mixture fraction variance, (c) progress variable one, (d) progress variable two.

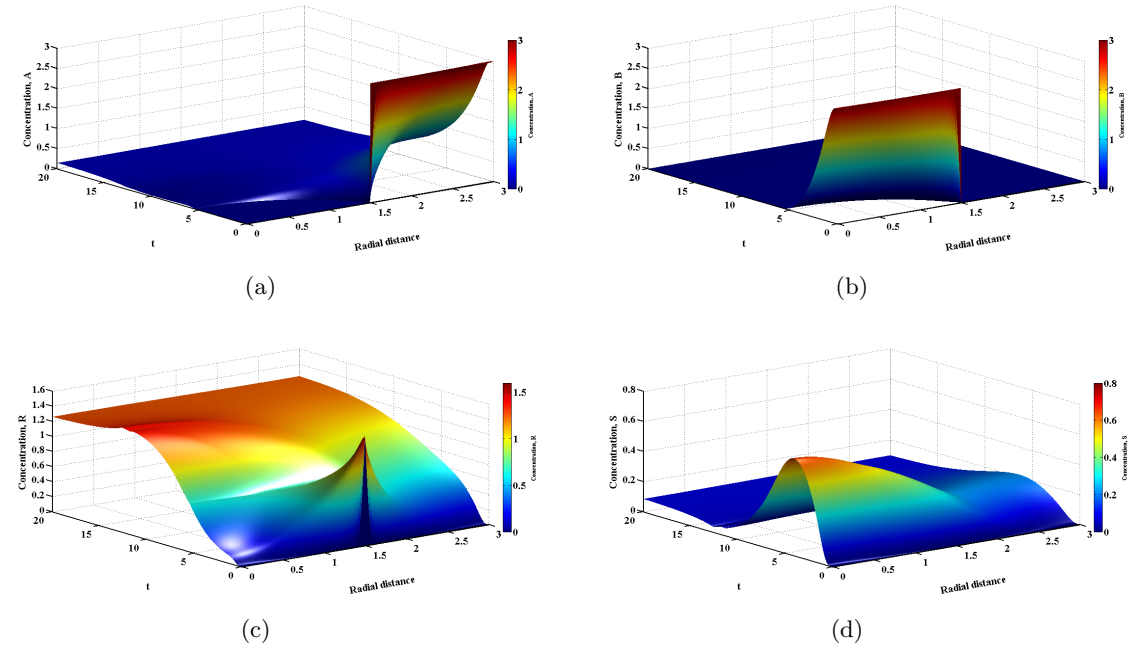

Figure 4.10: CQMOM-FP fast reaction – (a) concentration of species A, (b) concentration of species B, (c) concentration of species R, (d) concentration of species S.

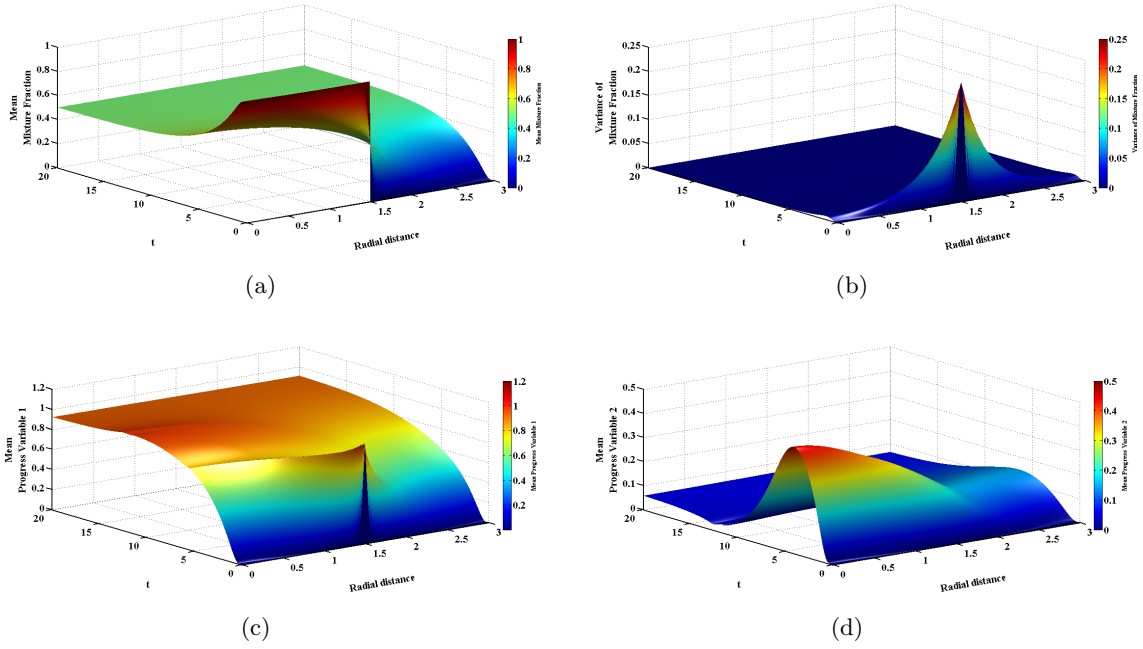

Figure 4.11: CQMOM-FP fast reaction – (a) mean mixture fraction, (b) mean mixture fraction variance, (c) progress variable one, (d) progress variable two.

methods. Different quantities obtained by CQMOM and DQMOM were reported at final time step. Finally, the efficiency of algorithms is reported. CQMOM compare to DQMOM is faster according to the time of simulations obtained in the same condition. The advantage of using CQMOM is that it conserves a larger number of moments than DQMOM, by definition. In DQMOM, transport equations for weights and abscissae are solved which are non-conserved quantities while in CQMOM, moments are transported.

4.8 Acknowledgment

Partial support from the National Science Foundation of the United States, under the SI2–SSE award NSF–ACI 1440443 is gratefully acknowledged.

CHAPTER 5. A QUADRATURE-BASED CFD MODEL FOR TURBULENT REACTING FLOWS COUPLED WITH POPULATION BALANCE

Abstract

A comprehensive model based on conditional quadrature method of moments (CQMOM) was developed to solve turbulent mixing problems associated with population balance equations (PBE) by approximating the evolution equation of the composition probability density function (PDF) for the moments of the PBE. The well-established Interaction-by-Exchange-with-the-Mean (IEM) model was used to close the PDF evolution equation. The new CQMOM methodology was coupled to a quadrature-based PBE solver for univariate problems, which relies on the extended quadrature method of moments (EQMOM). The two procedures were implemented into the OpenQBMM® framework, which leverages the OpenFOAM® CFD toolbox. The CQMOM approach for mixing problems was first tested considering two consecutive competitive reactions to verify the implementation and validate the proposed approach. The coupled turbulent mixing-PBE approach was then used to investigate polymer aggregation in a multi-inlet vortex reactor (MIVR), typically used to perform flash nanoprecipitation for the production of nanoparticles used in pharmaceutical applications. Results showing the predicted mixture fraction, reactant and product concentration fields and the polymer particle size distribution are shown.

5.1 Introduction

Modeling of turbulent mixing and reacting flows is relevant to many engineering applications. Examples of such applications are the spreading of contaminants in the atmosphere (Meyer and

Jenny, 2013), and optimizing the fuel efficiency at internal combustion engines (Raman and Pitsch, 2007; Wang and Kim, 2015; Stollinger and Heinz, 2010). Moreover, in reacting flows, chemical compositions can be determined by turbulent mixing and chemical reactions. For this purpose, the statistical methods are often used. In Reynolds-averaged Navier-Stokes (RANS) simulations, transport equations of statistically averaged quantities like mean flow velocity are solved (Fox, 2003; Pope, 2000). While dealing with reactive flows, the reaction source terms in these simulations are not closed (Meyer and Jenny, 2009). To overcome the closure problem in turbulent transport and chemical reaction, PDF methods are applied. The advantage of using PDF method is that it provides the entire information on joint composition PDF. However, there is a need of mixing models for molecular diffusion. Large number of mixing models have been proposed in literature (Curl, 1963; Villermaux and Falk, 1994; Tsai and Fox, 1995; Fox, 1992b, 1994; Subramaniam and Pope, 1998; Meyer and Jenny, 2009). In this study, we use interaction by exchange with the mean (IEM) model due to its simple form. In this model all the scalars mix at the same rate (Fox, 2003).

Approximate solution of a composition PDF can be determined using several approaches, including the method of classes (Balakin et al., 2014; Bannari et al., 2008; Becker et al., 2011; Hounslow et al., 1988; Hounslow, 1990; Kumar and Ramkrishna, 1996a,b; Puel et al., 2003). It consists in discretizing the PDF with respect to internal coordinate into a discrete number of classes. Depend on the order of pre-defined form of the distribution it is called zero-order class methods (Vanni, 2000) or high-order class methods Muhr et al. (1996). Although this method is intuitive and accurate, it is computationally expensive due to a large number of classes required to properly capture the PDF. Lin et al. (2002); Meimaroglou and Kiparissides (2007); Rosner and Yu (2001); Smith and Matsoukas (1998); Zhao et al. (2007) used Monte Carlo methods to solve the PDF transport equation, which however present challenges in term of computational cost for practical applications. A successful and sufficiently accurate approach to finding the approximate solution of composition PDF transport equation is the quadrature method of moments (QMOM) proposed by (McGraw, 1997) for aerosol applications and extensively applied to chemical engineering application (Marchisio et al., 2003b; Marchisio and Fox, 2013). In this approach, the PDF is represented by a weighted summation of Dirac delta functions, which is

defined by a set of moments (Wheeler, 1974).

In direct quadrature method of moments (DQMOM) the discrete representation of the PDF was used (Marchisio and Fox, 2005) to derive the transport equation for the quadrature weights and abscissae. However, this method is affected by shortcomings related to the conservation of moments due to the fact that weights and abscissae are not conserved quantities to transport (Yuan et al., 2012).

In order to overcome this limitation, we use the conditional quadrature method of moments introduce by Yuan and Fox (2011). In this method, a moment-inversion algorithm based on the adaptive quadrature of conditional composition moments is used to approximate the continuous distributions. It has been shown that this method always yields realizable distribution functions Yuan and Fox (2011).

One of the methods to produce nanoparticles is flash nanoprecipitation (FNP) which requires fast mixing (Johnson and Prud'homme, 2003). For aggregation of particles during FNP process, the particle size distribution has to be as narrow as possible due to constraints on the desired PSD for the product. This requires good mixing to take place at the micro scale. Rapid micromixing increases the stability of nanoparticles (Cheng, 2010; Liu et al., 2008). High mixing rates can be achieved in confined impinging jet (CIJ) reactors. They are constituted by a cylindrical chamber, where two inlet streams collide each other and create an impinging plane. This is the region characterized by fast production and dissipation of turbulent kinetic energy (Gavi et al., 2007). Mixing in the CIJ can be in the order of milliseconds, but CIJ mixers are limited by the requirement of equal momenta of two streams.

To overcome the limitations of the confined impinging jets (CIJ) reactors, recently a multi-inlet vortex reactor is developed (Cheng, 2010; Cheng and Fox, 2010; Cheng et al., 2010; Liu et al., 2015, 2016). The idea behind the MIVR is that the momentum from each inlet drives the micromixing. The MIVR achieves fast mixing by inducing turbulent swirling flow from four inlet streams. The inlet streams may have different momenta, unlike the CIJ reactors. To investigate the mixing, reaction, and aggregation process, a computational fluid dynamics (CFD) model is developed based on the quadrature-based moment method (QBMM) and tested at MIVR.

The present work proposes the new model based on conditional quadrature method of moments to solve the joint composition PDF. Two models are introduced. First, the model for the problems related to mixing and two competitive consecutive reactions and second a model for problems related to aggregation of nanoparticles are introduced. The proposed procedure is then applied to the MIVR.

The remainder of this paper is structured as below. In Sec. 5.2 we present the composition PDF evolution equation and closure models we solve using the QBMM. In Sec. 5.3 we introduce the model based on conditional quadrature method of moments for turbulent reacting flow. In Sec. 5.4, we present the algorithm used to solve the problems related to turbulent mixing and reacting flows. Consecutive competitive reactions are considered and their effect is included by solving the composition PDF for progress variables of each reaction. Later, in Sec. 5.5, we introduce the univariate population balance transport equation for flash nanoprecipitation process to describe the polymer aggregation phenomena. In Sec. 5.6, we describe an algorithm to investigate the aggregation of nanoparticles. Finally in Sec. 5.7, 5.8, 5.9, and 5.10, we apply the introduced models to predict the mixing and reaction field and particle size distribution inside the MIVR.

5.2 Transported PDF method for turbulent reacting flow

The evolution of joint composition PDF $f(\psi; \mathbf{x}, t)$ was obtained by Fox (2003) and it can be described as:

$$\underbrace{\frac{\partial f}{\partial t}}_{\text{rate of change}} + \underbrace{\langle U_i \rangle \frac{\partial f}{\partial x_i}}_{\substack{\text{convection in physical space} \\ \text{due to the mean velocity} \\ \text{(macromixing)}}} - \underbrace{\frac{\partial}{\partial x_i}\left(\langle u_i \mid \boldsymbol{\psi} \rangle f\right)}_{\substack{\text{convection in physical space due to} \\ \text{the scalar conditioned velocity fluctuations} \\ \text{(mesomixing)}}} =$$

$$\underbrace{-\frac{\partial}{\partial \psi_i}\left[\left(\Gamma_i \nabla^2 \phi_i' \mid \boldsymbol{\psi}\right) f\right] - \frac{\partial}{\partial \psi_i}\left[\left(\Gamma_i \nabla^2 \langle \phi_i \rangle + S_i(\boldsymbol{\psi})\right) f\right]}_{\substack{\text{transport in composition space due} \\ \text{to the molecular mixing and reaction} \\ \text{(micromixing)}}}. \quad (5.1)$$

The mesomixing term can be closed using a gradient-diffusion model (Fox, 2003):

$$\langle u_i \mid \boldsymbol{\psi} \rangle = -\frac{\Gamma_t}{f}\frac{\partial f}{\partial x_i}. \tag{5.2}$$

Chemical kinetics are assumed to be closed and the only remaining unclosed term in Eq. 5.1 is the one related to micromixing. A molecular mixing model able of estimating the passive scalar changes is needed to close the related term. In this study, we use the interaction by exchange with the mean (IEM) model to close the micromixing. The IEM model is the simplest model in chemical-reaction engineering and computational combustion (Villermaux and Falk, 1994; Dopazo and O'Brien, 1973). It assumes a linear relaxation of the concentration towards its mean (Fox, 2003; Pope, 2000; Choi et al., 2008) and reads:

$$\left\langle \Gamma \nabla^2 \phi_i' | \psi \right\rangle = \frac{\epsilon_{\phi_i}}{2\left\langle \phi_i'^2 \right\rangle} \left(\langle \phi_i \rangle - \psi_i \right). \tag{5.3}$$

In our study, we consider a PDF of three internal coordinates, i.e. mixture fraction, progress variable one and two. Thus we can rewrite the Eq. 5.1 as:

$$\begin{aligned} \frac{\partial f}{\partial t} + \langle U \rangle \frac{\partial f}{\partial \mathbf{x}} - \frac{\partial f}{\partial \mathbf{x}}\left(\Gamma_t \frac{\partial f}{\partial \mathbf{x}}\right) = &-\frac{\partial}{\partial \xi}\left[\left(\frac{\varepsilon_\xi}{\langle \xi'^2 \rangle}\left(\langle \xi \rangle - \xi\right) + S\left(\xi\right)\right) f\right] \\ &- \frac{\partial}{\partial Y_1}\left[\left(\frac{\varepsilon_{Y_1}}{\left\langle Y_1'^2 \right\rangle}\left(\langle Y_1 \rangle - Y_1\right) + S\left(Y_1\right)\right) f\right] \\ &- \frac{\partial}{\partial Y_2}\left[\left(\frac{\varepsilon_{Y_2}}{\left\langle Y_2'^2 \right\rangle}\left(\langle Y_2 \rangle - Y_2\right) + S\left(Y_2\right)\right) f\right], \end{aligned} \tag{5.4}$$

where ξ, Y_1 and Y_2 are mixture fraction, progress variable one and progress variable two respectively, $\langle \cdot \rangle$ is mean of scalar, $f\left(\xi, Y_1, Y_2; \mathbf{x}, t\right)$ probability density function, $\left\langle \cdot'^2 \right\rangle$ is variance of the scalar, ε is dissipation factor, t is time, $\langle U \rangle$ is mean velocity and Γ_t denotes turbulent diffusivity. In this study we consider the consecutive competitive reaction:

$$\begin{aligned} A + B &\rightarrow R \\ B + R &\rightarrow S, \end{aligned} \tag{5.5}$$

where the A and B are the reactants, R is the primary product and S is the bi-product. Thus chemical source terms can be defined as:

$$\begin{aligned}\mathcal{R}_1(\xi, Y_1, Y_2) &= \xi_{st} k_1 c_{B_0} \left(\frac{1-\xi}{1-\xi_{st}} - Y_1\right)\left(\frac{\xi}{\xi_{st}} - Y_1 - Y_2\right), \\ \mathcal{R}_2(\xi, Y_1, Y_2) &= \xi_{st} k_2 c_{B_0} (Y_1 - Y_2)\left(\frac{\xi}{\xi_{st}} - Y_1 - Y_2\right),\end{aligned} \tag{5.6}$$

where c_{A_0} denotes initial concentration of a reactant A, c_{B_0} initial concentration of a reactant B, k_1 reaction rate constant for the first reaction and k_2 reaction rate constant for the second reaction. The ξ_{st} stoichiometric mixture fraction can also be described as:

$$\xi_{st} = \frac{c_{A_0}}{c_{A_0} + c_{B_0}}. \tag{5.7}$$

Implementing the reaction source terms, transport equation finally can be written as:

$$\begin{aligned}\frac{\partial f}{\partial t} + \langle U \rangle \frac{\partial f}{\partial \mathbf{x}} - \frac{\partial}{\partial \mathbf{x}}\left(\Gamma_t \frac{\partial f}{\partial \mathbf{x}}\right) = &-\frac{\partial}{\partial \xi}\left[\frac{\varepsilon_\xi}{\langle \xi'^2 \rangle}(\langle \xi \rangle - \xi) f\right] \\ &- \frac{\partial}{\partial Y_1}\left[\frac{\varepsilon_{Y_1}}{\langle Y_1'^2 \rangle}(\langle Y_1 \rangle - Y_1) + \mathcal{R}_1(\xi, Y_1, Y_2) f\right] \\ &- \frac{\partial}{\partial Y_2}\left[\frac{\varepsilon_{Y_2}}{\langle Y_2'^2 \rangle}(\langle Y_2 \rangle - Y_2) + \mathcal{R}_2(\xi, Y_1, Y_2) f\right].\end{aligned} \tag{5.8}$$

5.3 Solution of the turbulent reacting flow using the conditional quadrature method of moments (CQMOM)

It is convenient to introduce the conditional density functions $f(Y_2 \mid \xi, Y_1)$ and $f(Y_1 \mid \xi)$ which are corresponds to the conditional density function for Y_2, given fixed values for the ξ and Y_1, and the conditional density function for Y_1, given fixed values for the ξ respectively. Then the conditional density function related to the mixture fraction and the progress variables can be expressed as:

$$f = f(\xi, Y_1, Y_2) = f(Y_2 \mid \xi, Y_1) f(\xi, Y_1) = f(Y_2 \mid \xi, Y_1) f(Y_1 \mid \xi) f(\xi). \tag{5.9}$$

The conditional moments can be expressed using the conditional density functions and can be defined by

$$\left\langle Y_1^j \right\rangle (\xi) \equiv \int Y_1^j f\left(Y_1 \mid \xi\right) \mathrm{d}Y_1 \tag{5.10}$$

and

$$\left\langle Y_2^k \right\rangle (\xi, Y_1) \equiv \int Y_2^k f\left(Y_2 \mid \xi, Y_1\right) \mathrm{d}Y_2 \tag{5.11}$$

Let M_{njk} denote the moments of f, where the non-negative integers n,j and k represents the order for each scalar, e.g. mixture fraction and progress variable one and progress variable two. Thus the moments of joint composition PDF in integral form are defined as:

$$M_{njk}\left(\mathbf{x}, t\right) = \iiint \xi^n Y_1^j Y_2^k f\left(\xi, Y_1, Y_2; \mathbf{x}, t\right) \mathrm{d}\xi \mathrm{d}Y_1 \mathrm{d}Y_2. \tag{5.12}$$

Using the same definition it is possible to show that:

$$M_{nj0} = \iint \xi^n Y_1^j f\left(\xi, Y_1\right) \mathrm{d}\xi \mathrm{d}Y_1 = \int \xi^n \left\langle Y_1^j \right\rangle (\xi) f\left(\xi\right) \mathrm{d}\xi \tag{5.13}$$

and

$$M_{njk} = \iint \xi^n Y_1^j \left\langle Y_2^k \right\rangle (\xi, Y_1) f\left(\xi, Y_1\right) \mathrm{d}\xi \mathrm{d}Y_1 \tag{5.14}$$

In quadrature-based moment method (QBMM) the scalar distribution function can be represented by:

$$f\left(\boldsymbol{\phi}\right) = \sum_{\alpha=1}^{\mathrm{N}} w_\alpha \delta\left(\phi - \phi_\alpha\right), \tag{5.15}$$

where $\phi_\alpha = (\xi, Y_1, Y_2)$ represent the scalar of interest and w_α are the weights. To simplify the problem, we will assume that only mean values for the conditional scalars are necessary, e.g. we assume that $\mathrm{N}_2 = \mathrm{N}_3 = 1$. The number of the primary nodes are $\mathrm{N}_1 = 2$. This assumption yields to the fact that the conditional weights becomes unity by definition. We also assume that the primary moments represent the mixture fraction while the conditional moments are

representing the progress variables, Y_1 and Y_2. Implementing Eq. 5.15 into Eq. 5.14, f can be expressed as:

$$f(\xi, Y_1, Y_2) = \sum_{\alpha=1}^{N_1} w_\alpha \delta(\xi - \xi_\alpha)\,\delta(Y_1 - Y_{1;\alpha})\,\delta(Y_2 - Y_{2;\alpha})\,. \tag{5.16}$$

Given the assumptions above, we reconstruct the coefficient matrices for the CQMOM (Yuan and Fox, 2011):

$$\mathbf{V} = \begin{bmatrix} 1 & 1 \\ \xi_1 & \xi_2 \end{bmatrix}, \quad \text{and} \quad \mathbf{R} = \begin{bmatrix} w_1 & 0 \\ 0 & w_2 \end{bmatrix}. \tag{5.17}$$

Using the coefficient matrices, the set of equation can be written to find the conditional moments from the original transported moments. These equations can be expressed as:

$$\mathbf{VR} \begin{bmatrix} Y_{1;1} & Y_{2;1} \\ Y_{1;2} & Y_{2;2} \end{bmatrix} = \begin{bmatrix} M_{010} & M_{001} \\ M_{110} & M_{101} \end{bmatrix}. \tag{5.18}$$

$$\begin{bmatrix} Y_{1;1} & Y_{2;1} \\ Y_{1;2} & Y_{2;2} \end{bmatrix} = \frac{1}{w_1 w_2 \xi_2 - w_1 w_2 \xi_1} \begin{bmatrix} w_2\xi_2 & -w_2 \\ -w_1\xi_1 & w_1 \end{bmatrix} \begin{bmatrix} M_{010} & M_{001} \\ M_{110} & M_{101} \end{bmatrix}. \tag{5.19}$$

In other words we can express the conditional moments as:

$$\begin{aligned} Y_{1;1} &= \frac{1}{w_1(\xi_2 - \xi_1)}\left[\xi_2 M_{010} - M_{110}\right], \\ Y_{1;2} &= \frac{1}{w_2(\xi_2 - \xi_1)}\left[-\xi_1 M_{010} + M_{110}\right], \\ Y_{2;1} &= \frac{1}{w_1(\xi_2 - \xi_1)}\left[\xi_2 M_{001} - M_{101}\right], \\ Y_{2;2} &= \frac{1}{w_2(\xi_2 - \xi_1)}\left[-\xi_1 M_{001} + M_{101}\right]. \end{aligned} \tag{5.20}$$

In terms of the quadrature, Eq. 5.16 can be expressed for the assumed case as:

$$M_{njk} = \sum_{\alpha=1}^{N_1} w_\alpha \xi_\alpha^n Y_{1;\alpha}^j Y_{2;\alpha}^k. \tag{5.21}$$

Using the definition for the moments, we can rewrite the transport equations in the form of moments. Then transport equations for the integer moments will be defined as:

$$\frac{\partial M_{njk}}{\partial t}+\langle U\rangle\frac{\partial M_{njk}}{\partial \mathbf{x}}-\frac{\partial}{\partial \mathbf{x}}\left(\Gamma_t\frac{\partial M_{njk}}{\partial \mathbf{x}}\right)=\frac{n\varepsilon_\xi}{\langle\xi'^2\rangle}\left(M_{n-1jk}M_{100}-M_{njk}\right)$$
$$+\sum_{\alpha=1}^{\mathrm{N}_1}w_\alpha\mathcal{R}_1\left(\xi_\alpha,Y_{1;\alpha},Y_{2;\alpha}\right)\left(j\xi_\alpha^nY_{1;\alpha}^{j-1}Y_{2;\alpha}^k\right)$$
$$+\sum_{\alpha=1}^{\mathrm{N}_1}w_\alpha\mathcal{R}_2\left(\xi_\alpha,Y_{1;\alpha},Y_{2;\alpha}\right)\left(k\xi_\alpha^nY_{1;\alpha}^{j}Y_{2;\alpha}^{k-1}\right). \quad (5.22)$$

Using the scale similarity:

$$\frac{\varepsilon_\xi}{\langle\xi'^2\rangle}=C_\xi\frac{\varepsilon}{k} \quad (5.23)$$

with $C_\xi\approx 2$, we can rewrite transport equation for moments as:

$$\frac{\partial M_{njk}}{\partial t}+\langle U\rangle\frac{\partial M_{njk}}{\partial \mathbf{x}}-\frac{\partial}{\partial \mathbf{x}}\left(\Gamma_t\frac{\partial M_{njk}}{\partial \mathbf{x}}\right)=nC_\xi\frac{\varepsilon}{k}\left(M_{n-1jk}M_{100}-M_{njk}\right)$$
$$+\sum_{\alpha=1}^{\mathrm{N}_1}w_\alpha\mathcal{R}_1\left(\xi_\alpha,Y_{1;\alpha},Y_{2;\alpha}\right)\left(j\xi_\alpha^nY_{1;\alpha}^{j-1}Y_{2;\alpha}^k\right)$$
$$+\sum_{\alpha=1}^{\mathrm{N}_1}w_\alpha\mathcal{R}_2\left(\xi_\alpha,Y_{1;\alpha},Y_{2;\alpha}\right)\left(k\xi_\alpha^nY_{1;\alpha}^{j}Y_{2;\alpha}^{k-1}\right). \quad (5.24)$$

Turbulent diffusivity Γ_t is defined as

$$\Gamma_t=\frac{C_\mu}{Sc_T}\frac{k^2}{\varepsilon}, \quad (5.25)$$

with $C_\mu=0.09$ and $Sc_T=0.7$.

5.4 CQMOM algorithm and chemical kinetics

Here, we present the procedure we used to implement the CQMOM model. The mixture fraction is considered to be the primary direction and the progress variable one and progress variable two are considered to be the conditional directions. Below are the steps we follow to solve the problem:

- We initialize the number of nodes per each direction.

- We consider the two primary node and one conditional node for the second and third direction. Choosing of one node is due to the fact that there is no information and closure for the cross terms that may appear at the right hand side of the equation between mixture fraction and chemical kinetics. Also we are only interested in the mean values of the progress variables for the first and second reaction.

- We use initial values for the concentrations to calculate the stoichiometric mixture fraction.

- We initialize moments of PDF.

$$\begin{array}{lll} M_{000} & M_{010} & M_{001} \\ M_{100} & M_{110} & M_{101} \\ M_{200} & & \\ M_{300} & & \end{array} \tag{5.26}$$

- We invert the moments of the mixture fraction e.g. M_{000}, M_{100}, M_{200} and M_{300} using the Wheeler (1974) algorithm to obtain the primary weights, p_α, and primary abscissae, ξ_α.

- Using the conditional moments of second and third direction, we find the abscissae of the progress variables for the node 1 and node 2.

- Using the mean values for the mixture fraction (M_{100}), progress variable one (M_{010}) and progress variable two (M_{001}) we calculate the concentration using the equations below:

$$\begin{aligned} c_A &= c_{A_0}\left[1-\xi-\left(1-\xi_{st}\right)Y_1\right], \\ c_B &= c_{B_0}\left[\xi-\xi_{st}\left(Y_1+Y_2\right)\right], \\ c_R &= c_{B_0}\xi_{st}\left(Y_1-Y_2\right), \\ c_S &= c_{B_0}\xi_{st}Y_2. \end{aligned} \tag{5.27}$$

- We use the current values of the moments for the next time step and implement the same procedure for the next step until the end of the simulation.

5.5 Population balance equation

A univariate population balance equation is used in this study for the flash nanoprecipitation process to describe the aggregation phenomena. The number density f represents the number of nanoparticles per unit volume. Due to the nature of FNP process, breakage rarely happens and thus it is neglected in this study. The evolution equation for the population of polymers during mixing process is then represented as

$$\frac{\partial f}{\partial t}+\langle U\rangle\frac{\partial f}{\partial \mathbf{x}}-\frac{\partial}{\partial \mathbf{x}}\left(\Gamma_t\frac{\partial f}{\partial \mathbf{x}}\right)=-\frac{\partial}{\partial \xi}\left[\frac{\varepsilon_\xi}{\langle \xi'^2\rangle}\left(\langle\xi\rangle-\xi\right)f\right] - \frac{\partial}{\partial\langle \underline{m}\rangle}\left[\frac{\varepsilon_\xi}{\langle \xi'^2\rangle}\left(\langle \underline{m}\rangle-\underline{m}\right)+\underline{R}\left(\xi,\underline{m}\right)f\right] \quad (5.28)$$

where $f\left(\xi,L;\mathbf{x},t\right)$ represents the jpoint composition PDF of mixture fraction and PBE, $\underline{m}$ is the moment vector for PBE, Γ_t is the turbulent diffusivity and $\langle U\rangle$ is the mean velocity. It should be mentioned that the IEM model used the same mixing time scale for all components of PDF. $\underline{R}\left(\xi,\underline{m}\right)=\mathrm{d}\underline{m}/\mathrm{d}t$ is change of moments in PBE given mixture fraction and it is described as

$$R\left(\xi,\underline{m}\right)=\underbrace{\frac{L^2}{2}\int_0^L\frac{\beta\left(\left(L^3-\lambda^3\right)^{1/3},\lambda\right)}{\left(L^3-\lambda^3\right)^{2/3}}f\left(\left(L^3-\lambda^3\right)^{1/3};\mathbf{x},t\right)f\left(\lambda;\mathbf{x},t\right)\mathrm{d}\lambda}_{\text{birth of particles due to aggregation}} \underbrace{-f\left(L;\mathbf{x},t\right)\int_0^\infty\beta\left(L,\lambda\right)f\left(\lambda;\mathbf{x},t\right)\mathrm{d}\lambda}_{\text{death of particles due to aggregation}}. \quad (5.29)$$

$\beta\left(p,i\right)$ is the kernel describing aggregation between two particles. In previous studies (Cheng and Fox, 2010; Cheng et al., 2010), details about the aggregation kernel is well described. Here we use three types of aggregation kernel:

- Free coupling

$$\beta_{1,1}^{free}=4\pi\Theta_p\left(D_1+D_1\right)\left(R_1^{coll}+R_1^{coll}\right) \quad (5.30)$$

- Unimer insertion

$$\beta_{p,1}^{ins}=4\pi\theta_pA_{1,p}^{ins}\frac{\left(R_p^{coll}+R_p^{coll}\right)\left(R_p^{coll}+R_p^{cor}+R_1^{coll}\right)\left(D_p+D_1\right)D_{p,1}^{ins}}{\left(D_p+D_1\right)R_p^{cor}+\left(R_p^{coll}+R_1^{coll}\right)D_{p,1}^{ins}} \quad (5.31)$$

Table 5.1: Parameters used at aggregation kernel β.

Functions	Formula
Θ	Heaviside function
D_p	Diffusion rate $= k_B T/\left(6\pi\eta_s R_p\right)$
R_p	Diffusion radius $= \left(pN_A v\right)^{v_A} + pN_B^{v_B} v^{1/3}$
R_p^{coll}	Collision radius $= \left(pN_A v\right)^{1/3}$
R_p^{cor}	Corona radius $= N_B^{v_B} i^{(1-v_B)/2} v^{1/3}$
$A_{1,p}^{ins}$	Efficiency factor $= \exp\left(-\alpha\left(1,0\right) i^{1/2} p\right)$, α : constant
$A_{1,p}^{fus}$	Efficiency factor $= \exp\left(-\alpha\left(1,0\right) \max\left(p^{1/2}, i^{1/2}\right) \min\left(p,i\right)\right)$, α : constant
Parameters	
k_B	Boltzmann constant
T	Temperature
η_s	solvent viscosity
v_c	unit volume of organic molecule
v	unit volume of polymer monomer
N_A, N_B	unit number of monomers in A block or B block
v_A, v_B	Flory exponent
c_p	initial polymer concentration
c^{cor}	corona polymer concentration

- Aggregation fusion

$$\beta_{p,i}^{fus} = 4\pi\theta_p A_{1,p}^{fus} \frac{\left(R_p^{coll} + R_i^{coll}\right)\left(R_p^{coll} + R_p^{cor} + R_i^{coll} + R_i^{cor}\right)\left(D_p + D_i\right) D_{p,i}^{fus}}{\left(D_p + D_i\right)\left(R_p^{cor} + R_i^{cor}\right) + \left(R_p^{coll} + R_i^{coll}\right) D_{p,i}^{fus}} \tag{5.32}$$

We describe the parameters shown in aggregation kernel in Tab. 5.1.

Finally applying the moment definition, we can write the source terms as

$$\underline{R}\left(\xi, \underline{m}\right) = \frac{1}{2}\sum_{i=1}^{\mathrm{N}} w_i \sum_{j=1}^{\mathrm{N}} w_j \left(L_i^3 + L_j^3\right)^{k/3} \beta\left(L_i, L_j\right) - \sum_{i=1}^{\mathrm{N}} w_i L_i^k \sum_{j=1}^{\mathrm{N}} w_j \beta\left(L_i, L_j\right), \tag{5.33}$$

where L_i and L_j are the particles with different sizes in the same environment. Transport equations for mixture fraction can be written as

$$\frac{\partial M_k}{\partial t} + \langle U\rangle \frac{\partial M_k}{\partial \mathbf{x}} - \frac{\partial}{\partial \mathbf{x}}\left(\Gamma_t \frac{\partial M_k}{\partial \mathbf{x}}\right) = \frac{k\varepsilon_\xi}{\langle \xi'^2\rangle}\left(M_{k-1}M_1 - M_k\right), \tag{5.34}$$

and conditional moments of PBE can be described as

$$\frac{\partial \langle \underline{m} \rangle}{\partial t} + \langle U \rangle \frac{\partial \langle \underline{m} \rangle}{\partial \mathbf{x}} - \frac{\partial}{\partial \mathbf{x}} \left(\Gamma_t \frac{\partial \langle \underline{m} \rangle}{\partial \mathbf{x}} \right) = \langle \underline{R}(\xi, \underline{m}) \rangle , \tag{5.35}$$

$$\frac{\partial \langle \xi \underline{m} \rangle}{\partial t} + \langle U \rangle \frac{\partial \langle \xi \underline{m} \rangle}{\partial \mathbf{x}} - \frac{\partial}{\partial \mathbf{x}} \left(\Gamma_t \frac{\partial \xi \langle \underline{m} \rangle}{\partial \mathbf{x}} \right) = \frac{\varepsilon_\xi}{\langle \xi'^2 \rangle} \left(\langle \xi \rangle \langle \underline{m} \rangle - \langle \xi \underline{m} \rangle \right) + \langle \xi \underline{R}(\xi, \underline{m}) \rangle . \tag{5.36}$$

Source terms at Eq. 5.35 and Eq. 5.36 are defined as

$$\begin{aligned} \langle \underline{R}(\xi, \underline{m}) \rangle &= \sum_{\alpha=1}^{2} p_\alpha \underline{R}(\xi, \underline{m}) \\ \langle \xi \underline{R}(\xi, \underline{m}) \rangle &= \sum_{\alpha=1}^{2} p_\alpha \xi_\alpha \underline{R}(\xi, \underline{m}) \end{aligned} \tag{5.37}$$

5.6 Algorithm to solve aggregation in multi-inlet vortex reactor

A sequential workflow is used to investigate the aggregation of nano-particles inside MIVR contains three parts. First we the velocity, $\langle U \rangle$ and turbulence fields, k and ε are first obtained by solving the steady state flow field. Later, the mean mixture fraction is obtained by solving the transport equations of mixture fraction moments. Finally, particle size distribution is obtained by solving the population balance equation (PBE) using an extended quadrature method of moments. We assume that particles have small Stokes number and do not affect the fluid motion. Also, the flash nanoprecipitation does not significantly affect mixing. Once we obtained the moments of mixture fraction, we solve two sets of equations to obtain the moments of PBE in each environment from the conditional moments. Thus we have

$$\begin{aligned} \langle \underline{m} \rangle &= p_1 \underline{m}_1 + p_2 \underline{m}_2 \\ \langle \xi \underline{m} \rangle &= p_1 \xi_1 \underline{m}_1 + p_2 \xi_2 \underline{m}_2, \end{aligned} \tag{5.38}$$

where $\underline{m}_1$ and $\underline{m}_2$ are the moment vector of PBE in each environment. Solving this set of equations we have

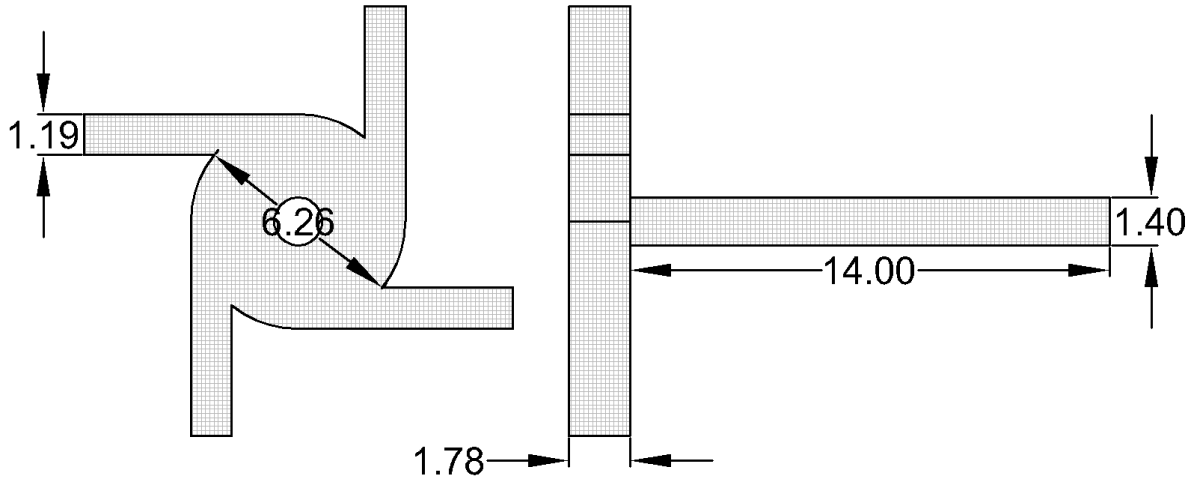

Figure 5.1: Geometry of the mixing chamber. All dimensions are reported in mm.

$$\underline{m}_1 = \frac{\langle \underline{m} \rangle \, \xi_2 - \langle \xi \underline{m} \rangle}{p_1 \, (\xi_2 - \xi_1)}$$
$$\underline{m}_2 = \frac{\langle \xi \underline{m} \rangle - \langle \underline{m} \rangle \, \xi_1}{p_2 \, (\xi_2 - \xi_1)}, \tag{5.39}$$

Once we obtained the PBE moments in each environment, we invert them and find the weights and abscissae related to particle sizes. To solve the PBE moments in each environment, we will use an extended quadrature method of moments with log-normal kernel density function (LnEQMOM) Madadi-Kandjani and Passalacqua (2015). We use `pbeTransportFoam` a solver based on OpenQBMM® framework, which leverages the OpenFOAM® CFD toolbox.

5.7 Case setup

Fig. 5.1 shows the simulation geometry. The vortex reactor has four inlets attached tangentially to the main circular chamber. The reactor outlet is perpendicular to the main chamber. Dimensions of vortex reactor are four identical inlet channels with width $w = 1.19$ mm and height $H = 1.78$ mm, the radius of mixing chamber is $R = 3.13$ mm and the outlet radius of $r = 0.7$ mm. The inlet streams have equal velocities. Two opposing streams contain solvent and the other two are non-solvent.

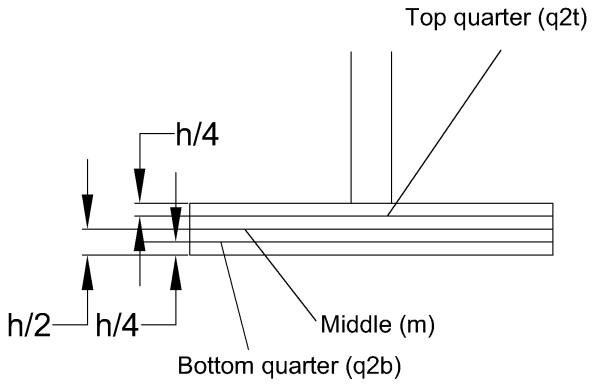

Figure 5.2: Three plates definition where the results are reported.

There are three plates defined to report the results which are located in the middle of the chamber top quarter and bottom quarter. These plates are shown in Fig. 5.2.

5.8 Fluid field

In order to obtain the concentration fields inside the MIVR, we first solve the flow field to obtain the velocity and turbulence fields. Flow rates are all equal in four streams in this study. We define the Reynolds number Re_j in terms of characteristic inlet velocity U_j by

$$Re_j = \frac{d_h U_j}{\nu}, \tag{5.40}$$

where d_h is the hydraulic diameter of the inlet channel and ν is the kinematic viscosity of fluid. In this study we assume $U_j = 0.1670$ m s^{-1} which results $Re_j = 240$. The velocity and turbulence fields are first obtained by solving the $k - \varepsilon$ model with a wall function. The flow field is solved using `simpleFoam` which is a solver from an open source software OpenFOAM®. In previous studies, the LES results were used to determine the accuracy of $k - \varepsilon$ predictions (Cheng, 2010).

Fig. 5.3 shows the solution obtained using this setup. As shown, MIVR generates swirling flow with higher turbulent intensity in the center of the mixing chamber. Most of the interactions happen in the center of the chamber and thus it is the place where the turbulent kinetic energy

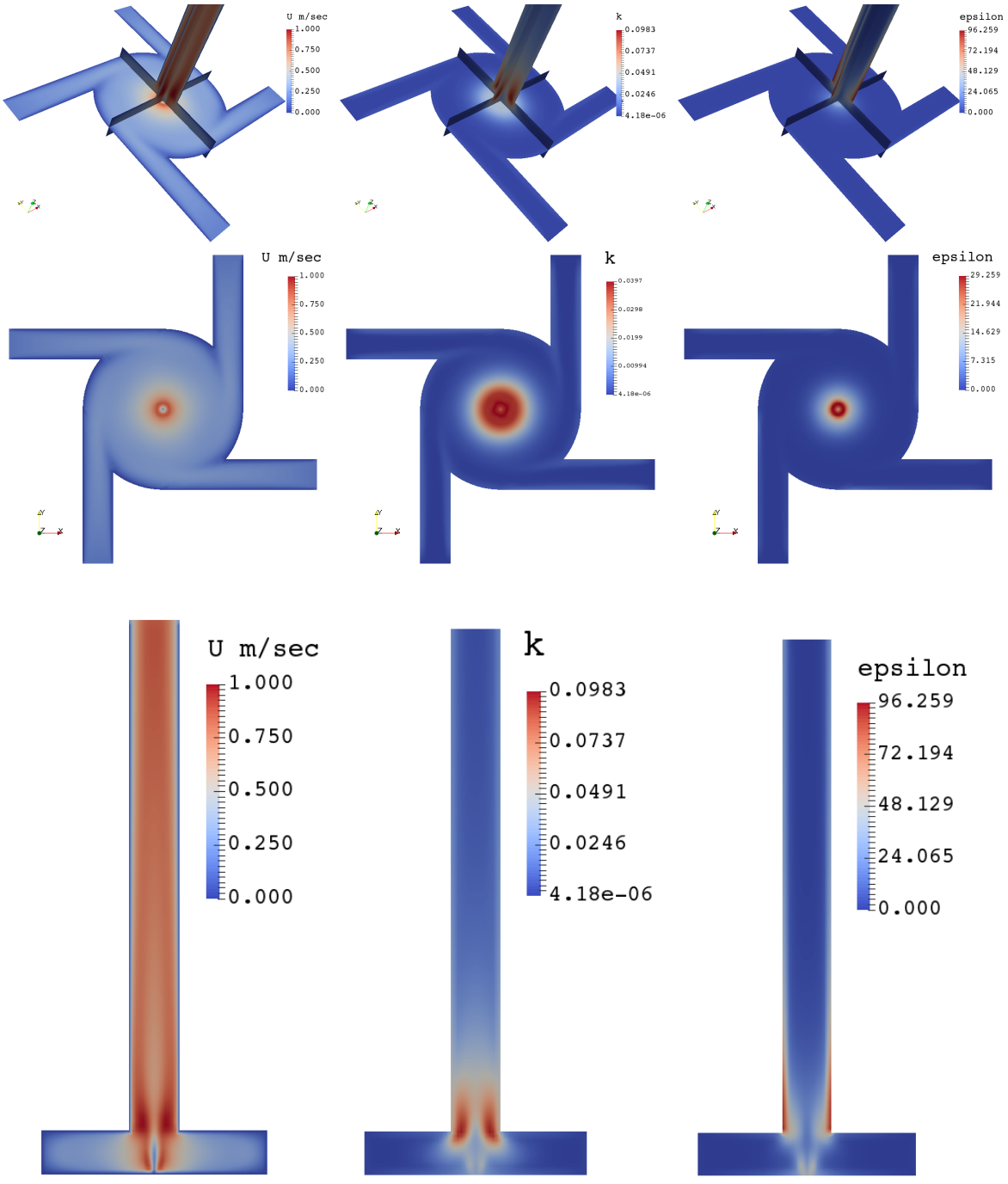

(a) (b) (c)

Figure 5.3: Steady state solution of the (a) velocity, (b) turbulent kinetic and (c) turbulent dissipation of the flow.

(k) and turbulent dissipation (ε) is higher. It is also the place where the mixing and reaction mostly happen. The values of k and ε are higher at the intersection of the outlet and the main chamber where the flow strikes with the wall while it makes the transition from a big chamber to the small volume of the outlet. When the stream velocities are increased, the Re_j will increase. This increases the turbulent flow area and provides a more homogeneous mixing flow.

5.9 Mixing in multi-inlet vortex reactor

The mixture fraction represents the mixing progress. Initially, two opposing streams are A and the other two opposing streams are B. The streams have equal velocities as it is addressed in Sec. 5.8. We assume that the streams containing B have a mixture fraction of $\langle\xi\rangle = 1$ and the other two opposing streams with A have mixture fraction $\langle\xi\rangle = 0$. Fig. 5.4 shows the concentration of A and B species and the mean mixture fraction inside the system. As mixing proceed, in the equal feed ratio case which we are studying here, mixture fraction tends toward the complete mixing where $\langle\xi\rangle = 0.5$. In this case, $\langle\xi\rangle = 0.5$ when the mixing simulation is fully converged. In flash nanoprecipitation processes $\langle\xi\rangle$ is key since the solvent and non-solvent should reach a specific ratio to precipitate. This will be discussed later in Sec. 5.11.

Fig. 5.5 shows the converged mixing solution for the case under study.

Generally, the large scale mixing are mainly influenced by the geometry of the reactor and small scale mixing are determined by the energy dissipation and viscosity. In this study, the mean mixture fraction can be written as

$$\langle\xi\rangle = M_{100}, \tag{5.41}$$

while the mixture fraction variance in the form of moments can be written as

$$\langle\xi'^2\rangle = M_{200} - M_{100}^2. \tag{5.42}$$

Fig. 5.6 shows the mean and variance of the mixture fraction in the different height of the mixing chamber. Mean mixture fraction is mostly homogeneous in the middle of mixing chamber, while

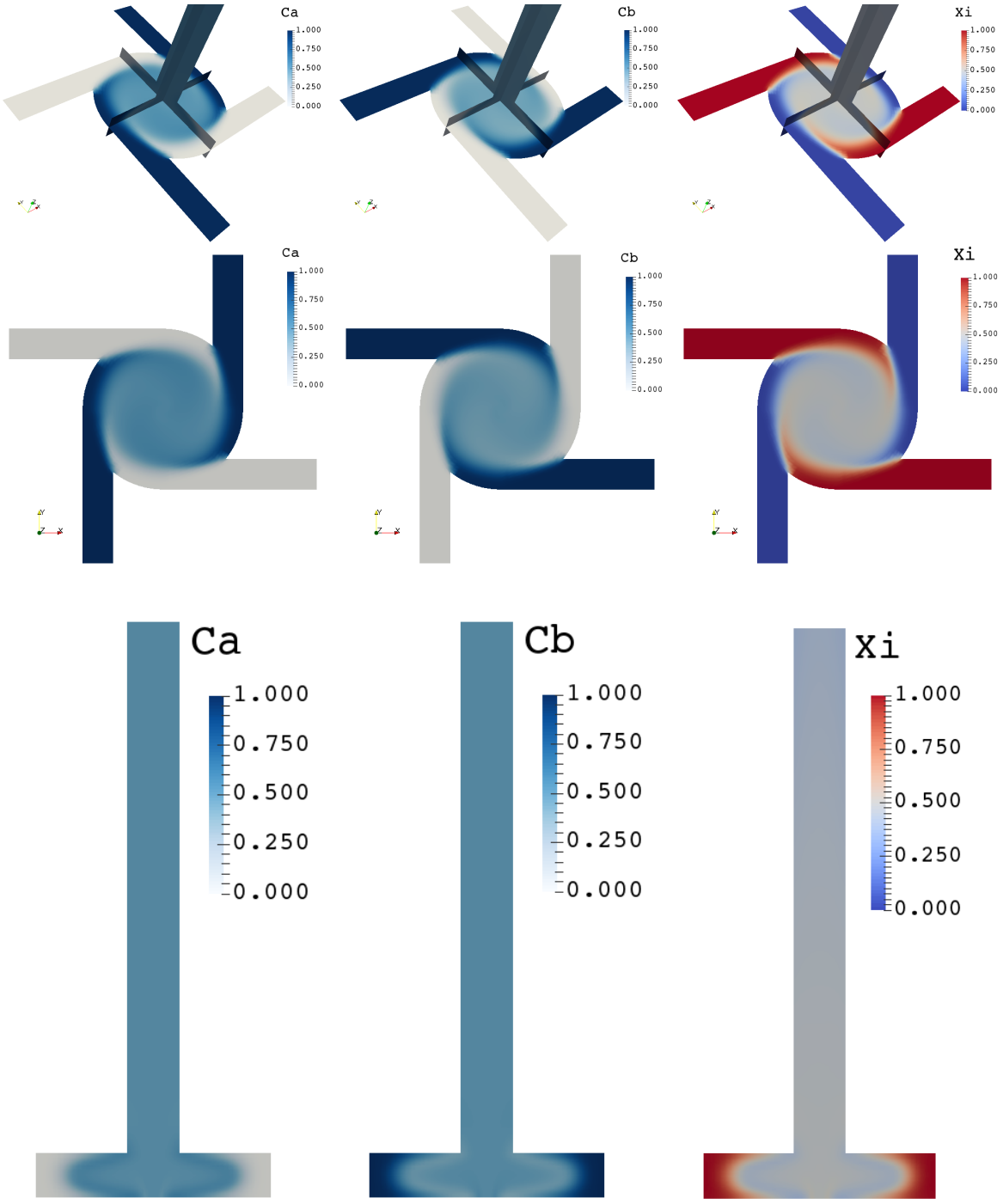

(a) (b) (c)

Figure 5.4: Steady state solution of the (a) concentration A, (b) concentration B and (c) mixture fraction.

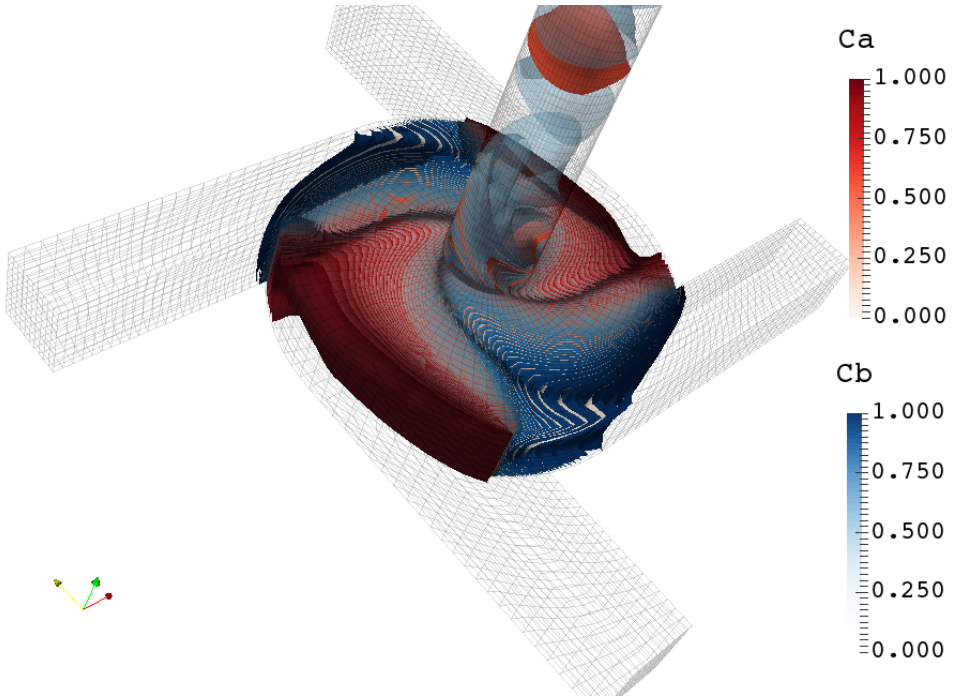

Figure 5.5: Mixture fraction obtained from mixing of two environments shown inside the chamber, reaching a steady state at mixture fraction equal to 0.5.

in the quarter bottom and quarter top, there a slight variation from the mean. At the middle of the chamber, $\langle \xi'^2 \rangle$ is nearly zero, which indicates the mixing mostly affected by the small-scale segregation in these areas. Near to inlet streams, the mixture fraction variance is high which indicates the mixing mostly is affected by the large scale segregation.

5.10 Reaction in multi-inlet vortex reactor

In order to obtain the concentration fields inside the MIVR, we first solve the flow field to obtain the velocity and turbulence fields. Later we use these values to solve the moment transport equations for the joint composition PDF to obtain the mean values for the mixture fraction, M_{100}, reaction progress variable one, M_{010}, and reaction progress variable two, M_{001}. Later we use Eq. 5.27 to calculate the concentration of reactants and product and bi-product during the process.

Fig. 5.7 shows the concentration of the species obtained during the competitive consecutive inside the reaction chamber. Two opposing inlet streams contain species A and the two other

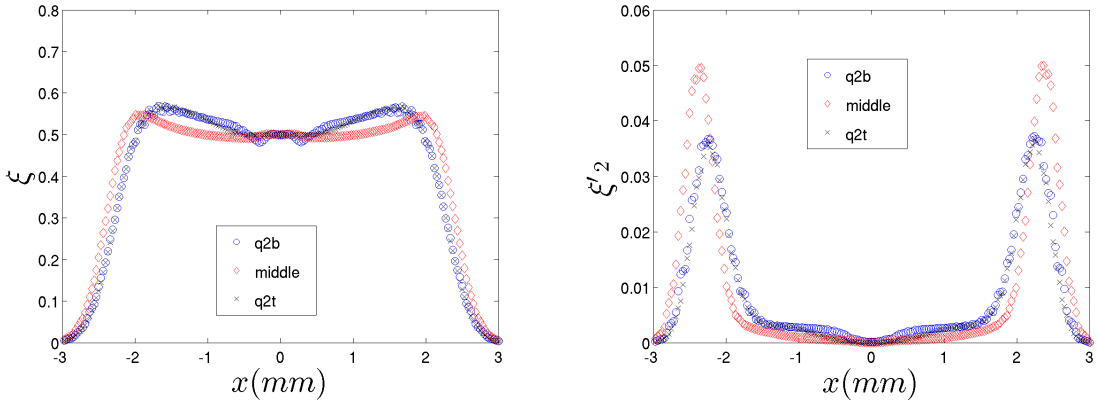

(a) (b)

Figure 5.6: The (a) mixture fraction and (b) variance inside the mixing chamber shown in three plates, middle (m), top quarter (q2t) and bottom quarter (q2b).

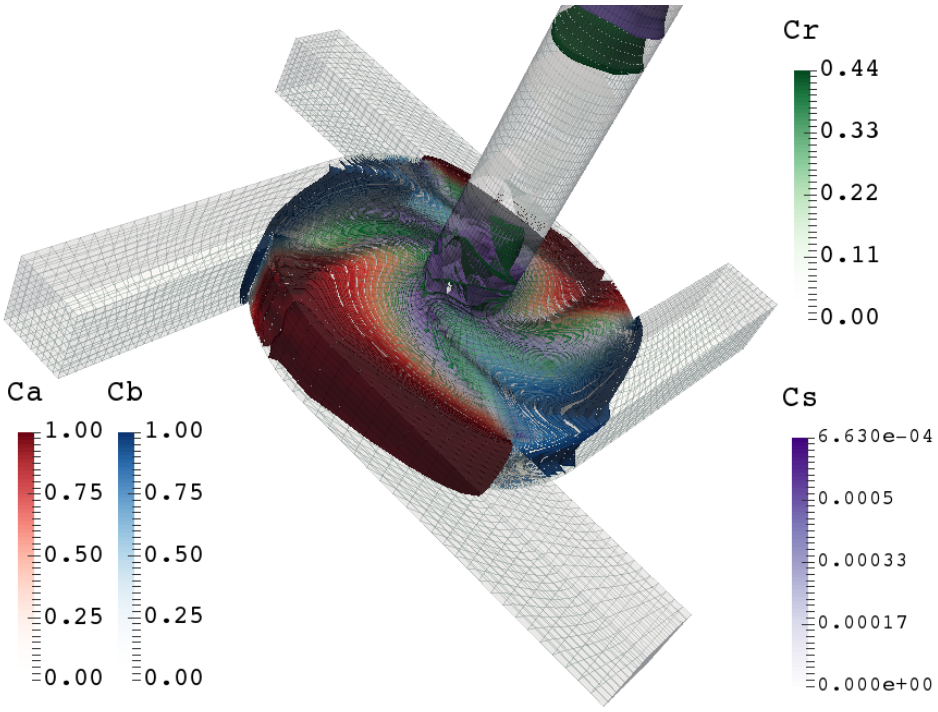

Figure 5.7: The concentration of four species for competitive consecutive reaction.

inlets contain species B. Initially, the reactor is filled up with A. Once the B is injected into the chamber, they start reacting and produce R and S. Since the rate of reaction, k_1, is higher for the first reaction, mostly the main product R appears in the system, while the parallel reaction which produces bi-product, S, happens when the R meets the B and A is not present. Fig. 5.8 and Fig. 5.9 show the concentration of each species at the middle plate of chamber and the middle slice at the outlet. It shows the rapid reaction between A and B. Middle of the reaction chamber is the place where the product, R and bi-product, S have a higher concentration. The product R forms rapidly in the reaction zone and moves toward the exit, while the bi-product S forms more slowly. As it is discussed previously, the concentration of R is higher due to the high reaction rate of the first reaction compare to the parallel reaction which is almost $O\left(10^3\right)$. The byproduct S is produced due to the presence of R and B when A is absent due to the mixing limitation.

5.11 Aggregation in multi-inlet vortex reactor

A bivariate PBE is implemented for the FNP process to describe the aggregation of the polymers and organics. Due to the nature of the FNP process breakage rarely occurs and thus is neglected in this study. The two environments are solved as passive scalars. In the FNP process, both the polymer and organics are dissolved in the solvent. The boundary conditions for scalars in solvent and solvent are as below. $m(0,0)_1$ is set to be one, while $m(k=1-4,l=0)_1 = p_{ini}/(p_{ini}+q_{ini})$, and $m(k=0,l=1)_1 = q_{ini}/(p_{ini}+q_{ini})$. Other moments are defined to be zero at the boundaries. The initial concentration of polymer is $p_{ini} = 5.583 mol/m^3$ and that of organics is $q_{ini} = 49.496 mol/m^3$. When the mixture fraction changes $0.1 < \xi < 0.4$, in environment 1 and 2, aggregation starts. We look into the properties of moments field rather than the particle sizes distribution since moments themselves represents important statics such as number density and particle mean size. Averaged values and contour plots of moments related to the number density and aggregates sizes are shown in Fig. 5.10 and Fig. 5.11. The $m(0,0)$ representing the total number density of the aggregates is equal to a normalized value of 1 in environment 1, where all the polymers and organics were dissolved initially. It decreases from 1 toward the mean $\langle m(0,0) = \xi_1 m(0,0)_1 + \xi_2 m(0,0)_2 \rangle$. Inside the chamber it has diffferent distribution due

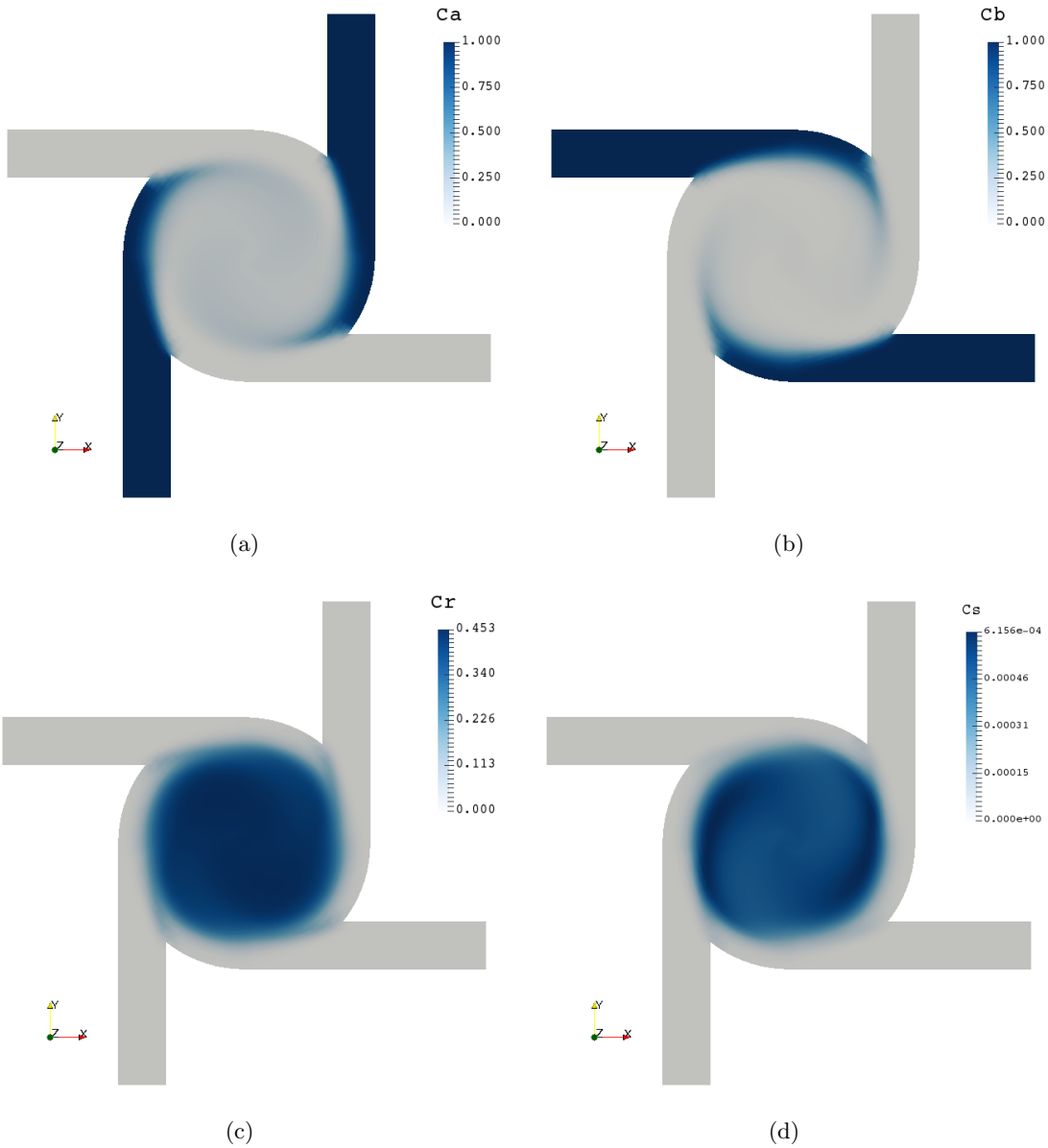

Figure 5.8: Steady state solution of the (a) concentration A, (b) concentration B, (c) concentration R and (d) concentration S.

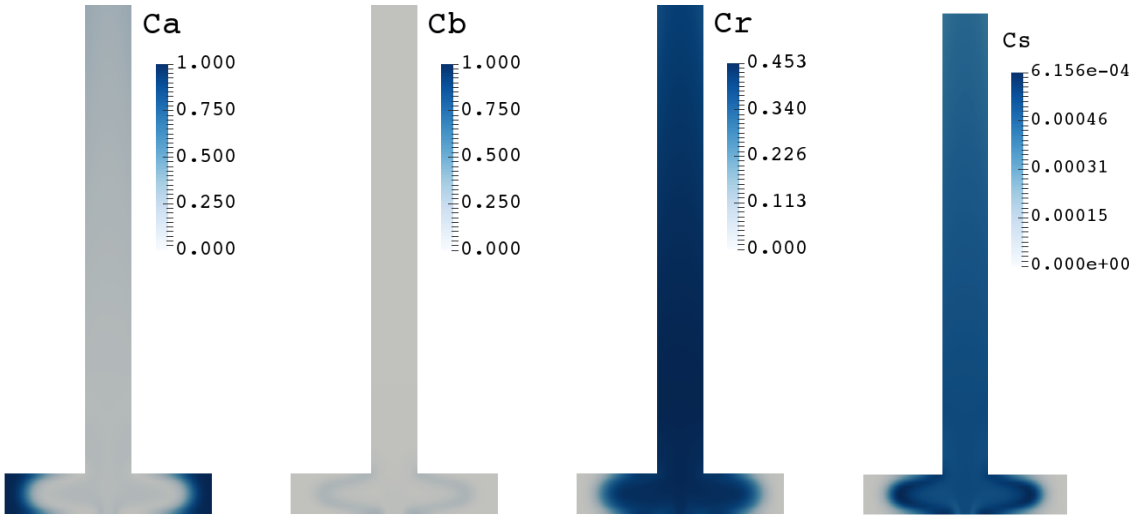

(a) (b) (c) (d)

Figure 5.9: Steady state solution of the (a) concentration A, (b) concentration B, (c) concentration R and (d) concentration S.

to different mixing levels.

5.12 Conclusion

This study addresses comprehensive models for turbulent reactive flows and flash nanoprecipitation. Conditional quadrature method of moments approach was introduced for the turbulent reacting flows. The transport equation for the moments of PDF was described for the mixing and consecutive competitive reactions. Initially, the model is used for the problems encounter with mixing. Later the model is validated for the problems where the reaction of species happens along mixing. The solvers for the mixing and reaction problems uses OpenQBMM® structure which leverage from an open source software OpenFOAM®. The new model was also introduced for flash nanoprecipitation. The model combines a PBE with aggregation of species and scalar mixing models. CQMOM is efficient in reducing the number of moments required to model the system.

The approach was applied to the CFD simulation of multi-inlet vortex reactor. First, the simple mixing was considered and the mixture fraction and concentration of each species for mixing

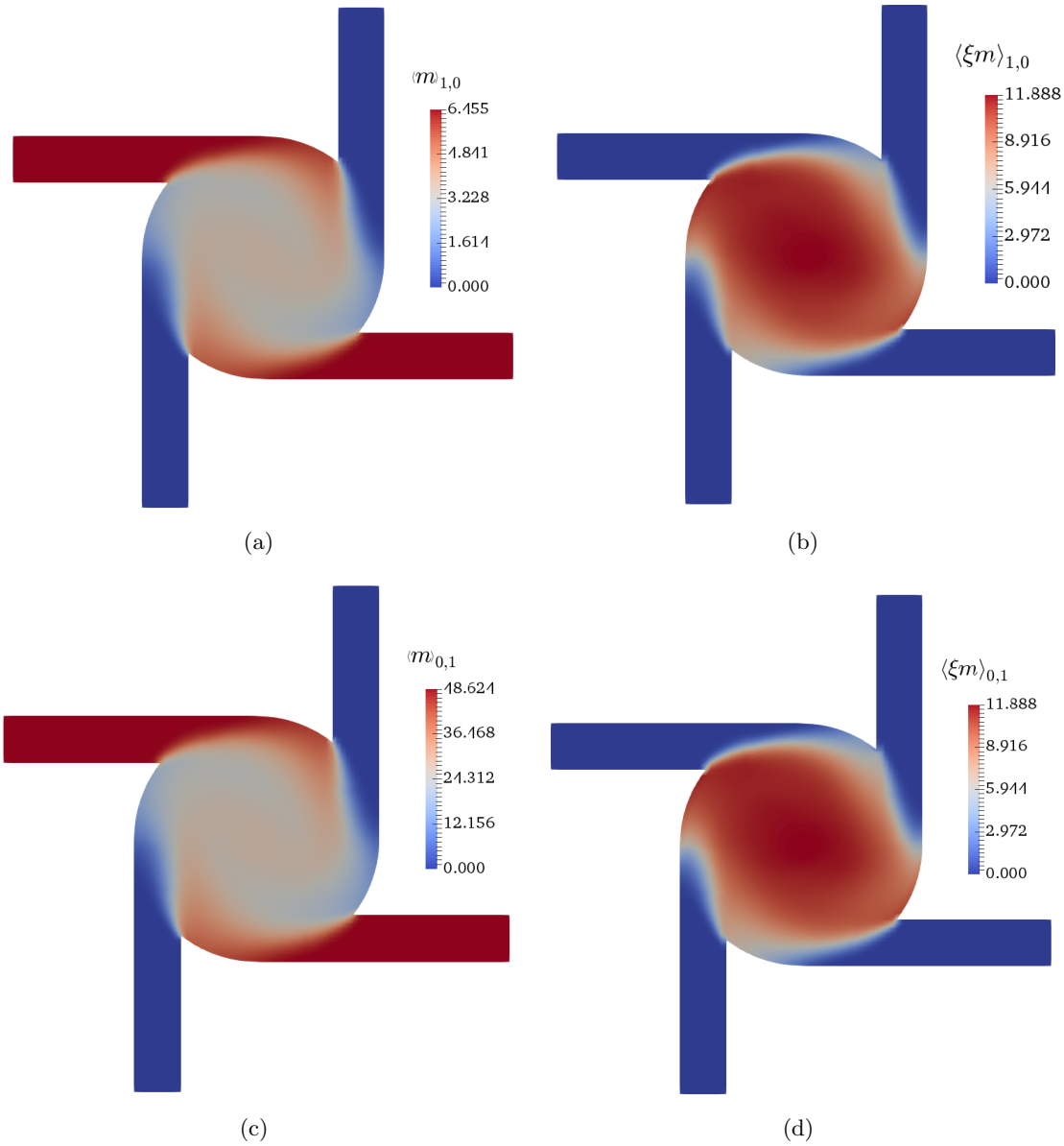

Figure 5.10: Steady state solution of the weighted population balance equation of (a) $\langle M_{10} \rangle$ and (b) $\langle M_{01} \rangle$, and weighted mixture population balance equation of (c) $\langle M_{10} \rangle$ and (d) $\langle M_{01} \rangle$.

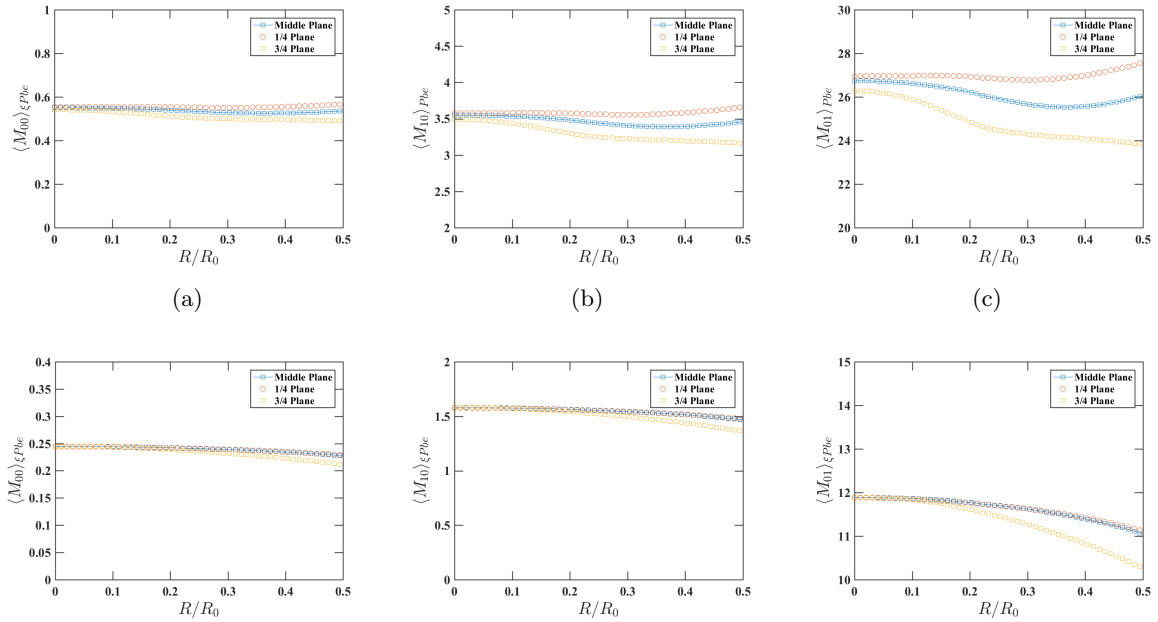

Figure 5.11: Steady state solution of the weighted population balance equation of (a) $\langle M_{00}\rangle$, (b) $\langle M_{10}\rangle$, (c) $\langle M_{01}\rangle$ and weighted mixture population balance equation of (d) $\langle M_{00}\rangle$ (e) $\langle M_{10}\rangle$ and (f) $\langle M_{01}\rangle$.

were reported at the MIVR. Later the consecutive competitive reaction besides the mixing was considered to take into account the effect of it. Simulation results show the consistency on physics of the phenomena. Finally, in the CFD simulation results for flash nanoprecipitation, different aggregation zones, and particle size distribution are accounted.

The ability of the CFD to quantify and predict mixing and consecutive competitive reaction is quite striking. It demonstrates that the CFD simulations can be used to optimize the design and functionality of the MIVR.

CHAPTER 6. SUMMARY

The objective of this thesis is to use quadrature-based moment method in multiphase systems and turbulent reacting flows. Simulation of physical systems require a robust and accurate methods with optimized cost. While well-established methods like direct numerical simulations (DNS) provides accurate results, they are often expensive from the computational cost to be applied to a large-scale system and thus there is a need to use models beside averaged transport equations. The idea behind quadrature-based moment methods (QBMM) is to transport moments of the PDF. While quadrature method of moments uses Dirac delta functions as the basis function, recently established approach, an extended quadrature method of moments (EQMOM) uses smooth non-negative kernel density functions as a base function to represent more complex PDFs with few nodes.

In this study, first, the new approach base on the log-normal kernel density function (KDF) for the extended quadrature method of moments (EQMOM) is presented. The approach is implemented to the population balance equation where the population of particles can be described as a number density function (NDF). Later the approach is tested and validated for the problems with aggregation and breakup of the particles. The basic idea of using the log-normal KDF is due the physical observation in experimental and numerical studies which report that the size distribution of particles in fluids tends to be log-normal. We verified the numerical procedure to reconstruct the NDF using LnEQMOM by considering a distribution obtained as a linear combination of two log-normal distributions with different mean and variance. The results show good agreement with the analytical function. We discussed the solution of the PBE for aggregation and breakup problems. Two types of calculation were performed to investigate the predictive capabilities of Ln-EQMOM. First, the moments of the rigorous NDF reported by Vanni (2000) were computed for each of the cases considered. The computed moments were

then used as input to Ln-EQMOM to obtain the reconstructed NDF. Results were compared to the rigorous NDF and to the reconstruction obtained with γ-EQMOM (Yuan et al., 2012). Later the moment transport equations for Ln-EQMOM closures with the appropriate source terms were integrated to obtain the approximate distribution for each of the cases under consideration, starting from the initial conditions. Ln-EQMOM provides more accurate results for the time evolution of the zero-order moment and of the mean particle size than QMOM for aggregation and breakup problems. This improvement is achieved using a lower number of primary quadrature nodes than the standard QMOM procedure. Ln-EQMOM also appeared to be numerically more robust when compared to γ-EQMOM, due to the structure of the system of equations used in the numerical procedure.

As another approach in this study, the EQMOM with β kernel density function was applied to find an approximate solution of the Fokker-Planck turbulent mixing model. Two form of the conditional scalar dissipation $\langle\epsilon|\phi\rangle$ are used to approximate the transported PDF of any arbitrary distribution. Three cases were examined to validate the EQMOM-FP against the results obtained with the DNS of Eswaran and Pope (1988). Later, the capability of the EQMOM-FP to predict the time evolution of a bivariate joint scalar PDF was demonstrated considering the cases studied by Juneja and Pope (1996). In these cases, the EQMOM-FP approach predicted the evolution of the marginal PDFs towards Gaussian, showing the capability of the approach of being applied to solve mixing problems. In both test cases, results obtained by the EQMOM-FP are in good agreement with the DNS results in the cases examined. Finally, the EQMOM-FP approach was examined against results obtained with the mapping closures (MC) approach. Results reveal the EQMOM-FP predicts the reconstruction of PDF in agreement with the MC results.

It is possible to formulate the problem with a joint composition PDF where the PDF includes information on both mixing and reaction of the scalar together. In this way, the higher number of internal coordinates will be considered according to the nature of the reaction. In this project three different reaction models, competitive consecutive, one reaction and fast reaction with both IEM and FP mixing were considered. Initially, correction terms of direct quadrature method of moments which is well studied in Fox (2003) are derived from the joint composition

PDF. Later, a new model based on conditional quadrature method of moments is used to solve the transport equation for the joint composition PDF. The advantage of CQMOM based model to the DQMOM is that it conserves a larger number of moments. Also, in DQMOM, transport equations are written for non-conserved quantities while in CQMOM the transport equations are written for the moments which are the conserved quantities. Also, CQMOM does not have the singularities introduced at the problem because of the correction terms added to the transport equation. In this study, the reaction system is written in terms of reaction progress variables and the mixture fraction. Then the joint composition PDF is introduced for mixture fraction and progress variables as internal coordinates and the quadrature based moments method were applied to close the transport equation. A string is initialized with two species and the evolution of the scalars are studied. The concentration of species is then reported. Finally, the two model for the mixing for different reaction systems provides the similar conclusion and they are in agreement with the results obtained with DQMOM. In all the cases most of the S produced near to the stream B where there is a high probability of presence for B and R. Also in all cases, the mixture fraction tend to be a homogeneous mixture. Since the rate of the first reaction is higher than the second reaction, the progress variable for the first reaction is higher in value than the one for the second reaction.

APPENDIX A. NUMERICAL APPROXIMATION OF INTEGRALS IN THE PBE

We briefly summarize here the procedures to approximate the integrals that appear in the source terms of the PBE.

A.1 Gauss-Hermite quadrature

The first approach to perform the numerical integration of the source terms using known Gaussian quadrature formulae is to rely on a change of variable to reduce the quadrature problem to the well known case of Gaussian-Hermite quadrature (Gautschi, 2004). We illustrate the procedure considering the integral

$$\int_0^\infty g(\xi)\,\delta_\sigma(\xi,\mu)\,\mathrm{d}\xi = \int_0^\infty g(\xi)\,\frac{1}{\xi\sigma\sqrt{2\pi}}\,\mathrm{e}^{-\frac{(\ln\xi-\mu)^2}{2\sigma^2}}\,\mathrm{d}\xi. \tag{A.1}$$

We set

$$\frac{(\ln\xi-\mu)^2}{2\sigma^2} = s^2 \Rightarrow \xi = \mathrm{e}^{\sigma s\sqrt{2}+\mu}, \tag{A.2}$$

and so we can write the differential of ξ as

$$\mathrm{d}\xi = \sqrt{2}\sigma\,\mathrm{e}^{\sigma s\sqrt{2}+\mu}\,\mathrm{d}s. \tag{A.3}$$

Thus, the original integral becomes

$$\int_{-\infty}^\infty \frac{g\left(\mathrm{e}^{\sqrt{2}\sigma s+\mu}\right)\mathrm{e}^{-s^2}\,\sqrt{2}\sigma\,\mathrm{e}^{\sqrt{2}\sigma s+\mu}}{\mathrm{e}^{\sqrt{2}\sigma s+\mu}\,\sigma\sqrt{2\pi}}\mathrm{d}s = \frac{1}{\sqrt{\pi}}\int_{-\infty}^\infty g\left(\mathrm{e}^{\sqrt{2}\sigma s+\mu}\right)\mathrm{e}^{-s^2}\,\mathrm{d}s, \tag{A.4}$$

which can be approximated using standard Gauss-Hermite formula (Gautschi, 2004).

A.2 Gauss-Stieltjes-Wigert quadrature

The quadrature formula obtained in A.1 is exact for polynomials of $\psi = \ln x$. A quadrature formula exact for polynomials of x is obtained considering the Stieltjes-Wigert polynomials

(Weisstein, 1998; Wilck, 2001), which are orthogonal to the log-normal distribution. The three-term recurrence relation that defines these polynomials is (Wilck, 2001):

$$P_{-1} = 0, \quad P_0 = 1, \quad P_{i+1} = (x - a_i)P_i - b_i P_{i-1}, \quad i = 1, 2, \ldots, \tag{A.5}$$

where

$$\begin{aligned} &a_0 = \eta, \quad a_i = \eta^{2i-1}\left[\left(\eta^2 + 1\right)\eta^{2i} - 1\right], \\ &b_0 = 0, \quad b_i = \eta^{6i-4}(\eta^{2i} - 1), \\ &\eta = \mathrm{e}^{\sigma^2/2}. \end{aligned} \tag{A.6}$$

The values of the quadrature weights and abscissae for both the approaches are found by solving an eigenvalue problem as explained in Wilf (1962); Golub and Welsch (1969); Dette (1997). We illustrate the procedure considering the integral

$$\int_0^\infty g(\xi)\,\delta_\sigma(\xi, \mu)\,\mathrm{d}\xi = \int_0^\infty g(\xi)\,\frac{1}{\xi\sigma\sqrt{2\pi}}\,\mathrm{e}^{-\frac{(\ln\xi-\mu)^2}{2\sigma^2}}\,\mathrm{d}\xi. \tag{A.7}$$

We set

$$\ln\xi - \mu = \ln s \Rightarrow \xi = s\,\mathrm{e}^{\mu},$$

and so we can write the differential of ξ as

$$\mathrm{d}\xi = \mathrm{e}^{\mu}\,\mathrm{d}s. \tag{A.8}$$

Thus the original integral becomes

$$\int_0^\infty \frac{g(s\,\mathrm{e}^{\mu})\,\mathrm{e}^{-\frac{\ln^2 s}{2\sigma^2}}\,\mathrm{e}^{\mu}}{s\,\mathrm{e}^{\mu}\,\sigma\sqrt{2\pi}}\mathrm{d}s = \int_0^\infty g(s\,\mathrm{e}^{\mu})\,w(s)\,\mathrm{d}s, \tag{A.9}$$

with

$$w(s) = \frac{\mathrm{e}^{-\frac{\ln^2 s}{2\sigma^2}}}{s\sigma\sqrt{2\pi}}. \tag{A.10}$$

BIBLIOGRAPHY

Akroyd, J., Smith, A. J., McGlashan, L. R., and Kraft, M. (2010). Numerical investigation of DQMOM-IEM as a turbulent reaction closure. *Chemical Engineering Science*, 65(6):1915–1924.

Alopaeus, V., Laakkonen, M., and Aittamaa, J. (2006). Solution of population balances with breakage and agglomeration by high-order moment-conserving method of classes. *Chemical Engineering Science*, 61(20):6732–6752.

Alopaeus, V., Laakkonen, M., and Aittamaa, J. (2008). Solution of population balances by high order moment-conserving method of classes: reconstruction of a non-negative density distribution. *Chemical Engineering Science*, 63(10):2741–2751.

Athanassoulis, G. A. and Gavriliadis, P. N. (2002). The truncated Hausdorff moment problem solved by using kernel density functions. *Probabilistic Engineering Mechanics*, 17(3):273–291.

Balakin, B. V., Hoffmann, A. C., and Kosinski, P. (2014). Coupling STAR-CD with a population-balance technique based on the classes method. *Powder Technology*, 257:47–54.

Bannari, R., Kerdouss, F., Selma, B., Bannari, A., and Proulx, P. (2008). Three-dimensional mathematical modeling of dispersed two-phase flow using class method of population balance in bubble columns. *Computers & Chemical Engineering*, 32(12):3224–3237.

Becker, P. J., Puel, F., Henry, R., and Sheibat-Othman, N. (2011). Investigation of discrete population balance models and breakage kernels for dilute emulsification systems. *Industrial & Engineering Chemistry Research*, 50(19):11358–11374.

Bove, S., Solberg, T., and Hjertager, B. H. (2005). A novel algorithm for solving population balance equations: the parallel parent and daughter classes. Derivation, analysis and testing. *Chemical Engineering Science*, 60(5):1449–1464.

Broadwell, J. E. and Breidenthal, R. E. (1982). A simple model of mixing and chemical reaction in a turbulent shear layer. *Journal of Fluid Mechanics*, 125:397–410.

Cao, R. R., Wang, H., and Pope, S. B. (2007). The effect of mixing models in PDF calculations of piloted jet flames. *Proceedings of the Combustion Institute*, 31(1):1543–1550.

Capecelatro, J., Desjardins, O., and Fox, R. (2014). Numerical study of collisional particle dynamics in cluster-induced turbulence. *Journal of Fluid Mechanics*, 747:R2–1–R2–13.

Carrica, P. M., Drew, D., Bonetto, F., and Lahey Jr, R. T. (1999). A polydisperse model for bubbly two-phase flow around a surface ship. *International Journal of Multiphase Flow*, 25(2):257–305.

Cassiani, M., Franzese, P., and Giostra, U. (2005). A PDF micromixing model of dispersion for atmospheric flow. Part I: development of the model, application to homogeneous turbulence and to neutral boundary layer. *Atmospheric Environment*, 39(8):1457–1469.

Chalons, C., Fox, R., and Massot, M. (2010). A multi-Gaussian quadrature method of moments for gas-particle flows in a LES framework. *Studying Turbulence Using Numerical Simulation Databases, Center for Turbulence Research, Summer Program 2010, Stanford University*, pages 347–358.

Chen, H., Chen, S., and Kraichnan, R. H. (1989). Probability distribution of a stochastically advected scalar field. *Physical Review Letters*, 63(24):2657–2660.

Cheng, J. C. (2010). A comrehensive model study for Flash Nanoprecipitation: computational fluid dynamics, micro- particle image velocimetry, and population balance modeling. *Iowa State University, Ames, Iowa, USA*.

Cheng, J. C. and Fox, R. O. (2010). Kinetic Modeling of Nanoprecipitation using CFD Coupled with a Population Balance. *Industrial & Engineering Chemistry Research*, 49(21):10651–10662.

Cheng, J. C., Vigil, R., and Fox, R. (2010). A competitive aggregation model for Flash Nano-Precipitation. *Journal of Colloid and Interface Science*, 351(2):330–342.

Choi, H. S., Park, T. S., and Suzuki, K. (2008). Turbulent mixing of a passive scalar in confined multiple jet flows of a micro combustor. *International Journal of Heat and Mass Transfer*, 51(17–18):4276–4286.

Cremer, M. A., McMurtry, P. A., and Kerstein, A. R. (1994). Effects of turbulence length scale distribution on scalar mixing in homogeneous turbulent flow. *Physics of Fluids*, 6(6):2143–2153.

Curl, R. L. (1963). Dispersed phase mixing: I. Theory and effects in simple reactors. *AIChE Journal*, 9(2):175–181.

Danckwerts, P. V. (1958). The effect of incomplete mixing on homogeneous reactions. *Chemical Engineering Science*, 8(12):93–102.

Desjardins, O., Fox, R., and Villedieu, P. (2008). A quadrature-based moment method for dilute fluid-particle flows. *Journal of Computational Physics*, 227(4):2514–2539.

Dette, H. (1997). *The Theory of Canonical Moments with Applications in Statistics, Probability and Analysis*. John Wiley & Sons, New York.

Diemer, R. B. and Olson, J. H. (2002). A moment methodology for coagulation and breakage problems: Part 2moment models and distribution reconstruction. *Chemical Engineering Science*, 57(12):2211–2228.

Dopazo, C. (1994). Recent development in pdf methods. In Libby, P. A. and Williams, F. A., editors, *Turbulent Reacting Flows*, pages 357–474. New York: Academic Press.

Dopazo, C. and O'Brien, E. E. (1973). Isochoric turbulent mixing of two rapidly reacting chemical species with chemical heat release. *Physics of Fluids*, 16(12):2075–2081.

Efendiev, Y. and Zachariah, M. R. (2002). Hybrid Monte Carlo Method for Simulation of Two-Component Aerosol Coagulation and Phase Segregation. *Journal of Colloid and Interface Science*, 249(1):30–43.

Eswaran, V. and Pope, S. B. (1988). Direct numerical simulations of the turbulent mixing of a passive scalar. *Physics of Fluids*, 31:506–520.

Falola, A., Borissova, A., and Wang, X. Z. (2013). Extended method of moment for general population balance models including size dependent growth rate, aggregation and breakage kernels. *Computers & Chemical Engineering*, 56:1–11.

Fokker, A. D. (1914). Die mittlere Energie rotierender elektrischer Dipole im Strahlungsfeld. *Annalen der Physik*, 348(5):810–820.

Fox, R., Laurent, F., and Massot, M. (2008). Numerical simulation of spray coalescence in an Eulerian framework: Direct quadrature method of moments and multi-fluid method. *Journal of Computational Physics*, 227(6):3058–3088.

Fox, R. O. (1992a). Computation of turbulent reactive flows: first- principles macro/micromixing models using probability density function methods. *Chemical Engineering Science*, 47(9–11):2853–2858.

Fox, R. O. (1992b). The Fokker–Planck closure for turbulent molecular mixing: Passive scalars. *Physics of Fluids*, 4(6):1230–1244.

Fox, R. O. (1994). Improved Fokker–Planck model for the joint scalar, scalar gradient PDF. *Physics of Fluids*, 6(1):334–348.

Fox, R. O. (1998). On the relationship between Lagrangian micromixing models and computational fluid dynamics. *Chemical Engineering and Processing: Process Intensification*, 37(6):521–535.

Fox, R. O. (1999). The Lagrangian spectral relaxation model for differential diffusion in homogeneous turbulence. *Physics of Fluids*, 11(6):1550–1571.

Fox, R. O. (2003). Computational models for turbulent reacting flows. Cambridge University Press.

Fox, R. O. (2009). Optimal Moment Sets for Multivariate Direct Quadrature Method of Moments. *Industrial & Engineering Chemistry Research*, 48(21):9686–9696.

Frankel, S. H., Madnia, C. K., and Givi, P. (1992). Modeling of the reactant conversion rate in a turbulent shear flow. *Chemical Engineering Communications*, 113(1):197–209.

Garcia, A. L., van den Broeck, C., Aertsens, M., and Serneels, R. (1987). A Monte Carlo simulation of coagulation. *Physica A: Statistical Mechanics and its Applications*, 143(3):535–546.

Garmory, A., Kim, I. S., Britter, R. E., and Mastorakos, E. (2009). Simulations of the dispersion of reactive pollutants in a street canyon, considering different chemical mechanisms and micromixing. *Atmospheric Environment*, 43(31):4670–4680.

Garmory, A. and Mastorakos, E. (2008). Aerosol nucleation and growth in a turbulent jet using the Stochastic Fields method. *Chemical Engineering Science*, 63(16):4078–4089.

Garmory, A., Richardson, E. S., and Mastorakos, E. (2006). Micromixing effects in a reacting plume by the Stochastic Fields method. *Atmospheric Environment*, 40(6):1078–1091.

Gautschi, W. (2004). *Orthogonal Polynomials: Computation and Approximation*. Oxford University Press.

Gavi, E., Rivautella, L., Marchisio, D. L., Vanni, M., Barresi, A. A., and Baldi, G. (2007). CFD modelling of nano-particle precipitation in confined impinging jet reactors. *Chemical Engineering Research and Design*, 85(5):735–744.

Gelbard, F. and Seinfeld, J. H. (1978). Numerical solution of the dynamic equation for particulate systems. *Journal of Computational Physics*, 28(3):357–375.

Gillespie, D. T. (1976). A general method for numerically simulating the stochastic time evolution of coupled chemical reactions. *Journal of Computational Physics*, 22(4):403–434.

Girimaji, S. S. (1991). Assumed β-pdf model for turbulent mixing: validation and extension to multiple scalar mixing. *Combustion Science and Technology*, 78:177.

Golub, G. H. and Welsch, J. H. (1969). Calculation of gauss quadrature rules. *Mathematics of Computation*, 23(106):221–230.

Goodson, M. and Kraft, M. (2002). An efficient stochastic algorithm for simulating nano-particle dynamics. *Journal of Computational Physics*, 183(1):210–232.

Gordon, R. G. (1968). Error bounds in equilibrium statistical mechanics. *Journal of Mathematical Physics*, 9:655–662.

Greenberg, J. B., Alibagli, D., and Tambour, Y. (1986). An opposed jet quasi-monodisperse spray diffusion flame. *Combustion Science and Technology*, 50(4-6):255–270.

Greenberg, J. B., Silverman, I., and Tambour, Y. (1993). On the origins of spray sectional conservation equations. *Combustion and Flame*, 93(12):90–96.

Hounslow, M., Ryall, R., and Marshall, V. (1988). Discretized population balance for nucleation, growth, and aggregation. *AIChE Journal*, 34(11):1821–1832.

Hounslow, M. J. (1990). A discretized population balance for continuous systems at steady state. *AIChE Journal*, 36(1):106–116.

Hu, X., Passalacqua, A., and Fox, R. O. (2015). Application of quadrature-based uncertainty quantification to the NETL small-scale challenge problem SSCP-I. *Powder Technology*, 272:100–112.

Hulburt, H. M. and Katz, S. (1964). Some problems in particle technology: A statistical mechanical formulation. *Chemical Engineering Science*, 19(8):555–574.

Johnson, B. K. and Prud'homme, R. K. (2003). Chemical processing and micromixing in confined impinging jets. *AIChE Journal*, 49(9):2264–2282.

Jones, W. P. and Navarro-Martinez, S. (2007). Large eddy simulation of autoignition with a subgrid probability density function method. *Combustion and Flame*, 150(3):170–187.

Jones, W. P. and Navarro-Martinez, S. (2009). Numerical Study of n-Heptane Auto-ignition Using LES-PDF Methods. *Flow, Turbulence and Combustion*, 83(3):407–423.

Jones, W. P., Navarro-Martinez, S., and Rhl, O. (2007). Large eddy simulation of hydrogen auto-ignition with a probability density function method. *Proceedings of the Combustion Institute*, 31(2):1765–1771.

Juneja, A. and Pope, S. B. (1996). A DNS study of turbulent mixing of two passive scalars. *Physics of Fluids*, 8(8):2161–2184.

Kolmogoroff, A. (1931). ber die analytischen Methoden in der Wahrscheinlichkeitsrechnung. *Mathematische Annalen*, 104(1):415–458.

Koochesfahani, M. M. and Dimotakis, P. E. (1986). Mixing and chemical reactions in a turbulent liquid mixing layer. *Journal of Fluid Mechanics*, 170:83–112.

Kraichnan, R. H. (1989). Closures for probability distributions. *Bulletin of the American Physical Society*, 34:2298.

Kraichnan, R. H. (1990). Models of intermittency in hydrodynamic turbulence. *Physical Review Letters*, 65(5):575–578.

Kruis, F. E., Maisels, A., and Fissan, H. (2000). Direct simulation Monte Carlo method for particle coagulation and aggregation. *AIChE Journal*, 46(9):1735–1742.

Kumar, P. and Narayanan, S. (2006). Solution of Fokker-Planck equation by finite element and finite difference methods for nonlinear systems. *Sadhana - Academy Proceedings in Engineering Sciences*, 31:445–461.

Kumar, S. and Ramkrishna, D. (1996a). On the solution of population balance equations by discretization – I. A fixed pivot technique. *Chemical Engineering Science*, 51(8):1311–1332.

Kumar, S. and Ramkrishna, D. (1996b). On the solution of population balance equations by discretization – II. A moving pivot technique. *Chemical Engineering Science*, 51(8):1333–1342.

Lage, P. L. C. (2011). On the representation of QMOM as a weighted-residual method – The dual-quadrature method of generalized moments. *Computers & Chemical Engineering*, 35(11):2186–2203.

Lasheras, J. C., Eastwood, C., Martinez-Bazan, C., and Montanes, J. L. (2002). A review of statistical models for the break-up of an immiscible fluid immersed into a fully developed turbulent flow. *International Journal of Multiphase Flow*, 28(2):247–278.

Launder, B. E. and Sandham, N. D. (2002). *Closure Strategies for Turbulent and Transitional Flows*. Cambridge University Press, Cambridge.

Laurent, F. and Nguyen, T. T. (2017). Realizable second-order finite-volume schemes for the advection of moment sets of the particle size distribution. *Journal of Computational Physics*, 337:309–338.

Lee, K. and Matsoukas, T. (2000). Simultaneous coagulation and break-up using constant-n monte carlo. *Powder Technology*, 110(12):82–89.

Lee, K. W. (1983). Change of particle size distribution during Brownian coagulation. *Journal of Colloid and Interface Science*, 92(2):315–325.

Liffman, K. (1992). A direct simulation Monte-Carlo method for cluster coagulation. *Journal of Computational Physics*, 100(1):116–127.

Limpert, E., Stahel, W. A., and Abbt, M. (2001). Log-normal distribution across the sciences: keys and clues. *BioScience*, 51(5):341–352.

Lin, Y., Lee, K., and Matsoukas, T. (2002). Solution of the population balance equation using constant-number Monte Carlo. *Chemical Engineering Science*, 57(12):2241–2252.

Liu, Y., Cheng, C., Liu, Y., Prudhomme, R. K., and Fox, R. O. (2008). Mixing in a multi-inlet vortex mixer (MIVM) for flash nano-precipitation. *Chemical Engineering Science*, 63(11):2829–2842.

Liu, Z., Fox, R. O., Hill, J. C., and Olsen, M. G. (2015). A Batchelor Vortex Model for Mean Velocity of Turbulent Swirling Flow in a Macroscale Multi-Inlet Vortex Reactor. *Journal of Fluids Engineering*, 137(4):041204–041204.

Liu, Z., Passalacqua, A., Olsen, M. G., Fox, R. O., and Hill, J. C. (2016). Dynamic delayed detached eddy simulation of a multi-inlet vortex reactor. *AIChE Journal*, 62(7):2570–2578.

Luhar, A. K. and Sawford, B. L. (2005). Micromixing modelling of mean and fluctuating scalar fields in the convective boundary layer. *Atmospheric Environment*, 39(35):6673–6685.

Madadi-Kandjani, E. and Passalacqua, A. (2015). An extended quadrature-based moment method with log-normal kernel density functions. *Chemical Engineering Science*, 131:323–339.

Madnia, C. K., Frankel, S. H., and Givi, P. (1991). Direct numerical simulations of the unmixedness in a homogeneous reacting turbulent flow. *Chemical Engineering Communications*, 109(1):19–29.

Magnus, W., Oberhettinger, F., and Soni, R. P. (1966). *Formulas and theorems for the special functions of mathematical physics*. Springer–Verlag, Berlin.

Marchisio, D. L. and Fox, R. O. (2005). Solution of population balance equations using the direct quadrature method of moments. *Journal of Aerosol Science*, 36(1):43–73.

Marchisio, D. L. and Fox, R. O. (2013). *Computational Models for Polydisperse Particulate and Multiphase Systems*. Cambridge University Press, Cambridge.

Marchisio, D. L., Pikturna, J. T., Fox, R. O., Vigil, R. D., and Barresi, A. A. (2003a). Quadrature method of moments for population-balance equations. *AIChE Journal*, 49(5):1266–1276.

Marchisio, D. L., Vigil, R., and Fox, R. O. (2003b). Quadrature method of moments for aggregation-breakage processes. *Journal of Colloid and Interface Science*, 258(2):322–334.

Massot, M., Laurent, F., Kah, D., and de Chaisemartin, S. (2010). A robust moment method for evaluation of the disappearance rate of evaporating sprays. *SIAM Journal on Applied Mathematics*, 70(8):3203–3234.

McGraw, R. (1997). Description of aerosol dynamics by the quadrature method of moments. *Aerosol Science and Technology*, 27(2):255–265.

McMurtry, P. A. and Givi, P. (1989). Direct numerical simulations of mixing and reaction in a nonpremixed homogeneous turbulent flow. *Combustion and Flame*, 77(2):171–185.

Mead, L. R. and Papanicolaou, N. (1984). Maximum entropy in the problem of moments. *Journal of Mathematical Physics*, 25(8):2404–2417.

Meimaroglou, D. and Kiparissides, C. (2007). Monte Carlo simulation for the solution of the bi-variate dynamic population balance equation in batch particulate systems. *Chemical Engineering Science*, 62(1820):5295–5299.

Meyer, D. W. (2010). A new particle interaction mixing model for turbulent dispersion and turbulent reactive flows. *Physics of Fluids*, 22(3):035103.

Meyer, D. W. and Jenny, P. (2006). A mixing model for turbulent flows based on parameterized scalar profiles. *Physics of Fluids*, 18(3):035105.

Meyer, D. W. and Jenny, P. (2009). Micromixing models for turbulent flows. *Journal of Computational Physics*, 228(4):1275–1293.

Meyer, D. W. and Jenny, P. (2013). Accurate and computationally efficient mixing models for the simulation of turbulent mixing with PDF methods. *Journal of Computational Physics*, 247:192–207.

Muhr, H., David, R., Villermaux, J., and Jezequel, P. H. (1996). Crystallization and precipitation engineering-VI. Solving population balance in the case of the precipitation of silver bromide crystals with high primary nucleation rates by using the first order upwind differentiation. *Chemical Engineering Science*, 51(2):309–319.

Mungal, M. G. and Dimotakis, P. E. (1984). Mixing and combustion with low heat release in a turbulent shear layer. *Journal of Fluid Mechanics*, 148:349–382.

Nguyen, T. T., Laurent, F., Fox, R. O., and Massot, M. (2016). Solution of population balance equations in applications with fine particles: Mathematical modeling and numerical schemes. *Journal of Computational Physics*, 325:129–156.

Nooren, P. A., Wouters, H. A., Peeters, T. W. J., Roekaerts, D., Maas, U., and Schmidt, D. (1997). Monte Carlo PDF modelling of a turbulent natural-gas diffusion flame. *Combustion Theory and Modelling*, 1(1):79–96.

O'Brien, E. E. (1980). The probability density function (pdf) approach to reacting turbulent flows. In Libby, P. A. and Williams, F. A., editors, *Turbulent Reacting Flows*, number 44 in Topics in Applied Physics, pages 185–218. Springer Berlin Heidelberg.

O'Brien, E. E. and Jiang, T.-L. (1991). The conditional dissipation rate of an initially binary scalar in homogeneous turbulence. *Physics of Fluids A: Fluid Dynamics*, 3(12):3121–3123.

Overholt, M. R. and Pope, S. B. (1996). Direct numerical simulation of a passive scalar with imposed mean gradient in isotropic turbulence. *Physics of Fluids*, 8(11):3128–3148.

Perthame, B. (1992). Second-Order Boltzmann Schemes for Compressible Euler Equations in One and Two Space Dimensions. *SIAM Journal on Numerical Analysis*, 29(1):1–19.

Peters, N. (2000). *Turbulent Combustion*. Cambridge University Press, Cambridge, 1 edition.

Petitti, M., Nasuti, A., Marchisio, D. L., Vanni, M., Baldi, G., Mancini, N., and Podenzani, F. (2010). Bubble size distribution modeling in stirred gas-liquid reactors with QMOM augmented by a new correction algorithm. *AIChE Journal*, 56(1):36–53.

Pitsch, H. (2006). Large-Eddy Simulation of Turbulent Combustion. *Annual Review of Fluid Mechanics*, 38(1):453–482.

Poinsot, T. and Veynante, D. (2005). *Theoretical and Numerical Combustion, Second Edition*. R.T. Edwards, Inc., Philadelphia, 2 edition.

Pope, S. B. (1991). Mapping closures for turbulent mixing and reaction. *Theoretical and Computational Fluid Dynamics*, 2(5-6):255–270.

Pope, S. B. (2000). *Turbulent Flows*. Cambridge University Press, Cambridge.

Pope, S. B. (2013). A model for turbulent mixing based on shadow-position conditioning. *Physics of Fluids*, 25(11):110803.

Popov, P. P. and Pope, S. B. (2014). Large eddy simulation/probability density function simulations of bluff body stabilized flames. *Combustion and Flame*, 161(12):3100–3133.

Popov, P. P., Wang, H., and Pope, S. B. (2015). Specific volume coupling and convergence properties in hybrid particle/finite volume algorithms for turbulent reactive flows. *Journal of Computational Physics*, 294:110–126.

Pratsinis, S. E. (1988). Simultaneous nucleation, condensation, and coagulation in aerosol reactors. *Journal of Colloid and Interface Science*, 124(2):416–427.

Puel, F., Fevotte, G., and Klein, J. P. (2003). Simulation and analysis of industrial crystallization processes through multidimensional population balance equations. part 1: a resolution algorithm based on the method of classes. *Chemical Engineering Science*, 58(16):3715–3727.

Raman, V. and Pitsch, H. (2007). A consistent LES/filtered-density function formulation for the simulation of turbulent flames with detailed chemistry. *Proceedings of the Combustion Institute*, 31(2):1711–1719.

Ramkrishna, D. (2000). *Population balances: theory and applications to particulate systems in engineering*. Academic Press.

Randolph, A. (1964). A population balance for countable entities. *The Canadian Journal of Chemical Engineering*, 42(6):280–281.

Randolph, A. D. and Larson, M. A. (1988). *Theory of particulate processes: analysis and techniques of continuous crystallization*. Academic Press.

Reyes, J. N. J. (1989). Statistically derived conservation equations for fluid particle flows.

Richardson, E. S. and Chen, J. H. (2012). Application of PDF mixing models to premixed flames with differential diffusion. *Combustion and Flame*, 159(7):2398–2414.

Risken, H. (1989). *The Fokker-Planck Equation*, volume 18 of *Springer Series in Synergetics*. Springer Berlin Heidelberg, Berlin, Heidelberg.

Rosner, D. E. and Yu, S. (2001). MC simulation of aerosol aggregation and simultaneous spheroidization. *AIChE Journal*, 47(3):545–561.

Sabelnikov, V. and Soulard, O. (2005). Rapidly decorrelating velocity-field model as a tool for solving one-point Fokker-Planck equations for probability density functions of turbulent reactive scalars. *Physical Review E*, 72(1):016301.

Sabelnikov, V. and Soulard, O. (2006). White in Time Scalar Advection Model as a Tool for Solving Joint Composition PDF Equations. *Flow, Turbulence and Combustion*, 77(1-4):333–357.

Sawford, B. L. (2004). Micro-mixing modelling of scalar fluctuations for plumes in homogeneous turbulence. *Flow, Turbulence and Combustion*, 72(2-4):133–160.

Sawford, B. L. (2006). Lagrangian modeling of scalar statistics in a double scalar mixing layer. *Physics of Fluids*, 18(8):085108.

Shohat, J. A. and Tamarkin, J. D. (1943). *The Problem of Moments*. American Mathematical Soc.

Silva, L. F. L. R., Rodrigues, R. C., Mitre, J. F., and Lage, P. L. C. (2010). Comparison of the accuracy and performance of quadrature-based methods for population balance problems with simultaneous breakage and aggregation. *Computers & Chemical Engineering*, 34(3):286–297.

Smith, M. and Matsoukas, T. (1998). Constant-number Monte Carlo simulation of population balances. *Chemical Engineering Science*, 53(9):1777–1786.

Smoluchowski, M. v. (1916). Drei vortrge ber diffusion, brownsche bewegung und koagulation von kolloidteilchen. In Simon, H. T. and Debye, P., editors, *Physikalische Zeitschrift*, number 17, pages 557–585. S. Hirzel, Leipzig.

Spencer, B. F. and Bergman, L. A. (1993). On the numerical solution of the Fokker-Planck equation for nonlinear stochastic systems. *Nonlinear Dynamics*, 4(4):357–372.

Stollinger, M. and Heinz, S. (2010). Evaluation of scalar mixing and time scale models in PDF simulations of a turbulent premixed flame. *Combustion and Flame*, 157(9):1671–1685.

Subramaniam, S. and Pope, S. B. (1998). A mixing model for turbulent reactive flows based on Euclidean minimum spanning trees. *Combustion and Flame*, 115(4):487–514.

Sundaram, B., Klimenko, A. Y., Cleary, M. J., and Ge, Y. (2016). A direct approach to generalized multiple mapping conditioning for selected turbulent diffusion flame cases. *Combustion Theory and Modelling*, 20(4):735–764.

Tagliani, A. (1999). Hausdorff moment problem and maximum entropy: A unified approach. *Applied Mathematics and Computation*, 105(23):291–305.

Tsai, K. and Fox, R. O. (1994). PDF simulation of a turbulent seriesparallel reaction in an axisymmetric reactor. *Chemical Engineering Science*, 49(24):5141–5158.

Tsai, K. and Fox, R. O. (1995). Modeling multiple reactive scalar mixing with the generalized IEM model. *Physics of Fluids*, 7(11):2820–2830.

Valino, L. (1998). A Field Monte Carlo Formulation for Calculating the Probability Density Function of a Single Scalar in a Turbulent Flow. *Flow, Turbulence and Combustion*, 60(2):157–172.

Vanni, M. (2000). Approximate population balance equations for aggregation-breakage processes. *Journal of Colloid and Interface Science*, 221(2):143–160.

Vikas, V., Hauck, C., Wang, Z., and Fox, R. (2013a). Radiation transport modeling using extended quadrature method of moments. *Journal of Computational Physics*, 246:221–241.

Vikas, V., Wang, Z. J., and Fox, R. O. (2013b). Realizable high-order finite-volume schemes for quadrature-based moment methods applied to diffusion population balance equations. *Journal of Computational Physics*, 249:162–179.

Vikas, V., Wang, Z. J., Passalacqua, A., and Fox, R. O. (2011). Realizable high-order finite-volume schemes for quadrature-based moment methods. *Journal of Computational Physics*, 230(13):5328–5352.

Villermaux, J. and Devillon (1972). Represntation de la coalescence et de la redispersion des domaines de sgrgation dans un fluide par un modle d'interaction phnomnologique. In *In Proceedings of the 2nd International Symposium on Chemical Reaction Engineering*, pages 1–13. New York: Elsevier.

Villermaux, J. and Falk, L. (1994). A generalized mixing model for initial contacting of reactive fluids. *Chemical Engineering Science*, 49(24, Part 2):5127–5140.

Wang, H. and Kim, K. (2015). Effect of molecular transport on PDF modeling of turbulent non-premixed flames. *Proceedings of the Combustion Institute*, 35(2):1137–1145.

Wang, L. and Fox, R. O. (2004). Comparison of micromixing models for CFD simulation of nanoparticle formation. *AIChE Journal*, 50(9):2217–2232.

Wang, L., Marchisio, D., Vigil, R., and Fox, R. (2005a). CFD simulation of aggregation and breakage processes in laminar Taylor–Couette flow. *Journal of Colloid and Interface Science*, 282(2):380–396.

Wang, L., Vigil, R. D., and Fox, R. O. (2005b). CFD simulation of shear-induced aggregation and breakage in turbulent Taylor–Couette flow. *Journal of Colloid and Interface Science*, 285(1):167–178.

Weisstein, E. W. (1998). *CRC Concise Encyclopedia of Mathematics*. CRC Press.

Wheeler, J. C. (1974). Modified moments and Gaussian quadratures. *Rocky Mountain Journal of Mathematics*, 4:287–296.

Wilck, M. (2001). A general approximation method for solving integrals containing a lognormal weighting function. *Journal of Aerosol Science*, 32(9):1111–1116.

Wilf, H. S. (1962). *Mathematics for the Physical Sciences*. Dover Publications, New York.

Williams, M. M. R. and Loyalka, S. K. (1991). *Aerosol Science: Theory and Practice*. Pergamon, Oxford ; New York, 1^{st} edition.

Wright, D. L. (2007). Numerical advection of moments of the particle size distribution in eulerian models. *Journal of Aerosol Science*, 38(3):352–369.

Yeung, P. K., Donzis, D. A., and Sreenivasan, K. R. (2005). High-Reynolds-number simulation of turbulent mixing. *Physics of Fluids*, 17(8):081703.

Yeung, P. K., Xu, S., and Sreenivasan, K. R. (2002). Schmidt number effects on turbulent transport with uniform mean scalar gradient. *Physics of Fluids*, 14(12):4178–4191.

Yuan, C. and Fox, R. (2011). Conditional quadrature method of moments for kinetic equations. *Journal of Computational Physics*, 230(22):8216–8246.

Yuan, C., Laurent, F., and Fox, R. (2012). An extended quadrature method of moments for population balance equations. *Journal of Aerosol Science*, 51:1–23.

Zhao, H., Kruis, F. E., and Zheng, C. (2009). Reducing statistical noise and extending the size spectrum by applying weighted simulation particles in Monte Carlo simulation of coagulation. *Aerosol Science and Technology*, 43(8):781–793.

Zhao, H., Maisels, A., Matsoukas, T., and Zheng, C. (2007). Analysis of four Monte Carlo methods for the solution of population balances in dispersed systems. *Powder Technology*, 173(1):38–50.

Zhao, H. and Zheng, C. (2013). A population balance-Monte Carlo method for particle coagulation in spatially inhomogeneous systems. *Computers & Fluids*, 71:196–207.

Zhao, X.-Y., Bhagatwala, A., Chen, J. H., Haworth, D. C., and Pope, S. B. (2016). An a priori DNS study of the shadow-position mixing model. *Combustion and Flame*, 165:223–245.